APPLICATION OF THE FINITE ELEMENT METHOD
TO THE VIBRATION ANALYSIS OF AXIAL FLOW TURBINES

by

G. Jeyaraj Wilson

B.E. (Civil), Madras University, India, 1966

M.E. (Struct.), Indian Institute of Science,

Bangalore, India, 1968

A thesis submitted to the Faculty of Graduate Studies
in partial fulfilment of the requirements for the degree of
Doctor of Philosophy in Mechanical Engineering.

Carleton University

Ottawa, Ontario

October, 1972

The undersigned hereby recommend to the Faculty of Graduate Studies, Carleton University, acceptance of this thesis, "Application of the Finite Element Method to the Vibration Analysis of Axial Flow Turbines," submitted by G. Jeyaraj Wilson, in partial fulfilment of the requirements for the degree of Doctor of Philosophy in Mechanical Engineering.

Dean of the Faculty of Engineering

Supervisor

External Examiner

The undersigned hereby recommend to the Faculty of Graduate Studies, Carleton University, acceptance of this thesis, "Application of the Finite Element Method to the Vibration Analysis of Axial Flow Turbines," submitted by G. Jeyaraj Wilson, in partial fulfilment of the requirements for the degree of Doctor of Philosophy in Mechanical Engineering.

Dean of the Faculty of Engineering

Supervisor

External Examiner

ABSTRACT

The finite element method is applied to the vibration analysis of axial flow turbine rotors.

Using the axi-symmetric properties of the configuration of such rotors, several new finite elements are developed to describe the bending and stretching of thin or moderately thick circular plates, and which are characterised by only four or eight degrees of freedom. These elements incorporate the 'desired number of diametral nodes in their dynamic deflection functions, and allow for any specified thickness variation in the radial direction. In addition, the effects of in-plane stresses, which might arise from rotation or radial temperature gradient, and the effects of transverse shear and rotary inertia in moderately thick plates, are readily accounted for. The accuracy and convergence of these elements is demonstrated by numerical comparison with both exact and experimental data for discs.

Making the assumption that blade dynamic loadings on the rim of a vibrating blade-disc system are continuously distributed, a method of coupling blade and disc vibration is formulated. For non-rotating configurations of simple geometry an exact solution for the coupled blade-disc frequencies and mode shapes is developed.

For configurations more representative of practical turbine rotors a finite element model is detailed; this model takes into account arbitrary disc profile and in-plane stresses, taper and twist in the blades, and allows for transverse shear and rotary inertia in both disc and blades where this is thought necessary. Numerical calculations are presented which demonstrate the convergence and accuracy of this finite element model on predicting the natural frequencies of both simple and complex bladed rotors.

Considerable effort has been made to make the computer programs developed for the numerical calculations in this work of practical usefulness to the designer, Thus these are given in some detail, and feature several options which allow flexibility to calculate disc stresses, disc alone vibration, blade alone vibration, and coupled blade-disc vibration frequencies; in the vibration analysis options are available to include effects of in-plane stresses due to rotation or thermal gradient, transverse shear, and rotary inertia.

ACKNOWLEDGEMENTS

The author wishes to express his deep sense of gratitude and sincere appreciation to Professor J. Kirkhope for his valuable guidance and the many suggestions throughout the course of this investigation, and for painstakingly reading the manuscript and suggesting its improvement.

The author is grateful to Dr. E. K. Armstrong, Head of Vibration Engineering, Rolls-Royce (1971) Limited, for providing experimental data on an actual turbine rotor. Very special thanks are due to Mr. R. W. Harris, senior undergraduate student at Carleton University (1969-70), for obtaining experimental results for the bladed disc models.

This work was supported by the National Research Council of Canada through Operating Grant A-7283.

Finally, the author will be forever grateful to his wife, Jeya, for her help and patient understanding during the preparation of this thesis.

CONTENTS

LIST OF PRINCIPAL SYMBOLS

a - inner radius of turbine disc;

A - area of cross-section of rim;blade;

a_1 - constants in assumed deflection functions;

b - outer radius of turbine disc;

b_b - thickness of uniform blade;

b_r - breadth of rim;

c - constant used to define variation of σ_r;

d - constant used to define variation of σ_r;

d_b - chord of uniform blade;

d_r - depth of rim;

D - flexural rigidity of disc;

e - constant used to define variation of σ_ξ;

e_1 - distance from the inner boundary to centroid of rim;

e_2 - distance from centroid to outer boundary of rim;

E - Young's modulus;

E - energy;

f - constant used to define variation of σ_ξ;

$F(r)$ - centrifugal force;

$h(r)$ - thickness of turbine disc at radius r;

h_0 - thickness at the centre of the disc;

I – moment of inertia of blade section;

J – polar moment of inertia of blade section;

k – shear constant used in Timoshenko beam;

k = $(\rho h\omega^2/D)^{1/2}$

K_G – St. Venant torsional stiffness of the blade cross-section;

ℓ – length of blade element; length of blade;

L – length of blade;

m – number of nodal diameters;

M_r – radial bending moment;

$M_{r\xi}$ – twisting moment;

n – number of nodal circles;

N – number of finite elements used in a model;

p – radial stress coefficient;

P_i – integrals appearing in stiffness or inertia matrices;

q – tangential stress coefficient;

Q_i – integrals appearing in stiffness or inertia matrices;

r – radial distance;

R – radius at the root of the blade;

R_g – radius to the centre of gravity of the blade;

R_i – integrals appearing in the element matrices;

R_O – centroidal radius of rim;

S_i – integrals appearing in the element matrices;

t – time in seconds;

T – kinetic energy;

$T(r)$ - temperature at radius r;

u - radial displacement at the middle plane of the disc;

U - strain energy;

v - deflection of the blade along the tangential direction;

v^* - deflection of the blade along the I_{min} direction;

w - axial deflection of the disc, rim and blade;

w^* - deflection of the blade along the I,,, direction;

Z - number of blades in the rotor;

α - constant defining thiclcness variation of element;

α^* - coefficient of thermal expansion;

β - constant defining thickness variation of element;

γ_v - additional rotation due to transverse shear in the tangential direction;

γ_v^* - additional rotation due to transverse shear in the T_{min} direction;

γ_w - additional rotation due to transverse shear in the axial direction;

γ_w^* - additional rotation due to transverse shear in the I_{max} direction;

δ - stagger angle;

ε_r -radial strain in the middle plane of the disc;

ε_ξ - tangential strain in the middle plane of the disc;

θ - radial rotation;

T(r) - temperature at radius r;

u - radial displacement at the middle plane of the disc;

U - strain energy;

v - deflection of the blade along the tangential direction;

v* - deflection of the blade along the I_{min} direction;

w - axial deflection of the disc, rim and blade;

w* - deflection of the blade along the I,,, direction;

Z - number of blades in the rotor;

a - constant defining thickness variation of element;

α^* - coefficient of thermal expansion;

β - constant defining thickness variation of element;

γ_v - additional rotation due to transverse shear in the tangential direction;

γ_v^* - additional rotation due to transverse shear in the I_{min} direction;

γ_w - additional rotation due to transverse shear in the axial direction;

γ_w^* - additional rotation due to transverse shear in the I_{max} direction;

δ - stagger angle;

ε_r - radial strain in the middle plane of the disc;

ε_ξ - tangential strain in the middle plane of the disc;

θ - radial rotation;

θ^* - rotation of blade in the I,,, direction;

λ - nondimensional frequency parameter;

λ_1 = $(\omega^2\rho/EI_1)^{1/4}$;

λ_2 = $(\omega^2\rho/EI_2)^{1/4}$;

λ_3 = $(J/GK_G)^{1/2}$;

μ - radius of gyration of a rectangular blade section in a principal direction;

ν - Poisson's ratio;

ξ - angle in radians measured from the reference antinode;

ρ - mass density of material;

σ_o - shrinkfit pressure at the hub;

σ_r - radial stress in the middle plane of the disc;

σ_x - stress along the length of the blade;

σ_ξ - tangential stress in the middle plane of the disc;

ϕ - angle of twist of the blade;

ψ - tangential rotation of the blade;

ψ^* - rotation of blade in the I_{min} direction;

ω - circular frequency in radians/second;

Ω - angular velocity of rotor in radians/second;

Ω^* - nondimensional rotation of a uniform blade.

$\{f_c\}$ - consistent load vector resulting from rotation;

$\{f_t\}$ - consistent load vector resulting from temperature gradient;

$\{q_b\}$ - blade element displacement vector;

$\{q_b^*\}$ - blade element displacement vector along the principal directions;

$\{q_B\}$ - blade subsystem displacement vector;

$\{\overline{q}_d\}$ - disc element displacement vector;

$\{\overline{q}_d^o\}$ - circular disc element displacement vector;

$\{q_D\}$ - disc subsystem displacement vector;

$\{q_R\}$ - rim subsystem displacement vector;

$\{q_S\}$ - rotor system displacement vector;

$\{Q_B\}$ - blade subsystem load vector;

$\{Q_D\}$ - disc subsystem load vector;

$\{Q_R\}$ - rim subsystem load vector;

$\{Q_S\}$ - rotor system load vector;

$[B_d^a]$ - 'B' matrix of rotating blade element;

$[B_d]$ - 'B' matrix of thin plate elements;

$[B_d^t]$ - 'B' matrix of Thick Disc Elements;

$[B_d^o]$ - 'B' matrix of thin plate circular elements;

[C] - diagonal matrix with diagonal terms cos $m\xi$

$[D_B]$ - dynamic stiffness matrix of the blade subsystem;

$[D_D]$ - dynamic stiffness matrix of the disc subsystem;

$[D_R]$ - dynamic stiffness matrix of the rim subsystem;

$[D_S]$ - dynamic stiffness matrix of the rotor system;

[E] - a matrix;

$[k_b^a]$ - 'k' matrix of a rotating blade element;

$[k_d]$ - 'k' matrix of thin plate bending annular element;

$[k_d^a]$ – 'k' matrix of the thin plate bending element resulting from rotation;

$[k_d^t]$ – 'k' matrix of the Thick Disc Elements;

$[k_d^o]$ – 'k' matrix of the thin plate bending circular element;

$[k_d^p]$ – 'k' matrix of the plane stress annular element;

$[k_{do}^a]$ – 'k' matrix of the thin plate bending circular element resulting from rotation;

$[k_{do}^p]$ – 'k' matrix of the plane stress circular element;

$[k_t^a]$ – 'k' matrix of a blade torsional element due to rotation;

$[k_v^a]$ – 'k' matrix of a blade bending element due to rotation, for bending in the plane of rotation;

$[k_w^a]$ – 'k' matrix of a blade bending element due to rotation, for bending out of plane of rotation;

$[K_b]$ – blade element stiffness matrix;

$[K_b^a]$ – additional stiffness matrix due to rotation of the blade element;

$[K_b^t]$ – blade element torsional stiffness matrix;

$[K_b^v]$ – blade element stiffness matrix for bending in the I_{min} direction;

$[K_b^w]$ – blade element stiffness matrix for bending in the I_{max} direction;

$[K_b^*]$ – blade element stiffness matrix corresponding to deflections along the principal directions;

$[K_B]$ – blade subsystem stiffness matrix;

$[K_d]$ – thin plate bending element stiffness matrix;

$[K_D]$ – disc subsystem stiffness matrix;

$[K_d^a]$ – additional stiffness matrix due to in-plane stresses of the thin plate bending annular element;

$[K_d^p]$ - plane stress annular element stiffness matrix;

$[K_d^t]$ - Thick Disc Element stiffness matrix;

$[K_d^o]$ - thin plate bending circular element stiffness matrix;

$[K_{do}^a]$ - additional stiffness matrix due to in-plane stresses of the thin plate bending circular element;

$[K_{do}^p]$ - plane stress circular element stiffness matrix;

$[K_R]$ - rim subsystem stiffness matrix;

$[K_S]$ - rotor system stiffness matrix;

$[m_d]$ - 'm' matrix of the thin plate bending annular element;

$[m_d^t]$ - 'm' matrix of the Thick Disc Elements;

$[m_d^o]$ - 'm' matrix of the thin plate bending circular element;

$[M_b]$ - blade element inertia matrix;

$[M_b^t]$ - blade torsional element inertia matrix;

$[M_b^v]$ - blade element inertia matrix for bending in the I_{min} direction;

$[M_b^w]$ - blade element inertia matrix for bending in the I_{max} direction;

$[M_b^*]$ - blade element inertia matrix corresponding to deflections along the principal directions;

$[M_B]$ - blade subsystem inertia matrix;

$[M_d]$ - thin plate bending element inertia matrix;

$[M_D]$ - disc subsystem inertia matrix;

$[M_d^t]$ - Thick Disc Element inertia matrix;

$[M_d^o]$ - thin plate bending circular element inertia matrix;

$[M_R]$ - rim subsystem inertia matrix;

$[M_S]$ - rotor system inertia matrix;

$[R]$ - rotation matrix;

LIST OF FIGURES

CHAPTER1

INTRODUCTION

1.1 PRELIMINARY

The stress and vibration analysis of almost every part of a gas turbine is of major concern to the designer. The bladed disc, which transmits torque from the blades to the shaft of the engine, constitutes an important part of the turbine. The problem of optimizing the disc configuration becomes more significant with the ever increasing demand for higher power and lighter weight of the gas turbine. The continuing emphasis on longer life together with reliable and safe operation in severe environments requires greater accuracy and speed in the mechanical analysis of the various parts of the turbine, especially the bladed disc.

The objective of present day structural design is to arrive at the most efficient structure, subjected to certain constraint conditions, for the specified load and temperature environment. In the design of the bladed disc certain geometrical restrictions may be imposed on the profile of the disc by its functional aspects as well as the geometry of other parts of the turbine. In addition, certain behavioural constraints, such as keeping the lowest natural frequency of the disc above some specified limit, may also be imposed. Hence, the design of the bladed rotor will normally require the accurate analysis of several trial profiles until the satisfactory one is reached. It is therefore essential that the designer has available simple, reliable and accurate methods of analysis.

In a turbine disc, in addition to the stresses resulting from bending, torsion and temperature gradient, very high stresses develop due to the centrifugal forces at high speeds. These stresses constitute the major portion of the total stresses and are not reduced by the thickening of the disc. Consequently the material unavoidably works at its limit, and hence the accuracy required on the predictions of these stresses is very high. Structural vibrations of the rotor, which might be torsional, or radial,but which are most predominantly axial, may also produce high stresses and lead to fatigue failures which are not understood on the basis of high steady stresses alone. Inorder to avoid strong resonant vibrations within the operating range of the machine, itis essential that the designer should be able to predict accurately the natural frequencies of the rotating bladed rotor, .

The complexity of the system makes it impossible to consider the entire system with all its generalities, for the analysis. In general the component parts of the rotor are analysed separately, and evenso making several simplifying assumptions to facilitate the analysis. Invariably both the disc and the loading are considered to be axisymmetric while analysing the stresses. When the vibration of the bladed-rotor is examined, the problem is simplified, in most cases, by assuming either rigid blades attached to a flexible vibrating disc, or, more commonly, flexible vibrating blades attached to a rigid disc.

The stress analysis of typical rotating discs for axial flow rotors is quite well understood, and reliable methods for calculation of steady stresses from rotation and thermal loading are available. Determination of steady stresses in the blade is also generally satisfactory, although there remain problems with highly twisted low aspect ratio configurations.

On the other hand, the determination of the vibratory behaviour of bladed rotors is less well defined. The effects of transverse shear and rotary inertia are generally neglected, leading to substantial discrepancies with experimental data in many rotors. More important, both experimental and theoretical studies indicate that coupling between-the blades and the disc cannot be neglected. It is now increasingly recognized that the significant vibration of many axial flow turbines involves combined participation by both blades and disc. This coupling between blades and disc can substantially modify the natural frequencies of the system (1), is thought to strongly influence the distribution of vibratory stresses in the blades (2-5), and can lead in some instances to aeroelastic instability (6).

A recent example of fatigue failure of turbine rotor blades resulting from coupling between blade and disc vibration is described by Morgan et al (7). Fatigue cracks were found either in the top serration of the fir tree roots or in the blade form starting at the trailing edge near the root. The resonance of the first flapwise mode (1F) with sixth orderexcitationwas thought to be the most probable cause. Modifications were made both to the blade fixings and to stiffen the disc which proved successful.

Figure 1.1, taken from the above mentioned reference, illustrates the influence of disc flexibility on the frequencies of the coupled blade-disc system, especially the first "flapwise" (1F) and the first "edgewise" (1E) modes, Here these two sets of frequencies, obtained experimentally, are plotted against engine speed and engine excitationorder, for two different rotors, one with a thick disc (solid line), and the other with a thin disc (broken line). These rotors had the same blades. As seen from the figure, when the disc is thick, disc flexibility has *very* little effect on the system frequencies. The reduction in frequencies with speed of rotation is probably due to reduction of elastic modulus with temperature and some disc effect. In the operating range of 6000 to 8000 rpm, we have only a few resonances for this rotor. The 1F modes of the blade areexcited only with engine orders 6 and 7, and the 1E modes with engine orders 10, 11, and 12. But when the disc is thin, within the operating range we have a large number of resonances. In this case we have the 1F modes with engine orders 2 to 7, and the 1E modes with engine orders 9 to 12. Thus the authors state that, "identification of the failure mode was difficult," because of the many resonances present. It should also be noted that, when the disc is thin, the 1E modeexcitedby engine order 8 lies just above the operating range. Since eight combustors were present in the engine, engine order 8 was particularly significant.

In summary, while the designer has available reliable methods for determining steady stresses in axial flow turbines, methods of determining the vibratory behaviour are much less adequate. Any realistic vibratory analysis of practical rotors should consider the effects of centrifugal and thermal stresses, the effects of transverse shear and rotary inertia and the effects of dynamic coupling between the vibrating blades and the vibrating disc. It is on these aspects of the vibratory behaviour of turbine discs, that the work described below is focussed.

1.2 REVIEW OF LITERATURE

Much work has been published describing typical stress and vibration problems encountered with axial flow turbine and compressor rotors. The publications of Shannon (8), Blackwell (9), Armstrong and Stevenson (10), Armstrong and Williams (11), Waldren et al (12), Goatham et al (13), and Petricone and Sisto (14), and NASA Technical Report TR R-54 (15) give excellent background and references to the problems encountered with aircraft power plant,

1.2.1 Stress Analysis of Turbine Discs

Much of the published work on the stress analysis of turbine discs deals with plane stress solutions, and three dimensional treatments are sparse. The reason for this is that when the thickness of the disc is small compared to the radius, the variation of the tangential and radial stresses over the thickness can be neglected and, taking mean values, satisfactory two dimensional approximations can be made.

Exact solutions with this plane stress approximation are available for several non-uniform profiles. Comprehensive reviews of early exact solutions of the problem are given in the classic works of Stodola (16) and Biezeno and Grammel (17). Several disc profiles suchas exponential, hyperbolic, and conical radial thickness variation have been considered.

More recently Manna (18) has also treated several unconventional profiles where the thickness can be represented as

$$h = h_o [1 - (r/b.)^{2/q}]^p \qquad (1.1)$$

where h_o is the thickness at the axis of rotation and b is the outer radius of the disc, q is a positive integer and p is greater than 2. Such an expression leads to a remarkably wide range of profiles, and is amenable to exact solution in terms of hypergeometric series.

Of the numerical methods which have been developed, Donath (19) first devised an approximate method where the actual disc is replaced by a model consisting of a series of rings of uniform thickness; and further improvement of this method was made by Grammcl (17).

. Manson (20,21) and others (22) have also replaced the disc by a series of uniform thickness rings, and solved the governing differential equations by finite difference methods.

This approach has formed the basis of the most widely used techniques for stress analysis of practical axial flow turbine discs. Further developments by Manson (23) extended the method to include elasto-plastic behaviour of the disc material, and, ofcourse, these methods readily allow for both centrifugal inertia forces and radial thermal gradients.

Several other techniques have also been employed for numerical solution of the plane stress problem. Mote (24) has used stress functions with undetermined constants which are adjusted to satisfy the thermal and inplane boundary conditions. Bogdanoff et al (25) have calculated the stresses in a disc by numerical integration of the plane stress equations of classical elasticity theory, Soo (26) has used a matrix technique for this problem.

In recent years, requirements for increased analysis accuracy and the use of relatively thick disc profiles has focussed attention on the three dimensional stress distribution present. The axial stress, neglected in thin disc analysis, can have a substantial effect on disc burst speed. Haigh and Murdoch (27) have considered axially symmetrical turbine wheels of appreciable thickness for which the thin disc theory gives only approximate results. Their analysts is based on three dimensional equlibrium equations. The solutions are obtained with a digital computer by relaxing the two governing equations using stress functions.

Radial flow rotors, while not of immediate concern in this work, are increasingly used and present most difficult problems in analysing the three dimensional stress distribution present. Such rotors are generally of asymmetric profile. Kobayashi and Trumpler (28) have developed a solution for the three dimensional stress analysis of such asymmetric discs. First the plane strain problem of a long rotating cylinder is considered. Then the surface tractions acting on a disc cut off from this cylinder are eliminated by a relaxation procedure employing Southwell stress functions. The solutions are obtained numerically using a digital computer. Only centrifugal forces are considered, and extension of this method for the calculation of thermal stress in the disc is outlined; Swansson (29) has used the two dimensional approach of Schilhansl (30) for the above problem and his results agree well with those of Kohayashi and Trumpler (28) for certain cases. Thurgood (31) has suggested further improvements of this method and has studied the effect of including axial deflection in the analysis; which he found, to have significant effect on the stress distribution in the disc.

For this asymmetric problem the finite element method is of considerable interest, and some work has been published on this problem, Stordahl and Christensen (32) have treated the problem as axisymmetric and analysed the impeller using a finite element method, Chan and Hendrywood (33) have developed and used ring shaped elements of triangular cross-section in the analysis of radial flow impellers.

Besides the various numerical methods used, photo-elastic analysis has also been used in the stress analysis of rotating discs (34-37).

1.2.2 Vibration Analysis of Turbine Discs

The vibration of turbine discs and of circular or annular plates is characterised by modes having integer numbers of nodal diameters and circumferential nodal circles. Much of the early work on plates and discs is summarised in the texts by Prescott (38) and Stodola (16).

The vibration of rotating discs has been quite well understood since the classic work of Campbell (39) and Stodola (16). This vibration is also found to comprise wave patterns involving integer numbers of nodal diameters and nodal circles, these patterns rotating forwards or backwards in the disc. The angular velocities of these waves in the discs are;

forward wave f_m/m revs./second

backward wave $-f_m/m$ revs./second

where f_m is the frequency in cycles/second of the mode with m nodal diameters. If now the disc rotates with angular velocity Ω revs./second, then relative to a stationary observer we have;

forward wave $\Omega + f_m/m$ revs./second

backward wave $\Omega - f_m/m$ revs./second

The work of Campbell and Stodola established that the dangerous condition of operation was such that the backward wave Is stationary in space,

$$\Omega - f_m/m = 0 \qquad \text{or} \qquad f_m = m\,\Omega$$

Thus a mode with m nodal diameters is stronglyexcitedby the m^{th} order of rotational speed.

The mechanism by which only the backward wave is significant is complicated, and perhaps not yet completely understood, Tobias and Arnold (40,41) are generally credited with the most rational explanation to date, and they concluded that unavoidable dynamic imperfections of the disc can account for the phenomenon, The major task of the designer is to avoid the dangerous resonant condition where the backward wave is stationary in space, This involves the accurate prediction of the natural frequencies of the disc; these frequencies, while mainly dependent on thin disc elastic and inertia properties can be substantially modified by in-plane stresses and transverse shear and rotary inertia.

Exact solutions forconstant thickness, thin circular and annular plates are given in the excellent monograph by McLeod and Bishop (42). Vogel and Skinner (43) have given numerical data for the calculation of the natural frequencies of uniform circular and annular plates with various boundary conditions. Leissa (44) has collected most of theavailablenumerical data on this problem.

Exact solutions for thin plates of variable thickness are quite limited. Conway (45) has investigated the transverse vibrations of some variable thickness plates when Poisson's ratio is given particular values. Harris (46) has developed an exact solution for the free vibration of circular plates with parabolic thickness variations.

The transverse vibration of a circular plate of uniform thickness rotating about its axis with constant angular velocity has been studied by Lamb and Southwell (47,48). They have separated the effect of rotation and have solved the vibration problem of the membrane disc. When both' plate flexural stiffness and membrane forces are operative, the following relationship is used to get the natural frequencies of the disc

$$\omega^2 = \omega_1^2 + \omega_2^2 \qquad (1.2)$$

where ω is the lower bound of the combined frequency of the rotating disc, ω_1 is the frequency of the membrane disc where the plate flexural stiffness is neglected, and ω_2 is the frequency of the stationary disc in which membrane stresses are absent.

Ghosh (49) has extended this approach to plates of variable thickness. Eversman (50) has outlined a solution to this problem when both membrane stresses and disc bending stiffness are considered together.

For the vibration analysis of discs having general thickness profile several numerical methods have been used. References to Prescott (38), Stodola (16), and Biezeno and Grammel (17) gives a good summary of early numerical methods based on the assumption of very simple deflection shapes for the disc, Perhaps the most successful and widely adopted numerical method is due to Ehrich (51), who derived a transfer matrix approach. The arbitrary disc is replaced by a number of annular strips of constant thickness, Every alternate strip *is* considered to be massless, but to have the local elastic properties of the actual disc. The intermediate strips are considered to have the local inertial properties but no elasticity. The effect of in-plane stresses resulting from rotation is also accounted for. The natural frequencies of the disc are found by a trial and iterative procedure using the residual determinants derived for various boundary conditions.

Among the other numerical methods which have been used, Mote (24) and Soo(26) have used Rayleigh-Ritz procedure. Bleich (52) has used the collocation method, for the vibration analysis of circular discs.

Several workers have recently applied the finite element method to the problem. Anderson et al (53) have suggested the use of triangular elements for the vibration analysis of uniform annular plates. Olson and Lindberg (54) have developed and used circular and annular sector elements for the analysis of uniform circular and annular plates, Sawko and Merriman (55) and Singh and Ramaswamy (56) have developed'sector elements with sixteen and twenty degrees of freedom respectively and have applied these elements in the static analysis of plates only. Chernuka et al (57) have used a high precision triangular element with one curved side for the static analysis of plates with curved boundaries. This element is described by eighteen degrees of freedom, and probably represents the most refined description for plates with curved boundaries which has been reported so far. It should be noted that none of these finite element approaches makes use of the axisymmetric properties of a complete circular disc, and all result in a mathematical model which is described by a large number of degrees of freedom.

When thick discs are considered, frequencies calculated using thin plate theory differ substantially from experimental values. Three dimensional elasticity solutions should be used in such situations (58,59). For the analysis of moderately thick discs and for the higher modes of relatively thin discs, plate theories which take into account effects of transverse shear and rotary inertia can be used. It is well known that both these effects serve to decrease the computed frequencies because of additional flexibility and increased inertia.

Reissner(60) extended the classical thin plate theory to include transverse shear deformation for the static analysis of plates. A consistent theory for the dynamic behaviour of plates, including rotary inertia and transverse shear was then developed by Uflyand (61), followed by Mindlin (62), who derived the basic sixth order system of partial differential equatfons of motion along with potential and kinetic energy functions for this problem. He has also given a consistent set of equations relating moments and transverse shears to transverse deflection and bending rotations, Mindlin and Deresiewicz (63) have further developed and applied this theory, Moderately thick circular plates have been analysed by several investigators. Deresiewicz and Mindlin (64, 65) have considered the symmetrical vibration of circular plates. Callahan (66) used the Mindlin theory to derive characteristic determinants corresponding to eight separate sets of continuous boundary conditions for circular and eliptical plates. Bakshi and Callahan (67) have derived similar determinants for the vibration analysis of circular rings (annular plates). Onoe and Yano (68) have followed a different approach to this problem which they claim is applicable to the higher order vibrations of circular plates.

Very few numerical methods have been suggested for this problem, Pestel and Leckie (69) have derived transfer matrices for annular strips, which are used to model circular and annular discs, including transverse shear and rotary inertia. This is essentially an improvement of Ehrich's lumped mass model. Clough and Felippa (70) have incorporated a simple shear distortion mechanism into their refined quadrilateral finite element which they have used in the static analysis of circular plates including transverse shear.

No published work is available, to the knowledge of the author, on the vibration analysis of variable thickness discs where effects of transverse shear and rotary inertia are also included in the analysis; also no one has considered the effects of in-plane stresses together with transverse shear and rotary inertia even when the disc is uniform.

In contrast to the many theoretical results published on the vibration of turbine discs and circular plates, it is surprising how little experimental data has been published in the literature, Campbell (39) in his classic work obtained experimentally frequencies and mode shapes of steam turbine rotors and has studied the effect of rotation on the frequencies. Peterson (71) has tested annular and circular discs of both uniform and stepped sections in connection with the study of gear vibration. Recently French (72) has described experimentally observed vibration of gas turbine compressor discs. This paper does not appear to have been published in any Journal, however. Mote and Nieh (73) have investigated theoratically and experimentally the relationship between the state of disc membrane stress, critical rotation speed and the frequency spectrum in radially symmetric, uniform thickness, disc problems. Onoe and Yano (68) have obtained experimentally several frequencies of relatively small but thick circular discs, used in mechanical filters, and compared these with their analysis method.

1.2.3 Vibration Analysis of Axial Flow Turbine Blades

Much work has been published on the vibration analysis of axial flow turbine blades and a fairly complete review of the problems and various analytical methods used is given by Dokainish and Rawtani (74). Practical turbine blades have an aerofoil cross-section and possess, in addition to camber and longitudinal taper, a pretwist to allow for the variation in tangential velocity along the span of the blade. Since all these factors complicate the analysis, in practice, many simplifying assumptions are usually made in the analysis. In most of the analytical methods suggested for the analysis, the blades are idealized to behave as beams having radial variation in section properties and pretwist. Attachment to the disc in the case of "firtree" or "dovetail" slots is generally considered rigid (i.e, a cantilever beam) or by means of springs which represent, in some manner, the finite flexibility of the fixing. In the case of pin attachments, the rotational constraint about the axis of the pin is relaxed (13).

In many cases coupling between bending and twisting of the blade resulting from non-coincidence of the centroid and shear centre of the aerofoil section is ignored. There are difficulties in determining the shear centre of an aerofoil section. Bending-torsion coupling can also result from the fact that the blade aerofoil at the root is not in a plane parallel to the axis of rotation; this effect cannot be accounted for with a beam model,

. Considerable difficulty arises in determining the torsional stiffness, This comprises three contributions.

(a} The St. Venant torsional stiffness,

(b) Additional stiffness due to pretwist,

(c) Additional stiffness due to restrained warping at the root or at shrouds.

While determination of contribution (b) is complicated, this effect has been included in most refined blade models. The contribution (c) is particularly difficult to obtain even when complete warping restraint is assumed, and this effect has generally been neglected, or at best accounted for by some "effective shortening" of the blade.

The effects of transverse shear and rotary inertia on blade frequencies have generally been neglected, This is somewhat justified, because the limitations previously mentioned above generally result in unacceptable errors long before the effects of shear and rotary inertia become significant.

Beam type models have been successfully used for high aspect ratio, thin, compressor blades, and somewhat less successfully for high aspect ratio turbine blades. Calculated frequencies of engineering accuracy are usually limited to the first three or so modes of vibration.

The above limitations of a beam model become particularly evident with low aspect ratio blading, which is increasingly used, and the solution to such problems probably will require modelling the blade as a curved shell of varying thickness and curvature. Notwithstanding this, beam type models of turbine and compressor blades are still widely used.

In its simplest form the axial flow turbine blade is considered to be a tapered beam of rectangular cross-section without pretwist. Pinney (75) has given an exact solution, for the frequencies and mode shapes, for beams with certain types of taper. Perhaps the most widely adopted numerical method, for nonuniform beams, is the lumped mass method of Myklestad (76). Leckfe and Lindberg (77) were the first to develop the beam flexure finite element and to demonstrate its accuracy compared to other conventional lumped parameter methods. Later Lindberg (78) and Archer (79) developed finite elements for the analysis of tapered beams. Carnegie and Thomas (80) have given a method of analysis of cantilever beams of constant thickness and linear taper in breadth.

Even when a rectangular section is assumed for the blade, pretwisting couples bending in the two principal directions, Rosard (81) has investigated such coupled vibration of blades, In this analysis the blade is divided into a number of segments; the mass and elasticity are concentrated at stations, and a transfer matrix method is developed.

The bending vibrations of a pretwisted beam lead to two fourth order differential equations. A method of solving these two coupled equations is given by Troesch et al (82). Carnegie (83) has used Rayleigh's energy method to calculate the first frequency in bending of a pretwisted cantilever beam. The static deflection curve is used in the analysis. Slyper (84) has used the Stodola method for this problem, Dokumaci et al (85) have used the finite element technique with matrix displacement type analysis, for the determination of the bending frequencies of a pretwisted cantilever beam. They have derived the stiffness and mass matrices for a pretwlsted beam element of rectangular cross-section, Natural frequencies and mode shapes are obtained from the resulting eigen-value problem,

When the aerofoil section of the blade is considered the torsional vibration is also coupled with the bending vibration of the blade, Mandelson and Gendler (86,87) have suggested a method of analysis for the problem using the concept of station functions, Houbolt and Brooks (88) have derived the differential equations of the coupled bending-torsion vibration of twisted nonuniform blades, Dunham (89) has derived the equations of motion in a twisted coordinate system following the blade length and has used them for the determination of the first natural frequency. Carnegie (80) has used the Rayleigh method to find an expression for the calculation of the fundamental frequency of the blade.

Perhaps the most careful and complete treatment of the problem is that by Montoya (90) who has derived the governing differential equations for the vibration analysis of twisted blades of aerofoil section, including coupling between bending and torsion. Effect of rotation on both bending and torsion are also considered. Runge-Kutta numerical procedure is followed to solve the problem and the differential equations are converted into ten first order equations. Assuming unit values to each of the unknowns at the fixed end, corresponding values are found at the free end and are combined linearly, resulting in a set of equations. The boundary conditions at the free end require the determinant of these equations to vanish when the correct frequency value is assumed. Results obtained when twist and torsional coupling are neglected are compared with those obtained when these effects are considered; and it is shown that these effects should not be ignored,

When a rotating blade is considered, the additional stiffness due to the centrifugal forces should be considered. The centrifugal forces induce several additional coupling terms 'In the already complicated equations of motion. The effect of rotation on the bending frequencies has been considered by Sutherland (91) by using a Myklestad type tabular method of analysis. Plunkett (92) has developed matrix equations governing transverse vibration of a rotating cantilever beam. Bending vibrations in a plane inclined at *any* general angle to the plane of rotation has been investigated by Lo et al (93). They have also observed that the equations of motion contain a nonlinear term resulting from the Corfolis acceleration (94). Equations of motion for a rotating cantilever blade using Hamilton's principle have been derived by Carnegie (95).

Jarrett and Warner (96) and Targoff (97) have solved the problem of a rotating twisted blade idealizing the blade by a lumped mass system. Isakson and Eisley (98,99) have also used Myklestad type analysis for calculating the bending frequencies of pretwisted rotating beams. The effect of rotation on the torsional frequencies has been investigated by Bogdanoff and Horner (100,101) and by Brady and Targoff (102). Karupka and Baumanis (103) have derived the field equations for coupled bending-torsion vibrations of a rotating blade using Carnegie's formulation of the Lagrange equations of motion. Cowper (104) has developed a computer program to calculate the shear centre of any arbitrary ***cross-section.***

When the blades are thick, the classical Bernoulli-Euler beam theory for bending vibrations is known to give higher values of computed frequencies. In such cases transverse shear and rotary inertia should be included in the analysis. Rayleigh improved the classical theory considering rotary inertia of the cross-section of the beam. Timoshenko extended the theory to include the effects of transverse shear deformation. Prescott (38) and Volterra(105) have developed various Timoshenko type beam models. Huang (106) has given solutions of Timoshenko equations for a cantilever beam of rectangular cross-section. Carnegie and 'Thomas (107) have used the finite difference method for the bending vibration analysis of pretwisted cantilevers including the effects of transverse shear and rotary inertia.

Among the other published work connected with blade vibration; Gere (108) has derived differential equations, for the torsional vibrations of beams of thin walled open cross-section for which the shear centre and centroid coincide, including the effects of warping of the cross-section. Grinsted (109) has studied the complex nodal patterns of turbine blades; impeller vanes and discs, Ellington (110) has derived frequency equations for the modes of vibration of turbine blades laced at their tips. Pearson (111) and Sabatiuk and Sfsto (112) have discussed the aero-dynamics of turbine blade vibration.

As mentioned earlier beam type models are not applicable to low aspect ratio blades. Such blades are generally treated either as plates (113) or as shells (114).

1.2.4 Coupled Blade-Disc Vibration

The existence of coupling between the blades and disc and its influence on the natural frequencies of bladed rotors has been demonstrated by both experimental and theoretical studies. With a bladed disc it is found that similar concepts to that of the unbladed disc apply; the rotor oscillates in a coupled blade-disc mode characterised by diametral and circular nodes. The blades being constrained in the disc at the rim, will vibrate in 'bending motion *at* diametral anti-nodes, in torsional motion at nodes, and in combined bending-torsion elsewhere. The circular nodes may lie in the disc, but will more often be located in the blades. This whole pattern may rotate as in the disc alone case, and again the dangerous resonant vibration condition corresponds to an m nodal diameter mode exited by the m^{th} order of rotational speed.

The general features of the resonant conditions in a typical rotor may be illustrated in a Campbell or interference diagram, Figure 1.2. In this diagram are shown the resonances predicted assuming rigid blades on a flexible disc, and flexible blades on a rigid disc. For the former assumption the resonances occur when the m^{th} order of rotational speed is equal to the frequency of the disc mode with m nodal diameters. For the latter assumption the resonances occur whenever the various rotational excitation frequencies are equal to a blade natural frequency. The resonances of the combined blade disc system are modified as shown. These resonances again occur when an m nodal diameter mode is excited by the m^{th} engine order, and it is seen that the resulting motion degenerates to essentially disc vibration with rigid blades at low engine order excitationand high speed, and to blade vibration with a rigid disc at high engineexcitationand low speed.

The early work reported on the problem is based on very simplified models. Ellington and McCallion (115) have investigated the effect of elastic coupling, through the rim of the disc, on the frequencies of bending vibration using a simplified model. In this model the effect of twist, taper and obliquity is neglected and the blades are replaced by uniform blades fixed to the rim at their roots and vibrating in a plane parallel to the plane of the disc. For the analysis three adjacent blades are assumed to be parallel to each other and the portion of the rim joining them is taken as a straight continuous beam. A relationship between three slopes of the beam at the root of three adjacent blades are established and is used in the calculation of the natural frequencies.

Johnson and Bishop (116) have also examined an idealized bladed rotor consisting of identical mass-spring elements to represent the blades, connected to a rigid free mass which represents the disc. They examine the principal modes of such a model'and outline methods for determining the receptances (dynamic flexibility) of the system.

Wagner (2) extended this simplified model, representing each blade by a single degree of freedom system which has the same natural frequency and damping factor as that of a particular mode of the blade. These subsystems are attached to a common ring representing the disc.

Capriz (117) has developed equations for the analysis of the interaction between the disc and blades. Using available numerical methods, "a number of cases of practical interest have been studied," but, "comparision with experimental results has put in evidence discrepancies when modes with large numbers of nodal diameters were considered." No numerical results are presented in the paper and the paper does not appear to have been published in a Journal.

The first extensive investigations of the problem appear to be due to Armstrong (118). Armstrong et al (1,119) studied the problem by experimental investigation. Armstrong carried out experimental tests on model rotors with uniform discs and uniform untwisted blades attached to the disc at varying stagger angles. Based on approximate receptance relations, he developed a theoretical method for the analysis of the coupled system and was able to predict satisfactorily the frequencies of' the lower coupled modes of his models. The analysis was restricted to simple model configurations for which receptance relations could be easily obtained. The application to practical rotors was outlined.

At about the same time as Armstrong's work, Jager (120) developed a numerical method to predict the coupled system frequencies and mode shapes, using a transfer matrix technique based on a lumped mass model of the disc suggested by Ehrich (51) and a conventional lumped mass model of the blades treated as twisted beams. This method was therefore directly applicable to practical rotors of varying geometry, and included the stiffening effects resulting from rotation. This method has been adopted by several aircraft engine companies.

Dye (3) and Ewins (4,5) have studied the effects of detuning upon the vibration characteristics of bladed discs, in particular the variation in blade stresses which can result when the blades do not have identical frequencies. They concluded that this effect can result in a variation of vibratory stress from blade to blade by a factor as high as 1.25 approximately.

Carta (6) describes an aeroelastic instability condition which is governed by strong coupling between bending and torsion of the blades resulting from disc or shroud dynamic coupling.' This flutter condition is highly dependent on the coupled blade-disc: shroud mode shape, which must be accurately determined. He assumes such mode shapes are available from a Jager type calculation (120), and successfully predicts the instability for a number of bladed rotors.

Finally, a paper by Stargardter (121), which also appears not to have been published in a Journal, describes qualitative results obtained by vibrating rubber models at low rotational speeds, He describes the physical phenomena well, and presents some interesting photographs showing clearly the motions involved with bladed rotors.

1.3 OBJECT OF THE PRESENT INVESTIGATION

Since exact solutions of rotating discs are restricted to certain simple geometry and boundary conditions, numerical procedures must be adopted for the analysis of practical turbine discs and bladed rotors of general geometry. Although transfer matrix techniques have been applied to these problems by Ehrich (51) and Jager (120), these methods have two disadvantages. First, the use of mass lumping in the mathematical model of the system requires a large number of stations to be considered in both disc and blades if good accuracy is required, particularly for higher modes of vibration. Secondly, the natural frequencies are obtained by iterating with the frequency of vibration as a variable, and seeking the zeros of a frequency determinant. These results in a requirement for substantial computing time and storage, and not infrequently, the numerical conditioning difficulties with higher modes which arise In transfer matrix methods.

A more profitable approachwould be to use the finite element technique which has now become firmly established as a powerful method of analysis, This method allows refinements over the other numerical procedures and when applied to the vibration analysis results in an algebraic eigen value problem,

Although the circular and annular sector finite elements developed by Olson and Lindberg (54) and even triangular elements may be used in the vibration analysis of circular and annular discs, the use of these elements results in an eigenvalue problem of considerable magnitude, Inclusion of thickness variation and the effects of rotation etc., in these elements would be quite involved. Hence, itis desirable to develope simpler elements, particularly suitable for the vibration analysis of turbine discs, and which take advantage of the nature and geometry of the problem.

The main objective of this investigation, therefore, is to develope finite elements of annular geometry, in which radial thickness variation, the effects of in-plane stresses, and the effects of rotary inertia and transverse shear can be easily introduced, and to examine the behaviour of these elements in the analysis of simple and complex discs and bladed rotors.

Attention is to be focussed on developing methods of vibration analysis of rotating discs of general profile and bladed discs representative of practical turbine stages. Although reliable and efficient methods are available for the stress analysis of turbine discs, a plane stress finite element method compatible with the vibration analysis is developed. In the analysis of the bladed rotors, only asimplifiedmodel *is* to be assumed for the blades and the investigation emphasises the study of the coupling between the disc and blade motions. A thorough treatment of the blades in the light of the many complicating factors involved would require substantial amount of additional work and hence is not attempted here.

CHAPTER 2

VIBRATION ANALYSIS OF AXIAL FLOW TURBINE DISCS

2.1 INTRODUCTION

In this chapter a finite element model which will adequately represent a turbine disc having general thickness profile is developed for the vibration analysis of axial flow turbine discs. The disc is idealized to be both axisymmetric and symmetric about the middle plane. But, any general radial thickness profile is satisfactorily described by the model. Stiffening effects of in-plane stresses resulting from centrifugal and thermal loading and other boundary loadings, such as shrinkfit pressure at the hub, and blade loading at the rim are taken into account. This method of analysis which is based on thin plate theory, is then further extended to include the effects of transverse shear and rotary inertia, so that the method can be used in the analysis of moderately thick discs.

Detailed analysis of stress distribution across the thickness of the disc is not attempted; rather, a plane stress finite element method for computing the average stresses at the middle plane of the disc is developed. While this plane stress finite element model has little advantage in accuracy or efficiency over the extensively used finite difference schemes (20, 21), it has the one advantage here of being completely compatible with the analysis developed for the flexural vibration of the disc, since many of the matrix relations and operations are identical.

In section 2.2 thin plate bending finite elements having annular and circular geometry and radially varying thickness and which are particularly suitable for the vibration of thin discs are developed (122). Compared with other available finite elements for this type of problem, these new elements are described by a remarkably small number of degrees of freedom. The annular element has four degrees of freedom, while the circular element has only two or three. This is achieved by including the number of diametral nodes in the chosen displacement function for the element, and in effect this results in separate solutions for each diametral mode configuration.

In section 2.3 matrix expressions are derived which allow for the additional stiffness resulting from in-plane stresses in a thin disc. These assume that the in-plane stress distribution is known, i.e., precalculated by some means or other. In this work a plane stress annular finite element is developed and used to calculate the stress distribution; this appears to be new and could be readily extended to handle buckling problems of discs.

Finally, in section 2.4, two new methods of incorporating the effects of transverse shear and rotary inertia are developed, which will allow accurate analysis of moderately thick discs,

The convergence and accuracy of the finite element models are in each case critically examined by comparision with exact solutions, where available, and with experimental data, for both static and vibration problems.

2.2 ANNULAR AND CIRCULAR THIN PLATE BENDING ELEMENTS

2.2.1 Element Geometry and Deflection Functions

Figures 2.1 and 2.2 show the annular and circular thin plate bending finite elements with their associated degrees of freedom and diametral nodes. The annular element is bounded by two concentric circles and the circular element by a single circle, Any required number of diametral nodes is incorporated in the elements as follows.

Once the lateral deflection $\bar{w}$ and the radial slope $\bar{\theta}$ at any antinode, where ξ is taken to be zero, are specified, the deflection and slope at any other point at an angle ξ from some reference antinode can be expressed as, $\bar{w}$ cos $m\xi$ and

$\bar{\theta}$ cos $m\xi$, where m is the number of diametral nodes. Hence a suitable deflection function for w , the lateral deflection of the disc along the radial direction and an antinode, only remains to be chosen.

Irrespective of the number of diametral nodes, the annular element has four degrees of freedom. These are $\bar{w}_1$, $\bar{w}_2$, $\bar{\theta}_1$, and $\bar{\theta}_2$ as shown in Figure 2.1, where θ is defined as $\theta = -\frac{\partial w}{\partial r}$, For the circular element, as shown in Figure 2.2, the number of degrees of freedom vary with the number of diametral nodes, It should be observed that when m is zero $\bar{\theta}_1$ is zero, when m is odd $\bar{w}_1$ is zero and when m is even both $\bar{w}_1$ and $\bar{\theta}_1$ are zero. This indicatesthat while a single deflection function can be assumed for the annular element, three different deflection functions are to be assumed for the circular element, one for m = 0, another for m = 1,3,5,... and a third one for m = 2,4,6,... However, no suitable function could be found for the second case excepting when m = 1.

The following deflection functions are found suitable for the different cases mentioned.

$$w(r,\xi) = (a_1 + a_2 r + a_3 r^2 + a_4 r^3) \cos m\xi \; * \tag{2.1}$$

for the annular element;

$$w(r,\xi) = (a_1 + a_2 r^2 + a_3 r^3) \tag{2.2}$$

* The choice of cos $m\xi$ in the deflection function can be justified noting that the exact solution for an axisymmetric plate is of the form W = f(r) cos $m\xi$

for the circular element with $m = 0$;

$$w(r,\xi) = (a_1 r + a_2 r^2 + a_3 r^3) \cos \xi \tag{2.3}$$

for the circular element with $m = 1$;

$$w(r,\xi) = (a_1 r^2 + a_2 r^3) \cos m\xi \tag{2.4}$$

for the circular element with $m = 2,4,6,\ldots$ where $w(r,\xi)$ is the lateral deflection of a point on the middle surface of the plate at radius r and angle ξ measured from the reference antinode. The relationship of the deflection functions to those normally used for a beam element is evident. The deflection functions for the circular element are chosen considering the following conditions. For the circular element with $m = 0$ it is necessary to include the rigid body translation, and with $m = 1$ it is necessary to include the rigid body rotation about a diameter. The difficulty with $m = 3,5,7,\ldots$ arises from the need to retain the linear rotation term, but at the same time ensure that the circumferential curvature remains finite when $r = 0$. This is not possible with the simple form of deflection function chosen.

2.2.2 Element Stiffness and Inertia Matrices

The stiffness and inertia matrices of the annular element and the three different circular elements are obtained by substituting the assumed deflection functions into the strain energy and kinetic energy expressions of the elements and following well known procedures (123). For the thin plate annular element the strain energy is given by (124),

$$U = \frac{1}{2} \int_0^{2\pi} \int_{r_1}^{r_2} \{\chi\}^T [V] \{\chi\} \, r \, dr \, d\xi \tag{2.5}$$

where

$$[V] = D \begin{bmatrix} 1 & \nu & 0 \\ \nu & 1 & 0 \\ 0 & 0 & \frac{1-\nu}{2} \end{bmatrix} \tag{2.6}$$

and

$$\{\chi\} = \begin{bmatrix} -\dfrac{\partial^2 w}{\partial r^2} \\ -\dfrac{1}{r}\dfrac{\partial w}{\partial r} \quad \dfrac{1}{r^2}\dfrac{\partial^2 w}{\partial \xi^2} \\ \dfrac{2}{r}\dfrac{\partial^2 w}{\partial r \partial \xi} - \dfrac{2}{r^2}\dfrac{\partial w}{\partial \xi} \end{bmatrix} \tag{2.7}$$

Substituting (2.1) for w in (2.7)

$$\{\chi\} = [E] [B_d] \{\bar{q}_d\} \cos m\xi \tag{2.8}$$

where

$$\{\bar{q}_d\}^T = [\, \bar{w}_1 \;\; \bar{\theta}_1 \;\; \bar{w}_2 \;\; \bar{\theta}_2 \,] \quad ; \quad \theta = -\frac{\partial w}{\partial r} \tag{2.9}$$

and

$$[E] = \begin{bmatrix} 0 & 0 & -2 & -6r \\ \frac{m^2}{r^2} & \frac{1}{r}(m^2 - 1) & (m^2 - 2) & r\,(m^3 - 3) \\ -\frac{2m}{r^2}\tan m\xi & 0 & 2m \tan m\xi & 4mr \tan m\xi \end{bmatrix} \tag{2.10}$$

The matrix $[B_d]$ is given in Table 2.1. Substituting (2.8) in (2.5)

$$U = \frac{1}{2}\int_0^{2\pi}\int_{r_1}^{r_2} D\,\{\bar{q}_d\}^T [B_d]^T [E]^T [V] [E] [B_d] \{\bar{q}_d\}\; r \cos^2 m\xi \, dr \, d\xi \tag{2.11}$$

Therefore the stiffness matrix is given by

$$[K_d] = \int_0^{2\pi}\int_{r_1}^{r_2} D\,[B_d]^T [E]^T [V] [E] [B_d]\, r \cos^2 m\xi \, dr \, d\xi \tag{2.12}$$

or,

$$[K_d] = [B_d]^T [k_d] [B_d] \tag{2.13}$$

where

$$[k_d] = \int_0^{2\pi}\int_{r_1}^{r_2} D\,[E]^T [V] [E]\, r \cos^2 m\xi \, dr \, d\xi \tag{2.14}$$

The matrix $[k_d]$ is given in Table 2.2.

The kinetic energy of the annular element is given by

$$T = \frac{1}{2} \int_0^{2\pi} \int_{r_1}^{r_2} \rho\, h(r) \left(\frac{\partial w}{\partial t} \right)^2 r\, dr\, d\xi \tag{2.15}$$

Substituting (2.1) in (2.15)

$$T = \frac{1}{2} \int_0^{2\pi} \int_{r_1}^{r_2} \rho\, h(r)\, \{\dot{q}_d\}^T [B_d]^T \{s\}^T \{s\} [B_d] \{\dot{q}_d\}\, r \cos^2 m\xi\, dr\, d\xi \tag{2.16}$$

Where

$\{s\} = [\ 1\ \ r\ \ r^2\ \ r^3];$ and the dot denotes time derivative.

Therefore the inertia matrix is given by

$$[M_d] = \int_0^{2\pi} \int_{r_1}^{r_2} \rho\, h(r)\, [B_d]^T \{s\}^T \{s\} [B_d]\, r \cos^2 m\xi\, dr\, d\xi \tag{2.17}$$

or,

$$[M_d] = [B_d]^T [m_d] [B_d] \tag{2.18}$$

where

$$[m_d] = \int_0^{2\pi} \int_{r_1}^{r_2} \rho\, h(r)' \{s\}^T \{s\}\, r \cos^2 m\xi\, dr\, d\xi \tag{2.19}$$

The matrix $[m_d]$ is given in Table 2.3

In Tables 2.2 and 2.3 the integrals P_i and Q_i are.

given by

$$P_i = C\pi \frac{E}{12(1-\nu^2)} \int_{r_1}^{r_2} h^3(r)\, r^i \, dr \tag{2.20}$$

and

$$Q_i = C\pi\rho \int_{r_1}^{r_2} h(r)\, r^i \, dr \tag{2.21}$$

where

$$C = 2 \text{ when } m = 0 \text{ and } C = 1 \text{ when } m \geq 1 \tag{2.22}$$

The values of P_i and Q_i depend on the function assumed for $h(r)$. Any desired function can be assumed. If linear thickness variation within the element is assumed, then

$$h(r) = a + \beta r \tag{2.23}$$

where

$$a = \frac{h_1 r_2 - h_2 r_1}{r_2 - r_1} \quad ; \quad \text{and} \quad \beta = \frac{h_2 - h_1}{r_2 - r_1} \tag{2.24}$$

If parabolic thickness variation within the element is assumed, then

$$h(r) = a + \beta r^2 \tag{2.25}$$

where

$$a = \frac{h_1 r_2^2 - h_2 r_1^2}{r_2^2 - r_1^2} \quad ; \quad \text{and} \quad \beta = \frac{h_2 - h_1}{r_2^2 - r_1^2} \tag{2.26}$$

The two cases above require the thickness to be known only at the inner and outer boundaries of the element. Any other desired expressions for $h(r)$ can be assumed and the corresponding values of P_i and Q_i evaluated.

The stiffness and inertia matrices of the thin plate circular elements are derived in a similar manner and these are given by

$$[K_d^o] = [B_d^o]^T [k_d^o] [B_d^o]$$

and (2.27)

$$[M_d^o] = [B_d^o]^T [m_d^o] [B_d^o]$$

The matrices $[B_d^o]$, $[k_d^o]$, and $[m_d^o]$ and the corresponding deflection vector' $\{q_d^o\}$ are given in Tables 2.4 to 2.6, for the three different circular elements. Here again the integrals P_i and Q_i are evaluated assuming desired functions for h(r).

These element.stiffness matrices [Kd] and inertia matrices $[M_d]$ can be assembled by conventional methods to get the disc system stiffness matrix $[K_D]$ and inertia matrix $[M_D]$, for a model of the disc comprising several elements. The dynamic stiffness relation for the disc becomes;

$$\{Q_D\} = \{ [K_D] - \omega^2 [M_D] \} \{q_D\} \qquad (2.28)$$

where $\{q_D\}$ is the disc deflection vector and $\{Q_D\}$ is the vector of corresponding generalised forces. For free vibration of the disc all the terms of $\{Q_D\}$ are zero, and Equation 2.28 becomes an algebraic eigen value problem which is solved to yield the natural frequencies and mode shapes of the disc. Such a calculation would be repeated for each diametral mode configuration.

In static problems the inertia matrix $[M_D]$ disappears and $\{Q_D\}$ is the vector of external generalised forces at the nodes of the finite element model of the disc.

Displacement boundary conditions only are applied by deleting the appropriate rows and columns of the stiffness and inertia matrices of the disc.

2.2.3 Application to Thin Plate Vibration Problems

The convergence properties and accuracy of the finite elements developed above for the vibration of thin plates are examined by comparing the nondimensional frequency parameter $\lambda = \omega\, b^2\sqrt{\frac{\rho h_o}{D_o}}$ obtained, with available exact solutions. h_o and D_o are the thickness and the flexural rigidity of the plates considered. When a variable thickness plate is considered, these are the values at the centre of the plate.

(A) For a first example, complete circular plates having uniform thickness are considered. When these plates are modelled with several annular elements and one circular element at the centre as shown in Figure 2.3 , the results are restricted to modes with m = 0,1,2,4,6, etc., only because of the difficulty in choosing a suitable deflection function for the circular element with odd values of m other than unity. The solutions obtained for plates with simply supported, clamped and free outer boundaries are given in Tables 2.7 to 2.9, in which m and n are the diametral and circular node numbers respectively. These plates can also be modelled by approximating the complete plate by an annular plate having a very small central hole as shown in Figure 2.3. Only annular elements are used in this case and hence results are obtained for any value of m. The results obtained with a radius ratio $a/b = 0.001$ for the three cases considered above are given in Tables 2.10 to 2.12 along with available exact solutions of complete circular plates. Comparing results from Tables 2.7 to 2.12 it is seen that the presence of the central hole has only very small effect and in practical problems the use of annular elements alone would be satisfactory.

Convergence of the solution with number of elements is seen to be extremely rapid in all cases and monotonic from above as would be expected. Frequencies of engineering accuracy are obtained with very few elements; thus the use of number of elements N = (Number of modes desired -t 1) will in all cases give frequencies accurate to approximately 2% or better.

In Figure 2.4 the percentage absolute error in the first six frequencies of the simply supported plate, calculated using annular elements alone, are plotted against number of elements used in the model.

(B) As a second example, annular plates of uniform thickness are considered. These are modelled with the annular elements only. Results obtained for plates with radius ratios $a/b = 0.1$ and 0.5 are given in Tables 2.13 to 2.18 together with the available exact solutions. The remarks made in (A) above regarding convergence and accuracy of the solution also clearly hold for these examples.

(C) The third example chosen is that of a complete free circular plate having parabolic variation in thickness, $h(r) = h_o \{ 1 - (r/b)^{\overset{3}{2}} \}$, as shown in Figure 2.5, and for which exact solutions have been obtained by Harris (46), when the plate is free along the outer boundary. The plate is approximated by considering an annular plate with $a/b = 0.001$ and using only the annular elements with parabolic thickness variation. The results are presented in Table 2.19. The effect of using elements with linear thickness variation instead of parabolic thickness variation within the element is also studied and the results are given in Table 2.20.

Comparing results of Table 2.19 and 2.20 it will be noted that convergence is rapid with either model, but that while the model using parabolic thickness elements converges monotonically and is an upper bound solution as expected, the convergence of the model using linear elements, where an approximation of the geometry is made, is from below, at least for the first mode, and is not monotonic for the higher modes. Convergence and accuracy of the finite element solution with true thickness modelling is quite remarkable.

(D) In a final example, the efficiency of the procedure using annular elements can be judged by comparision with results obtained using sector elements. Such a comparision is made for a uniform freeplate in Table (2.21). Olson and Lindberg (54) model the plate with a grid of three sector elements radially, and 12 circumferentially. Using symmetry their resulting model has 55 degrees of freedom. The results obtained with the 3 x 12 grid of sector elements are compared with those obtained using two and four annular element models. It is seen that the use of only two annular elements, resulting in only six degrees of freedom, gives more accurate results than the use of sector elements. Moreover the identification of the particular modes is easier with the annular element. The sector element model yields two values of frequency for the (2,0) and (5,0) modes; these solutions appear to be associated with nodal diameters in the vibrating plate passing through nodes in the grid mesh, and passing between the nodes in the grid mesh respectivly.

It should be pointed out that the use of annular elements will involve solution of the eigen value problem once for each nodal diameter configuration. Notwithstanding this there remains considerable saving in storage and computer time requirements. In addition the use of the sector elements is ofcourse not restricted to complete annular and circular plates, unlike the annular and circular elements.

Apart from these examples, where vibration problems are considered, the elements developed here may be applied to static problems also, by superposing the solutions obtained by expressing the applied load in it's Fourier components. The results of several such studies are briefly described in Appendix A.

2.3 THE EFFECT OF IN-PLANE STRESSES ON THE VIBRATION OF THIN DISCS

The stiffening effect of centrifugal and thermal stresses is significant in practical rotors, and must be taken into account in any realistic analysis. If centrifugal stresses only are considered, these are proportional to the square of the rotational speed, and additional stif'fness terms may be derived which will also be proportional to the square of the rotational speed. Thermal stresses, however, have no relationship with the rotational speed. This suggests that a method of including both effects should be formulated assuming that stresses in the rotor are already known.

In section 2.3.1 a stiffness matrix is derived which is dependent on the in-plane stresses present in the disc. This matrix simply adds to the basic elastic matrix equation to give the total stiffness matrix of the element. The radial and tangential stress values used in this additional stiffness matrix may be obtained by any method, but in section 2.3.2 a plane stress annular finite element is derived which is used to calculate these stresses in this work. This has the advantage here being compatible with the annular bending element, and many of the matrix relations and operations are seen to be identical.

The accuracy and convergenceoffirst the method of stress analysis and second the resulting stiffening effect on the disc vibration, is examined with several numerical examples in section 2.3.3.

2.3.1 Additional Stiffness Matrix for the Annular Element due to In-Plane Stresses

When in-plane radial stress σ_r and tangential stress σ_ξ are present at the middle plane of the annular thin plate element, the following additional terms arise in the strain energy equation (124), of the annular element, Figure 2.1,

$$U = \frac{1}{2} \int_0^{2\pi} \int_{r_1}^{r_2} \{ \sigma_r (\frac{\partial w}{\partial r})^2 + \frac{\sigma_\xi}{r^2} (\frac{\partial w}{\partial \xi})^2 \} h(r) \, r \, dr \, d\xi \tag{2.29}$$

Assuming the deflection function, Equation 2.1, as before, and substituting in the above strain energy expression, additional stiffness coefficients for the annular element are readily derived corresponding to the deflection vector,

$$\{\bar{q}_d\}^T = [\bar{w}_1 \quad \bar{\theta}_1 \quad \bar{w}_2 \quad \bar{\theta}_2] \tag{2.30}$$

The additional stiffness matrix is

$$[K_d^a] = [B_d]^T [k_d^a] [B_d] \tag{2.31}$$

where the matrices $[B_d]$ and $[k_d^a]$ are given in Tables 2.1 and 2.22 The integrals R_i and S_i appearing in the elements of the matrix $[k_d^a]$ are given by

$$R_i = C\pi \int_{r_1}^{r_2} r^i \, h(r) \, \sigma_r(r) \, dr \tag{2.32}$$

$$S_i = C\pi \int_{r_1}^{r_2} r^i \, h(r) \, \sigma_\xi(r) \, dr \tag{2.33}$$

It is convenient to assume linear variations, within the element, of $h(r)$, $\sigma_r(r)$, and $\sigma_\xi(r)$ requiring that the values need only be known at the nodal points.

assuming

$$h(r) = \alpha + \beta r \; ; \; \sigma_r(r) = c + dr \; ; \text{ and } \sigma_\xi(r) = e + fr \qquad (2.34)$$

then

$$\alpha = (h_1 r_2 - h_2 r_1)/(r_2 - r_1) \; ; \; \beta = (h_2 - h_1)/(r_2 - r_1)$$

$$c = (\sigma_{r1} r_2 - \sigma_{r2} r_1)/(r_2 - r1) \; ; d = (\sigma_{r2} - \sigma_{r1})/(r_2 - r1)$$

$$e = (\sigma_{\xi 1} r_2 - \sigma_{\xi 2} r_1)/(r_2 - r_1) \; ; f = (\sigma_{\xi 2} - \sigma_{\xi 1})/(r_2 - r_1)$$

$$(2.35)$$

and

$$R_i = C\pi \int_{r_1}^{r_2} r^i (a + \beta r)(c + dr)\, dr \qquad (2.36)$$

$$S_i = C\pi \int_{r_1}^{r_2} r^i (a + \beta r)(e + fr)\, dr \qquad (2.37)$$

2.3.2 Plane Stress Finite Element For Thin Discs

When a disc rotates at speed, very high radial and tangential stresses are generally produced by the centrifugal inertia force. The presence of radial temperature gradient can substantially modify the total stress distribution and in extreme cases has been known to result in buckling at the rim. Shrinkfit pressure at the hub, in certain cases, can also modify the centrifugal stress distribution. The result of all these effects produces an in-plane stress distribution in the disc, which changes the flexural stiffness of the disc. The variation of these stresses across the thickness of the disc is generally ignored in axial flow rotors.

By taking advantage of the axisymmetric nature of the problem, plane stress finite elements of annular and circular geometry are developed below for use in the stress analysis of discs. These elements incorporate radial thickness variation. Consistent load vectors (123) are used to replace the continuously distributed centrifugal and thermal loading, or any other axisymmetric external loading on either boundary.

Consider the axisymmetric stretching of an annular element with inner radius r_1 and outer radius r_2 and radially varying thickness $h(r)$. The geometry and deflections of the element are shown in Figure 2.6. The strain energy in the element is given by (124),

$$U = \frac{1}{2} \frac{2\pi}{(1 - \nu^2)} \int_{r_1}^{r_2} E\, h(r) \{ \varepsilon_r^2 + \varepsilon_\xi^2 + 2\varepsilon_r \varepsilon_\xi \}\, r\, dr \tag{2.38}$$

The radial and tangential strains in this case are

$$\varepsilon_r = \frac{du}{dr} \; ; \text{ and } \quad \varepsilon_\xi = \frac{u}{r} \tag{2.39}$$

where u is the radial displacement. Substituting the deflection function

$$u(r) = a_1 + a_2 r + a_3 r^2 + a_4 r^3 \tag{2.40}$$

in the strain energy expression and following standard procedure we arrive at the following expression for the stiffness matrix for the element,

$$[K_d^p] = [B_d]^T [k_d^p] [B_d] \tag{2.41}$$

corresponding to the deflection vector

$$\{q_d\}^T = [\, u_1 \quad \theta_1 \quad u_2 \quad \theta_2 \,] \tag{2.42}$$

where

$$\theta = -\frac{du}{dr} = -\varepsilon_r$$

The matrics $[B_d]$ and $[k_d^p]$ are given in Tables 2.1 and 2.30.

The integrals Q_i in Table 2.30 are given by

$$Q_i = \frac{2\pi E}{1-\nu^2} \int h(r)\, r^i \, dr \tag{2.43}$$

If linear thickness variation within the element is assumed, then

$$h(r) = \alpha + \beta r \tag{2.44}$$

where

$$\alpha = \frac{h_1 r_2 - h_2 r_1}{r_2 - r_1} \quad \text{and} \quad \beta = \frac{h_2 - h_1}{r_2 - r_1} \tag{2.45}$$

then,

$$Q_i = \frac{2\pi E}{1-\nu^2} \int_{r_1}^{r_2} (\alpha + \beta r)\, r^i \, dr \tag{2.46}$$

When $r_1 = 0$, the geometry of the element becomes circular. In this case $u_1 = 0$ and the element has only three degrees of freedom, and

$$\{q_d\}^T = [\ \theta_1\ u_2\ \theta_2\ ] \tag{2.47}$$

By assuming the deflection function

$$u(r) = a_1 r + a_2 r^2 + a_3 r^3 \tag{2.48}$$

the stiffness matrix of the element becomes,

$$[K^P_{do}] = [B_o]^T [k^P_{do}] [B_o] \tag{2.49}$$

The matrices $[B_o]$ and $[k^P_{do}]$ are given in Tables 2.4 and 2.31.

The integrals Q_{io} in Table 2.31 are given by

$$Q_{io} = \frac{2\pi E}{1 - \nu^2} \int_{r_1}^{r_2} h(r)\, r^i\, dr \tag{2.50}$$

Again when linear thickness variation is assumed within this element

$$h(r) = \alpha + \beta r \tag{2.51}$$

where

$$\alpha = h_1 \quad \text{and} \quad \beta = (h_2 - h_1)/r$$

then

$$Q_{io} = \frac{2\pi E}{1 - \nu^2} \int_{r_1}^{r_2} (\alpha + \beta r)\, r^i\, dr \tag{2.52}$$

The element stiffness matrices $[K^P_d]$ can be assembled by conventional methods to get the disc system stiffness matrix $[K^P_D]$. Now, theequilibriumcondition requires the following relation to be satisfied;

$$\{Q_D\} = [K^P_D]\, \{q_D\} \tag{2.53}$$

where $\{Q_D\}$ is the vector of generalised nodal forces and $\{q_D\}$ is the vector of unknown nodal displacements.

Only displacement boundary conditions should be applied by deleting rows and columns in $[K_D^p]$ corresponding to displacements which are zero. Often the turbine disc is considered to be free at either boundary while analysing the stresses in the disc; here $[K_D^p]$ is not reduced. The simultaneous equations given by the relation (2.53) may be solved by conventional procedures; if matrix inversion is followed then,

$$\{q_D\} = [K_D^p]^{-1} \{Q_D\} \tag{2.54}$$

Thus all the nodal displacements are obtained.

The load vector $\{Q_D\}$ comprises several contributions. Thus the following should be considered.

(a) Rim loading resulting from blades should be added at the appropriate position of the vector. $\{Q_D\}$. If the number of blades present is Z, each with mass m^* and centre of gravity at radius R_g and if the rotational speed is Ω rad./sec., then this loading is $Zm^*\Omega^2R_g$.

(b) Shrinkfit pressure at the hub results in some loading at the inner radius a and is given by $2\pi\, a\, \sigma_o h(a)$, where σ_o is the shrinkfit pressure and $h(a)$ the thickness at radius a.

(c) Distributed centrifugal loading.

(d) Distributed thermal gradient loading.

For (c) and (d) equivalent consistent vectors of nodal forces are obtainedbyequating work done by the hypothetical nodal forces to work done by distributed centrifugal and thermal_ loading.

Consider the distributed centrifugal inertia loading first. When the disc is rotating with constant angular velocity Ω , by, equating the work done by the hypothetical nodal forces to the work done by the centrifugal force in the annular element, we obtain

$$\{q_d\}^T \{f_c\} = \int_0^{2\pi} \int_{r_1}^{r_2} F(r)\ u(r) \qquad (2.55)$$

where

$$\{q_d\}^T = [\ u_1 \ \ \theta_1 \ u_2 \ \ \theta_2 \ ] \qquad (2.56)$$

$\{f_c\}$ - consistent vector of nodal loads.

$$F(r) = \rho\ \Omega^2\ r^2\ h(r)\ dr\ d\xi \qquad (2.57)$$

and

$$u(r) = [\ 1 \ \ r \ \ r^2 \ \ r^3\ ]\ [B_d]\ \{q_d\} \qquad (2.58)$$

Substituting for F(r) and u(r) in (2.55)

$$\{f_c\} = [B_d]^T \{g\} \qquad (2.59)$$

where

$$\{g\}^T = [\ g_2 \ \ g_3 \ g_4 \ \ g_5] \qquad (2.60)$$

and

$$g_i = 2\pi\rho\Omega^2 \int_{r_1}^{r_2} h(r)\ r^i\ dr \tag{2.61}$$

When linear thickness variation within the element is assumed, then

$$h(r) = a + \beta r \tag{2.62}$$

and

$$a = \frac{h_1 r_2 - h_2 r_1}{r_2 - r_1} \quad \text{and} \quad \beta = \frac{h_2 - h_1}{r_2 - r_1} \tag{2.63}$$

then

$$g_i = 2\pi\rho\Omega^2 \int_{r_1}^{r_2} (a + \beta r)\ r^i\ dr \tag{2.64}$$

When the disc is subjected to axisymmetrical radial temperature gradient the thermal loading is replaced by the consistent vector given below. For the annular element,

$$\begin{bmatrix} \varepsilon_r \\ \varepsilon_\xi \end{bmatrix} = \begin{bmatrix} \frac{du}{dr} \\ \frac{u}{r} \end{bmatrix} = \begin{bmatrix} 0 & 1 & 2r & 3r^2 \\ \frac{1}{r} & 1 & r & r^2 \end{bmatrix} [B_d]\ \{q_d\}$$

$$= [E]\ [B_d]\ \{q_d\} \tag{2.65}$$

$$\begin{bmatrix} \sigma_r \\ \sigma_\xi \end{bmatrix} = \frac{E}{1 - \nu^2} \begin{bmatrix} 1 & \nu \\ \nu & 1 \end{bmatrix} \begin{bmatrix} \varepsilon_r \\ \varepsilon_\xi \end{bmatrix} - \frac{E\alpha^*\ T(r)}{1 - \nu} \begin{bmatrix} 1 \\ 1 \end{bmatrix} \tag{2.66}$$

where

α^* – coefficient of thermal expansion of the material of the disc.

$T(r)$ – temperature at any radius r.**

Equating the work done by the temperature gradient to that by the consistent load vector $\{f_t\}$

$$\int_0^{2\pi}\int_{r_1}^{r_2}\{\frac{E}{1-\nu^2}\{q_d\}^T[B_d]^T\ [E]^T\begin{bmatrix}1 & \nu\\ \nu & 1\end{bmatrix}[E]\ [B_d]\{q_d\}$$

$$-\frac{E}{1-\nu}\ \alpha^*\ T(r)\ [B_d]^T\ [E]^T\ \{q_d\}^T\begin{bmatrix}1\\1\end{bmatrix}\}h(r)\ r\ dr\ d\xi$$

$$=\{q_d\}^T\ [K_d^p]\{q_d\}-\{q_d\}^T\{f_t\} \tag{2.67}$$

Now,

$$[K_d^p]=\frac{E}{1-\nu^2}\int_0^{2\pi}\int_{r_1}^{r_2}[B_d]^T[E]^T\begin{bmatrix}1 & \nu\\ \nu & 1\end{bmatrix}[E]\ [B_d]\ h(r)\ r\ dr\ d\xi \tag{2.68}$$

Therefore

$$\{f_t\}=\frac{2\pi E\alpha^*}{1-\nu}\ [B_d]^T\int_{r_1}^{r_2}h(r)\ T(r)\ [E]^T\begin{bmatrix}1\\1\end{bmatrix}r\ dr\ d\xi$$

$$=[B_d]^T\{g\} \tag{2.69}$$

where

$$\{g\}=[\ g_o\ g_1\ g_2\ g_3\ ] \tag{2.70}$$

and

$$g_i=\frac{2\pi E\alpha^*}{1-\nu}\int h(r)\ T(r)\ r^i\ dr \tag{2.71}$$

** Note that $T(r)$ is the change in temperature from a stress free temperature state.

When linear thickness and temperature variations within the element are assumed, then

$$h(r) = \alpha + \beta r \tag{2.72}$$

where

$$\alpha = \frac{h_1 r_2 - h_2 r_1}{r_2 - r_1} \quad \text{and} \quad \beta = \frac{h_2 - h_1}{r_2 - r_1} \tag{2.73}$$

and

$$T(r) = c + dr \tag{2.74}$$

where

$$c = \frac{T_1 r_2 - T_2 r_1}{r_2 - r_1} \quad \text{and} \quad d = \frac{T_2 - T_1}{r_2 - r_1} \tag{2.75}$$

and therefore,

$$g_i = \frac{2\pi E\alpha^*}{1 - \nu} \int_{r_1}^{r_2} (\alpha + \beta r)(c + dr)\, r^i \, dr \tag{2.76}$$

As already mentioned the load vector $\{Q_D\}$ comprises of the above individual contributions where applicable. Now Equation 2.54 can be solved to obtain the system displacement vector. The stresses are then calculated as follows. In the case of axisymmetric stretching of the disc the shearing stress $\tau_{r\xi}$ is zero and hence the stress strain relationship becomes,

$$\begin{bmatrix} \sigma_r \\ \sigma_\xi \end{bmatrix} = \frac{E}{1 - \nu^2} \begin{bmatrix} 1 & \nu \\ \nu & 1 \end{bmatrix} \begin{bmatrix} \varepsilon_r \\ \varepsilon_\xi \end{bmatrix} - \frac{E\ \alpha^* T(r)}{1 - \nu} \begin{bmatrix} 1 \\ 1 \end{bmatrix} \tag{2.77}$$

The last term on the right hand side of the above equation vanishes if there is no temperature gradient. Now the strain vector can be expressed in terms of the assumed deflection function; which in effect gives a relationship betweenstrain and the nodal displacements.

$$\begin{bmatrix} \varepsilon_r \\ \varepsilon_\xi \end{bmatrix} = \begin{bmatrix} \frac{du}{dr} \\ \frac{u}{r} \end{bmatrix} = \begin{bmatrix} 0 & 1 & 2r & 3r^2 \\ \frac{1}{r} & 1 & r & r^2 \end{bmatrix} [B_d]\ \{q_d\} \qquad (2.78)$$

The above relationship together with Equation 2.77 can be used to get the stresses σ_r and σ_ξ at any radius r. In such a situation $\{q_d\}$ is the deflection vector of the element inside which the point in question lies.

Generally we are interested in the stresses at the nodal points of the model only, and the following procedure should be followed. Consider an element between nodes i and i+l. The deflection vector of this element is

$$\{q_d\}^T = [\ u_i \quad \theta_i \quad u_{i+1} \quad \theta_{i+1}\ ] \qquad (2.79)$$

This vector is obtained from the system deflection vector $\{q_D\}$. Now, making use of the relationships (2.77) and (2.78), we get

$$\begin{bmatrix} \sigma_{ri} \\ \sigma_{\xi i} \\ \sigma_{ri+1} \\ \sigma_{\xi i+1} \end{bmatrix} = \frac{E}{1-\nu^2} \begin{bmatrix} 1 & \nu & 0 & 0 \\ \nu & 1 & 0 & 0 \\ 0 & 0 & 1 & \nu \\ 0 & 0 & \nu & 0 \end{bmatrix} \begin{bmatrix} 0 & 1 & 2r_i & 3r_i^2 \\ \frac{1}{r_i} & 1 & r_i & r_i^2 \\ 0 & 1 & 2r_{i+1} & 3r_{i+1}^2 \\ \frac{1}{r_{ii-l}} & 1 & r_{i+1} & r_{i+1}^2 \end{bmatrix} [B_d]\{q_d\} - \frac{E\alpha^*}{1-\nu} \begin{bmatrix} T_i \\ T_{i+1} \\ T_i \\ T_{i+1} \end{bmatrix}$$

(2.80)

When there is no temperature gradient in the disc the last term in the above equation vanishes. These same stresses can be found using the deflection vectors of the adjacent elements also. Note that in this case the stresses at a node are uniquely defined since both u and du/dr happen to be degrees of freedom chosen; thus there will not be any difference in the values calculated using adjacent elements.

2.3.3 Numerical Applications

The convergence properties and accuracy of the plane stress annular element developed are first examined by comparing with exact solutions the values of stresses calculated using these elements. Both centrifugal and thermal loading are considered. The accuracy of the use of the additional stiffness coefficients derived for the vibration of rotating discs is then assessed by comparing frequency values calculated with these coefficients and the thin plate annular elements, with exact and experimental values.

(A) First uniform annular discs with the extreme value of a/b = 0.001 and the more typical value 0.2, rotating with uniform angular velocity Ω were considered. Radial stress coefficients $p = (\sigma_r/\rho\,\Omega^2 b^2) \times 10^4$; and tangential stress coefficients $q = (\sigma_\xi/\rho\,\Omega^2 b^2) \times 10^4$ were calculated for these discs with the plane stress annular elements, and these are given in Tables 2.25 to 2.28 along with exact solutions. From these results it is seen that when a/b is very small, 0.001, the finite element results are in error at the inner boundary and are unacceptable. However, at points away from the inner boundary, agreement between finite element and exact solutions is good. For such cases it is necessary to use many elements, eg. 8 or 16 elements, in Tables 2.25 and 2.26, and to disregard the stress value obtained at the inner boundary. When the value of a/b is increased to 0.2, the finite element results at the inner boundary also become very much closer to the exact values, Tables 2.27 and 2.28. In both cases convergence is rapid and results with engineering accuracy are obtained with four to eight elements. In Figure 2.7, the stress coefficients p 'and q calculated, for a disc with a/b = 0.2, using plane stress annular elements are compared with exact solutions graphically.

(B) For a second example, an annular disc with a/b = 0.2 and hyperbolic radial thickness variation (17), $h(r) = h(b)/r^{i}$, when $i = 1$, rotating with uniform angular velocity Ω was considered. The stress coefficients p and q obtained with plane stress annular elements with linear thickness variation are given in Tables 2.29 and 2.30 along with exact solutions. Agreement between finite element and exact solutions is good and convergence is rapid with increasing number of elements.

(C) Next, temperature stresses in two uniform annular discs with a/b = 0.001 and 0.2 were considered. The discs were subjected to radially varying temperature gradient, $T(r) = T(b)\ \frac{r}{b}$. Radial stress coefficients $p = \{\sigma_r / E * T(b)\} \times 10^4$, and tangential stress coefficients $q = \{\sigma_\xi / E\alpha * T(b)) \times 10^4$, calculated with the plane stress annular elements, are given in Tables 2.31 to 2.34, along with exact solutions. Remarks made under (A) above, regarding accuracy and convergence of results, hold for these cases also.

(D) The stresses obtained using plane stress elements are now used as initial in-plane stresses in the vibration analysis of rotating discs. Ignoring bending stiffness of the disc and considering only the stiffness due to the initial stresses, frequency coefficients $\lambda = (\omega_1 / \Omega)^2$ of the membrane disc, where ω_1 is the natural frequency of the membrane disc and Ω, the speed of rotation, were calculated. The values of λ obtained, for a centrally clamped disc, are given in Table 2.35 along with the exact values given by Lamb and Southwell (47). These values were also calculated taking exact stress values at nodal points and are given in Table 2.36. A value of a/b = 0.001 was assumed to facilitate modelling the disc with annular elements only. In both cases linear variations of the stresses within the element were assumed. In either case the membrane frequencies are calculated within 3% or better using only four elements.

(E) Finally, the variation of the natural frequencies with speed of rotation of a thin annular disc with a/b = 0.5, b = 8.0 in. and h = 0.04 in. was studied. Both the disc bending stiffness and the additional stiffness resulting from centrifugal stresses were considered together. Natural frequencies ω_{mn} of this disc rotating at 0, 1000, .., 4000 rpm, calculated using eight thin plate bending and plane stress annular elements are given in Table 2.37. Convergence of results with increasing number of elements, for 3000 rpm, are shown in Table 2.38. The relationship between the natural frequencies ω_{mn} of a rotating disc and the harmonic exeitation frequency ζ is given by (73)

$$\zeta = \omega_{mn} \pm m\,\Omega \qquad (2.81)$$

where m is the number of nodal diameters and Ω is the speed of rotation of the disc. Mote and Nieh (73) have measured experimentally values of ζ for this disc. In Figure 2.8 values of ζ obtained from finite element results have been plotted against rpm, for the first mode of diametral nodes 0 to 5. The calculated frequencies lie very close to the experimental points showing excellent agreement between these results.

2.4 THE EFFECT OF TRANSVERSE SHEAR AND ROTARY INERTIA ON THE VIBRATION OF MODERATELY THICK DISCS

Computed frequencies using thin plate theory are always found to be higher than the experimentally measured ones when thick discs and the higher modes of relatively thin discs are considered. An improved plate theory, which considers transverse shear and rotary inertia, would result in satisfactory analysis when the discs are moderately thick. The effect of transverse shear is to produce additional rotation and deflection; and that of rotary inertia is to increase the inertia. Thus both these effects serve to decrease the computed frequencies.

A coefficient κ^2, known as shear coefficient, is introduced to take into account the shear stress distribution across the depth of the plate.' Mindlin (62) has used a value $\kappa^2 = \pi^2/12$, which is close to the normally used value of 5/6 for rectangular section Timoshcnko beam. When moderately thick uniform circular and annular plates are considered the frequency determinants derived by Callahan (66) and Bakshi and Callahan (67) can be used; however, as mentioned previously, there is'no simple exact solution for thick discs of varying thickness.

In this section, a finite element approach is described which can readily be used in the analysis of discs with radial thickness variation. Two new finite elements, both of annular geometry and having radial thickness taper, are developed. These elements require additional degrees of freedom to take into account transverse shear effects. The efficiency of these elements is examined by comparing calculated frequency values with experimental values published by other investigators. For uniform discs, the exact values are computed using Mindlin's theory for comparision with finite element results. These exact values use the method of Bakshi and Callahan (67). Since their paper contains many typographical errors the frequency determinant resulting for a free annular plate is given along with a brief summary of Mindlin's equations in Appendix B.

In the finite element analysis of moderately thick turbine discs, additional strain energy due to transverse shear and addftional kinetic energy due to rotary inertia must be taken into account in obtaining the element matrices. For an annular element, the complete strain energy and kinetic energy expressions are given below when these additional energies are included (62).

$$U = \frac{1}{2}\int_0^{2\pi}\int_{r_1}^{r_2} D\,\{\chi_b\}^T \begin{bmatrix} 1 & \nu & 0 \\ \nu & 1 & 0 \\ 0 & 0 & \frac{1-\nu}{2} \end{bmatrix} \{\chi_b\} r\, dr d\xi$$

$$+ \frac{1}{2}\int_0^{2\pi}\int_{r_1}^{r_2} \kappa^2 G h(r)\, \{\chi_s\}^T \begin{bmatrix} 1 & 0 \\ 0 & 1 \end{bmatrix} \{\chi_s\} r\, dr d\xi \qquad (2.82)$$

where

$$\{\chi_s\} = \begin{bmatrix} \gamma_r \\ \gamma_\xi \end{bmatrix} \qquad (2.83)$$

and

$$\{\chi_b\} = \begin{bmatrix} \dfrac{\partial\psi_r}{\partial r} \\ \dfrac{\psi_r}{r} + \dfrac{1}{r}\dfrac{\partial\psi_\xi}{\partial\xi} \\ \dfrac{1}{r}\dfrac{\partial\psi_r}{\partial\xi} - \dfrac{\psi_\xi}{r} + \dfrac{\partial\psi_\xi}{\partial r} \end{bmatrix} \tag{2.84}$$

and

$$\begin{aligned} T = & \frac{1}{2}\int_0^{2\pi}\int_{r_1}^{r_2} \rho h(r) \left(\frac{\partial w}{\partial t}\right)^2 r\, dr d\xi \\ & + \frac{1}{2}\int_0^{2\pi}\int_{r_1}^{r_2} \frac{\rho h^3(r)}{12} \left[\left\{\frac{\partial\psi_r}{\partial t}\right\}^2 + \left\{\frac{\partial\psi_\xi}{\partial t}\right\}^2 \right] r\, dr d\xi \end{aligned} \tag{2.85}$$

where

$$\psi_r = -\frac{\partial w}{\partial r} + \gamma_r \quad ; \qquad \psi_\xi = -\frac{1}{r}\frac{\partial w}{\partial\xi} + \gamma_\xi \tag{2.86}$$

and, γ_r and γ_ξ are the additional radial and circumferential rotations resulting from transverse shear.

2.4.1 Annular Plate Bending Finite Elements Including Transverse Shear And Rotary Inertia.

(A) Thick Disc Element-1

In this case, in addition to the total deflections $\bar{w}$ and radial rotations $\bar{\psi}_r$ along an antinode at either boundary of the annular element, the radial and tangential shear rotations $\overline{\gamma}_r$ and $\overline{\gamma}_\xi$ are taken as additional degrees of freedom. Figure 2.9 shows this element with two nodal diameters and the degrees of freedom considered, Hence, the deflection vector, which has eight degrees of freedom, is

$$\{q_d\}^T = [\ \overline{w}_1 \ \ \overline{\psi}_{r1} \ \ \overline{\gamma}_{r1} \ \ \overline{\gamma}_{\xi 1} \ \ \overline{w}_2 \ \ \overline{\psi}_{r2} \ \ \overline{\gamma}_{r2} \ \ \overline{\gamma}_{\xi 2}\ ] \qquad (2.87)$$

This formulation of the element configuration follows closly that of Pryor et al (125), who recently examined the static loading solutions for thick plates using rectangular finite elements. Now, assuming the deflection functions

$$\begin{aligned} w(r,\xi) &= (a_1 + a_2 r + a_3 r^2 + a_4 r^3) \cos m\xi \\ \gamma_r(r,\xi) &= (a_5 + a_6 r) \cos m\xi \qquad (2.88) \\ \gamma_\xi(r,\xi) &= (a_7 + a_8 r) \sin m\xi \end{aligned}$$

and substituting these into the energy equations, Equations 2.82 and 2.85, we obtain the stiffness and inertia matrices of the element as

$$[K_d^t] = [B_d^t]^T [k_d^t] [B_d^t]$$

and (2.89)

$$[M_d^t] = [B_d^t]^T [m_d^t] [B_d^t]$$

where

$$[B_d^t]^{-1} = \begin{bmatrix} 1 & r_1 & r_1^2 & r_1^3 & 0 & 0 & 0 & 0 \\ 0 & -1 & -2r_1 & -3r_1^2 & 1 & r_1 & 0 & 0 \\ 0 & 0 & 0 & 0 & 1 & r_1 & 0 & 0 \\ 0 & 0 & 0 & 0 & 0 & 0 & 1 & r_1 \\ 1 & r_2 & r_2^2 & r_2^3 & 0 & 0 & 0 & 0 \\ 0 & -1 & -2r_2 & -3r_2^2 & 1 & r_2 & 0 & 0 \\ 0\,0 & 0\,0 & 0\,0 & 0\,0 & 1\,0 & r_2\,0 & 1\,0 & r_2\,0 \end{bmatrix} \qquad (2.90)$$

and

$$[k_d^t] = \begin{bmatrix} [k_d] & [k_d^1] \\ [k_d^1]^T & [k_d^2] \end{bmatrix} \qquad (2.91)$$

The matrix $[k_d]$ is the same matrix of the thin plate bending annular element developed in section 2.2.2 and is given in Table 2.2. The matrices $[k_d^1]$ and $[k_d^2]$ are given in Table 2.39, where

$$P_i = C\pi \frac{E}{12(1-\nu^2)} \int_{r_1}^{r_2} h^3(r)\, r^i dr; \qquad Q_i = C\pi G\kappa^2 \int_{r_1}^{r_2} h(r)\, r^i dr \qquad (2.92)$$

$$[m_d^t] = \begin{bmatrix} [m_d] & [0] \\ [0] & [0] \end{bmatrix} + [m_d^1] \qquad (2.93)$$

where

$$[B_d^t]^{-1} = \begin{bmatrix} 1 & r_1 & r_1^2 & r_1^3 & 0 & 0 & 0 & 0 \\ 0 & -1 & -2r_1 & -3r_1^2 & 1 & r_1 & 0 & 0 \\ 0 & 0 & 0 & 0 & 1 & r_1 & 0 & 0 \\ 0 & 0 & 0 & 0 & 0 & 0 & 1 & r_1 \\ 1 & r_2 & r_2^2 & r_2^3 & 0 & 0 & 0 & 0 \\ 0 & -1 & -2r_2 & -3r_2^2 & 1 & r_2 & 0 & 0 \\ 0 & 0 & 0 & 0 & 1 & r_2 & 0 & 0 \\ 0 & 0 & 0 & 0 & 0 & 0 & 1 & r_2 \end{bmatrix} \tag{2.90}$$

and

$$[k_d^t] = \begin{bmatrix} [k_d] & [k_d^1] \\ [k_d^1]^T & [k_d^2] \end{bmatrix} \tag{2.91}$$

The matrix $[k_d]$ is the same matrix of the thin plate bending annular element developed in section 2.2.2 and is given in Table 2.2. The matrices $[k_d^1]$ and $[k_d^2]$ are given in Table 2.39, where

$$P_i = C\pi \frac{E}{12(1-\nu^2)} \int_{r_1}^{r_2} h^3(r)\ r^i dr; \qquad Q_i = C\pi G\kappa^2 \int_{r_1}^{r_2} h(r)\ r^i dr \tag{2.92}$$

$$[m_d^t] = \begin{bmatrix} [m_d] & [0] \\ [0] & [0] \end{bmatrix} + [m_d^1] \tag{2.93}$$

where $[m_d]$ is the same matrix of the thin plate bending annular element, developed in section 2.2.2, and is given in Table 2.3. The matrix $[m_d^1]$ is given in Table 2.40, where

$$P_i = C\pi \frac{\rho}{12} \int_{r_1}^{r_2} h^3(r)\, r^i \, dr \tag{2.94}$$

Linear thickness variation can be assumed within the element in evaluating the integrals, Equations 2.92 and 2.94.

When this element is used the following boundary conditions should be satisfied.

Simply supported boundary	$\overline{w} = 0$
Clamped boundary	$\overline{w} = 0$; $\overline{\psi}_r = 0$
Free boundary	$\overline{\gamma}_r = 0$

(B) Thick Disc Element-2

An alternative method of considering the effects of transverse shear and rotary inertia is to treat separately the deformations due to bending and transverse shear. The efficiency of this approach was first examined in the static bending analysis of thick rectangular plates and this work is described with some detail in Appendix C. It is demonstrated that this approach has considerable advantages for static problems (126). Below, this method of analysis is applied to the vibration analysis of moderately thick circular plates. An annular plate bending element with eight degrees of freedom is developed. In this element, in addition to the deflections and rotations due to bending, those due to transverse shear are taken to be the additional degrees of freedom.

In the formulation of this finite element, the contributions of bending and transverse shear are separated, thus

$$w = w^b + w^s \tag{2.95}$$

and further it is assumed that the rotations ψ_r and ψ_ξ are due to bending alone.

$$\psi_r = -\frac{\partial w^b}{\partial r} \quad \text{and} \quad \psi_\xi = -\frac{1}{r}\frac{\partial w^b}{\partial \xi} \tag{2.96}$$

Then the rotations γ_r and γ_ξ are due to shear deformation alone.

$$\gamma_r = -\frac{\partial w^s}{\partial r} \quad \text{and} \quad \gamma_\xi = -\frac{1}{r}\frac{\partial w^s}{\partial \xi} \tag{2.97}$$

Taking these shear deflections and rotations in addition to those due to bending as degrees of freedom, the deflection vector of the element Is

$$\{\overline{q}_d\} = \begin{bmatrix} \{\overline{q}_d^b\} \\ \\ \{\overline{q}_d^s\} \end{bmatrix} \tag{2.98}$$

where

$$\{\bar{q}_d^b\}^T = [\ \bar{w}_1^b \quad \bar{\psi}_{r1} \quad \bar{w}_2^b \quad \bar{\psi}_{r2}\ ]$$

and

$$\{\bar{q}_d^s\}^T = [\ \bar{w}_1^s \quad \bar{\gamma}_{r1} \quad \bar{w}_2^s \quad \bar{\gamma}_{r2}\ ]$$

Figure 2.10 shows this element with two nodal diameters and the degrees of freedom. Assuming the deflection functions,

$$\begin{aligned} w^b(r,\xi) &= (a_1 + a_2 r + a_3 r^2 + a_4 r^3) \cos m\xi \\ w^s(r,\xi) &= (a_5 + a_6 r + a_7 r^2 + a_8 r^3) \cos m\xi \end{aligned} \tag{2.99}$$

and substituting in the energy expressions, Equations 2.82 and 2.85, we obtain the stiffness and inertia matrices.

$$[K_d^t] = [B_d^t]^T [k_d^t] [B_d^t]$$

and (2.100)

$$[M_d^t] = [B_d^t]^T [m_d^t] [B_d^t]$$

where

$$[B_d^t] = \begin{bmatrix} [B_d] & [0] \\ [0] & [B_d] \end{bmatrix} \tag{2.101}$$

and

$$[k_d^t] = \begin{bmatrix} [k_d] & [0] \\ [0] & [k_d^s] \end{bmatrix} \tag{2.102}$$

where the matrices $[B_d]$ and $[k_d]$ are the same as those of the annular thin plate bending element, developed in section 2.2.2, and are given in Tables 2.1 and 2.2. The matrix $[k_d^s]$ is given in Table 2.41, where

$$Q_i = C\pi\ \kappa^2 G \int_{r_1}^{r_2} h(r)\ r^i\ dr \qquad (2.103)$$

and

$$[m_d^t] = \begin{bmatrix} [m_d] & [m_d] \\ [m_d] & [m_d] \end{bmatrix} + \begin{bmatrix} [m_d^r] & [0] \\ [0] & [0] \end{bmatrix} \qquad (2.104)$$

where the matrix $[m_d]$ is the same as that of the thin plate bending annular element, developed in section 2.2.2, and is given in Table 2.3. The matrix $[m_d^r]$ is given in Table 2.42, where

$$P_i = C\pi\ \frac{\rho}{12} \int_{r_1}^{r_2} h\ (r)\ r^i\ dr \qquad (2.105)$$

When this element is used the following boundary conditions should be satisfied.

Simply supported boundary	$\bar{w}^b = 0$; $\bar{w}^s = 0$
Clamped boundary	$\bar{w}^b = 0$; $\bar{w}^s = 0$; $\bar{\psi}_r = 0$
Free boundary	$\bar{\gamma}_r = 0$

2.4.2 Numerical Applications

The efficiency and convergence properties of these two thick disc elements are now examined by comparing frequency values computed using these elements with experimental data, for both uniform and nonuniform discs. In the case of uniform discs, the exact values are also calculated using Mindlin's theory for comparision.

(A) The first example is a small circular disc 75 mm in diameter and 5 mm thick, for which some of the experimental frequencies are given by Onoe and Yano (68). A small hole is assumed at the centre of the disc with a/b = 0.001. Frequencies calculated using both thick disc elements are given in Tables 2.43 and 2.44, along with exact and experimental values. Modes of vibration with m = 0 to 3 are considered. Comparision of results in Tables 2.43 and 2.44 shows little difference between results of Element-1 and Element-2; and both results compare well with exact and experimental data. The disc was completely free and therefore free body modes exist for m = 0 and 1. In these cases convergence is from below, atleast for the first mode. In all the other cases-convergence is from above, as would be expected, and is rapid.

(B) A number of fairly thick discs and rings were chosen as the second example, The dimensions of these discs and rings are given in Tables 2.45 and 2.46 along with the first frequency (m=2, n=0) values calculated using these thick disc elements. Experimental results are given by Peterson (71) for all these cases. Comparision of results in Tables 2.45 and 2.46 shows that when complete discs are considered both the elements perform well and calculated and experimental results are close. But in the case of rings Element-l gives good results whereas there is a large difference between calculated and experimental values with Element-2. Practically there is no convergence with this element. Such poor performance of Element-2 may be due to the difficulty in imposing correct boundary conditions when this element is used,

(C) As the third example two rings with different thick nesses were chosen. Experimental results for these rings for m = 2 and n = 0 are given by Rao(127); and are originally due to Peterson (71). Only Element-l is used in this case and the calculated frequencies are given in Table 2.47 along with exact and experimental results. The dimensions of these rings are also given in Table 2.47. Agreement between the calculated and experimental results is good.

(D) Discs with stepped section and fillets were examined next. Three such discs were considered. Except the web thickness other dimensions are the same, Figure 2.11. Only one frequency (m = 2, n= 0) in each case was calculated and are given in Table 2.48 along with experimental values. Agreement between calculated and experimental values is good. These discs were modelled with five elements as shown in Figure 2.11.

(E) The final example chosen is a practical turbine disc. The dimensions, material constants and experimentally measured frequencies for this disc were provided by Dr. E. K. Armstrong of Rolls-Royce (1971) Ltd. The profile of this disc is given in Figure 2.12, and the thickness at various radial distances are given in Table 2.49. This disc was modelled with 4, 6 and 8 elements using Element-l, and the mass of castellations present at the end of the disc was lumped at the outer boundary, Finite element results are given along with experimental frequencies in Table 2.50. Frequencies calculated using 8 thin plate elements also are given for comparision. Values calculated with thick disc elements are in much closer agreement with the experimental results. It is also perhaps worth noting that the error between calculated frequencies, with 8 elements, and experimental values is consistently 6% to 8% high; this suggests the possibility that the nominal modulus of elasticity used may be in error.

CHAPTER 3

VIBRATION ANALYSIS OF AXIAL FLOW TTJRBINE BLADES

3.1 INTRODUCTION

Since the purpose of this investigation has more emphasis on the coupling effect between the disc and the array of blades in a bladed disc, a refined analysis of the blade is not attempted here. Much work has been published on this area, as was noted in the literature survey in chapter 1, and several methods of analysis of blade alone case are available. Such methods consider the blade with its aerofoil section and most of the other complicating factors such as camber, pretwist, longitudinal taper, root flexibility etc.

In this investigation the blade is idealized to behave as a beam having arbitrary variations in section properties and pretwist along its span. It is assumed that the centroidal and flexural axes coincide, ie the shear centre coincides with the centroid and there is no coupling between bending and torsion within the blade.

. In section 3.2 an idealization of a blade segment using available beam finite elements is outlined. The effect of and the presence of other stresses in the blade modifies substantially the natural frequencies of the blade. Therefore, in section 3.3, additional stiffness coefficients resulting from these effects are derived to be included in the bending and torsional stiffness matrices of the element chosen. In section 3.4 a new beam bending finite element with six degrees of freedom is developed; where transverse shear and rotary inertia effects are taken into account. Finally in section 3.5, the method of analysis of pretwisted blades is described.

Numerical results showing the effects of rotation, transverse shear and rotary inertia and pretwist are given along with other available solutions,

3.2 MODELLING OF BLADE SEGMENTS USING AVAILABLE BEAM FINITE ELEMENTS

Figure 3.1 shows a nonuniform blade element with the coordinate system chosen. Oz is the engine axis and Oy and Ox are the tangential and radial directions respectively. The minor principal axis Oz* of the blade cross-section is inclined at an angle δ to the engine axis Oz. When this blade element is considered to behave according to Euler-Bernoulli beam theory, well known beam finite elements described by several authors (78,79) can be used. In such cases, the element has four degrees of freedom in each principal direction in bending and two in torsion. These are, as shown in Figure 3.1, v_1^*, ψ_1^*, v_2^* and ψ_2^* in bending along the minor principal direction, w_1^*, θ_1^*, w_2^* and θ_2^* in bending along the major principal direction and ϕ_1 and ϕ_2 in torsion. Since there is no coupling between bending in the principal directions and between bending and torsion, the element matrices are not coupled. Therefore corresponding to the displacement vector,

$$\{q_b^*\}^T = [\ v_1^* \quad \psi_1^* \quad v_2^* \quad \psi_2^* \quad w_1^* \quad \theta_1^* \quad w_2^* \quad \theta_2^* \quad \phi_1^* \quad \phi_2^*\ ] \tag{3.1}$$

the element stiffness and inertia matrices are given by

$$[K_b^*] = \begin{bmatrix} [K_b^v] & [\ 0\ ] & [\ 0\ ] \\ [\ 0\ ] & [K_b^w] & [\ 0\ ] \\ [\ 0\ ] & [\ 0\ ] & [K_b^t] \end{bmatrix}$$

(3.2)

$$[M_b^*] = \begin{bmatrix} [M_b^v] & [\ 0\ ] & [\ 0\ ] \\ [\ 0\ ] & [M_b^w] & [\ 0\ ] \\ [\ 0\ ] & [\ 0\ ] & [M_b^t] \end{bmatrix}$$

where ψ^* and θ^* are defined as

$$\psi^* = -\frac{\partial v^*}{\partial x} \quad \text{and} \quad \theta^* = -\frac{\partial w^*}{\partial x} \tag{3.3}$$

$[K_b^v]$ and $[M_b^v]$ are the bending stiffness and inertia matrices along the minor principal direction, $[K_b^w]$ and $[M_b^w]$ are the bending stiffness and inertia matrices along the major principal direction and $[K_b^t]$ and $[M_b^t]$ are the torsional stiffness and inertia matrices. Matrices $[K_b^v]$ and $[K_b^w]$ are identical and can be defined by the matrix $[K_b^c]$ in which appropriate values of moment of inertia corresponding to the required direction should be used. Matrices $[M_b^v]$ and $[M_b^w]$ are the same when rotary inertia is ignored and can be defined by the matrix $[M_b^c]$.

In Tables 3.1 and 3.2 matrices $[K_b^c]$, $[M_b^c]$, $[K_b^t]$ and $[M_b^t]$ are given for a beam element when linear variations of the moment of inertia I, the area of cross-section A, the torsional stiffness K_G, and the polar moment of inertia J are assumed.

3.3 EFFECT OF ROTATION

The additional terms arising in the energy expression of a blade element rotating with angular velocity Ω are given by (90)

$$U = \frac{1}{2}\int_{x_1}^{x_2} A\,\sigma_x \left\{ \left(\frac{\partial w}{\partial x}\right)^2 + \left(\frac{\partial v}{\partial x}\right)^2 \right\} dx - \frac{1}{2}\rho\Omega^2 \int_{x_1}^{x_2} A\,(v)^2\,dx$$
$$+ \frac{1}{2}\int_{x_1}^{x_2} \sigma_x\, J \left(\frac{\partial \phi}{\partial x}\right)^2 dx - \frac{\rho\Omega^2}{2}\int_{x_1}^{x_2} (I_{max}-I_{min})(\phi)^2 \cos 2\delta\, dx \tag{3.4}$$

where σ_x is the stress along the length of the blade resulting from rotation. It should be noted that since Oz is the engine axis and Oy the tangential direction, the deflections w and v are perpendicular and parallel to the plane of rotation. Assuming the deflection functions,

$$v(x) = a_1 + a_2 x + a_3 x^2 + a_4 x^3$$

$$w(x) = a5 + a_6 x + a_7 x^2 + a_8 x^3 \tag{3.5}$$

$$\phi(x) = a_9 + a_{10} x$$

which are used to derive the basic beam matrices given in Tables 3.1 and 3.2, and substituting in the above strain energy equation we arrive at the additional stiffness matrix corresponding to the deflection vector

$$\{q_b\}^T = [\ v_1 \ \ \psi_1 \ \ w_1 \ \ \theta_1 \ \ \phi_1 \ \ v_2 \ \ \psi_2 \ \ w_2 \ \ \theta_2 \ \ \phi_2\ ] \tag{3.6}$$

as

$$[K_b^a] = [B_b^a]^T [k_b^a] [B_b^a] \tag{3.7}$$

where

$$[B_b^a]^{-1} = \begin{bmatrix} 1 & x_1 & x_1^2 & x_1^3 & 0 & 0 & 0 & 0 & 0 & 0 \\ 0 & -1 & -2x_1 & -3x_1^2 & 0 & 0 & 0 & 0 & 0 & 0 \\ 0 & 0 & 0 & 0 & 1 & x_1 & x_1^2 & x_1^3 & 0 & 0 \\ 0 & 0 & 0 & 0 & 0 & -1 & -2x_1 & -3x_1^2 & 0 & 0 \\ 0 & 0 & 0 & 0 & 0 & 0 & 0 & 0 & 1 & x_1 \\ 1 & x_2 & x_2^2 & x_2^3 & 0 & 0 & 0 & 0 & 0 & 0 \\ 0 & -1 & -2x_2 & -3x_2^2 & 0 & 0 & 0 & 0 & 0 & 0 \\ 0 & 0 & 0 & 0 & 1 & x_2 & x_2^2 & x_2^3 & 0 & 0 \\ 0 & 0 & 0 & 0 & 0 & -1 & -2x_2 & -3x_2^2 & 0 & 0 \\ 0 & 0 & 0 & 0 & 0 & 0 & 0 & 0 & 1 & x_2 \end{bmatrix} \quad (3.8)$$

and

$$[k_b^a] = \begin{bmatrix} [k_v^a] & [0] & [0] \\ [0] & [k_w^a] & [0] \\ [0] & [0] & [k_t^a] \end{bmatrix} \quad (3.9)$$

where the matrices $[k_v^a]$, $[k_w^a]$ and $[k_t^a]$ are given below.

$$[k_v^a] = \begin{bmatrix} 0 & 0 & 0 & 0 \\ 0 & R_0 & 2R_1 & 3R_2 \\ 0 & 2R_1 & 4R_2 & 6R_3 \\ 0 & 3R_2 & 6R_3 & 9R_4 \end{bmatrix} \quad (3.10)$$

$$[k_w^a] = \begin{bmatrix} S_0 & S_1 & S_2 & S_3 \\ S_1 & R_0+S_2 & 2R_1+S_3 & 3R_2+S_4 \\ S_2 & 2R_1+S_3 & 4R_2+S_4 & 6R_3+S_5 \\ S_3 & 3R_2+S_4 & 6R_3+S_5 & 9R_4+S_6 \end{bmatrix} \tag{3.11}$$

In the above matrices

$$R_i = \int_{x_1}^{x_2} \sigma_x A x^i \, dx \quad \text{and} \quad S_i = -\rho \Omega^2 \int_{x_1}^{x_2} A x^i \, dx \tag{3.12}$$

and

$$[k_t^a] = \begin{bmatrix} S_0 & S_1 \\ S_1 & R_0+S_2 \end{bmatrix} \tag{3.13}$$

where

$$\begin{aligned} R_i &= \int_{x_1}^{x_2} \sigma_x J x^i \, dx \\ S_i &= -\rho \Omega^2 \cos 2\theta \int_{x_1}^{x_2} (I_{max}-I_{min}) x^i \, dx \\ J &= (I_{max}+I_{min}) \end{aligned} \tag{3.14}$$

It is perhaps worth noting that the deflection vector $\{q_b\}$ given by Equation 3.6 is different from $\{q_b^*\}$ given by Equation 3.1. The bending displacements and rotations in vector $\{q_b\}$ are measured along the engine axis Oz and tangential direction Oy, whereas those in vector' $\{q_b^*\}$ are measured along the principal directions Oz* and Oy*. The torsional displacements in both cases are the same and are along the Ox axis. Since the angle δ between these two sets of coordinates vary along the length of the blade the individual element matrices given by Equation 3.2 should be transformed to the Oz-Oy coordinates before adding the additional stiffness coefficients derived in this section. This transformation is discussed in some detail in section 3.5.

In evaluating the integrals given by Equations 3.12 and 3.14 linear variations in I, A, σ_x and J can be assumed within the element. For a uniform beam element the additional stiffness matrices for bending parallel and perpendicular to the plane of rotation and for torsion are given in Tables 3.3 to 3.5, in closed form.

3.4 EFFECT OF TRANSVERSE SHEAR AND ROTARY INERTIA

In this section a new beam bending finite element which is compatible with the Thick Disc Element-l, developed in chapter 2, section 2.4.1, is developed. In the developement of this element transverse shear and rotary inertia are included, and in addition to the transverse deflection and rotation the additional rotation due to transverse shear is also taken as a degree of freedom in each node. Thus the element has six degrees of freedom.

Although two other Timoshenko beam finite element models developed by Archer (77) and Kapur (128) are available these are not compatible with the annular Thick Disc Element-l and thus these are not used here. It turns out, in fact, that the beam element derived hereunder is a marginal improvement in terms of convergence over those of Archer and Kapur.

Figure 3.2 shows a nonuniform blade element with the coordinate system chosen. Here again the minor principal axis Oz* is inclinedto the engine axis Oz at angle 6. The degrees of freedom of the element along the principal directions are shown in Figure 3.2. The rotations ψ* and ψ* in this case are defined as

$$\psi^* = -\frac{\partial v^*}{\partial x}+\gamma_v^* \quad \text{and} \quad \theta^* = -\frac{\partial w^*}{\partial x} + \gamma_w^* \qquad (3.15)$$

where γ_v^* and γ_w^* are the additional rotations due to transverse shear corresponding to the minor and major principal directions.

Since, in our case, there is no coupling between bending in the two principal directions, the bending stiffness matrices $[K_b^v]$ and $[K_b^w]$ and the inertia matrices $[M_b^v]$ and $[M_b^w]$ are similar to each other except that in each case corresponding values of section properties are used. Hence the stiffness and mass matrices for the minor principal direction only are derived here.

The strain energy and the kinetic energy in an element of the blade, shown in Figure 3.2, for the I_{min} direction, when transverse shear and rotary inertia are also considered, are

$$u = \frac{1}{2}\int_{x_1}^{x_2} EI_{min}\left(\frac{\partial\psi^*}{\partial x}\right)^2 dx + \frac{1}{2}\int_{x_1}^{x_2} kGA \quad (\gamma_v^*)^2\ dx \tag{3.16}$$

where

$$\psi^* = -\frac{\partial v^*}{\partial x} + \gamma_v^*$$

γ_v^* - rotation due to shear,

k - shear constant†,

A - area of cross-section of blade

and

$$T = \frac{1}{2}\int_{x_1}^{x_2} \rho A\left(\frac{\partial v^*}{\partial t}\right)^2 dx + \frac{1}{2}\int_{x_1}^{x_2} \rho I_{min}\left(\frac{\partial\psi^*}{\partial t}\right)^2 dx \tag{3.17}$$

Assuming the deflection functions

$$\begin{aligned} v^*(x) &= a_1 + a_2\,x + a_3\,x^2 + a_4\,x^3 \\ \gamma_v^*(x) &= a5 + a_6\ x \end{aligned} \tag{3.18}$$

---

† In view of difficulty in calculating k for an aerofoil section a value of 5/6 corresponding to a rectangular section is used.

and substituting in Equations 3.16 and 3.17, we arrive at the stiffness and inertia matrices of the element for the I_{min} direction as

$$[K_b^v] = [B_b]^T [k_b^v] [B_b]$$

and (3.19)

$$[M_b^v] = [B_b]^T [m_b^v] [B_b]$$

corresponding to the deflection vector

$$\{q_b^{v*}\}^T = [\ v_1^* \quad \psi_1^* \quad \gamma_{v1}^* \quad v_2^* \quad \psi_2^* \quad \gamma_{v2}^*\ ] \tag{3.20}$$

$$[B_b]^{-1} = \begin{bmatrix} 1 & x_1 & x_1^2 & x_1^3 & 0 & 0 \\ 0 & -1 & -2x_1 & -3x_1^2 & 1 & x_1 \\ 0 & 0 & 0 & 0 & 1 & x_1 \\ 1 & x_2 & x_2^2 & x_2^3 & 0 & 0 \\ 0 & -1 & -2x_2 & -3x_2^2 & 1 & x_2 \\ 0 & 0 & 0 & 0 & 1 & x_2 \end{bmatrix} \tag{3.21}$$

$$[k_b^v] = \begin{bmatrix} 0 & 0 & 0 & 0 & 0 & 0 \\ & 0 & 0 & 0 & 0 & 0 \\ & & 4R_0 & 12R_1 & 0 & -2R_0 \\ & & & 36R_2 & 0 & -6R_1 \\ & \text{Symmetrical} & & & S_0 & S_1 \\ & & & & & R_0+S_2 \end{bmatrix} \tag{3.22}$$

In the above matrix

$$R_i = \int_{x_1}^{x_2} EI_{min}\, x^i\, dx \quad \text{and} \quad S_i = \int_{x_1}^{x_2} kGA\, x^i\, dx \tag{3.23}$$

and

$$[m_b^v] = \begin{bmatrix} S_0 & S_1 & S_2 & S_3 & 0 & 0 \\ & R_0+S_2 & 2R_1+S_3 & 3R_2+S_4 & -R_0 & -R_1 \\ & & 4R_2+S_4 & 6R_3+S_5 & -2R_1 & -2R_2 \\ & & & 9R_4+S_6 & -3R_2 & -3R_3 \\ & \text{Symmetrical} & & & R_0 & R_1 \\ & & & & & R_2 \end{bmatrix} \tag{3.24}$$

In the above matrix

$$R_i = \int_{x_1}^{x_2} \rho I_{min}\, x^i\, dx \quad \text{and} \quad Si = \int_{x_1}^{x_2} \rho A\, x^i\, dx \tag{3.25}$$

The stiffness and inertia matrices of the element for the I_{max} direction are derived similarly and are given by

$$[K_b^w] = [B_b]^T [k_b^w] [B_b]$$

and (3.26)

$$[m_b^w] = [B_b]^T [m_b^w] [B_b]$$

The matrices $[k_b^w]$ and $[m_b^w]$ are given by Equations 3.22 and 3.24 when I_{min} is replaced by I_{max}.

Linear variations within the element of the area A, I_{min}, I_{max}, K_G and J of the blade section can be assumed requiring the values to be known only at the nodes. For an element of uniform section the stiffness and mass matrices are given in closed form in Tables 3.6, where I is either I_{min} or I_{max} depending on the direction considered. ℓ is the length of the element, and μ is the radius of gyration for the particular direction considered.

The following displacement boundary conditions should be applied when this element is used. For the I_{min} direction:

Simply supported edge	$v^* = 0$
Clamped edge	$v^* = o$; $\psi^* = 0$
Free edge	$\gamma_v^* = 0$

3.5 VIBRATION ANALYSIS OF PRETWISTED BLADES

When the blade is pretwisted it is modelled with straight elements staggered (inclined) at an angle δ to the engine axis.' For any particular element δ is the average pretwist angles of the actual blade measured at the two nodes of the element. Figure 3.3 shows a pretwisted blade and the finite element model with two straight elements.

In this case the individual element stiffness and inertia matrices $[K_b^*]$ and $[M_b^*]$, given by Equation 3.2, which correspond to the deflection vector $\{q_b^*\}$ whose elements are measured along the element principal directions, should be transformed to the engine axis (Oz-Oy coordinates). This requires a rotation matrix [R] relating $\{q_b^*\}$ and $\{q_b\}$

$$\{q_b^*\} = [R] \{q_b\} \tag{3.27}$$

Making use of the above relationship the stiffness and inertia matrices corresponding to the deflection vector $\{q_b\}$ are given by

$$[K_b] = [R]^T [K_b^*] [R]$$

and (3.28)

$$[M_b] = [R]^T [M_b^*] [R]$$

Once this transformation is done the element matrices can be assembled to get the blade system matrices $[K_B]$ and $[M_B]$. Additional stiffness coefficients resulting from rotation should be added to these matrices only after this transformation.

Figure 3.4 gives the relationships between coordinates appearing in the displacement vectors $\{q_b^*\}$ and $\{q_b\}$. Making use of these relationships the rotation matrix [R] is obtained. When transverse shear and rotary inertia are ignored the relationship between the deflection vectors $\{q_b^*\}$ and $\{q_b\}$ becomes

$$
\begin{Bmatrix} v_1^* \\ \psi_1^* \\ v_2^* \\ \psi_2^* \\ w_1^* \\ \theta_1^* \\ w_2^* \\ \theta_2^* \\ \phi_1 \\ \phi_2 \end{Bmatrix}
=
\begin{bmatrix}
c & 0 & s & 0 & 0 & 0 & 0 & 0 & 0 & 0 \\
0 & c & 0 & s & 0 & 0 & 0 & 0 & 0 & 0 \\
0 & 0 & 0 & 0 & 0 & c & 0 & s & 0 & 0 \\
0 & 0 & 0 & 0 & 0 & 0 & c & 0 & s & 0 \\
-s & 0 & c & 0 & 0 & 0 & 0 & 0 & 0 & 0 \\
0 & -s & 0 & c & 0 & 0 & 0 & 0 & 0 & 0 \\
0 & 0 & 0 & 0 & 0 & -s & 0 & c & 0 & 0 \\
0 & 0 & 0 & 0 & 0 & 0 & -s & 0 & c & 0 \\
0 & 0 & 0 & 0 & 1 & 0 & 0 & 0 & 0 & 0 \\
0 & 0 & 0 & 0 & 0 & 0 & 0 & 0 & 0 & 1
\end{bmatrix}
\begin{Bmatrix} v_1 \\ \psi_1 \\ w_1 \\ \theta_1 \\ \phi_1 \\ v_2 \\ \psi_2 \\ w_2 \\ \theta_2 \\ \phi_2 \end{Bmatrix}
$$

where (3.29)

$c = \cos\delta$ and $s = \sin\delta$

or

$$\{q_b^*\} = [R]\{q_b\}$$

Rearrangement of variables in $\{q_b\}$ is carried out to facilitate assembling the complete blade matrices. When transverse shear and rotary inertia are included in the analysis, then

$$\begin{Bmatrix} v_1^* \\ \psi_1^* \\ \gamma_{v1}^* \\ v_2^* \\ \psi_2^* \\ \gamma_{v2}^* \\ w_1^* \\ \theta_1^* \\ \gamma_{w1}^* \\ w_2^* \\ \theta_2^* \\ \gamma_{w2}^* \\ \phi_1 \\ \phi_2 \end{Bmatrix} = \begin{bmatrix} c & 0 & 0 & s & 0 & 0 & 0 & 0 & 0 & 0 & 0 & 0 & 0 & 0 \\ 0 & c & 0 & 0 & s & 0 & 0 & 0 & 0 & 0 & 0 & 0 & 0 & 0 \\ 0 & 0 & c & 0 & 0 & s & 0 & 0 & 0 & 0 & 0 & 0 & 0 & 0 \\ 0 & 0 & 0 & 0 & 0 & 0 & 0 & c & 0 & 0 & s & 0 & 0 & 0 \\ 0 & 0 & 0 & 0 & 0 & 0 & 0 & 0 & c & 0 & 0 & s & 0 & 0 \\ 0 & 0 & 0 & 0 & 0 & 0 & 0 & 0 & 0 & c & 0 & 0 & s & 0 \\ -s & 0 & 0 & c & 0 & 0 & 0 & 0 & 0 & 0 & 0 & 0 & 0 & 0 \\ 0 & -s & 0 & 0 & c & 0 & 0 & 0 & 0 & 0 & 0 & 0 & 0 & 0 \\ 0 & 0 & -s & 0 & 0 & c & 0 & 0 & 0 & 0 & 0 & 0 & 0 & 0 \\ 0 & 0 & 0 & 0 & 0 & 0 & 0 & -s & 0 & 0 & c & 0 & 0 & 0 \\ 0 & 0 & 0 & 0 & 0 & 0 & 0 & 0 & -s & 0 & 0 & c & 0 & 0 \\ 0 & 0 & 0 & 0 & 0 & 0 & 0 & 0 & 0 & -s & 0 & 0 & c & 0 \\ 0 & 0 & 0 & 0 & 0 & 0 & 1 & 0 & 0 & 0 & 0 & 0 & 0 & 0 \\ 0 & 0 & 0 & 0 & 0 & 0 & 0 & 0 & 0 & 0 & 0 & 0 & 0 & 1 \end{bmatrix} \begin{Bmatrix} v_1 \\ \psi_1 \\ \gamma_{v1} \\ w_1 \\ \theta_1 \\ \gamma_{w1} \\ \phi_1 \\ v_2 \\ \psi_2 \\ \gamma_{v2} \\ w_2 \\ \theta_2 \\ \gamma_{w2} \\ \phi_2 \end{Bmatrix} \tag{3.30}$$

where

$$c = \cos\delta \quad \text{and} \quad s = \sin\delta$$

or

$$\{q_b^*\} = [R]\ \{q_b\}$$

3.6 NUMERICAL APPLICATIONS

Numerical results are presented, in this section, which show the effects of rotation, transverse shear and rotary inertia and pretwist on the natural frequencies of uniform rectangular blades.

(A) . First, the variation of the first three nondimensional frequencies $\lambda = \sqrt{\frac{\rho A L^4}{EI}}$ of a uniform rectangular blade with the nondimensional rotation $\Omega^* = \Omega\sqrt{\frac{\rho A L^4}{EI}}$, and the influence of R/L ratio, where R is the radius at the root and L is the length of the blade, on these frequencies, were studied. Values of λ for vibration (a) out of plane of rotation and (b) in the plane of rotation, calculated using four elements, are given in Tables 3.7 to 3.12. In these calculations, the additional stiffness coefficients given in Tables 3.3 and 3.4 are added to the beam bending stiffness matrix.

Boyce (129) has calculated upper and lower bounds of λ for vibration out of plane of rotation for a few values of R/L ratios. In Figure 3.5, values of λ calculated with four elements have been plotted against the nondimensional rotation Ω^* for the value of R/L = 0.1. Only the first two modes of vibration are considered. The upper and lower bounds given by Boyce for this case lie close to the finite element curves.

(B) Next, the effect of transverse shear and rotary inertia on the natural frequencies of a uniform rectangular beam was studied using the new Timoshenko beam finite element developed in section 3.4. A value of k = 0.667 was used and the ratio u/L, where μ is the radius of gyration and L the length of the beam, was chosen to be 0.08. Nondimensional frequency parameter $\lambda = \omega\sqrt{\frac{\rho AL^4}{EI}}$ for a simply supported beam and a cantilever beam, computed using 1 to 6 element models are given in Tables 3.13 and 3.14 along with exact solutions. These results demonstrate the accuracy and convergence of the elements used. Results obtained by Kapur (128) and Archer (79) are also given for comparision in Tables 3.15 and 3.16. In Figures 3.6 and 3.7 percentage error versus number of degrees of freedom have been plotted for these three beam models.

(C) Finally, the efficiency of modelling twisted blades using untwisted beam elements was studied. Dokumaci et al (85) have used beam elements in which pretwist is incorporated, for this problem. They have. computed frequency parameters $\lambda^4 = \frac{\omega^2 \rho AL^4}{EI_{min}}$

for uniform rectangular twisted beams. Here values calculated using untwisted beam elements are compared with those of Dokumaci et al and those given by Anliker and Troesch (82) and Slyper (84). It is seen from the results in Table 3.17, that when the number of elements is increased the results converge rapidly to those given by Dokumaci et al indicatingthat in practical problems use of untwisted beam elements in modelling twisted blades would be satisfactory, thus avoiding the additional complication involved in formulating the beam element which incorporates pretwist.

CHAPTER 4

ANALYSIS OF COUPLED BLADE-DISC VIBRATION IN AXIAL FLOW TURBINES

4.1 INTRODUCTION

The vibration of a bladed rotor is found to be similar to that of an unbladed disc. The rotor oscillates in a coupled blade-disc mode which is also characterised by diametral and circular nodes, Figure 4.1. The blades, being constrained in the disc at the rim, will vibrate in bending motion at diametral antinodes, in torsional motion at nodes, and in combined bending-torsion elswhere, Figure 4.2. The circular nodes may lie in the disc, but will more commonly be located in the blades.

A method of analysis is developed in section 4.2 for bladed rotors with a large number of identical blades. The blade loading on the rim are assumed to be continuously distributed around the rim. With this assumption, formulation of an exact method of analysis is possible for rotors of nonrotating simple configurations. This method utilizes the exact dynamic stiffness coefficients for the disc, rim and the blade, and is detailed in section 4.3.

For rotors of more general geometry, a finite element method is developed, in section 4.4, which utilizes the annular plate bending element for the disc and the conventional beam element for the blades. This method includes the effect of a rim and torsional distorsions in the blades, which are ignored by other investigators (118,120). Effects of rotation, temperature' gradient and other in-plane stresses are also considered. The method is then extended to include transverse shear and rotary inertia both in the disc and blades.

A number of numerical studies are presented, in section 4.5, which examine critically the accuracy and convergence of the calculated solutions by comparision with experimental data for bladed rotors of simple and complex geometry.

4.2 METHOD OF ANALYSIS

4.2.1 System Configuration And Deflections

Figure 4.3 shows the idealized model of the rotor and for analysis purposes the rotor is considered as three distinct subsystems.

(1) The disc web described by thin plate theory,

(2) The disc rim treated as a solid compact ring,

(3) The array of blades, each of which is considered to behave as a beam described by Euler-Bernoulli theory.

Ignoring torsional vibration of the system about the oz axis and considering only the flexural vibration, the coordinates shown in Figure 4.3 areassumedto describe the distortions of the subsystems.

Considering stations 1,2,...,i in the disc as shown in Figure 4.3 the deflection vector for the disc is written as

$$[q_D(\xi)] = \begin{bmatrix} w_1(\xi) \\ \theta_1(\xi) \\ w_2(\xi) \\ \theta_2(\xi) \\ \cdot \\ \cdot \\ \cdot \\ w_i(\xi) \\ \theta_i(\xi) \end{bmatrix} \tag{4.1}$$

Considering only the centroidal distortions of the rim, the deflection vector for the rim is written as

$$[q_R(\xi)] = \begin{bmatrix} w_j(\xi) \\ \theta_j(\xi) \end{bmatrix} \tag{4.2}$$

For the blade with stations k, k+1, ... the deflection vector is written as

$$[q_B(\xi)] = \begin{bmatrix} v_k(\xi) \\ \psi_k(\xi) \\ v_{k+1}(\xi) \\ \psi_{k+1}(\xi) \\ \cdot \\ \cdot \\ \cdot \\ w_k(\xi) \\ \theta_k(\xi) \\ w_{k+1}(\xi) \\ \theta_{k+1}(\xi) \\ \cdot \\ \cdot \\ \cdot \\ \phi_k(\xi) \\ \phi_{k+1}(\xi) \\ \cdot \\ \cdot \\ \cdot \end{bmatrix} \tag{4.3}$$

Consider the system vibrating with m nodal diameters. If ξ is the angle measured from a reference diametral antinode, then for the disc subsystem,

$$\{q_D(\xi)\} = \begin{bmatrix} \bar{w}_1 \\ \bar{\theta}_1 \\ \cdot \\ \cdot \\ \cdot \\ \bar{w}_i \\ \bar{\theta}_i \end{bmatrix} \cos m\xi = \{\bar{q}_D\} \cos m\xi \qquad (4.4)$$

where $\bar{w}_1$, $\bar{\theta}_1$, . . . etc are the amplitudes of vibration at the reference antinode. Similarly for the rim

$$\{q_R(\xi)\} = \begin{bmatrix} \bar{w}_j \\ \bar{\theta}_j \end{bmatrix} \cos m\xi = \{\bar{q}_R\} \cos m\xi \qquad (4.5)$$

The blades are assumed to be fixed to the rim and are thus constrained to retain their orientation at the root. The flexural axes are assumed to coincide with the centroidal axis and hence there is no coupling between bending and torsion within the blade. Then a blade at an antinode is displaced in bending only as shown in Figure 4.2. However because of blade stagger, or in general, because of the pretwist in the blade, bending may take place in both axial and tangential planes. A blade at a node is displaced in torsion only. Blades at any other angular locations experience both bending and torsion. Thus the deflections of a blade at an angle may be written as

$$\{q_B(\xi)\} = \begin{bmatrix} \bar{v}_k \cos m\xi \\ \bar{\psi}_k \cos m\xi \\ \vdots \\ \bar{w}_k \cos m\xi \\ \bar{\theta}_k \cos m\xi \\ \vdots \\ \bar{\phi}_k \sin m\xi \\ \vdots \end{bmatrix} = [R]\{\bar{q}_B\} \tag{4.6}$$

where

$$[R] = \begin{bmatrix} [C] & [0] & [0] \\ [0] & [C] & [0] \\ [0] & [0] & [S] \end{bmatrix} \tag{4.7}$$

where [C] and [S] are diagonal matrices with diagonal terms $\cos m\xi$ and $\sin m\xi$ respectively, and $\bar{v}_k$, $\bar{\psi}_k$, ..., $\bar{w}_k$, $\bar{\theta}_k$,... are the bending amplitudes of the blade at the reference diametral antinode, while $\bar{\phi}_k$,... are the twisting amplitudes of the blade at a diametral node.

4.2.2 Dynamic Stiffness Of The Subsystems

The individual dynamic stiffness matrices are directly used for the disc and rim subsystems. Thus,

$$[D_D] = [K_D] - \omega^2 [M_D]$$

and (4.8)

$$[D_R] = [K_R] - \omega^2 [M_R]$$

where $[D_D]$,$[K_D]$ and [MD] are the dynamic stiffness, stiffness and mass matrices respectively of the disc corresponding to the deflection vector $\{\bar{q}_D\}$ and [DR] ,$[K_R]$ and $[M_R]$ are the corresponding matrices for the rim with respect to the deflection vector $\{\bar{q}_R\}$.

The dynamic stiffness matrix [D,] for the vibrating array of blades may be obtained from the stiffness and mass matrices $[K_B]$ and $[M_B]$ of a single blade in the following manner, provided we assume sufficient number of identical blades to be present on the rotor, such that the resulting loading on the rim can be considered to be continuously distributed in a sinusoidal pattern around the rotor as shown in Figure 4.2. This condition is likely to be satisfied in typical rotors vibrating-in modes involving low numbers of nodal diameters.

The dynamic stiffness relation for a blade vibrating at a frequency ω and located at a polar angle ξ from the reference antinode is

$$\{Q_B(\xi)\} = [\,[K_B] - \omega^2\,[M_B]\,]\,\{q_B(\xi)\} \tag{4.9}$$

where $\{q_B(\xi)\}$ is defined by Equation 4.3 and $\{Q_B(\xi)\}$ is the corresponding force vector. It should be noted that matrices $[K_B]$ and $[M_B]$ are independent of ξ.

Assuming that the blade loading on the rotor to be continuously distributed, the total energy, strain energy and kinetic energy, of the vibrating blades between the angles ξ and $\xi + d\xi$ is

$$dE = \frac{1}{2}\,\frac{Z}{2\pi}\,\{q_B(\xi)\}^T\,[\,[K_B] - \omega^2[M_B]\,]\,\{q_B(\xi)\}\,d\xi$$

where Z is the number of blades in the rotor. Substituting for $\{q_B\}$ from Equation 4.6

$$dE = \frac{1}{2}\,\frac{Z}{2\pi}\,\{\bar{q}_B\}^T\,[R]^T\,[\,[K_B] - \omega^2[M_B]\,]\,[R]\,\{\bar{q}_B\}\,d\xi$$

Integrating between the limits $\xi = 0$ and $\xi = 2\pi$ we get the total energy

$$E = \frac{1}{2}\,C\,\frac{Z}{2}\,\{\bar{q}_B\}^T\,[\,[K_B] - \omega^2[M_B]\,]\,\{\bar{q}_B\} \tag{4.10}$$

where

$C = 2$ if $m = 0$; and $C = 1$ if $m \geq 1$

Hence the required dynamic stiffness matrix of the vibrating array of blades corresponding to the deflection vector $\{\bar{q}_B\}$ is

$$[D_B] = C\frac{Z}{2}[\,[K_B] - \omega^2[M_B]\,] \tag{4.11}$$

4.2.3 Dynamic Coupling Of The Subsystems

The dynamic stiffness relation for the complete rotor system is obtained by combining the individual relations for the disc, rim and blade subsystems, taking into account the compatibility requirements at their boundaries.

The torsion of the blade at the root, $\phi_k(\xi)$, is related to the axial deflection $w_k(\xi)$; thus

$$\phi_k(\xi) = \frac{1}{R}\frac{\partial}{\partial\xi}\{w_k(\xi)\}$$

$$= -\frac{m}{R}\bar{w}_k \sin m\xi$$

Therefore

$$\bar{\phi}_k = -\frac{m}{R}\bar{w}_k \tag{4.12}$$

where R is the radius of the blade-rim attachment.

The remaining relations ensure compatibility between the three subsystems and hence depend on the nature of blade fixing. With the commonly used dovetail or fir-tree attachment cantilever blades can be assumed and in such cases the following, relations hold.

$$\bar{w}_i = \bar{w}_j + e_1 \bar{\theta}_j$$

$$\bar{\theta}_i = \bar{\theta}_j = \bar{\theta}_k$$

$$\bar{w}_k = \bar{w}_j - e_2 \bar{\theta}_j$$

$$\bar{u}_k = 0$$

$$\bar{\psi}_k = 0$$

where e_1 and e_2 are the distances from the rim centroidal axis to the disc-rim junction and blade-rim junction respectively, Figure 4.3. Considering such cantilever blades all the coordinates at stations j and k can be conveniently described in terms of $\bar{w}_i$ and $\bar{\theta}_i$ with the following transformation relations.

$$\begin{vmatrix} \bar{w}_j \\ \bar{\theta}_j \\ \bar{v}_k \\ \bar{\psi}_k \\ \bar{w}_k \\ \bar{\theta}_k \\ \bar{\phi}_k \end{vmatrix} = \begin{vmatrix} 1 & -e_1 \\ 0 & 1 \\ 0 & 0 \\ 0 & 0 \\ 1 & -(e_1+e_2) \\ 0 & 1 \\ -\frac{m}{R} & \frac{m}{R}(e_1+e_2) \end{vmatrix} \begin{bmatrix} \bar{w}_i \\ \bar{\theta}_i \end{bmatrix} \qquad (4.13)$$

This relationship is sufficient to allow assembly of the dynamic stiffness matrix of the coupled blade-rim-disc system.

4.3 EXACT SOLUTION OF NON-ROTATING ROTORS OF SIMPLE GEOMETRY

When non-rotating rotors with uniform disc and uniform blades are considered, exact dynamic stiffness matrices for the disc, rim and blades can be derived. This resulting solutions are exact in so far as thin plate theory, Euler-Bernoulli beam theory and the assumption of continuous blade loading hold true and are useful in examining the accuracy and convergence of the finite element solutions.

In such cases the disc dynamic matrix $[D_D]$ need be derived with respect to only the axial deflection $\bar{w}_i$ and the radial slope $\bar{\theta}_i$ at the outer boundary along the reference anti-node. Thus the disc deflection vector has only two generalised coordinates.

$$\overline{\{q_D\}} = \begin{bmatrix} \bar{w}_i \\ \bar{\theta}_i \end{bmatrix} \tag{4.14}$$

The derivation of the (2 x 2) dynamic stiffness matrix for a uniform annular disc with its inner boundary fixed and the outer boundary free is given below. Similar matrices for other boundary conditions at the inner boundary can be readily derived.

4.3.1 Dynamic Stiffness Of The Disc

The deflections $w_i(\xi)$ and' $\theta_i(\xi)$ have associated forces, corresponding to sinusoidal distributions of shear force and bending moment around the rotor, and which may be related to the deflections by a dynamic stiffness matrix for the case of a uniform thickness disc, either by inversion of the corresponding receptance matrix relation given by McLeod and Bishop (42), or directly as follows.

Consider a thin annular disc, of uniform thickness h, clamped at the inner radius a, and subjected to transverse shear force $V_i \cos m\xi\, e^{iwt}$ and radial bending moment $M_i \cos m\xi\, e^{i\omega t}$ around the outer radius b. The governing differential equation is,

$$\nabla^4 w(r,\xi) + \frac{\rho h}{D} \frac{\partial^2}{\partial t^2} \{ w(r,\xi)\} = 0 \tag{4.15}$$

where $w(r,\xi)$ is the transverse deflection, ρ is the material mass density, and D is the flexural rigidity.

For the case being considered the solution of this equation is

$$w(r,\xi) = [PJ_m(kr) + QY_m(kr) + RI_m(kr) + SK_m(kr)] \cos m\xi$$

$$= W(r) \cos m\xi \tag{4.16}$$

where

ω - vibratory frequency in rad./second,

$\overline{w}(r)$ - amplitude at an antinode,

J_m, Y_m - Bessel functions of first and second kind of integer order m,

I_m, K_m – modified Bessel functions of first and second kind of integer order m

$$k = \left(\frac{\rho h\, \omega^2}{D} \right)^{1/4}$$

Using the sign convention established in Figure 4.3

$$\theta = - \frac{\partial w}{\partial r}$$

$$Mr = - D \left[\frac{\partial^2 w}{\partial r^2} + \nu \left(\frac{1}{r} \frac{\partial w}{\partial r} + \frac{1}{r^2} \frac{\partial^2 w}{\partial \xi^2} \right) \right]$$

$$M_{r\xi} = D(1-\nu) \left[\frac{1}{r} \frac{\partial^2 w}{\partial r \partial \xi} - \frac{1}{r^2} \frac{\partial w}{\partial r} \right] \tag{4.17}$$

$$Q_r = - D \left[\frac{\partial^3 w}{\partial r^3} + \frac{1}{r} \frac{\partial^2 w}{\partial r^2} - \frac{1}{r^2} \frac{\partial w}{\partial r} + \frac{1}{r^2} \frac{\partial^3 w}{\partial r\, \partial \xi^2} + \frac{2}{r^3} \frac{\partial^2 w}{\partial \xi^2} \right]$$

$$V = Q_r - \frac{1}{r} \frac{\partial}{\partial \xi} M_{r\xi}$$

Substituting for $w(r,\xi)$ from Equation 4.16,

$$\theta(r,\xi) = - [\, PA_1(kr) + QA_2(kr) + RA_3(kr) + SA_4(kr) \,] \cos m\xi$$

$$= \overline{\theta}(r) \cos m\xi$$

$$M_r(r,\xi) = - [\, PA_5(kr) + QA_6(kr) + RA_7(kr) + SA_8(kr) \,] \cos m\xi$$

$$= \overline{M}_r(r) \cos m\xi$$

$$V(r,\xi) = -D\,[\,PA_9(kr) + QA_{10}(kr) + RA_{11}(kr) + SA_{12}(kr)\,]\cos m\xi$$

$$= \overline{V}(r)\cos m\xi \qquad (4.18)$$

where A_1 through A_{12} are linear combinations of the Bessel functions of order m and m-I-1, given in Table 4.1. Applying the boundary conditions

$$w(a,\xi) = 0 \qquad \theta(a,\xi) = 0$$

$$w(b,\xi) = w_i(\xi) \qquad \theta(b,\xi) = \theta_i(\xi)$$

$$V(b,\xi) = V_i(\xi) \qquad M_r(b,\xi) = M_{ri}(\xi)$$

and using Equations 4.16 and 4.18 gives,

$$\begin{bmatrix} V_i(\xi) \\ M_i(\xi) \end{bmatrix} = [D] \begin{bmatrix} w_i(\xi) \\ \theta_i(\xi) \end{bmatrix} \cos m\xi \qquad (4.19)$$

where [D] is the matrix given in Table 4.2

Consider a unit displacement vector $\begin{bmatrix} \overline{w}_i \\ \overline{\theta}_i \end{bmatrix}$ is imposed at the reference antinode, at the outer boundary, then following standard procedure the associated force vector will be,

$$\begin{bmatrix} \overline{V}_i \\ \overline{M}_i \end{bmatrix} = \int_0^{2\pi} [D] \begin{bmatrix} \overline{w}_i \\ \overline{\theta}_i \end{bmatrix} \cos^2 m\xi \; b \; d\xi \qquad (4.20)$$

$$= C\pi \;\; b \;\; [D] \begin{bmatrix} \bar{w}_i \\ \bar{\theta}_i \end{bmatrix}$$

where

$$C = 2 \text{ if } m = 0 \quad \text{and } C = 1 \text{ if } m \geq 1$$

Thus the required dynamic stiffness matrix is given by

$$[D_D] = C\pi \;\; b \;\; [D] \tag{4.21}$$

4.3.2 Dynamic Stiffness Of The Rim

The formulation of the exact dynamic stiffness relation for the rim, treated as a thin ring is well known (130). For a thin ring vibrating at frequency ω with m nodal diameters, when shear deformation and rotary inertia are neglected, it takes the form,

$$\begin{bmatrix} \bar{V}_j \\ \bar{M}_j \end{bmatrix} = [D_R] \begin{bmatrix} \bar{w}_j \\ \bar{\theta}_j \end{bmatrix} \tag{4.22}$$

where $[D_R]$ is the dynamic stiffness matrix of the ring and is given in Table 4.3.

4.3.3 Dynamic Stiffness Of The Blade Array

When we consider uniform untwisted blades, the dynamic stiffness relation for a single blade vibrating with frequency ω

and located at an angle ξ from the reference antinode is

$$\{Q_k\} = [D_b] \{q_k\} \tag{4.23}$$

where

$$\{q_k\} = \begin{bmatrix} v_k \\ \psi_k \\ w_k \\ \theta_k \\ \phi_k \end{bmatrix}$$

and the matrix $[D_b]$ is given in Table 4.4.

In Table 4.4

E, G - elastic moduli,

I_1, I_2 - principal minimum and maximum second moment of area of the blade cross-section respectively,

δ stagger angle; angle between the engine axis Oz and the I_{min} direction, Figure 3.1

K_G - St. Venant torsional stiffness of the blade cross-section,

and

$$\lambda_1 = \left(\frac{\omega^2 \rho}{EI_1} \right)^{1/4}$$

$$\lambda_2 = \left(\frac{\omega^2 \rho}{EI_2} \right)^{1/4}$$

$$\lambda_3 = \left(\frac{J}{GK_G} \right)^{1/2}$$

ρ - mass density of blade material,

J - mass polar moment of inertia of blade section,

ℓ - length of blade.

The matrix $[D_b]$ is of size (5x5), since only the five displacements at the root of the blade are involved. This matrix is readily obtained from the receptance relations tabulated for a free-free beam, (131), transformed from local principal axes, through stagger angle δ to the coordinate system used here.

From Equation 4.11, the dynamic stiffness matrix for the array of blades is obtained by multiplying that of a single blade by $C \frac{Z}{2}$, where Z is the number of blades in the rotor. Hence the dynamic stiffness matrix for the array of blades is

$$[D_B] = C \frac{Z}{2} [D_b] \tag{4.24}$$

4.3.4 Dynamic Stiffness Of The Disc-Rim-Blade System

The dynamic stiffness matrix for the complete rotor system is obtained by combining the individual matrices for the disc, rim and blades, taking into account the compatibility relations given by Equation 4.13. The result is a (2x2) dynamic stiffness relationship involving only the deflections $\bar{w}_i$ and $\bar{\theta}_i$ A non-trivial solution is obtained when the determinant of this matrix is zero, and corresponds to the natural frequencies of the system. For numerical calculations the zeros of the determinant are sought by iterating with the frequency ω as the variable.

4.4 FINITE ELEMENT SOLUTION OF ROTORS OF GENERAL GEOMETRY

For rotors of general geometry with arbitrary discs and pretwisted nonuniform blades numerical procedures are adopted to obtain the subsystem dynamic stiffness matrices $[D_D]$ and $[D_B]$ of the disc and the array of blades respectively. The annular plate bending finite elements developed in chapter- 2 can be readily used here.

4.4.1 Dynamic Stiffness Of The Disc-Rim-Blade System Neglecting Transverse Shear And Rotary Inertia

The method of analysis.described here utilizes the finite element models developed for the disc and blade in section 2.2 and 3.2. Thus the matrices $[K_D]$ and $[M_D]$ of the disc subsystem appearing in Equation 2.28 are directly used in the dynamic stiffness relation

$$\{\overline{Q}_D\} = [\ [K_D] - \omega^2 [M_D]\ ]\ \{\overline{q}_D\}$$

$$= [D_D]\ \{\overline{q}_D\} \tag{4.25}$$

matrix is zero, and corresponds to the natural frequencies of the system. For numerical calculations the zeros of the determinant are sought by iterating with the frequency ω as the variable.

4.4 FINITE ELEMENT SOLUTION OF ROTORS OF GENERAL GEOMETRY

For rotors of general geometry with arbitrary discs and pretwisted nonuniform blades numerical procedures are adopted to obtain the subsystem dynamic stiffness matrices $[D_D]$ and $[D_B]$ of the disc and the array of blades respectively. The annular plate bending finite elements developed in chapter 2 can be readily used here.

4.4.1 Dynamic Stiffness Of The Disc-Rim-Blade System Neglecting Transverse Shear And Rotary Inertia

The method of analysis.described here utilizes the finite element models developed for the disc and blade in section 2.2 and 3.2. Thus the matrices $[K_D]$ and $[M_D]$ of the disc subsystem appearing in Equation 2.28 are directly used in the dynamic stiffness relation

$$\{\overline{Q}_D\} = [\,[K_D] - \omega^2[M_D]\,]\,\{\overline{q}_D\}$$

$$= [D_D]\,\{\overline{q}_D\} \tag{4.25}$$

Similarly for the array of blades matrices $[K_B]$ and $[M_B]$ from Equation 3.2 are used here, thus,

$$\{\bar{Q}_B\} = C\pi \frac{Z}{2} [[K_B] - \omega^2 [M_B]] \{\bar{q}_B\}$$

$$= [D_B] \{\bar{q}_B\} \qquad (4.26)$$

In this analysis, the stations 1,2,..., i considered in section 4.2.1 are the finite element nodes in the disc subsystem and hence the disc deflection vector $\{\bar{q}_D\}$ is given by Equation 4.4. Similarly the stations k, k+l,... considered in section 4.2.1 are the finite element nodes in any of the blades and hence the blade subsystem deflection vector $\{q_B\}$ is given by Equation 4.6.

The number of degrees of freedom in each of these subsystems depend on the number of elements used in each case. The constraint conditions given by Equation 4.13, now gives the relationships between the degrees of freedom at nodes i,j and k, where j is the centroid of the rim. In this analysis, for the rim, the dynamic stiffness relation given by Equation 4.22 is used. The subsystems are coupled satisfying the relations given by Equation 4.13 and the following dynamic stiffness relation for the entire system is obtained.

$$\{\bar{Q}_S\} = [[K_S] - \omega^2 [M_S]] \{\bar{q}_S\} \qquad (4.27)$$

When free vibration of the system is considered Equation 4.27 reduces to an algebraic eigen value problem, which may be solved by any of the standard procedures. It should be noted that, here, as in the disc alone vibration problem, a set of eigen value problems result, one for each diametral mode configuration.

The use of the annular element for the disc makes it possible *to* effectively model discs with any arbitrary radial profile. Moreover, the initial in-plane stresses resulting from rotation and radial temperature gradient and other loading can be computed and their effect on the vibration frequencies of the system can be taken into account. Similarly variation in section properties of the blades, pretwist in the blades, and the effect of in-plane stresses in the blades are readily included.

4.4.2 Dynamic Stiffness Of The Disc-Rim-Blade System Including Transverse Shear And Rotary Inertia

In practical rotors the disc is moderately thick and the use of methods based on thin plate theory may not result in satisfactory analysis. Therefore, the finite element method of analysis developed is now extended to include transverse shear and rotary inertia, both in the disc and blades.

This analysis is very similar. to the one described in section 4.4.1 above for bladed rotors, except, now the rim, if present is considered to be a part of the disc. Hence, the whole rotor system is divided into two subsystems.

(1) The disc and rim subsystem described by Mindlin's plate theory,

(2) The array of blades, each of which is considered to behave as a beam described by Timoshenko beam theory.

The annular Thick Disk Element-l, developed in chapter 2, section 2.4, is used to model the disc and rim. The blades are modelled with the Timoshenko beam element described in chapter 3, section 3.4, Hence each station in the disc has four degrees of freedom and at station i these are, Figure 4.4,

$$\{\bar{q}_i\}^T = [\ \bar{w}_i \quad \bar{\theta}_i \quad \bar{\gamma}_{ri} \quad \bar{\gamma}_{\xi i}\ ] \tag{4.28}$$

Each station in the blade has seven degrees of freedom and at station k these afe,

$$\{\bar{q}_k\}^T = [\ \bar{v}_k \quad \bar{\psi}_k \quad \bar{\gamma}_{vk} \quad \bar{w}_k \quad \bar{\theta}_k \quad \bar{\gamma}_{wk} \quad \bar{\phi}_k\ ] \tag{4.29}$$

When the subsystems are connected together, the following relationships between the degrees of freedom at stations i and k exist, and these should be satisfied

$$\begin{bmatrix} \bar{v}_k \\ \bar{\psi}_k \\ \bar{\gamma}_{vk} \\ \bar{w}_k \\ \bar{\theta}_k \\ \bar{\gamma}_{wk} \\ \bar{\phi}_k \end{bmatrix} = \begin{bmatrix} 0 & 0 & 0 & 0 & 0 \\ 0 & 0 & 0 & 0 & 0 \\ 0 & 0 & 0 & 0 & 1 \\ 1 & 0 & 0 & 0 & 0 \\ 0 & 1 & 0 & 0 & 0 \\ 0 & 0 & 1 & 0 & 0 \\ -\frac{m}{R} & 0 & 0 & 1 & 0 \end{bmatrix} \begin{bmatrix} \bar{w}_i \\ \bar{\theta}_i \\ \bar{\gamma}_{ri} \\ \bar{\gamma}_{\xi i} \\ \bar{\gamma}_{vk} \end{bmatrix} \tag{4.30}$$

where R is the radius at the root of the blade

4.5 NUMERICAL APPLICATIONS

4.5.1 Comparision Of Exact And Finite Element Solutions For Simple Nonrotating Rotors

The validity and accuracy of the analysis developed in sections 4.3 and 4.4 have been assessed by comparing numerical results of the coupled frequencies with experimental data on three simple nonrotating bladed disc models. For the first two models experimental data were obtained by Mr. R. W. Harris, a senior undergraduate student at Carleton University. The third model is that used by Jager (120).

All these models are of mild steel and comprise uniform thickness annular discs clamped at the inner radius and uniform untwisted rectangular blades cantilevered at the outer boundary of the disc or rim. The blades are set at a stagger angle δ = 45" in models I and II, and at δ = 50" in model III. The dimensions. and other details of these models are given in Table 4.5. A rim is present in models I and II, but absent in III. The first six. cantilevered blade alone frequencies of these models are given in in Table 4.6. For models I and II experimental measurements of frequency were made by exciting the models using an electromagnet. A barium titanate accelerometer probe was used to detect resonance and to identify mode shapes. Figure 4.5 illustrates the vibrating bladed disc models with sand pattern showing nodal diameters.

Coupled system frequencies of thesethree models were calculated by finite element models comprising various numbers of elements. These frequencies were also calculated using the exact method. As already mentioned, these values are exact in so far the assumption of continuous blade loadings on the rim is valid. Also certain tolerances on the value of the determinant, which should otherwise be zero, were necessary.. The results of the finite element analysis should converge to the exact values as the number of elements are increased.

The numerical results for models I and I-I are given in Tables 4.7 and 4.8 along with experimental results. It is seen that agreement between finite element, exact and measured frequencies is excellent, and indeed that just two blade elements and two disc elements yield the first three to four modes for any untwisted rectangular blades cantilevered at the outer boundary of the disc or rim. The blades are set at a stagger angle δ = 45" in models I and II, and at δ = 50" in model III. The dimensions. and other details of these models are given in Table 4.5. A rim is present in models I and II, but absent in III. The first six. cantilevered blade alone frequencies of these models are given in in Table 4.6. For models I and 11 experimental measurements of frequency were made by exciting the models using an electromagnet. A barium titanate accelerometer probe was used to detect resonance and to identify mode shapes. Figure 4.5 illustrates the vibrating bladed disc models with sand pattern showing nodal diameters.

Coupled system frequencies of thesethree models were calculated by finite element models comprising various numbers of elements. These frequencies were also calculated using the exact method. As already mentioned, these values are exact in so far the assumption of continuous blade loadings on the rim is valid. Also certain tolerances on the value of the determinant, which should otherwise be zero, were necessary.. The results of the finite element analysis should converge to the exact values as the number of elements are increased.

The numerical results for models I and I-I are given in Tables 4.7 and 4.8 along with experimental results. It is seen that agreement between finite element, exact and measured frequencies is excellent, and indeed that just two blade elements and two disc elements yield the first three to four modes for any given nodal diameter configuration, with engineering accuracy for these models. Convergence of finite element solution is rapid and monotonic from above as expected.

The first six coupled system frequencies are plotted against increasing number of nodal diameters in Figures 4.6 and 4.7 for models I and II. As the number of nodal diameters increases, the combined frequencies should degenerate to the cantilevered blade alone frequencies and this is seen to be the case from these graphs.

In model III, which was used by Jager, no rim was present, so that the blades overhung the disc at the point of attachment. In Table 4.9 the numerical and experimental frequencies given by Jager are compared with the finite element and exact solutions. Jager's numerical model comprised ten lumped masses in the disc and ten lumped masses in the blades. Again it is seen that good agreement is obtained between the various frequencies; more important the efficiency of the finite element model is significantly better than that of the lumped mass model. The increasing divergence between calculated and measured values for the higher modes may result from the incomplete attachment of blades to disc, since the blade chord is much greater than the thickness of the disc.

4.5.2 The Effect Of System Parameters On The Frequencies Of Simple Nonrotating Rotors

It would be useful, as in most of the other engineering problems, to nondimensionalize the system frequencies of the bladed disc. In view of the unusually large number of parameters involved this is extremely difficult. Alternatively the variation of the frequencies with respect to a selected number of parameters, which would give some qualitative insight to the problem, may be studied. These parameters may be chosen to suit particular situations.

As an example, the effects of the following three parameters on the frequencies of a bladed disc are studied. The parameters considered are,

(1) $\frac{\ell}{b}$ ratio, where ℓ is the length of the blade and b is the outer radius of the disc,

(2) blade aspect ratio $\frac{\ell}{d_b}$, where d_b is the chord of the blade

(3) stagger angle 6.

Seven different cases of the model were studied. In all these cases the model comprises of an uniform disc with constant inner radius and thickness. The blades, which are uniform and untwisted, are cantilevered at the outer boundary of the disc with a stagger angle. In order to minimise the number of parameters the rim is omitted. The thickness to chord ratio is fixed at 8%, which is typical of compressor blading. Only the outer radius b of the disc, the length ℓ of the blade and the stagger angle δ are changed independently. The number of blades in the model depends on the chord of the blade, The various dimensions of the model for the seven cases considered are given in Table 4.10, and the first four cantilevered blade alone frequencies in Table 4.11.

In all these cases the first four system frequencies were calculated with the exact method for m = 2 to 6. These frequencies ω are divided by the first blade alone frequency ω_1^b and the ratio $\frac{\omega}{\omega_1^b}$ are given in Table4.13. Figures 4.8 to 4.10 show the variation of the first system frequency and Figures 4.11 to 4.13 the next three frequencies with respect to the three system parameters chosen.

From Figures 4.8 and 4.11 it is seen that when the value of $\frac{a}{b}$ is low, in other words when the blades are shorter compared to disc radius, the system frequencies are very low compared to the blade alone frequencies, at lower numbers of diametral nodes, and the vibration is controlled by the disc. These frequencies increase in their values with increasing number of diametral nodes and converge to the blade frequencies. Therefore the influence of disc is considerable when short blades are used, especially at lower values of m .

From Figures 4.9 and 4.12 it is seen that when the blade aspect ratio is lower the system frequencies are lower than the blade alone frequencies. In all the three cases considered the first blade frequencies are in bending in the I_{min} direction. Therefore with increasing number of nodal diameters the system frequencies converge to the first blade alone frequencies. But the higher modes of vibration of the blades in the three cases are different nature. Hence convergence of system frequencies are to the individual blade frequencies in each case.

From Figures 4.10 and 4.13 it is seen that for the first mode of vibration the system frequencies are lower for lower values of δ, the stagger angle. But for the higher modes this is reversed and the system frequencies are higher for lower values of δ. In the case of first, second, and fourth modes, where the blade frequencies are bending frequencies, the system frequencies converge rapidly to the blade alone frequencies with increasing values of m. But in the case of the third mode, where the blade frequency is a torsional frequency, convergence is slow with increasing value of m.

4.5.3 The Effect Of Rotation On The Frequencies Of Simple Rotors

When the bladed disc is rotating at speed, the centrifugal stresses developed both in the disc and the blades increase the stiffness of the entire system and the natural frequencies of the bladed disc are substancially modified.

In the finite element analysis of the bladed disc the effect of rotation can be readily included, since additional stiffness coefficients for the disc and blade elements are available. The stresses in the disc are calculated including the blade loading at the rim. The frequencies of bladed disc model I were calculated neglecting transverse shear and rotary inertia, but adding the centrifugal stiffening effect when the bladed disc was considered rotating at 3500 rpm and 7000 rpm, which are typical speeds of rotors of similar dimensions; Unfortunately no experimental or other numerical results are available to compare the results. These results are given in Table 4.14, along with the results of the stationary bladed disc. Comparision of results in Table 4.14 shows that variations in the frequencies are considerable at lower modes of vibration for each diametral node configuration, whereas frequencies of higher modes are not affected much.

4.5.4 The Effect Of Transverse Shear And Rotary Inertia On The Frequencies Of Simple Rotors

The finite element method of analysis outlined in section 4.4.2, which includes transverse shear and rotary inertia was applied in the analysis of bladed disc models I and II. The first six frequencies of each of the diametral node configuration, m = 2 to 6, obtained are given in Tables 4.15 and 4.16. These results should be expected to be lower than those in Tables 4.7 and 4.8, which were obtained neglecting transverse shear and rotary inertia in the analysis. Comparision of results in these tables show this to be true except in the case of a few lower modes when $m = 2$. This discrepancy is thought to be due to the difference in the models assumed for the rim. In the earlier case the rim is treated as a thin ring with constant radial slope from the inner to the outer boundaries. In the second case the rim is assumed to be a part of the disc and hence its radial slope can vary across the rim.

4.5.5 Calculated And Measured Frequencies Of A Complex Turbine Rotor

The finite element method of analysis developed for bladed discs was also used to calculate the natural frequencies of a complex turbine rotor. Experimental results and other data for this rotor were provided by Dr. Armstrong of Rolls Royce (1971) Ltd. The disc of the rotor is the same analysed in chapter 2, section 2.4.2. The dimensions of the disc are given in Table 2.49. Other details of the rotor are given in Figure 4.14. Section properties of the blades are given in Table 4.17.

Since the computed frequencies of the disc alone were satisfactory only when transverse shear and rotary inertia were included in the analysis, here also these effects were considered.

The blades of the rotor are of aerofoil section and have pretwist and other complicating factors, and therefore the Timoshenko beam finite element model used in the analysis should not be expected to give accurate results for the blades. No torsional stiffness data was made available for this aerofoil section; thus the effect of blade torsion is necessarily neglected. The cantilevered blade alone frequencies calculated with five Timoshenko beam elements are given in Table 4.18. As expected only the first computed frequency agrees closely with the experimental value.

The rotor was modelled with 6 Thick Disc Element-l and 5 Timoshenko beam elements. In both cases linear variations of section properties within the element were assumed. Details of the finite element model are given in Table 4.19. As mentioned earlier, the error in most of the disc computed frequencies is almost constant and is around 7%. This may be due to a higher value of Youngs modulus E assumed in the calculations. Therefore here the coupled frequencies were calculated using two different values for E_{disc}. These results are given in Table 4.20 along with experimental values. The first frequencies of each diametral node configuration are in fairly good agreement with the experimental results, Deviations in the second frequencies should be due to the inadequacy of the blade model. Use of an improved blade model should improve the results considerably.

CHAPTER 5

SUMMARY AND CONCLUSIONS

In this investigation of the application of the finite element method to the vibration analysis of axial flow turbines, the following important novel techniques have been evolved.

(1) New finite elements for the flexure of complete thin and moderately thick circular and annular plates (discs) have been derived, and critically examined for static and vibration problems.

(2) The formulation of these new disc elements has been extended to include the effects of in-plane stresses such as might result from rotation or thermal gradient. This aspect of the work is also new.

(3) A novel method of coupling blade bending and torsional vibration with disc flexural vibration has been formulated, which is particularly effective when combined with the refined modelling offered by the finite element method.

(4) An exact solution for coupled vibration of bladed rotors having simple geometry has been obtained.

The significant advantages of these developments are

(1) By making use of the axisymmetric properties of the problem, the resultingmathematicalmodel is described by a very small number of degrees of freedom compared with other finite element techniques, with corresponding savings in computer storage and time.

(2) The finite element method itself is known to demonsrate higher accuracy compared with conventional lumped mass models, due to a more correct description of the inertia properties.

(3) A very refined mathematical model results, since incorporation of varying thickness in these new elements is readily achieved. With other available finite element models, eg. sector elements, incorporation of thickness variation is difficult - indeed formidable.

(4) The formulation of the vibration problem for the disc or the bladed disc results in an algebraic eigenvalue problem, and avoids the numerical difficulties which often arise in the transfer matrix methods with higher modes which have close frequencies.

The accuracy and convergence of the methods developed have been critically examined by comparision with exact and/or experimental data in all cases, and the results obtained demonstrate the reliability and potential of these methods. In general these comparisions show excellent agreement. The exception, unfortunately, is the calculations carried out for the one complex (real) turbine rotor, for which some experimental data was available, and which gave somewhat indifferent results. In this case the blade model was clearly inadequate, and by comparision with the precision demonstrated on other test cases, it must be admitted that the disc alone results are also disappointing. In fairness, it should be pointed out that these experimental data were obtained on a single test, and may not be representative of the nominal disc frequencies.' A standard deviation in test results, amounting to 5% to 7% of the mean measured frequencies is not unusual for bladed turbine discs. In the authors opinion, this particular comparision, while disappointing, underlines the following further work necessary to clearly evaluate and improve the precision of the present bladed disc model:

(1) A need for further careful assessment of the calculated frequencies by comparision with experimental data on various complex rotors.

(2) A need for further refinement of the blade model, to include, as a first step, coupling between bending and torsional vibration within the blade (shear centre effect).

REFERENCES

(1) Armstrong, E. K., Christie, P. I., and Hague, W. M., "Natural Frequencies of Bladed Discs," Proc. Instn. Mech. Eng., Vol. 180, Part 31, 1966, pp. 110-123.

(2) Wagner, J. T., "Coupling of Turbomachine Blade Vibrations Through the Rotor," Trans. ASME, J. Eng. Power, Vol. 89, no. 4, 1967, pp. 502-512.

(3) Dye, R. C. F., and Henry, T. A., "Vibration Amplitudes of Compressor Blades Resulting From Scatter in Blade Natural Frequencies," Trans. ASME, J. Eng. Power, Vol. 91, no. 3, 1969, pp. 182-188.

(4) Ewins, D. J., "The Effect of Detuning Upon The Forced Vibrations of Bladed Discs," J. Sound and Vibration, Vol. 9, no. 1, 1969, pp. 65-79.

(5) Ewins, D.J., "A Study of Resonance Coincidence in Bladed Rotors," J. Mech. Eng. Sci., Vol. 12, no. 5, 1970, pp. 305-312.

(6) Carta, F. O., "Coupled Blade-Disc-Shroud Flutter Instabilities in Turbo-Jet Engine Rotors," Trans. ASME, J. Eng. Power, Vol. 89, no. 3, 1967, pp. 419-426.

(7) Morgan, S. G., et al., "Gas Turbine in The Royal Navy," ASME Paper No. 70-GT-10.

(8) Shannon, J. F., "Vibration Problems in Gas Turbine, Centrifugal and Axial Flow Compressors," Aero. Res. Council, R and M 2226, March 1945.

(9) Blackwell, B. D., "Some Investigations in The Field of Blade Engineering," J. Roy. Aero. Soc., vol. 62, 1958, pp. 633-646.

(10) Armstrong, E, K., and Stevenson, R. E., "Some Practical Aspects of Compressor Blade Vibration," J. Roy. Aero. Soc., vol. 64, 1960, pp. 117-130.

(11) Armstrong, E. K., and Williams, D. D., "Some Intake Flow Maldistribution Effects on Compressor Rotor Blade Vibration," J. Sound and Vibration, Vol. 3, no. 3, 1966, pp. 340-354.

(12) Waldren, N. E., et al.,
"Burst Strength of Rotating Discs," Proc. Instn. Mech. Engrs., Vol. 180, Pt. 1, no. 5, 1965-66, pp. 111-130.

(13) Goatham, J. I., et al.,
"Some Vibration Characteristics of Pin-Fixed Compressor Blades," Trans. ASME, J. Eng. Power, Vol. 89, no. 4, 1967, pp. 491-501.

(14) Petricone, R., and Sisto,
"Vibration Characteristics of Low Aspect Ratio Compressor Blades," Trans. ASME, J. Eng. Power, Vol. 93, no. 1, 1971, pp. 103-112.

(15) NASA
"Factors That Affect Operational Reliability of Turbojet Engines," NASA Technical Report, TR R-54, 1960.

(16) Stodola, A.,
Steam and Gas Turbines, Vo1.2, McGraw-Hill, New York, 1927.

(17) Biezeno, C. B., and Grammel, R.,
Engineering Dynamics, Vol. III, Blackie and Sons Ltd, London, 1954.

(18) Manna, F.,
"Rotating Disks of Unconventional Profiles," (in English) Meccanica, J. Italian Asso. Theo. and App. Mech. Vol. 3, no. 4, Dec. 1968, pp. 274-282.

(19) Donath, M.,
Die Berechnung rotierender Scheiben und Ringe, Second Edition, Julius Springer, Berlin, 1929.

(20) Manson, S. S.,
"The Determination of Elastic Stresses in Gas-Turbine Disks," NACA Technical Note No. 1279, 1947.

(21) Manson, S. S.,
"Direct Method of Design and Stress Analysis of Rotating Disks With Temperature Gradients," NACA Technical Note No. 1957, 1947.

(22) Seireg, A., and Surana, K. S.,
"Optimum Design of Rotating Disks," Trans. ASME, J. Eng. Ind. Vol. 92, no. 1, 1970, pp. l-10.

(23) Manson, S. S.,
'Analysis of Rotating Discs of Arbitrary Contour And Radial Temperature Distribution in The Region of Plastic Deformation," Proc. First US Nat. Cong. App. Mech., 1951, p. 569.

(24) Mote, C. D., Jr.
'Free Vibration of Initially Stressed Circular Disks,' Trans. ASME, J. Eng. for Ind., Vol. 87, 1965, pp. 258-264.

(25) Bogdanoff, J. L., et al.,
'Lateral Buckling of Rimmed Rotating Discs," Proc. Third US Nat. Cong. App. Mech., 1958, pp. 253-257.

(26) Soo, P. P.,
"An Energy Method of Natural Mode Frequency Analysis of A Turbine Disk Subjected to Uniform Rotation and Temperature Gradient," Developements in Mechanics, Proc. 10th Mid-Western Mech. Conf., Vol. 4, Aug. 1967, pp. 977-994.

(27) Haigh, R. E., and Murdoch, M. L.,
"Analysis of Centrifugal Stresses in Turbine Wheels," J. Mech. Eng. Sci., Vol. 5, no. 1, 1963, pp. 66-74.

(28) Kobayashi, A. S., and Trumpler, P. R.,
'Elastic Stresses in A Rotating Disc of General Profile," Int. J. Mech. Sci., Vol. 2, 1960, pp. 13-29.

(29) Swansson, N. S.,
'The Stress Analysis of A Radial Flow Impeller," Mech. Eng. Note 259, Aero. Res. Lab., Melbourne, Aug. 1963.

(30) Schilhansl, M. J.,
"Stress Analysis of A Radial Flow Rotor," Trans. ASME, Ser. A, Vol. 84, no. 1, 1962, pp. 124-130.

(31) Thurgood, D.A.,
"Stress Distribution in A Rotating Disc," The Engineer, Vol. 224, Dec. 1967, pp. 832-834.

(32) Stordahl, H., and Christensen, H.,
'Finite Element Analysis of Axisymmetric Rotors,' J. Strain Analysis, Vol. 4, no. 3, July 1969, pp. 163-168.

(33) Chan, A. S. L., and Henrywood, R. K.,
'The Analysis of Radial Flow Impellers By the Matrix Finite Element Method," Aero. J., Roy. Aero. Soc., Vol. 75, 1971, pp. 850-860.

(34) Fessler, H.,
"Centrifugal Stresses in Turbo-Alternator Rotors," Proc. Instn. Mech. Engrs., Vol. 173, no. 29, 1959, pp. 717-733.

(35) Guernsey, R.,
"Photoelastic Study of Centrifugal Stresses in A Single Wheel and Hub," Proc. Soc. Exp. Stress Analysis, Vol. 18, no. 1, Jan. 1961.

(36) Fessler, H., and Thorpe, T. E.,
"Centrifugal Stresses in Rotationally Symmetrical Gas-Turbine Discs," J. Strain Analysis, Vol. 3, no. 2, 1968, pp. 135-141.

(37) Thurgood, D. A.,
"Stresses in Asymmetric Discs," J. Strain Analysis, Vol. 4, no, 1, Jan. 1969, pp. 65-73.

(38) Prescott, J.,
Applied Elasticity, McGraw-Hill Book Co., Inc., New York, 1953.

(39) Campbell, W.,
"The Protection of Steam Turbine Disk Wheels From Axial Vibration," Trans. ASME, Vol. 46, 1924, pp. 31-160.

(40) Tobias, S. A., and Arnold, R. N.,
"The Influence of Dynamical Imperfections on the Vibration of Rotating Disks," Proc. Instn. Mech. Engrs. Vol. 171, 1957, pp. 669-690.

(41) Tobias, S. A.,
"Free Undamped Nonlinear Vibrations of Imperfect Circular Disks," Proc. Instn. Mech. Engrs., Vol. 171, 1957, pp. 691-701.

(42) McLeod, A. J., and Bishop, R. E. D.,
"The Forced Vibration of Circular Flat Plates," Mech. Eng. Sci. Monograph No. 1, Instn. Mech. Engrs., London, 1965.

(43) Vogel, S. M., and Skinner, D. W.,
"Natural Frequencies of Transversely Vibrating Uniform Annular Plates," Trans. ASME, J. App. Mech. Vol. 32, 1965, pp. 926-931.

(44) Leissa, A. W.,
Vibration of Plates, Scientific and Technical Information Division, NASA, Washington, 1969.

(45) Conway, H. D.,
"Some Special Solutions for the Flexural Vibration of Discs of Varying Thickness," Ing. Arch., Vol. 26, 1958, pp. 408-410.

(46) Harris, G. Z.,
"The Normal Modes of A Circular Plate of Variable Thickness," Quart. J. Mech. and App. Maths., Vol. 21, 1968, pp. 321-327.

(47) Lamb, H., and Southwell, K. V.,
"The Vibrations of A Spinning Disc," Proc. Roy. Soc. of London, Vol. 99, 1921, pp. 272-280.

(48) Southwell, R. V.,
"On the Free Transverse Vibrations of A Uniform Circular Disc Clamped at Its Centre; and on the Effects of Rotation," Proc. Roy. Soc. of London, Vol. 101, 1922, pp. 133-153.

(49) Ghosh, N. C.,
"Vibration of Rotating Disk of Variable Thickness," J. Sci. Eng. Res., India, Vol. 13, no. 2, pp. 315-322.

(50) Eversman, W., et al.,
"Free Vibration of A Centrally Clamped Spinning Circular Disk," AIAA J., Vol. 7, no, 10, 1969, pp. 2010-2012.

(51) Ehrich, F. F.,
"A Matrix Solution for the Vibration Modes of Non-Uniform Discs," Trans. ASME, J. App. Mech., Vol. 23, 1956, pp. 109-115.

(52) Bleich, J. J.,
'Computer Analysis of Flexural Vibrations of A Rotating Disc With an Arbitrary Profile," ASME Paper No. 65-WA/GTP-8.

(53) Anderson, R. G., et al.,
"Vibration and Stability of Plates Using Finite Elements," Int. J. Solids and Struct., Vol. 4, 1968, pp. 1031-1055.

(54) Olson, M. D., and Lindberg, G. M.,
"Annular and Circular Sector Finite Elements for Plate Bending," Int. J. Mech. Sci., Vol. 12, 1970, pp. 17-33.

(55) Sawko, F., and Merriman, P.A.,
"An Annular Segment Element for Plate Bending," Int. J. Num. Meth. Eng., Vol. 3, 1971, pp. 119-129.

(56) Singh, S., and Ramaswamy, G. S.,
"A Sector Element for Thin Plate Flexure," Int. J. Num. Meth. Eng., vol. 4, 1972, pp. 133-142.

(57) Chernuka, M.W., et al.,
"Finite Element Analysis of Plates With Curved Edges," Int. J. Num. Meth. Eng., Vol. 4, 1972, pp. 49-65.

(58) Srinivas, S., et al.,
"An Exact Analysis for Vibration of Simply-Supported Homogeneous and Laminated Thick Rectangular Plates," J. Sound and Vibr., Vol. 12, no.2, 1970, pp. 187-199.

(59) Potter, D. S., and Leedham, C. D.,
"Antisymmetric Vibrations of A Circular Plate," J. Acoust. Soc. Amer., Vol. 49, no.5, 1971, pp. 1521-1526.

(60) Reissner, E.,
"The Effect of Transverse Shear Deformation on the Bending of Elastic Plates," J. App. Mech., vol. 12, 1945, pp. 69-77.

(61) Uflyand, Y. S.,
"The Propagation of Waves in the Transverse Vibration of Bars and Plates," (in Russian) Akad. Nauk. SSSR, Prikl. Mat. Mech., Vol. 12, 1948, pp. 287-300.

(62) Mindlin, R. D.,
"Influence of Rotary Inertia and Shear on Flexural Motions of Isotropic Elastic Plates," J. App. Mech., Vol. 18, no. 1, March 1951, pp. 31-38.

(63) Mindlin, R. D., and Deresiewicz, H.,
"Thickness Shear And Flexural Vibrations of a Circular Disc," J. App. Phys., Vol. 25, no. 10, 1954, pp. 1329-1332.

(64) Deresiewicz, H., and Mindlin, R. D.,
"Axially Symmetric Flexural Vibrations of a Circular Disc," J. App. Mech., Vol. 22, no. 1, March 1955, pp. 86-88.

(65) Deresiewicz, H.,
"Symmetric Flexural Vibrations of a Clamped Circular Disk," J. App. Mech., Vol. 23, no.2, June 1956, p. 319.

(66) Callahan, W. R.,
"On the Flexural Vibrations of Circular and Elliptical Plates," Quart. Appl. Math., Vol. 13, 1956, pp. 371-380.

(67) Bakshi, J. S., and Callahan, W. R.,
"Flexural Vibrations of a Circular Ring When Transverse Shear and Rotary Inertia are Considered," J. Acoust. Soc. Amer., Vol. 40, no. 2, 1966, pp. 372-375.

(68) Onoe, M., and Yano, T.,
"Analysis of Flexural Vibrations of a Circular Disk," Electronic Communications in Japan, Vol. 51-A, no. 2, 1968, pp. 33-36.

(69) Pestel, E. C., and Leckie, P. A.,
Matrix Methods in Elastomechanics, McGraw-Hill Book Co., Inc., New York, 1963, pp. 404-408.

(70) Clough, R. W., and Fellippa, C.A.,
"A Refined Quadrilateral Element for Analysis of Plate Bending," Second Conf. on Matrix Meth. in Struct. Mech., Wright-Patterson AFB, Ohio, Oct. 1968.

(71) Peterson, R. E.,
"Natural Frequency of Gears," Trans. ASME, Vol. 52, APM-52-1, 1930, pp. 1-11.

(72) French,
"Aircraft Gas Turbine Rotating Compressor Disc Vibration," ASME Paper No. 65-WA/GTP-11.

(73) Mote, C. D., Jr., and Nieh, L. T.,
"Control of Circular Disk Stability With Membrane Stresses," Experimental Mechanics, Vol. 11, no. 11, 1971, pp. 490-498.

(74) Dokainish, M. A., and Rawtani, S.',
"A Review of the Analytical Methods for Vibration Analysis of Turbomachinery Blades," Dept. of Mech. Eng., McMaster University, Hamilton, Canada, 1969.

(75) Pinney, E.,
"Vibration Modes of Tapered Beams," Amer. Math. Monthly, Vol. 54, 1.947, pp. 391-394.

(76) Myklestad, N. O.,
"A New Method of Calculating Natural Modes of Uncoupled Bending Vibration of Airplane Wings and Other Types of Beams," J. Aero. Soc., Vol. 11, no. 4, 1944.

(77) Leckie, F. A., and Lindberg, G. M.,
"The Effect of Lumped Parameters on Beam Frequencies," The Aero. Quart., Vol. 14, Aug. 1963, pp. 224-240.

(78) Lindberg, G. M.,
"Vibration of Non-Uniform Beams," The Aero. Quart., Vol. 14, 1963, pp. 387-395.

(79) Archer, J. S.,
'Consistent Matrix Formulation for Structural Analysis Using Influence Co-efficient Techniques," AIM J., Vol. 3, 1965, pp. 1910-1918.

(80) Carnegie, W., and Thomas, J.,
"Vibration Characteristics of Turbine Blading," The Engineer, Vol. 224, no. 5831, 1967, pp. 545-547.

(81) Rosard, D. D.,
"Natural Frequencies of Twisted Cantilever Beams," Trans. ASME, J. App. Mech., Vol. 20, no. 2, 1953, pp. 241-244.

(82) Anliker, M., and Troesch, B. A.,
"Theory of Lateral Vibrations of Pretwisted Rods," Z.A.M.P., Vol. 14, 1963.

(83) Carnegie, W.,
'Vibrations of Pretwisted Cantilever Blading," Proc. Instn. Mech. Engrs., Vol. 173, no. 12, 1959, pp. 343-374.

(84) Slyper, H. A.,
"Coupled Bending Vibrations of Pretwisted Cantilever Beams," J. Mech. Eng. Sci., Vol. 4, no. 4, 1962, pp. 365-379.

(85) Dokumaci, E., et al.,
"Matrix Displacement Analysis of Coupled Bending-Bending Vibrations of Pretwisted Blading," J. Mech. Eng. Sci., Vol. 9, no. 4, 1967, pp. 247-254.

(86) Mendelson, A., and Gendler, S.,
"Analytical Determination of Coupled Bending-Torsion Vibrations of Cantilever Beams by Means of Static Functions," NACA TN 2135, 1950.

(87) Mendelson, A., and Gendler, S.,
"Analytical and Experimental Investigation on Effects of Twist on Vibrations of Cantilever Beams," NACA TN 2300, 1951.

(88) Houbolt, J. C., and Brooks; G. W.,
"Differential Equations of Motion for Combined Flapwise Bending, Chordwise Bending and Torsion of Twisted Non-Uniform Rotor Blades,' NACA TN 3905, 1957.

(89) Dunham, J.,
"The Lowest Natural Frequency of an Axial Compressor Blade," J. Roy. Aero. Soc., Vol. 62, 1958, pp. 677-680.

(90) Montoya, J.,
"Coupled Bending and Torsional Vibrations in a Twisted, Rotating Blade," Brown Boveri Review, Vol. 53, no. 3, March 1966, pp. 216-230.

(91) Sutherland, R. L.,
"Bending Vibration of a Rotating Blade, Vibrating in the Plane of Rotation," Trans. ASME, J. App. Mech., Vol. 16, 1949, pp. 389-394.

(92) Plunkett, R.,
"Free and Forced Vibration of Rotating Blades," J. Aero. sci., Vol. 18, no. 4, pp. 278-282.

(93) Lo,H., et al.,
"Bending Vibrations of Rotating Beams," Proc. First US Nat. Cong. App. Mech., 1951.

(94) Lo, H.,
"A Nonlinear Problem in Bending Vibration of a Rotating Beam," Trans. ASME, J. App. Mech., Vol. 19, no. 4,1952, pp. 461-464.

(95) Carnegie, W.,
"Vibrations of Rotating Cantilever Blading; Theoretical Approaches to the Frequency Problem Based on Energy Methods," J. Mech. Eng. Sci., Vol. 1, no. 3, 1959, pp. 235-240.

(96) Jarrett, G.W., and Warner, P. C.,
"The Vibration of Rotating, Tapered Twisted Beams," Trans. ASME, J. App. Mech., Vol. 20, no. 3, 1953, pp. 381-389.

(97) Targoff, W.,
"The Bending Vibrations of a Twisted Rotating Beam," Proc. Third Midwestern Conf. on Solid Mech., 1957.

(98) Isakson, G., and Eisley, J.G.,
"Natural Frequencies in Bending of Twisted Rotating Blades," NASA TN D-371, March 1960.

(99) Isakson, G., and Eisley, J. G.,
'Natural Frequencies in Coupled Bending and Torsion of Twisted Rotating and Non-Rotating Blades," NASA CR-65, 1964.

(100) Bogdanoff, J. L.,
'Influence of Secondary Inertia Terms on the Natural Frequencies of Rotating Beams," Trans. Trans. ASME, J. App. Mech., Vol. 22, 1955, pp. 587-591.

(101) Bogdanoff, J. L., and Horner, J. T.,
"Torsional Vibration of Rotating Twisted Beams," J. Aero. sci., Vol. 23, no. 4, 1956, pp. 393-395.

(102) Brady, W. G., and Targoff, W. P.,
"Uncoupled Torsional Vibrations of a Thin, Twisted, Rotating 'Beam," WADC Tech. Report 56-501, 1957.

(103) Krupka, R. M., and Baumanis, A. M.,
"Bending-Bending Mode of a Rotating Tapered Twisted Turbo-machine Blade Including Rotary Inertia and Shear Deformation," Trans. ASME, J. Eng. Ind., Vol. 91, no. 4, 1969, pp. 1017-1024.

(104) Cowper, G.R.,
"A Computer Programme for Calculating Shear Centres and Other Section Properties," Mem. No. ST-68, Nat. Aero. Est., N.R.C., Ottawa, Canada, March 1966.

(105) Volterra, E.,
"Second Approximations of Method of Internal Constraint and Its Applications," Int. J. Mech. Sci., Vol. 3, 1961,p.47.

(106) Huang, T. C.,
"Effect of Rotary Inertia and Shear on the Vibration of Beams Treated by Approximate Methods of Ritz and Galerkin," Proc. Third US Nat. Conc. of App. Mech., 1958, p. 189.

(107) Carnegie, W., and Thomas, J.,
'*The Effects of Shear Deformation and Rotary Inertia on the Lateral Frequencies of Cantilever Beams in Bending," Trans. ASME, J. Eng. Ind., Vol. 94, no. 1, 1972, pp. 267-278.

(108) Gere, J. M.,
"Torsional Vibrations of Beams of Thin-Walled Open Section," Trans. ASME, J. App. Mech., Vol. 21, 1954, 381-387.

(109) Grinsted, B.,
"Nodal Pattern Analysis," Proc. Instn. Mech. Engrs., Vol. 166, 1952, pp. 309-326.

(110) Ellington, J. P., and McCallion, H.,
"The Vibrations of Laced Turbine Blades," J. Roy. Aero. Sac., Vol. 61, no. 560, 1957, pp. 563-567.

(111) Pearson, H.,
"The Aerodynamics of Compressor Blade Vibration," Engine-ering, Vol. 196, no. 5098, pp. 473-476.

(112) Sabatiuk, A., and Sisto, F.,
"A Survey of Aerodynamic Excitation Problems in Turbo-machines," Trans. ASME, Vol. 78, 1956, pp. 555-564.

(113) Rawtani, S., and Dokainish, M. A.,
"Vibration Analysis of Pretwisted Cantilever Plates," Canadian Aero. and Space Inst., Trans., Vol. 2, no. 2, 1969.

(114) Olson, M. D., and Lindberg, G. M.,
"A Finite Cylindrical Shell Element and the Vibrations of a Curved Fan Blade," Aero. Report LR-497, N.R.C., Canada, Feb. 1968.

(115) Ellington, J. P., and McCallion, H.,
"Blade Frequency of Turbines; Effect of Disc Elasticity," Engineering, Vol. 187, no. 4862, May 1959, pp. 645-646.

(116) Johnson, D. C., and Bishop, B.E.D.,
"The Modes of Vibration of a Certain System Having a Number of Equal Frequencies," Trans. ASME, J. App. Mech. Vol. 23, 1956, pp. 379-384.

(117) Capriz, G.,
'Interaction Between Disk and Blades During Vibrations of a Thick-Bladed Turbine Disk," ASME Paper No. 67-VIBR-52.

(118) Armstrong, E. K.,
"An Investigation Into the Coupling Between Turbine Disc and Blade Vibration," Ph.D., Thesis, Cambridge Univ ., 1.955.

(119) Armstrong, E. K.,
"Recent Blade Vibration Techniques," Trans. ASME, J. Eng. Power, Vol. 89, no. 3, 1967, pp. 437-444.

(120) Jager, B.,
"Eigenfrequenzen einer Scheibe mit Verwundenen Schaufeln,' Zeitschrift fur Flugwissenschaften, Vol. 10, no. 12, 1962, pp. 439-446.

(121) Stargardter, H.,
"Dynamic Models of Vibrating Rotor Stages," ASME Paper No. 66-WA/GT 12, Winter Annual Meeting, 1966.

(122) Kirkhope, J., and Wilson, G. J.,
"Vibration of Circular and Annular Plates Using Finite Elements,' Int. J. Num. Meth. Eng., Vol. 4, 1972, pp. 181-193.

(123) Zienkiewicz, O. C., and Cheung, Y. K.,
The Finite Element Method in Structural and Continuum Mechanics, McGraw-Hill, London, 1967.

(124) Timoshenko, S. P., and Woinowsky-Krieger, S.,
Theory of Plates and Shells, Second Edition, McGraw-Hill Book Company, New York, 1959.

(125) Pryor, C. W., Barber, R. M., and Frederick, D.,
"Finite Element Bending Analysis of Reissner Plates," Proc. ASCE, J. Eng. Mech., Vol. 96, no. EM6, 1970, pp. 967-983.

(126) Wilson, G. J., and Kirkhope, J.,
Discussion on "Finite Element Bending Analysis of Reissner Plates," Proc. ASCE, J. Eng. Mech., Vol. 97, 1971, p. 1570.

(127) Rao, S. S.,
'Effects of Transverse Shear and Rotary Inertia on the Coupled Twist-Bending Vibrations of Circular Rings," J. Sound and Vib., Vol. 16, no. 4, 1971, pp. 567-580.

(128) Kapur, K. K.,
"Vibrations of a Timoshenko Beam, Using Finite-Element Approach," J. Acoust. Soc. Amer., Vol. 40, 1966, pp. 1058-1063.

(129) Boyce, W. E.,
"Effect of Hub Radius on the Vibrations of a Uniform Bar," Trans.ASME, J. App. Mech., Vol. 23, 1956, pp. 287-290.

(130) Kirkhope, J.,
"Vibrations of Systems of Elastically Coupled Concentric Rings," J. Acoust. Soc. Amer., Vol. 47, 1971, pp. 371-373.

(131) Bishop, R. E. D., and Johnson, D. C.,
The Mechanics of Vibration, Cambridge University Press, 1960.

(132) Kirkhope, J., and Wilson, G. J.,
"Analysis of Coupled Blade-Disc Vibration in Axial Flow Turbines and Fans," Proc. AIAA/ASME 12th Structures, Structural Dynamics and Materials Conference, Anaheim, Calif., April 1971.

(133) Herrman, L. R.,
'A Bending Analysis for Plates," Proc. First Conf. Matrix Methods Struct. Mech., Wright-Patterson AFB, Ohio, 1965.

(134) Smith, I, M.,
"A Finite Element Analysis for 'Moderately Thick' Rectangular Plates in Bending," Int. J. Mech. Sci., Vol. 10, 1968, pp. 563-570.

(135) Salerno, V. L., and Goldberg, M. A.,
"Effect of Shear Deformation on the Bending of Rectangular Plates," Trans. ASME, J. App. Mech., Vol. 27, 1960, pp. 54-58.

(136) Cowper, G. R., et al.,
"Static and Dynamic Applications of a High Precision Triangular Plate Bending Element," AIAA J. Vol. 7, 1969, pp. 1957-1965.

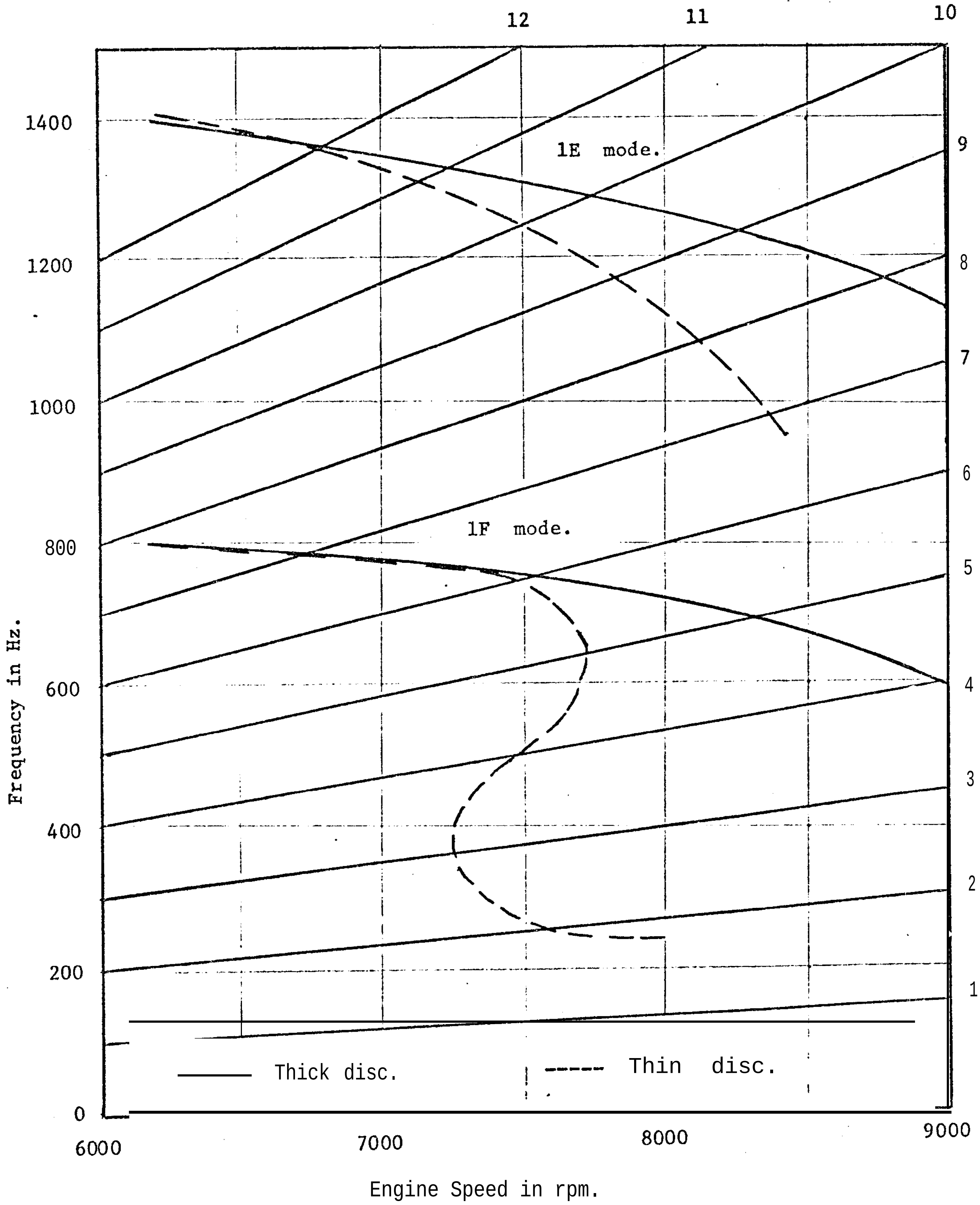

Figure 1.1 Effect of disc stiffness on the coupled blade-disc frequencies.

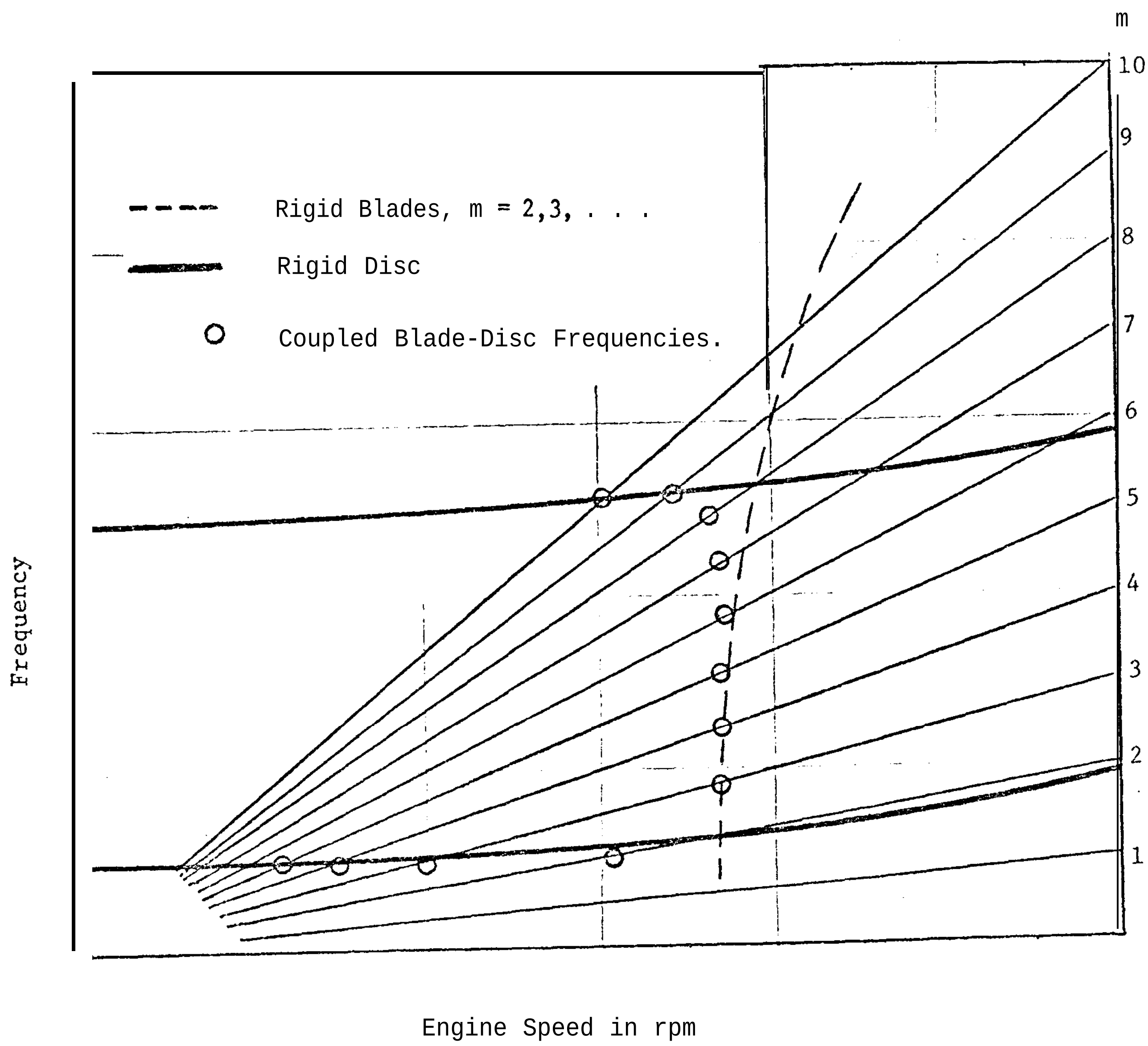

Figure 1.2 Interference diagram.

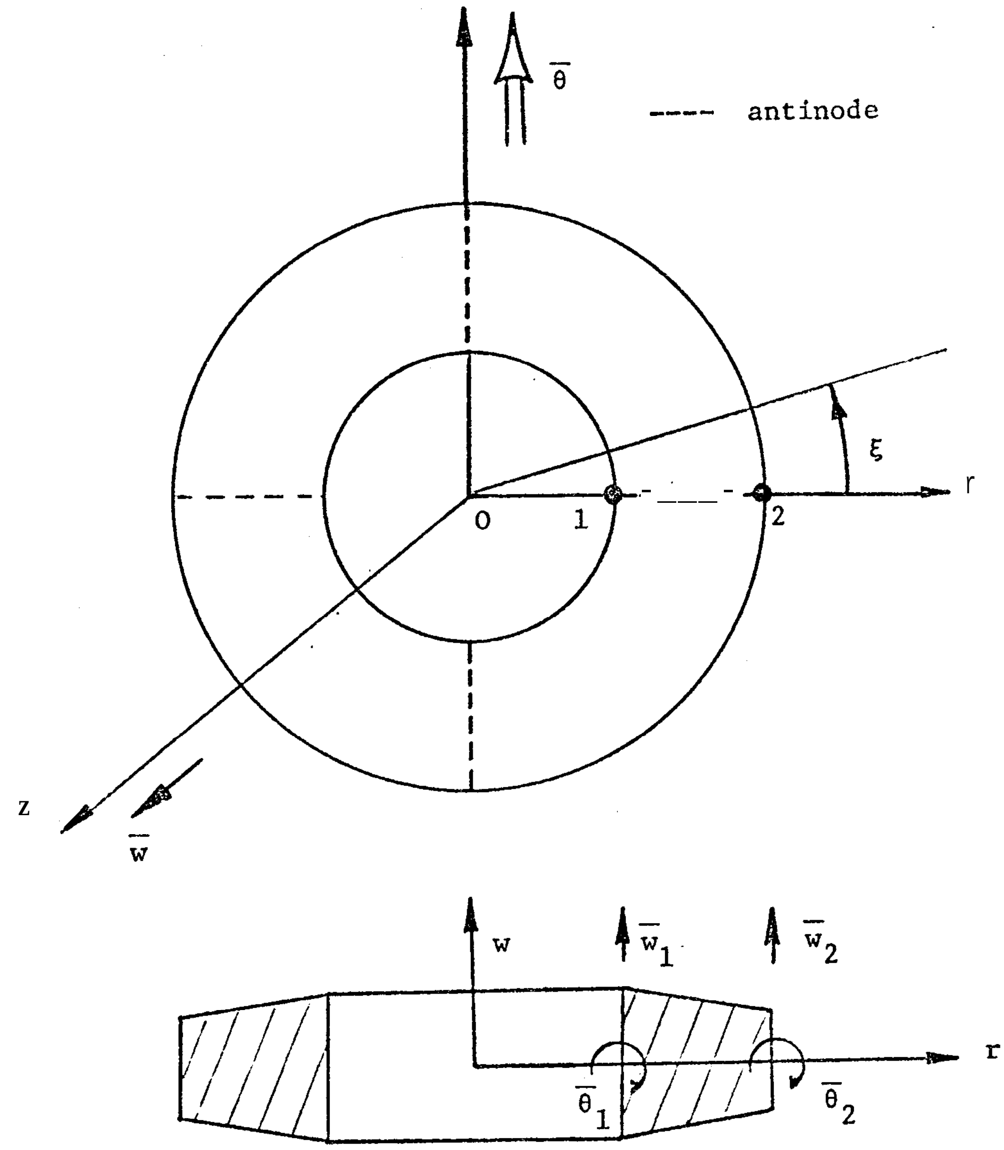

Figure 2.1 Thin plate bending annular element with two nodal diameters and linear thickness variation.

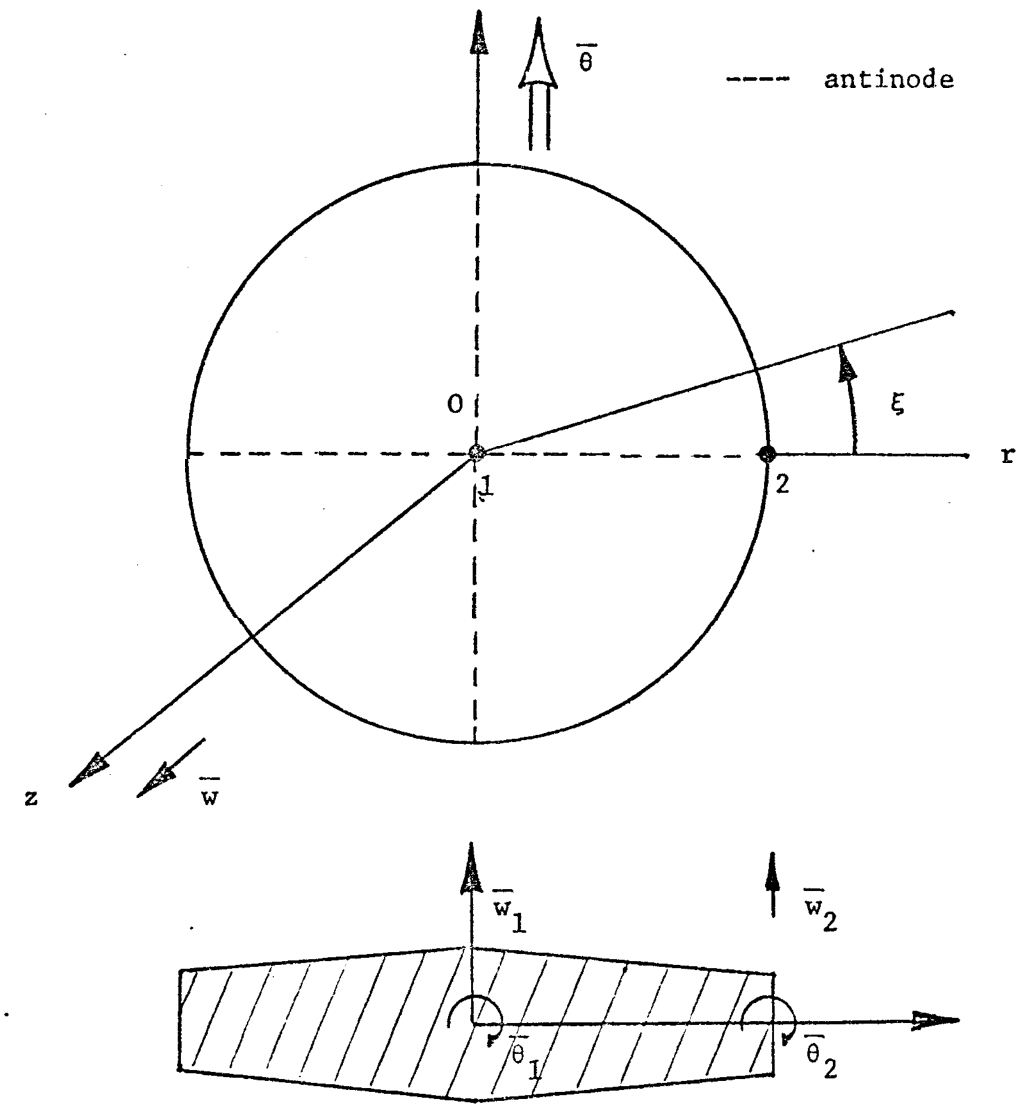

Figure 2.2 Thin plate bending circular element with two nodal diameters and linear thickness variation.

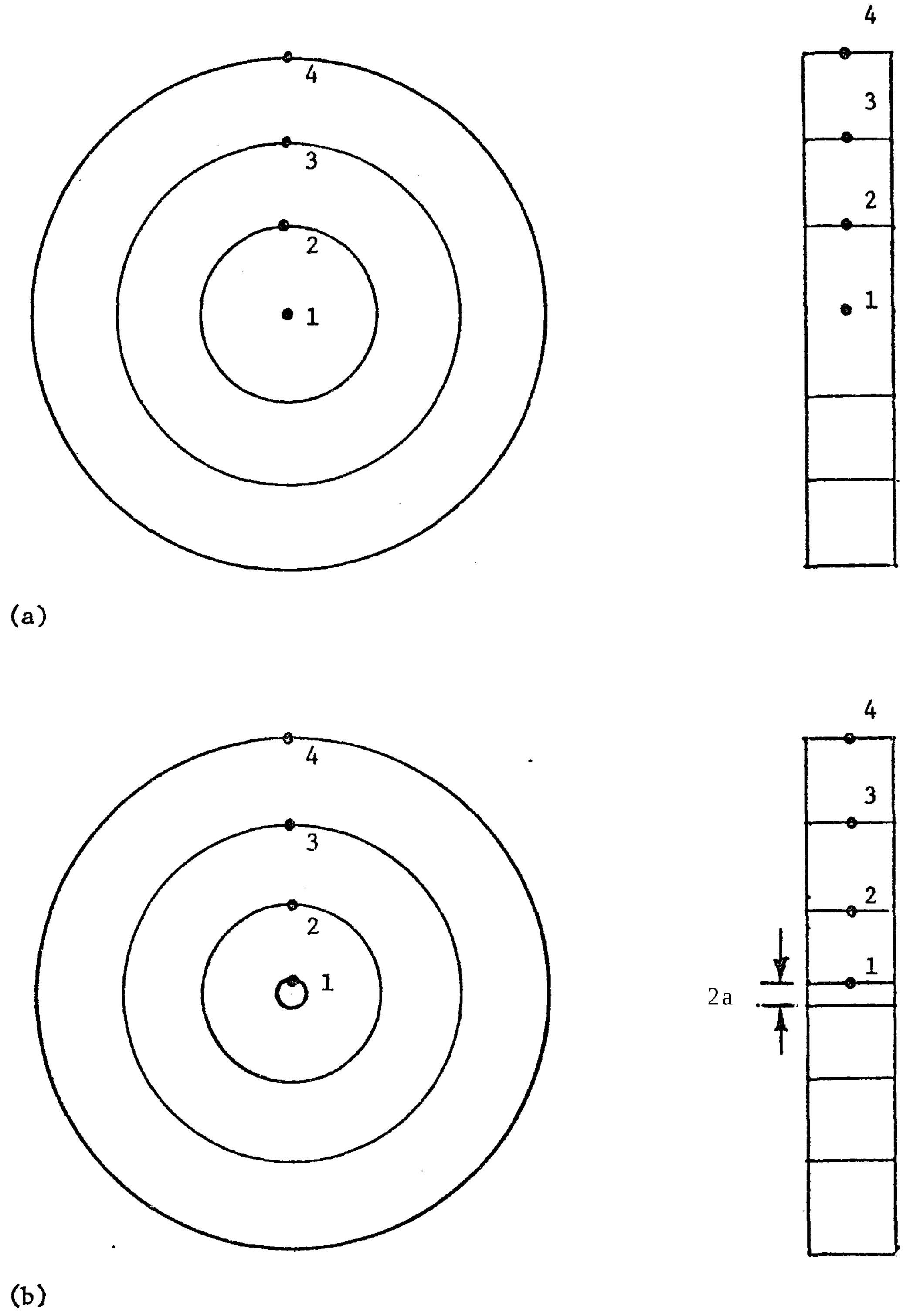

Figure 2.3 Modelled circular plate. (a) With one circular element and two annular elements. (b) With a small central hole and three annular elements.

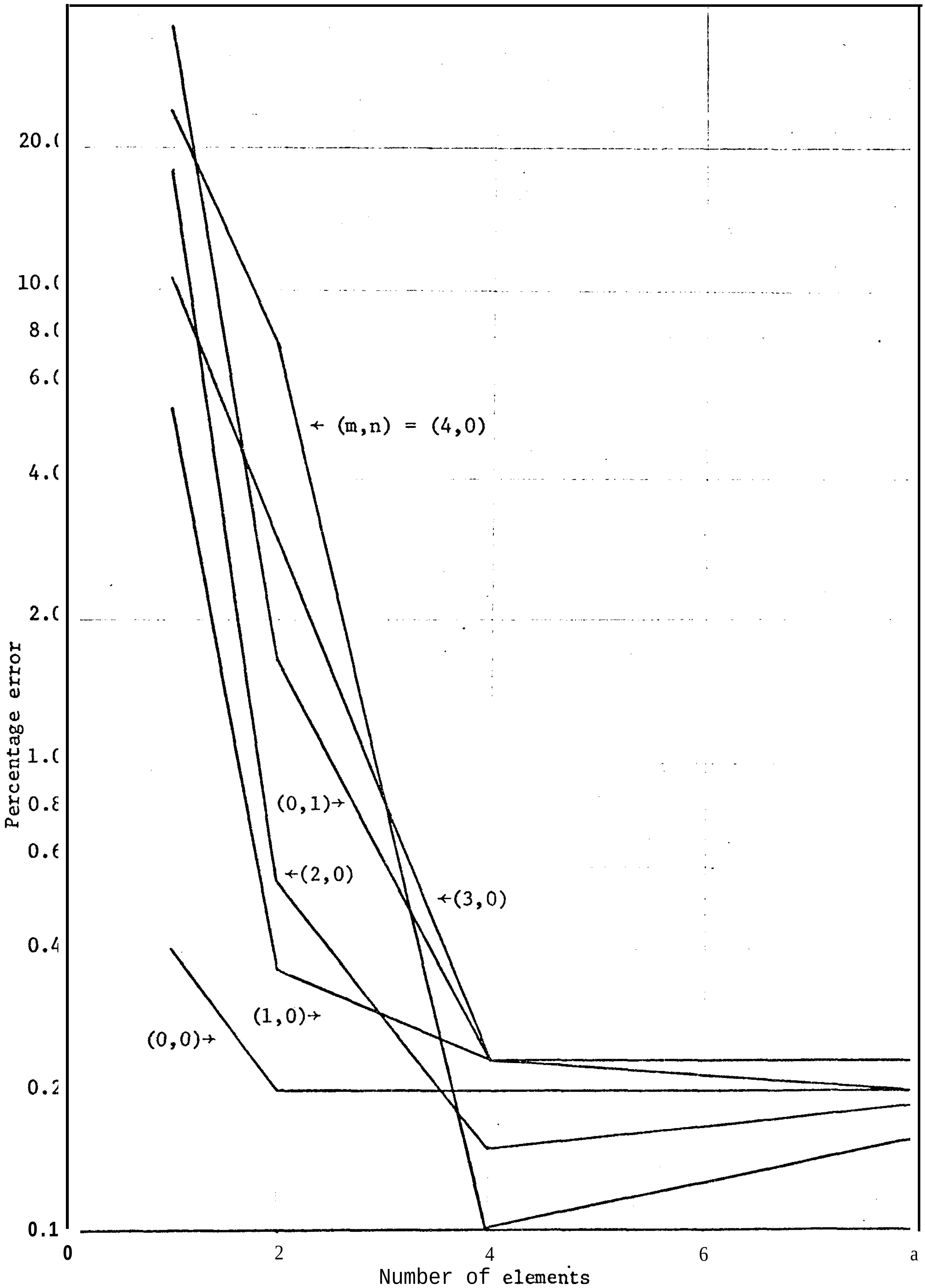

Figure 2.4 Percentage absolute error in the first six frequency coefficients of a simply supported circular plate modelled with thin plate bending annular elements.

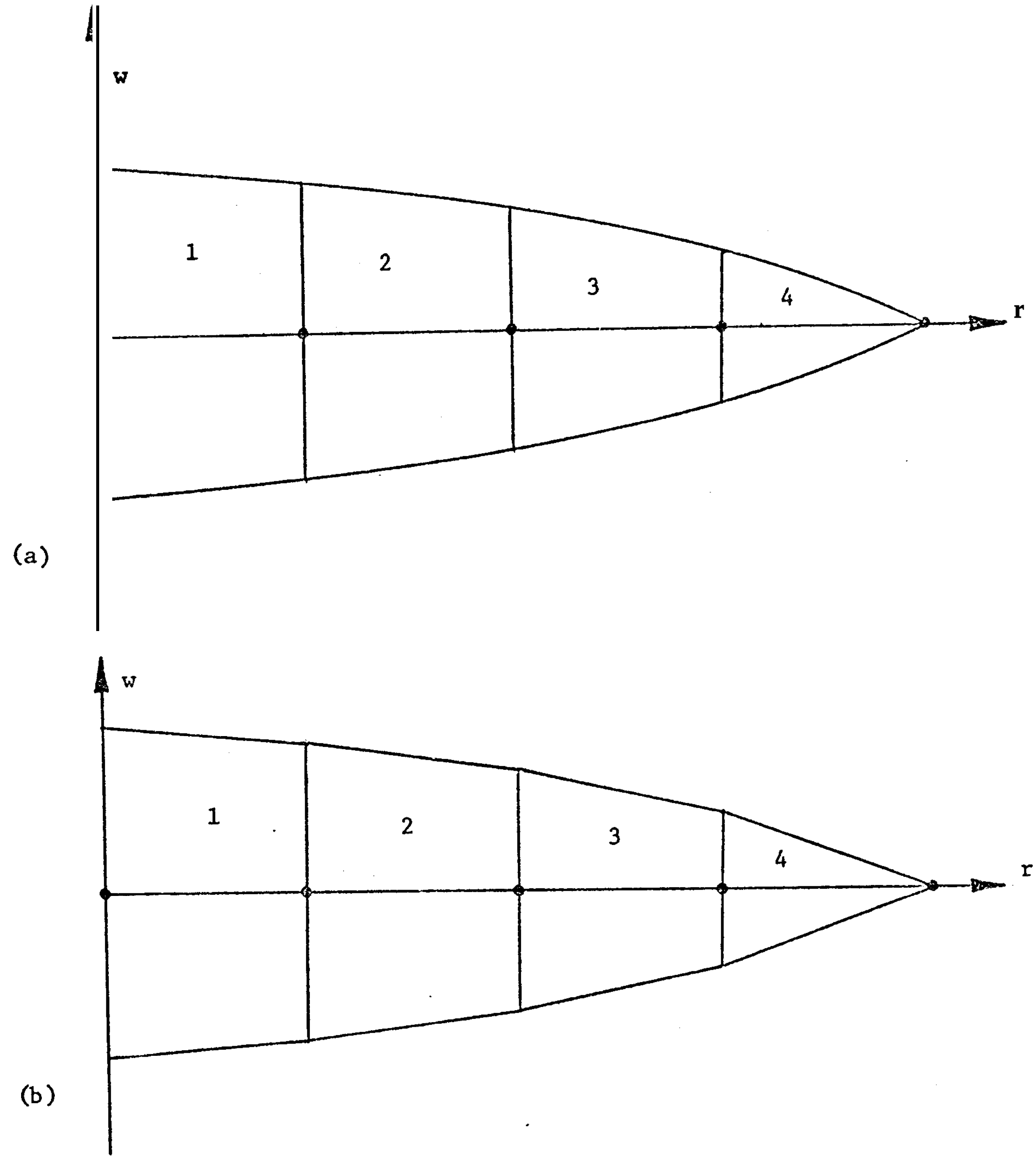

Figure 2.5 Modelled circular disc with parabolic thickness variation.
(a) Elements with parabolic thickness variation used.
(b) Elements with linear thickness variation used.

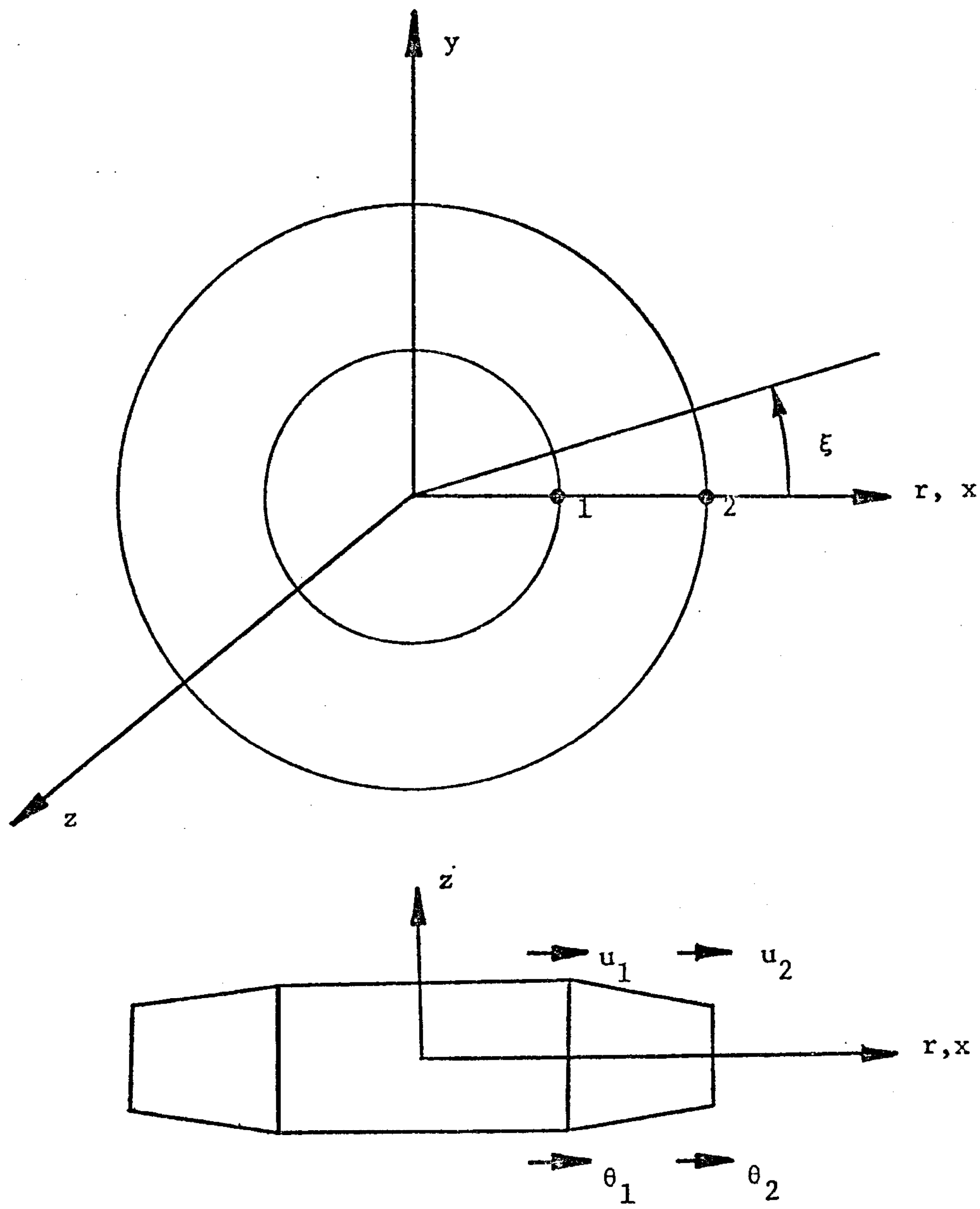

Figure **2.6** Plane stress annular element.

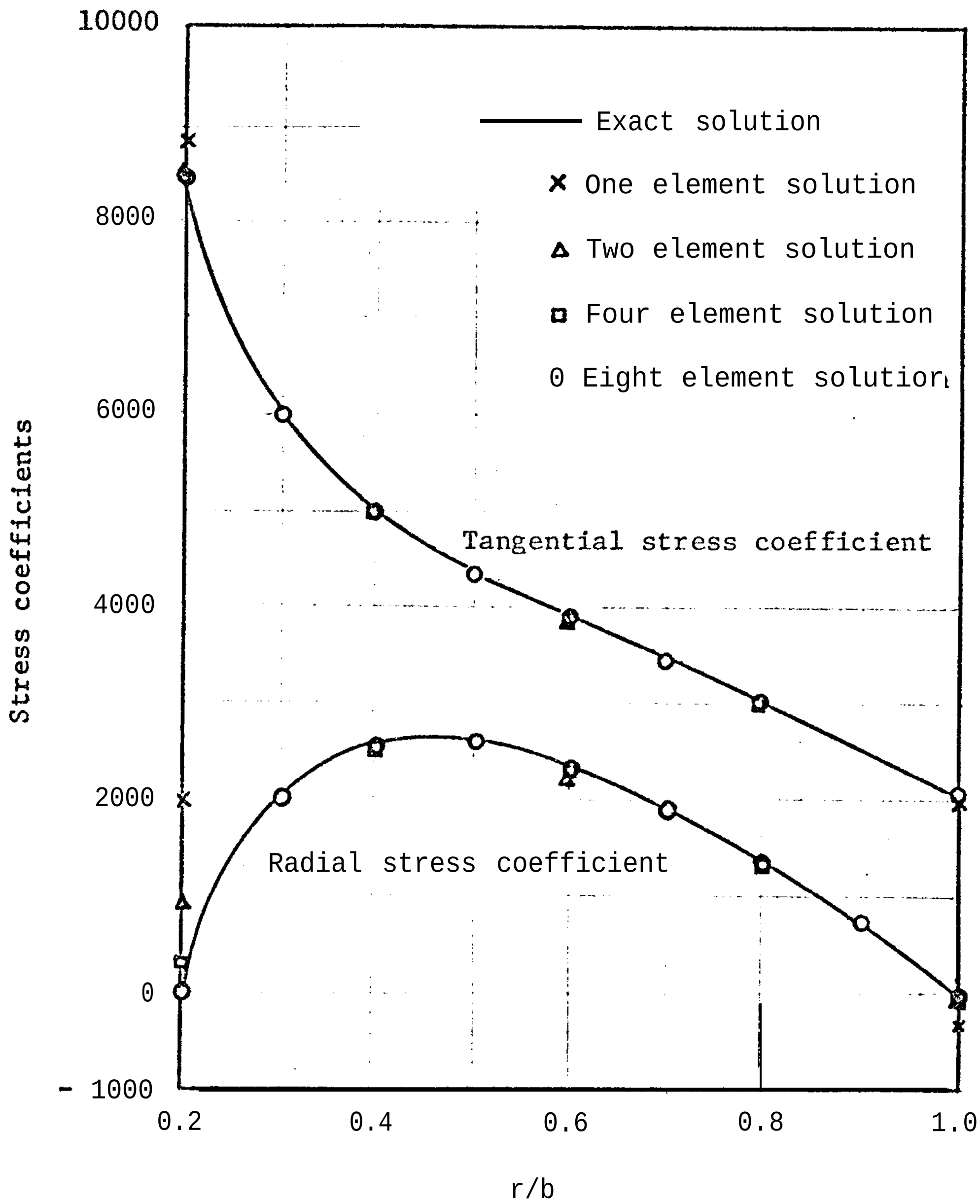

Figure 2.7 Radial and tangential stress coefficients for a uniform rotating disc, calculated using the plane stress annular element.

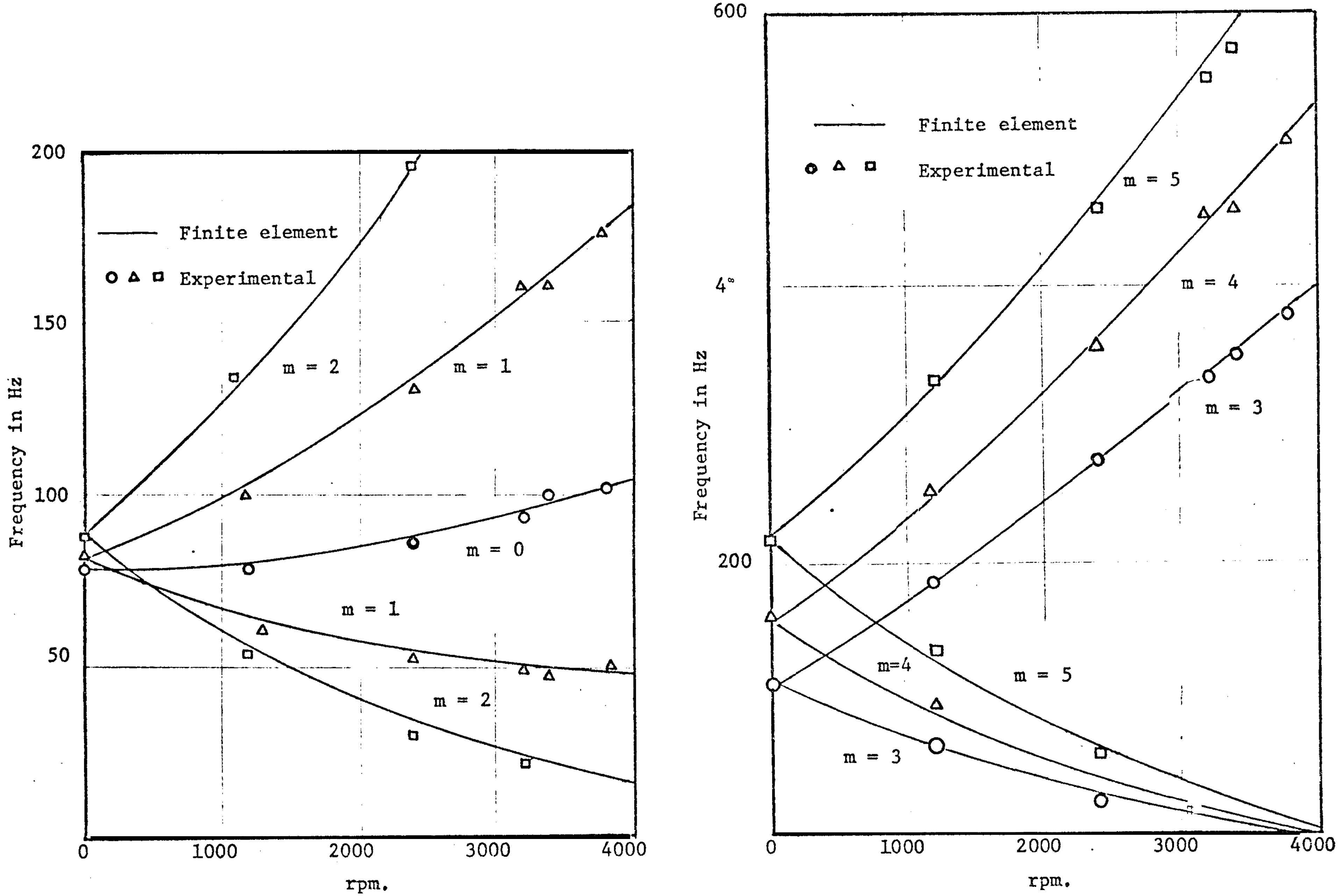

Figure 2.8 Variation of harmonic excitation frequencies with rotational speed of a thin annular plate.

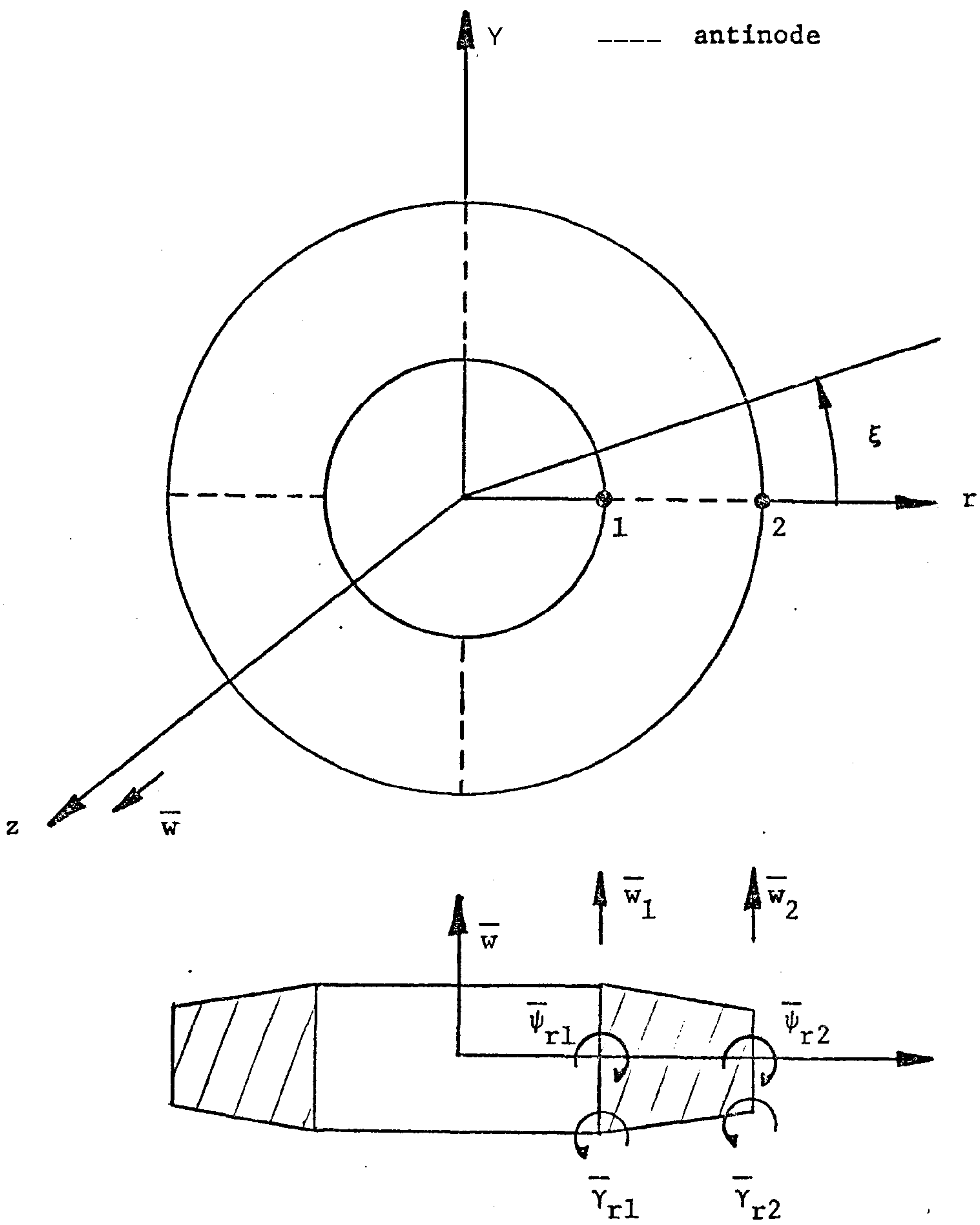

Figure 2.9 Thick Disc Element-1 with two nodal diameters and associated degrees of freedom.

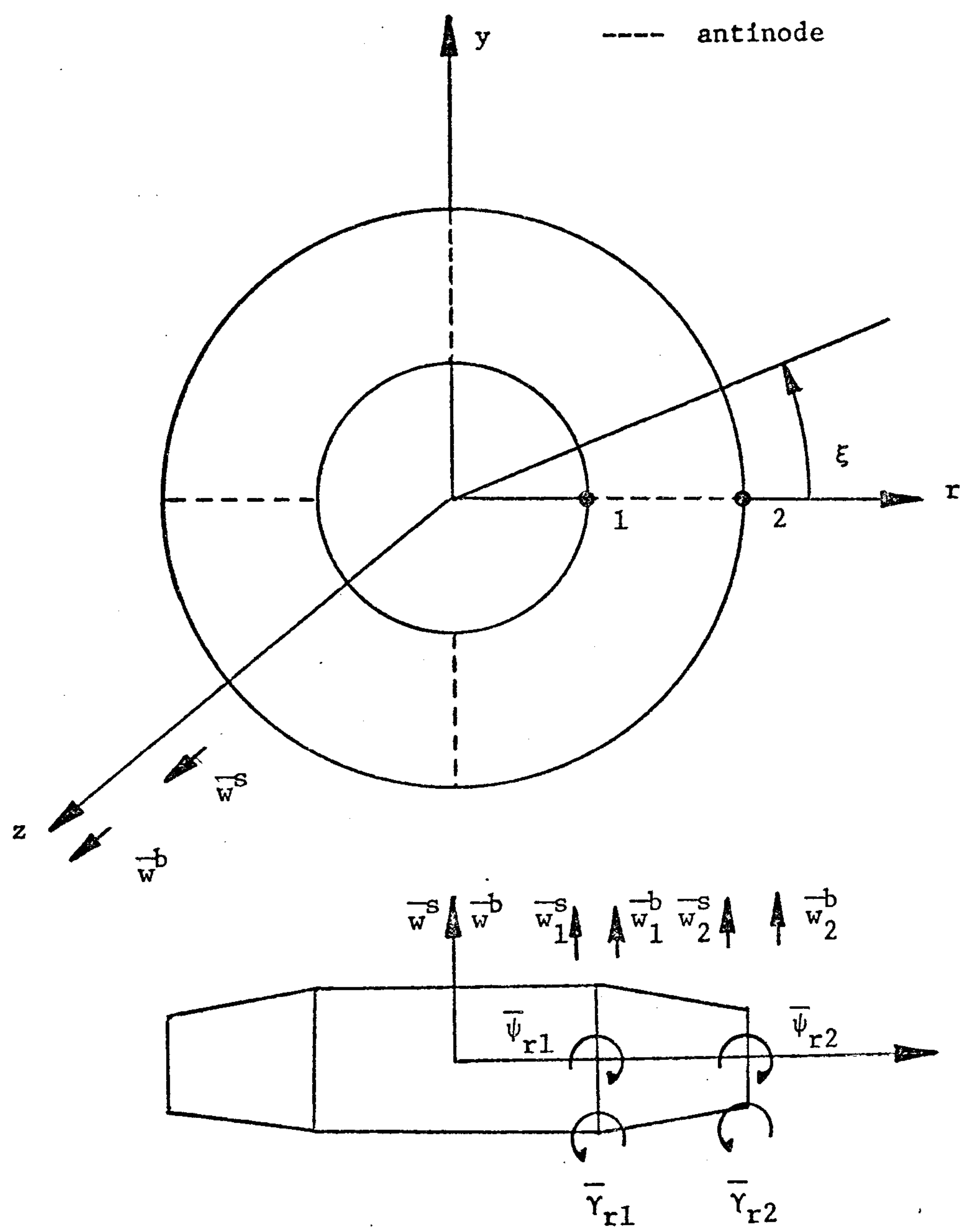

Figure 2. 10 Thick Disc Element-2 with two nodal diameters and associated degrees of freedom.

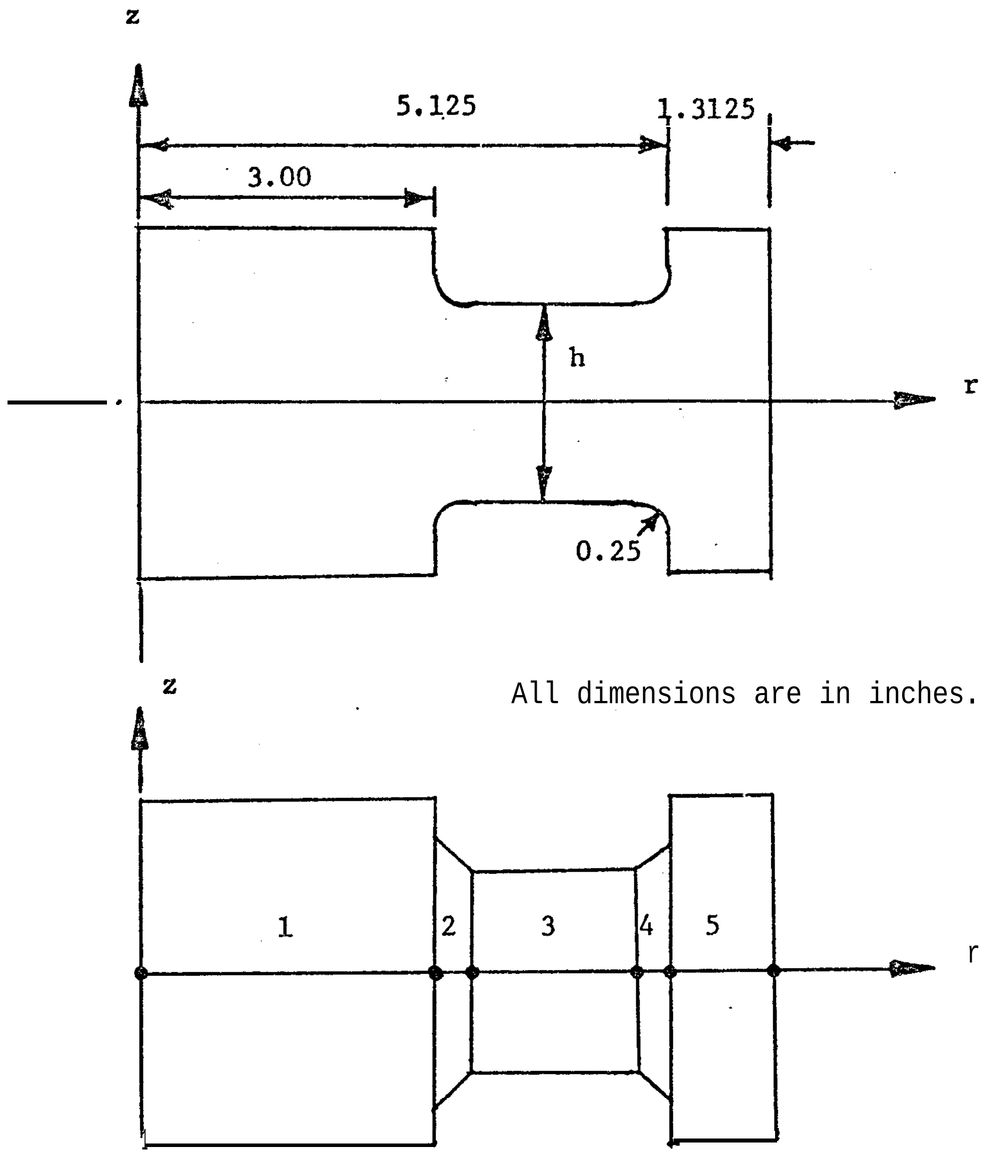

All dimensions are in inches.

Figure 2.11 Stepped circular disc and five element finite element model.

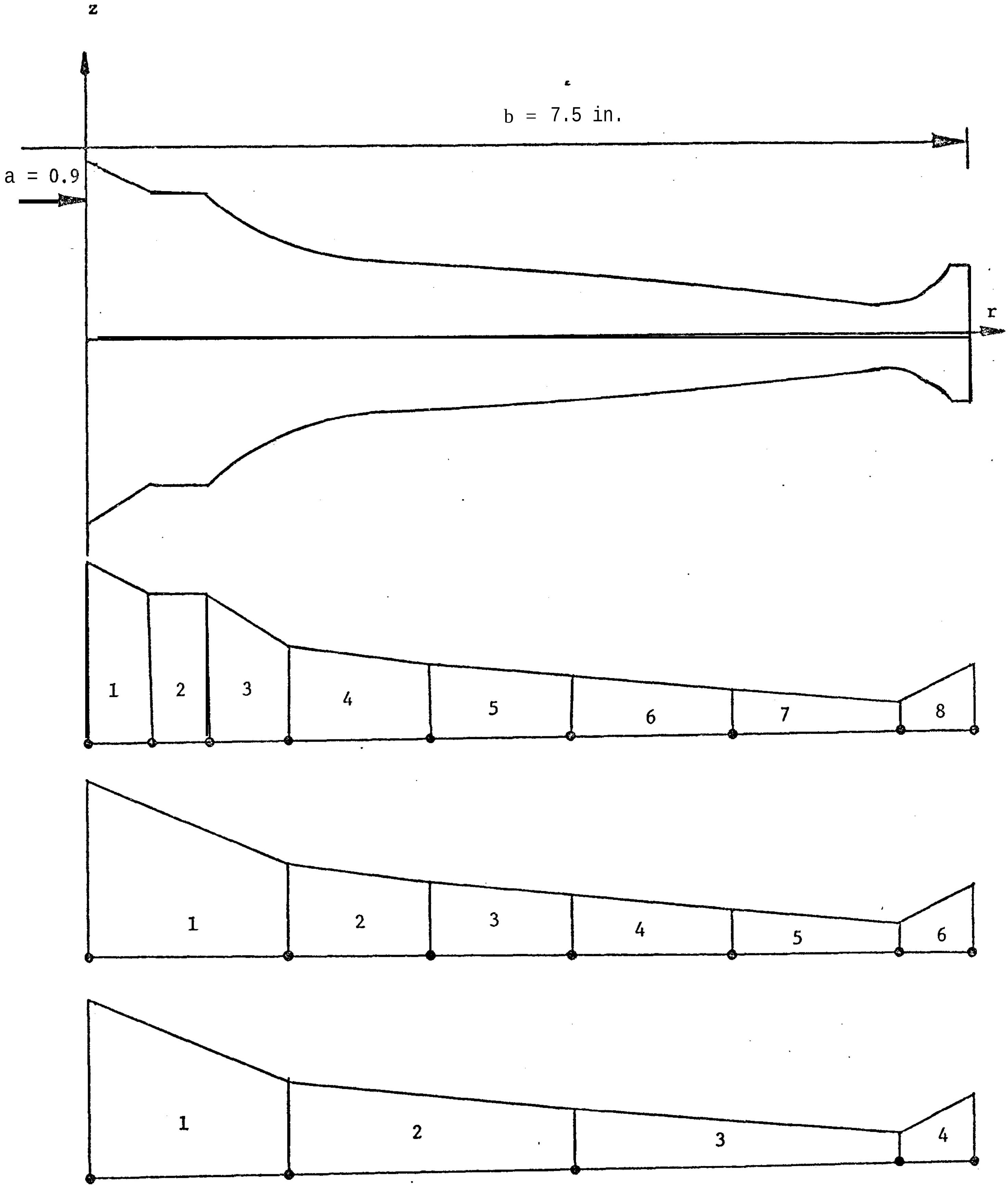

Figure 2.12 A practicl turbine disc and its finite element models.

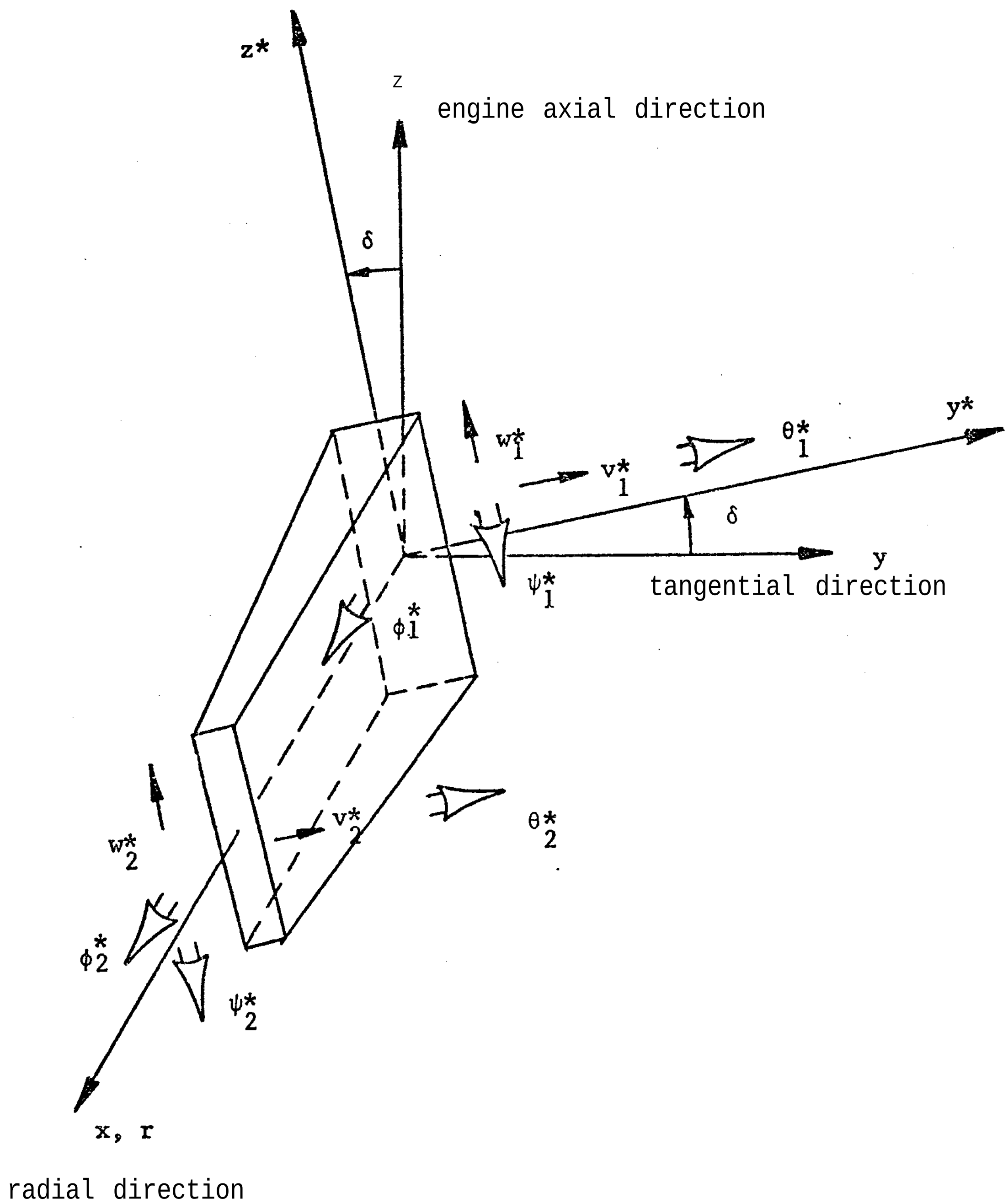

Figure 3.1 Blade element with associated degrees of freedom.

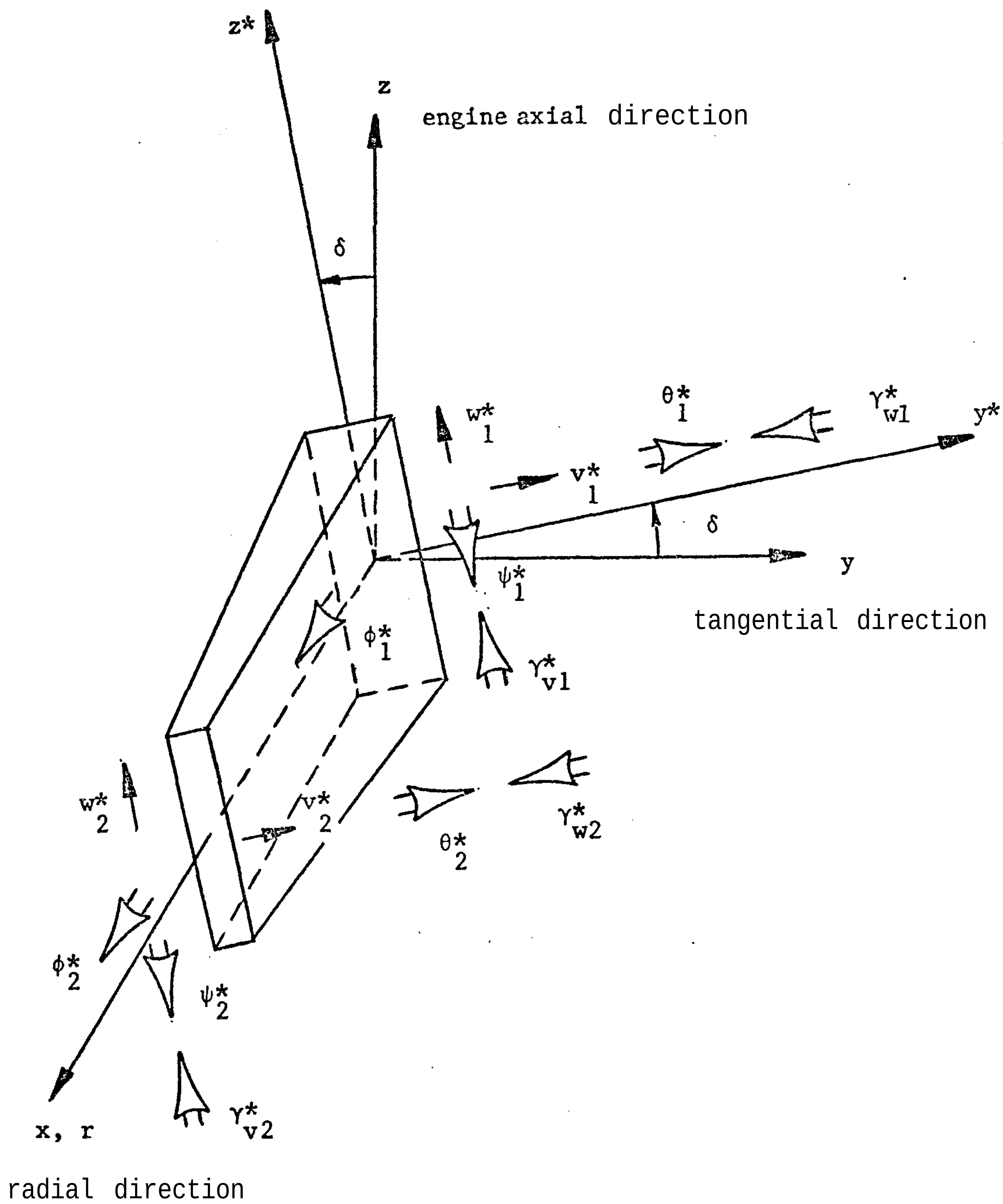

Figure 3.2 Blade element with associated degrees of freedom when transverse shear is considered.

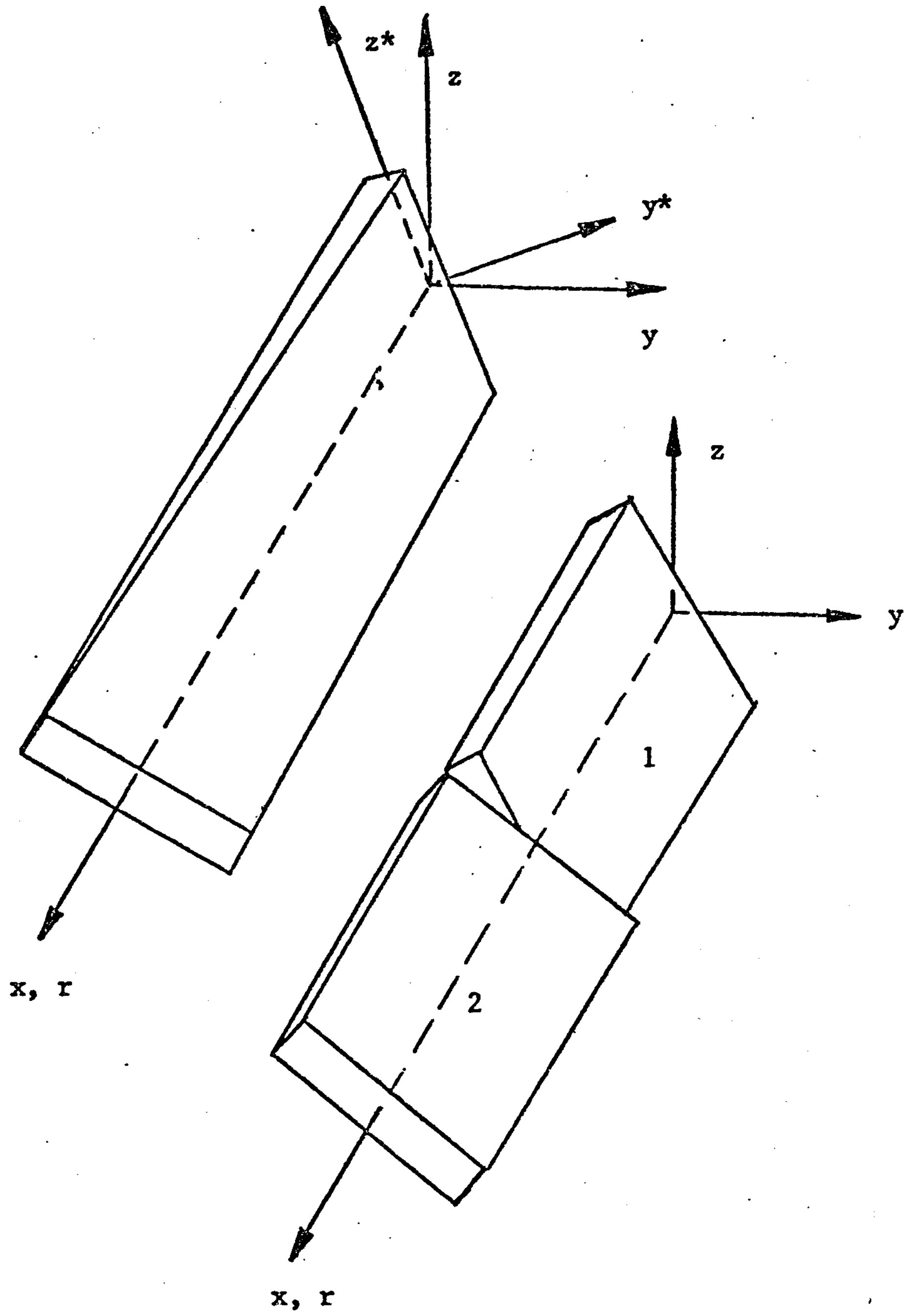

Figure 3.3 Pretwisted blade modelled with two straight beam elements.

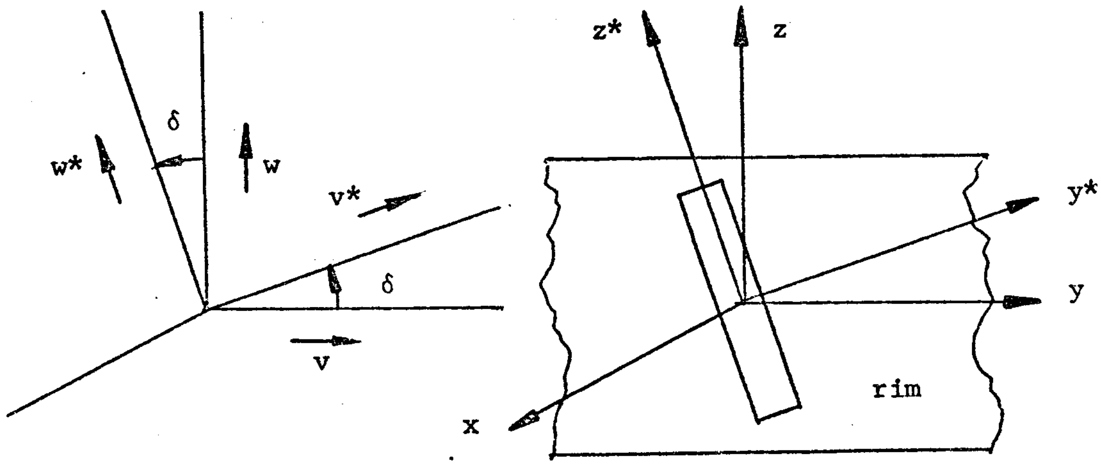

$$v^* = v\cos\delta + w\sin\delta$$

$$w^* = -v\sin\delta + w\cos\delta$$

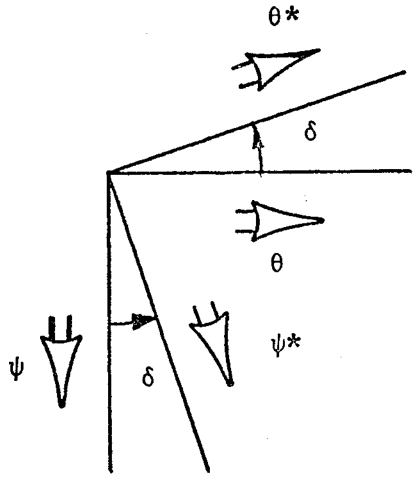

$$\psi^* = \psi\cos\delta + \theta\sin\delta$$

$$\theta^* = -\psi\sin\delta + \theta\cos\delta$$

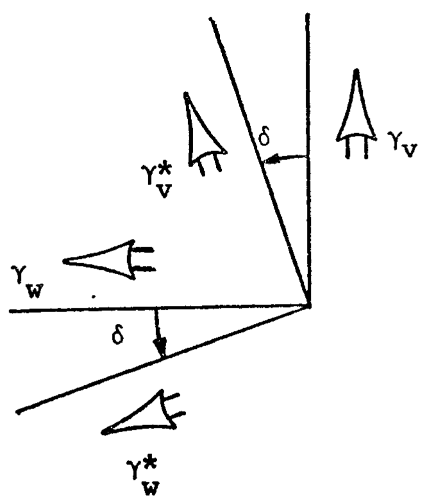

$$\gamma^*_v = \gamma_v\cos\delta + \gamma_w\sin\delta$$

$$\gamma^*_w = -\gamma_v\sin\delta + \gamma_w\cos\delta$$

Figure 3.4 Relationships between distortions along the principal directions and the coordinate system chosen.

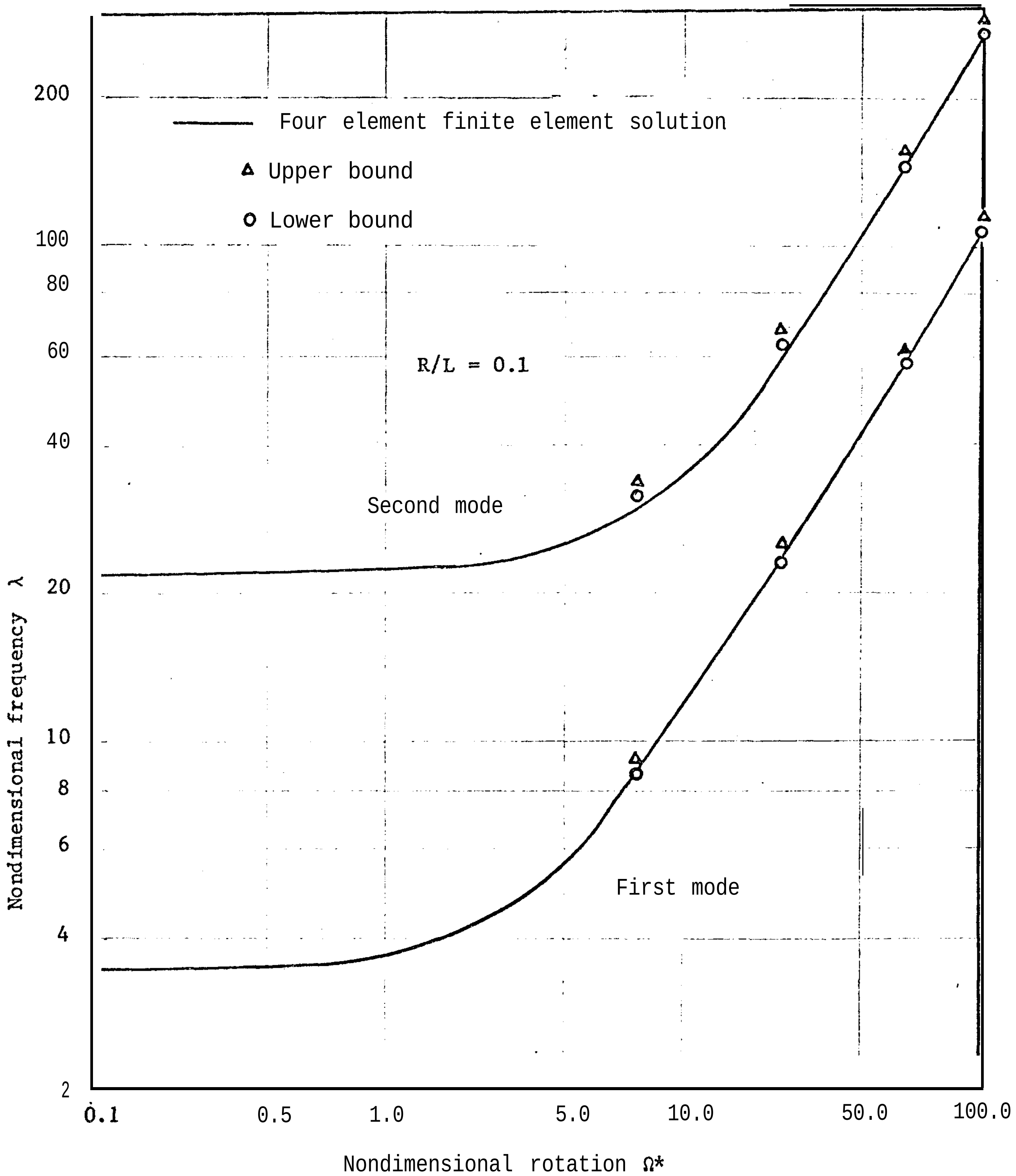

Figure 3.5 Variation of the first two frequencies of a rotating beam with speed of rotation - vibration out of plane of rotation.

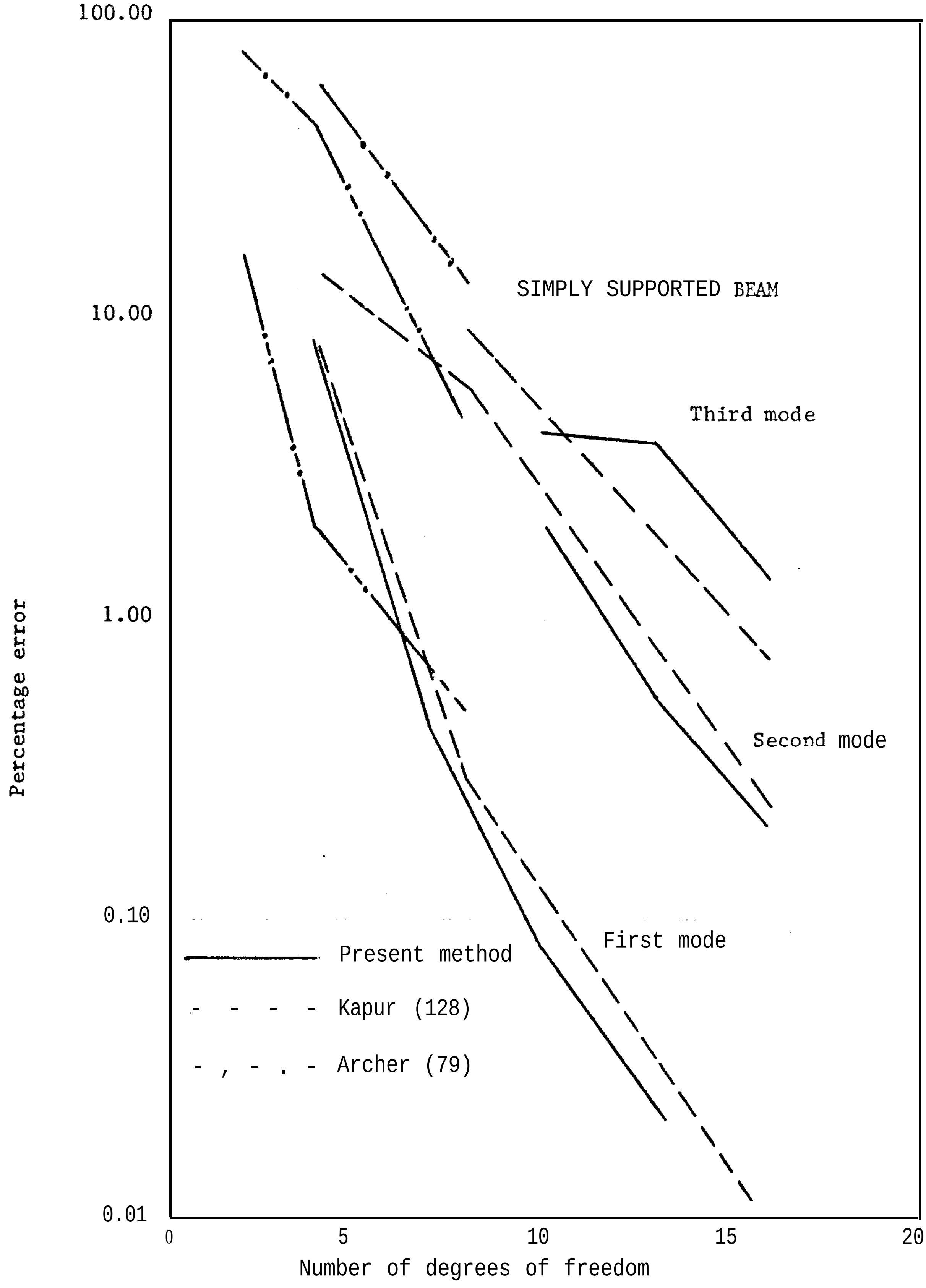

Figure 3.6 Percentage error versus degrees of freedom of Timoshenko beam elements.

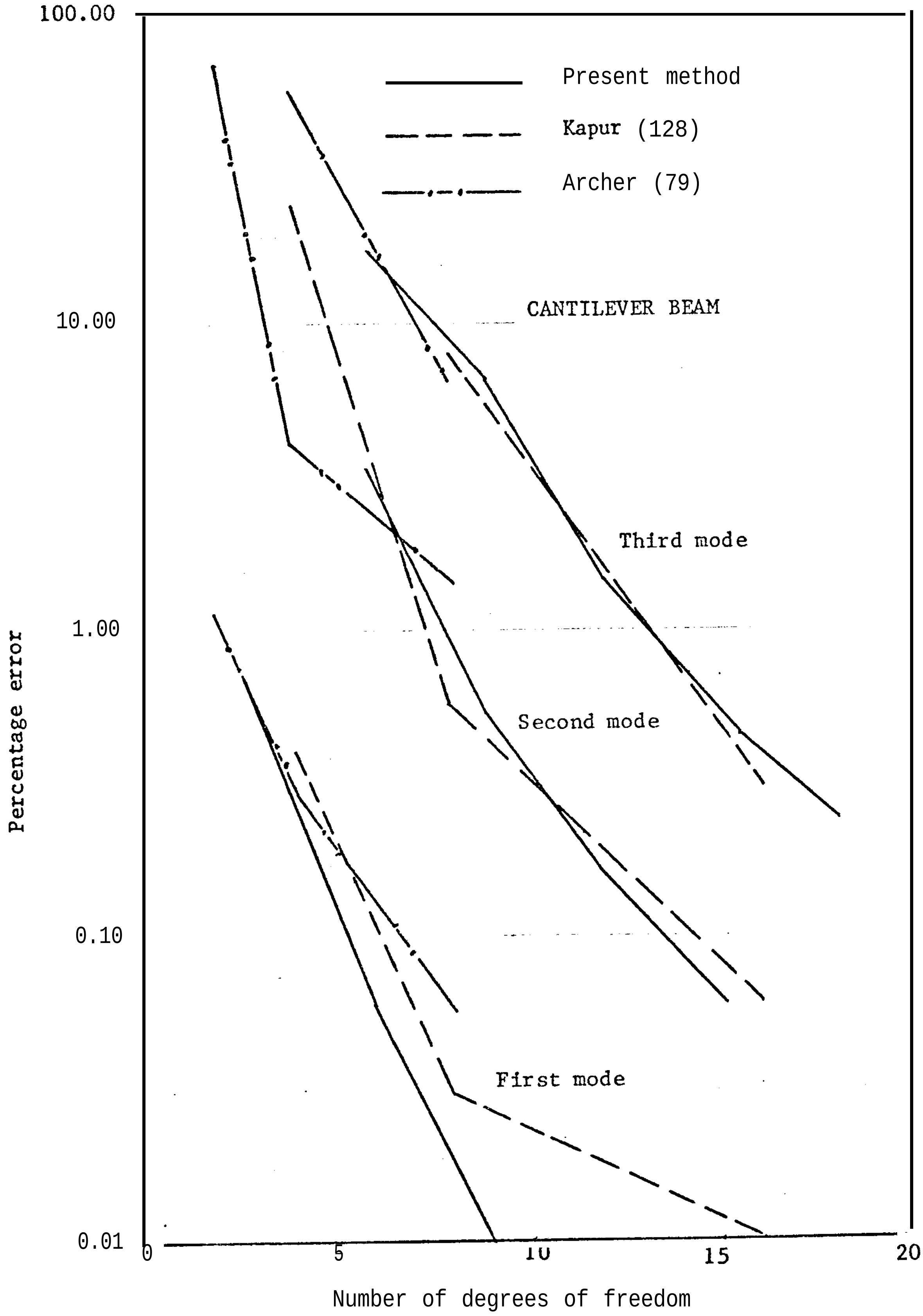

Figure 3.7 Percentage error versus degrees of freedom of Timoshenko beam elements.

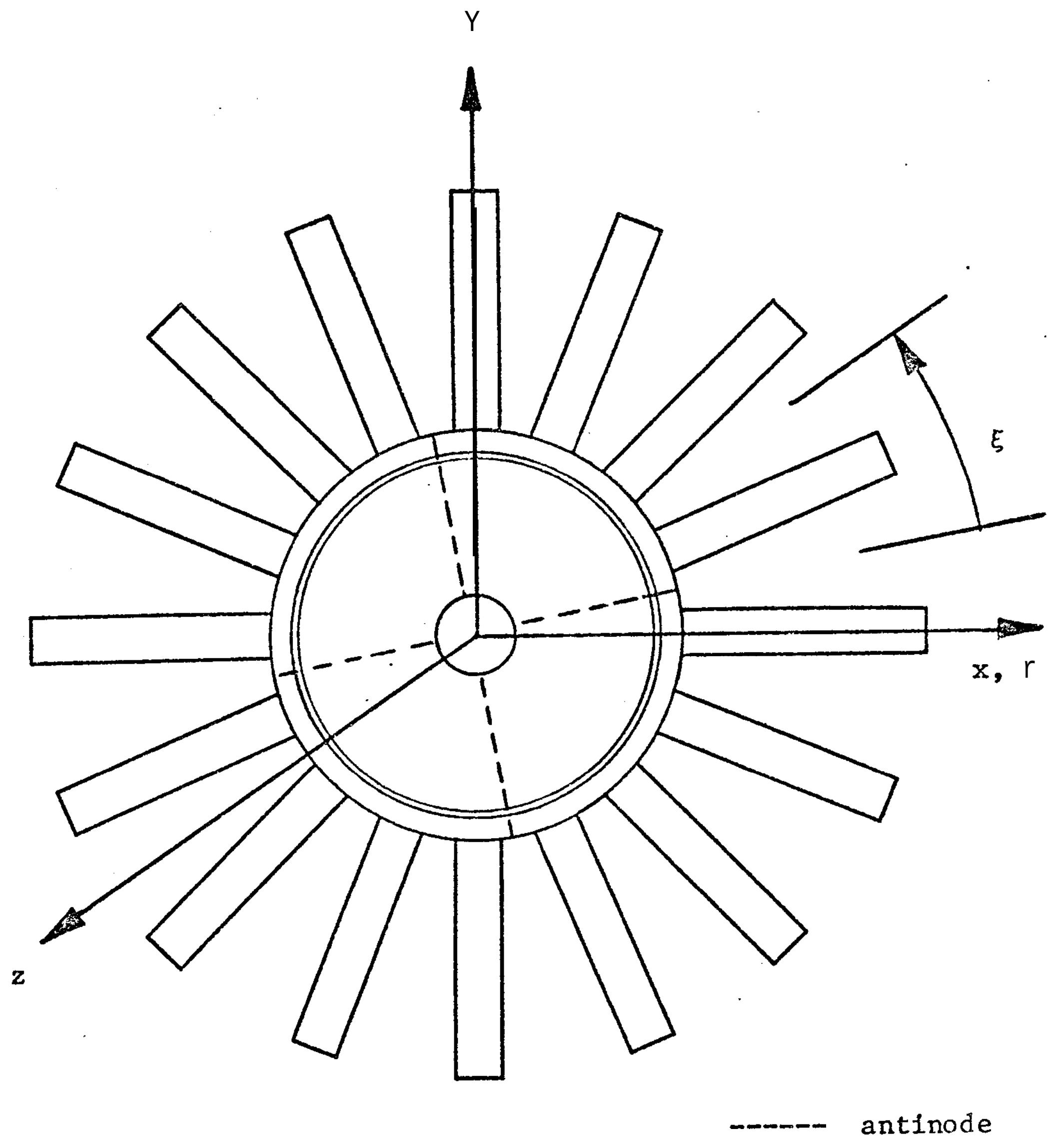

Figure 4.1 Bladed disc with two nodal diameters.

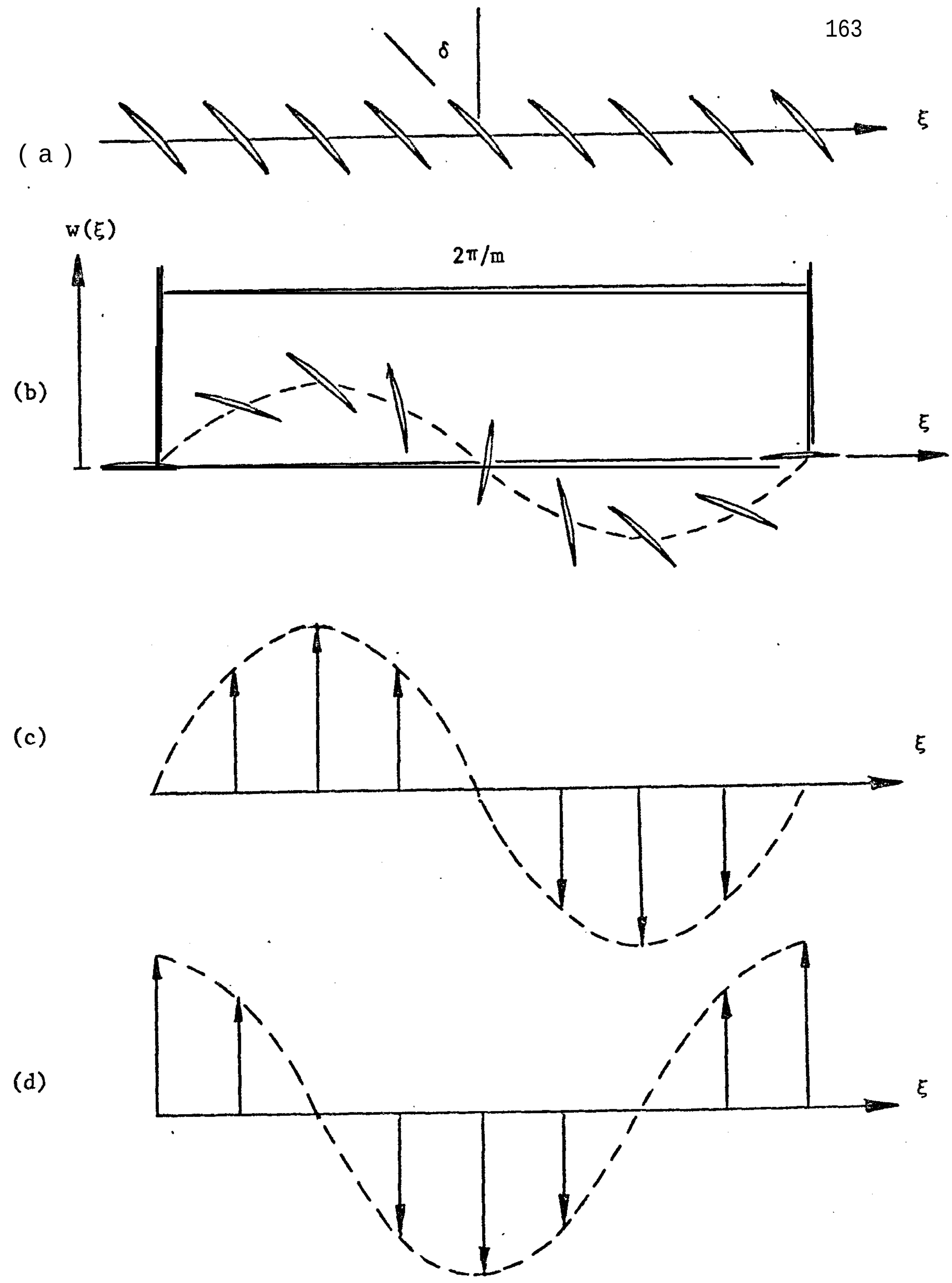

Figure 4.2 Rim deflections and forces. (a) undeflected position. (b) rim deflections. (c) blade shear force and bending moment. (d) blade torsional moment.

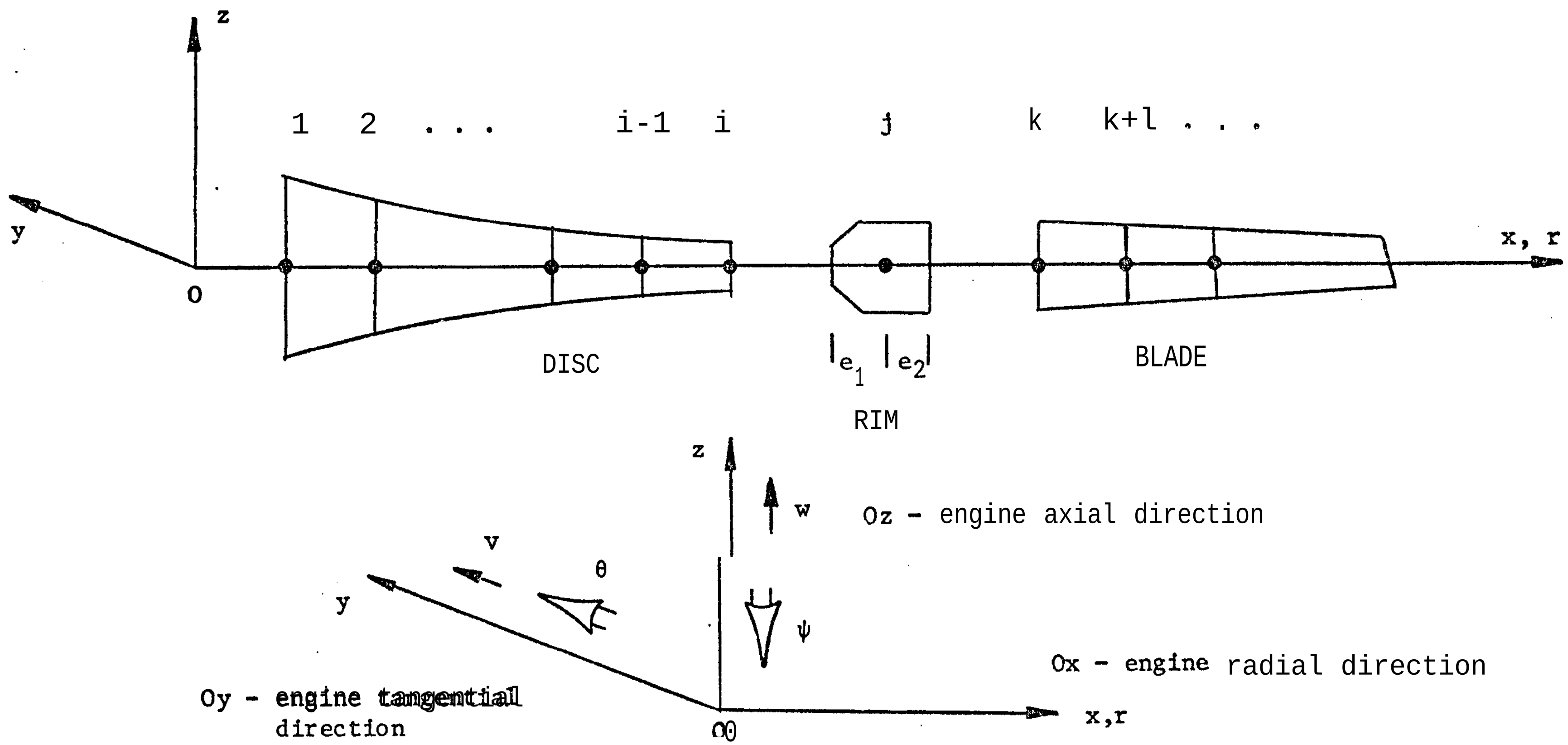

Figure 4.3 Bladed disc system configuration and deflections.

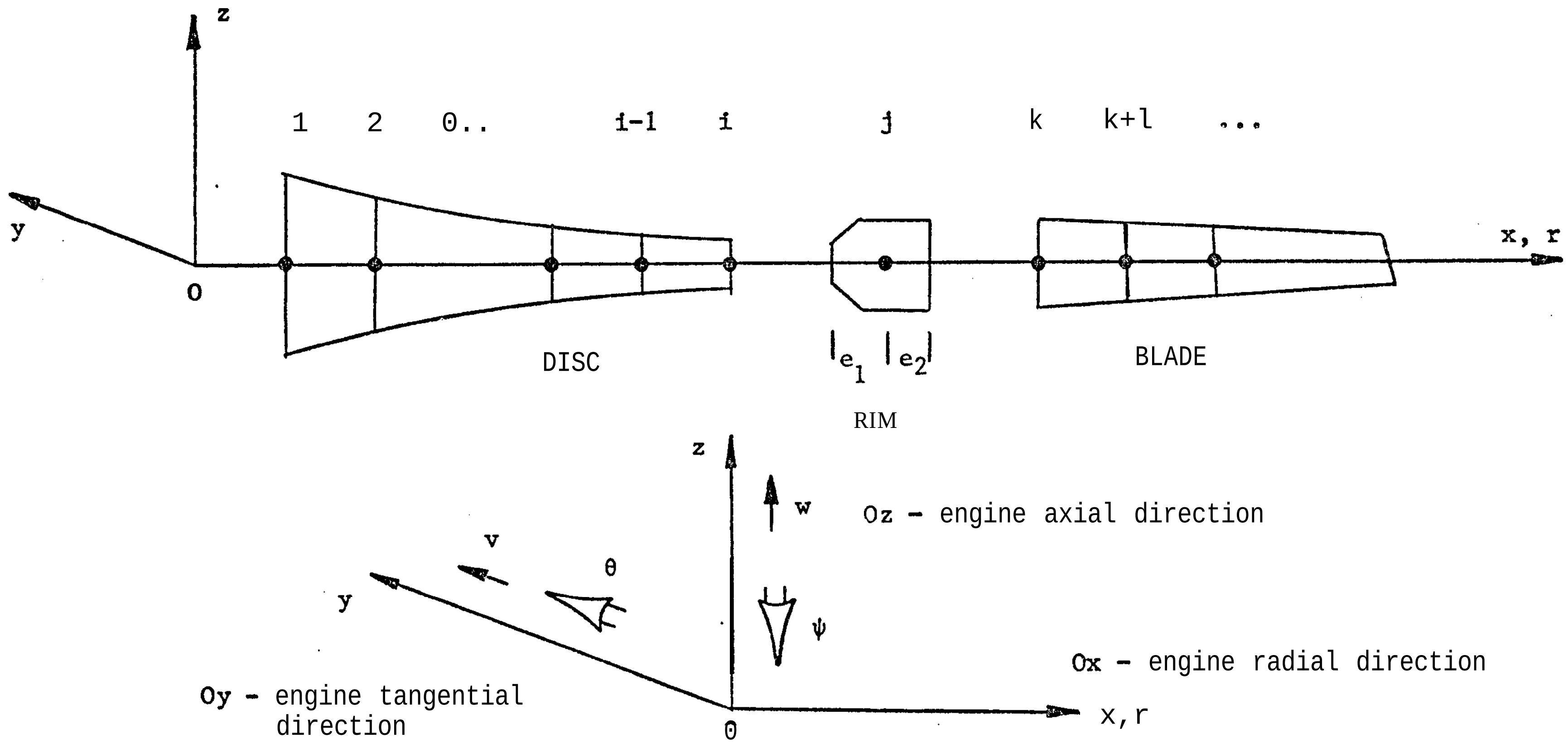

Figure 4.3 Bladed disc system configuration and deflections.

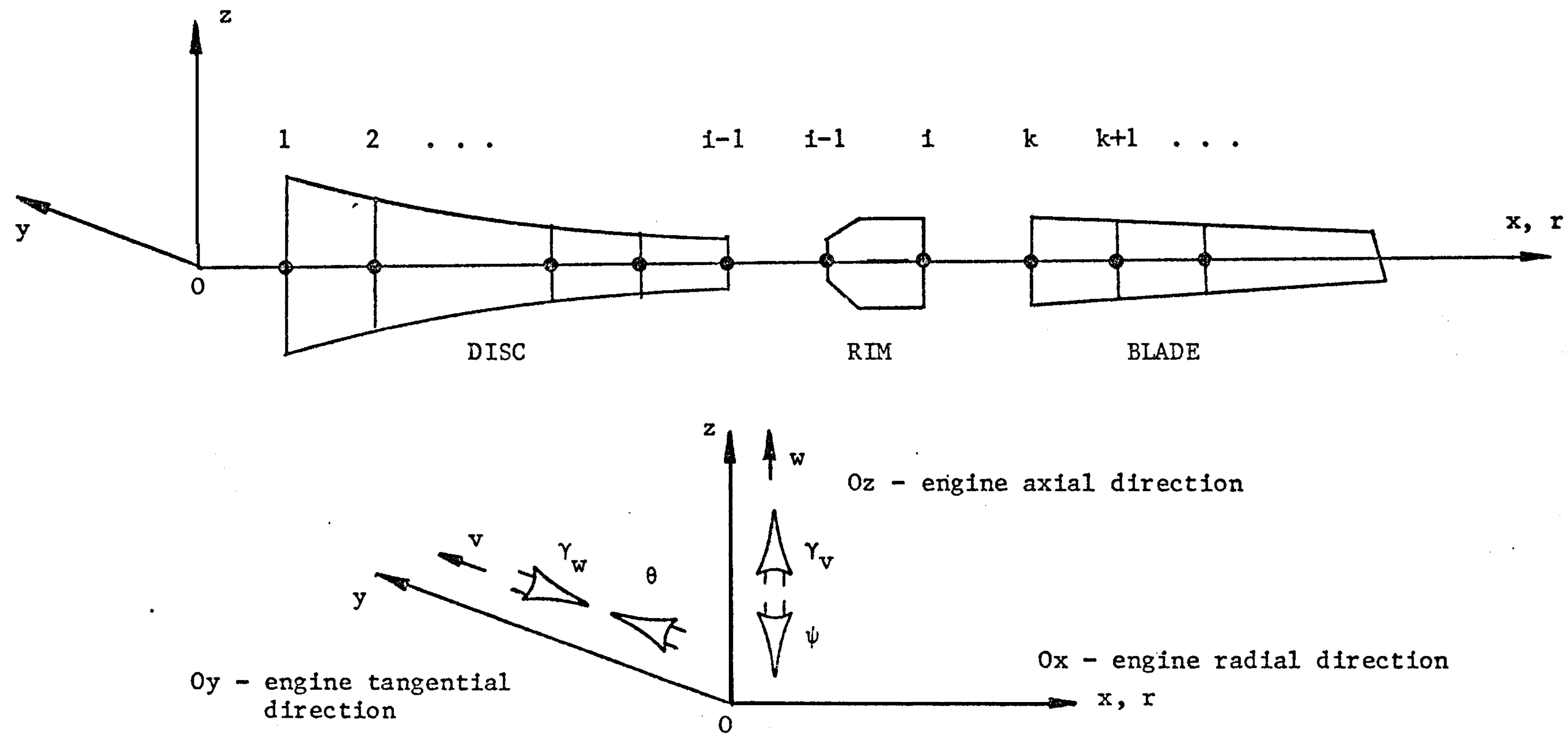

Figure 4.4 Bladed disc system configuration and deflections when transverse shear is also included.

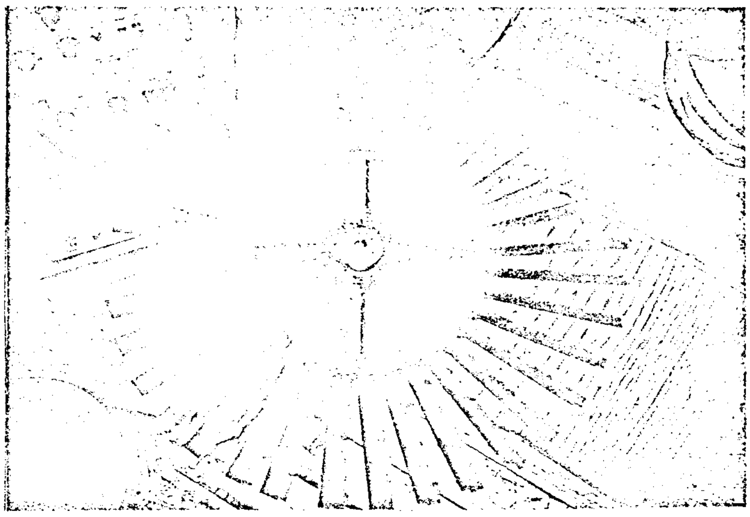

m = 2

Mode No. 4

ω = 1123 Hz

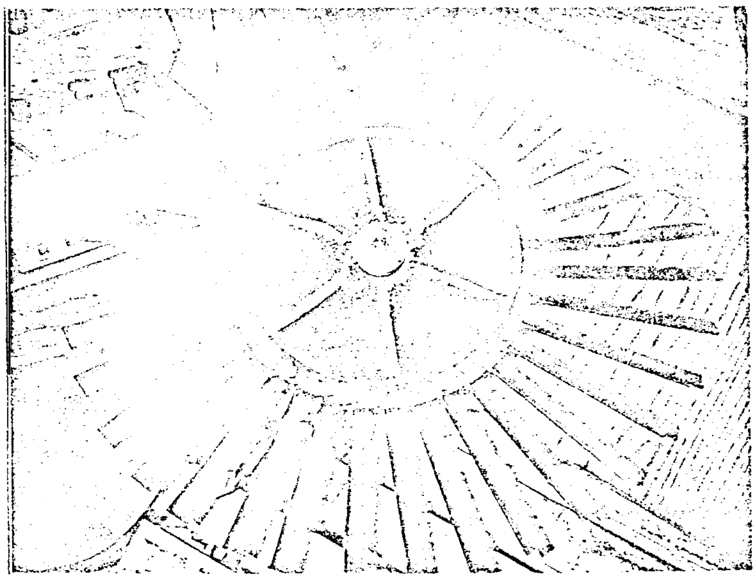

m = 3

Mode No. 5

ω = 1687 Hz

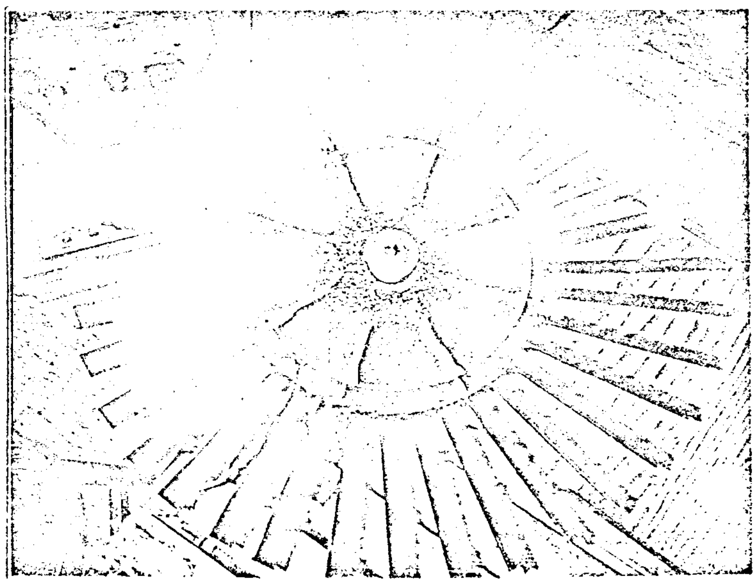

m = 4

Mode No. 6

ω = 2792 Hz

Figure 4.5 Sand pattern illustrating mode shapes of vibrating bladed disc models.

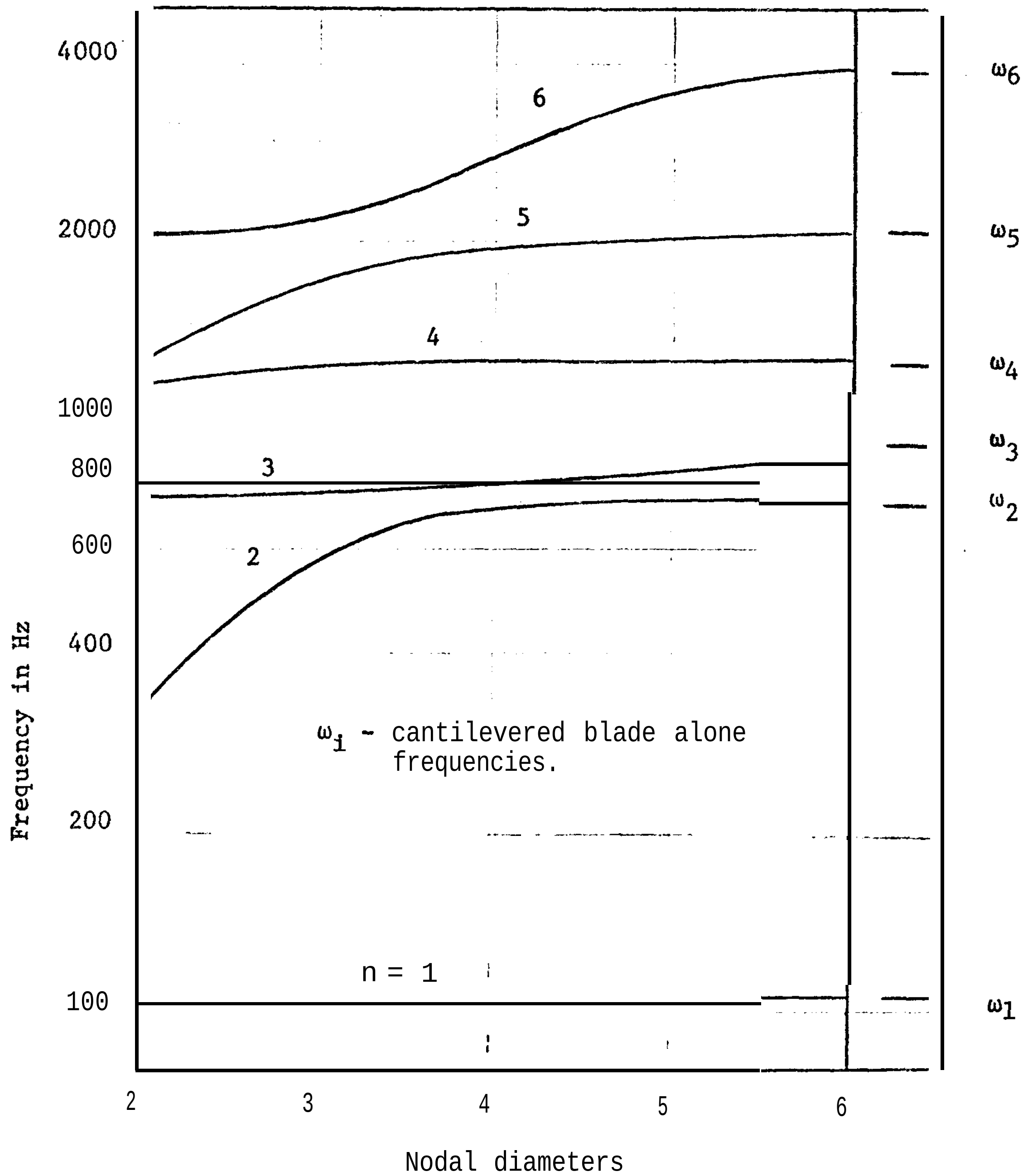

Figure 4.6 Variation of the first six coupled bladed disc frequencies with nodal diameters, Model I.

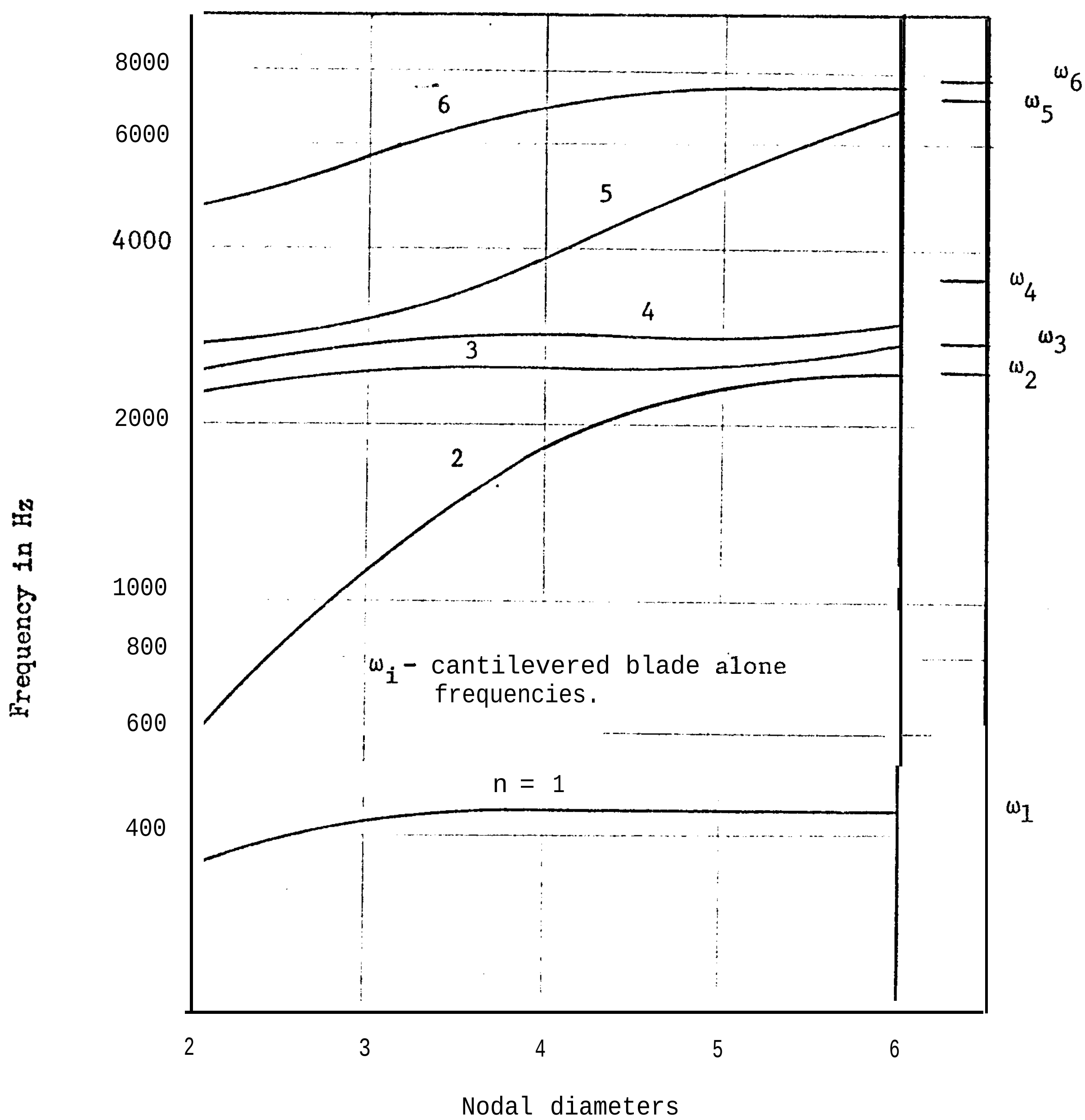

Figure 4.7 Variation of the first six coupled bladed disc frequencies with nodal diameters, Model II.

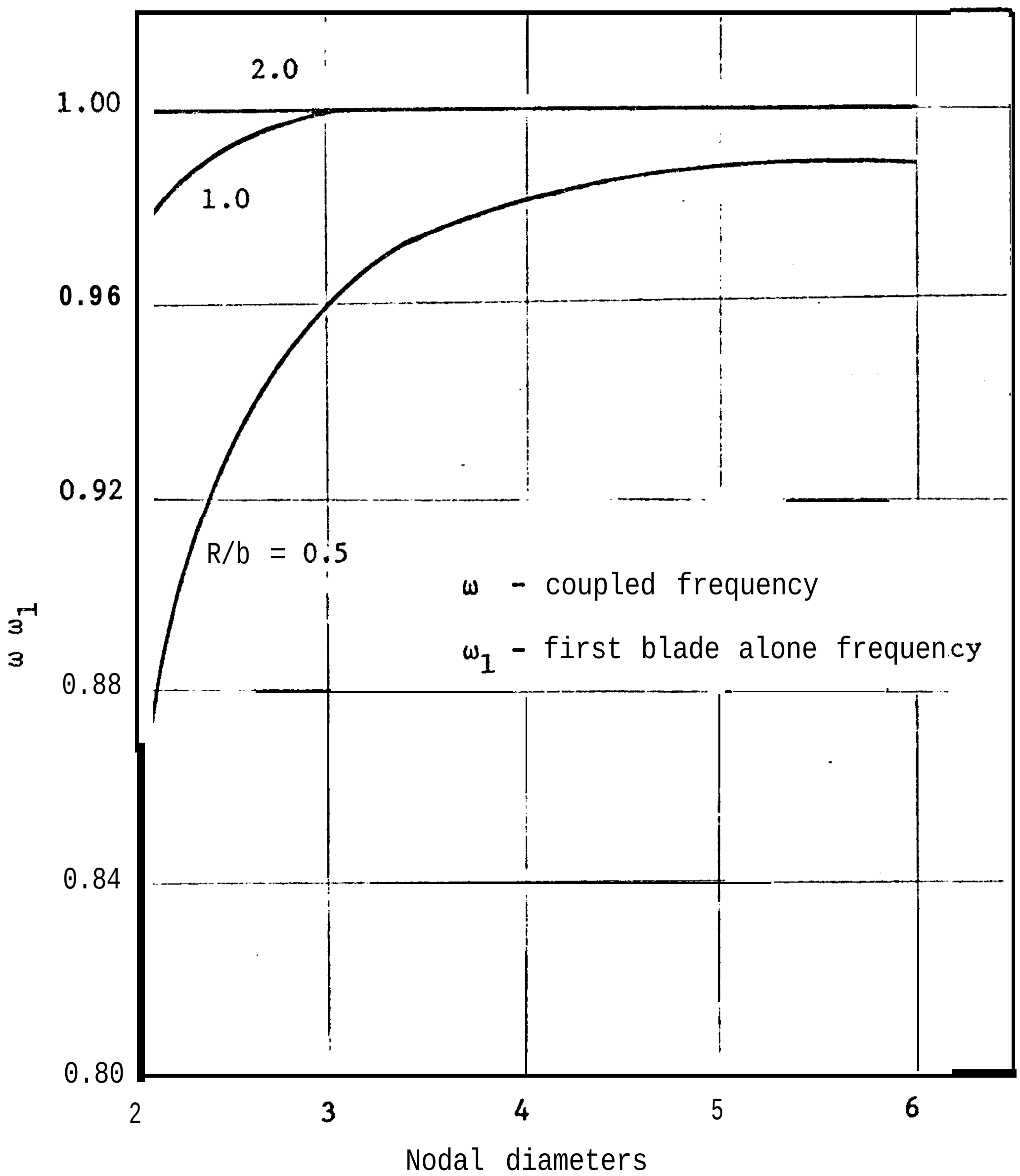

Figure 4.8 Influence of ℓ/b ratio on the first coupled bladed disc frequency.

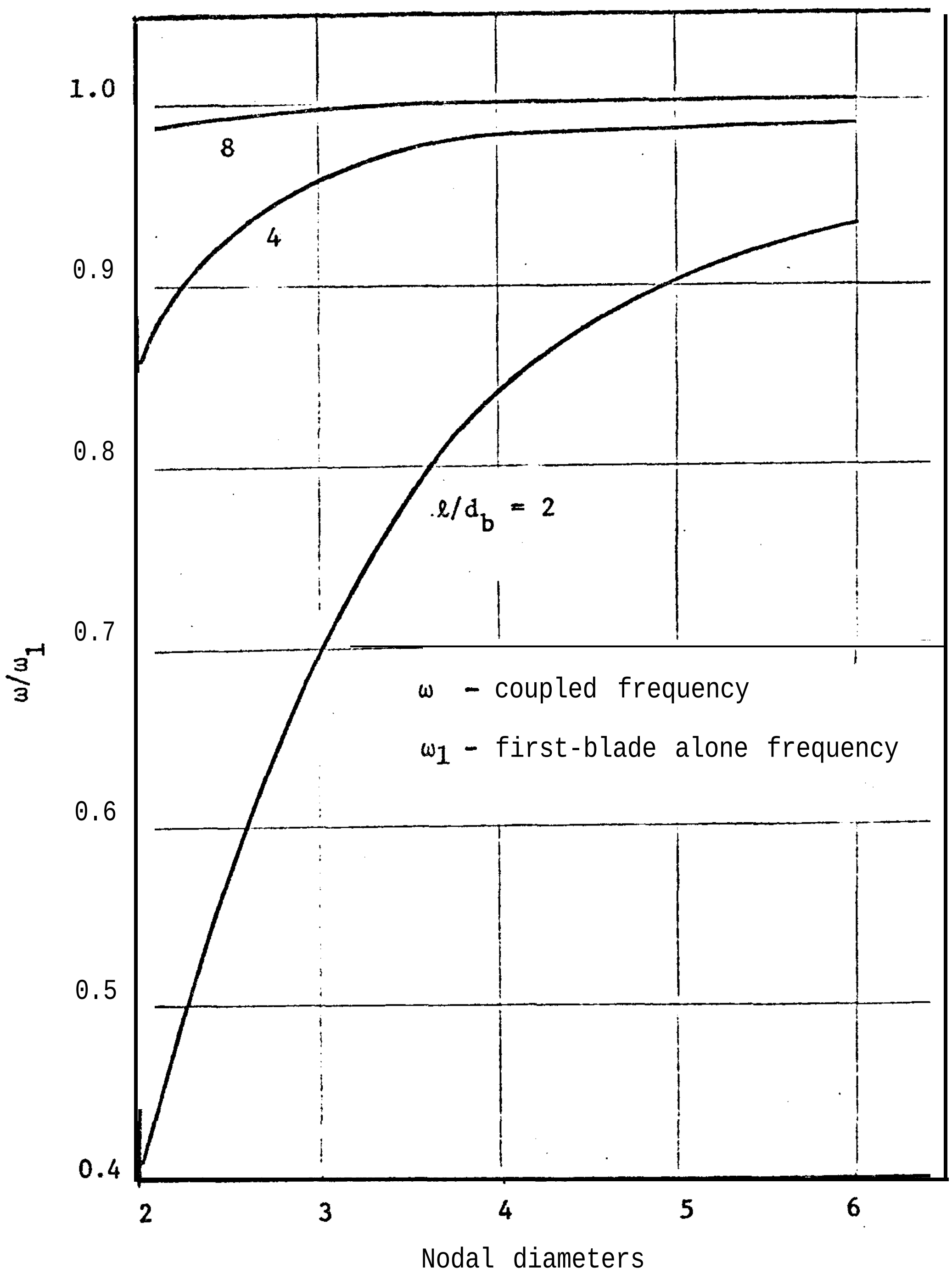

Figure 4.9 Influence of blade aspect ratio on the first coupled bladed disc frequency.

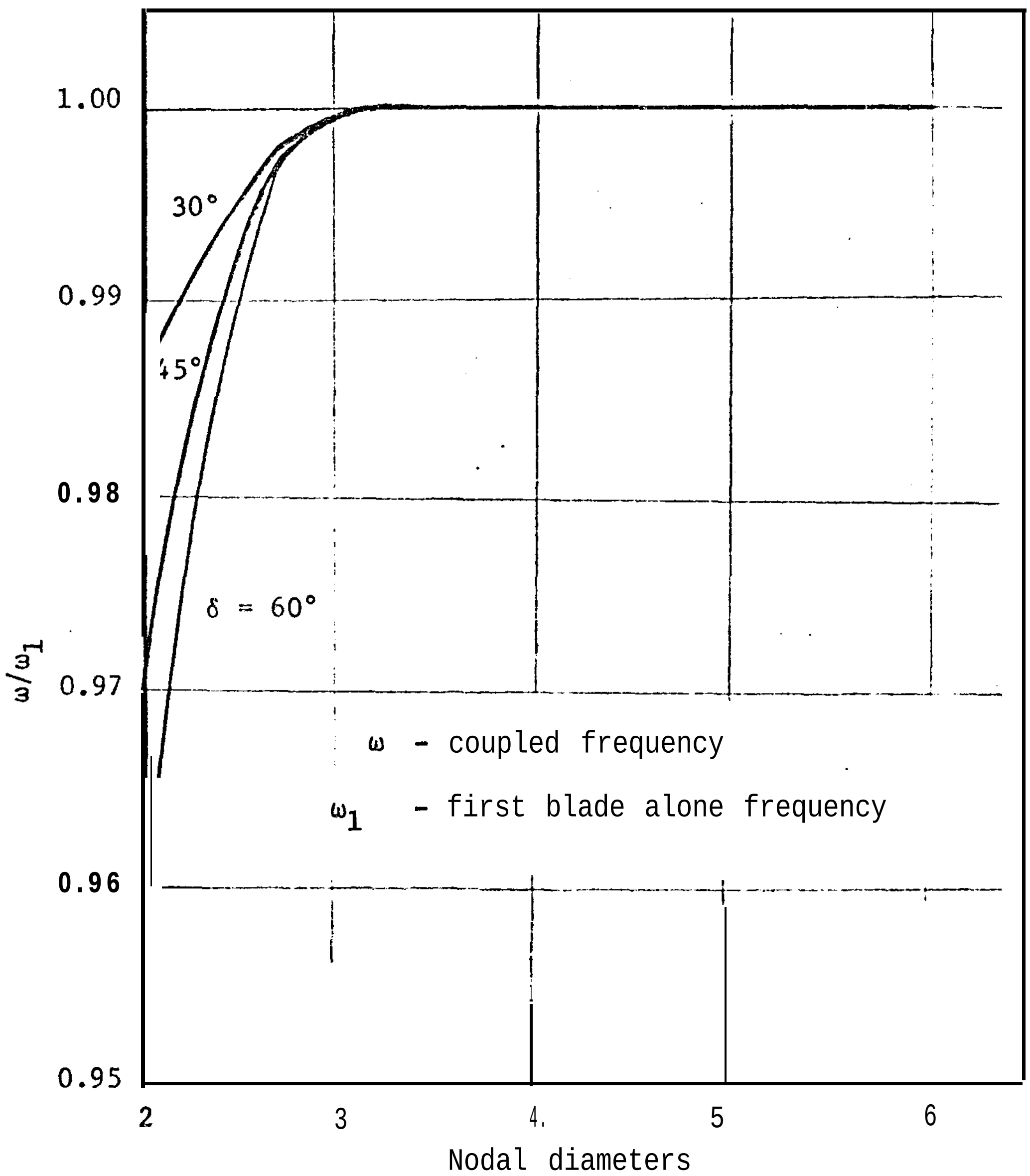

Figure 4.10 Influence of blade stagger angle on the first coupled bladed disc frequency.

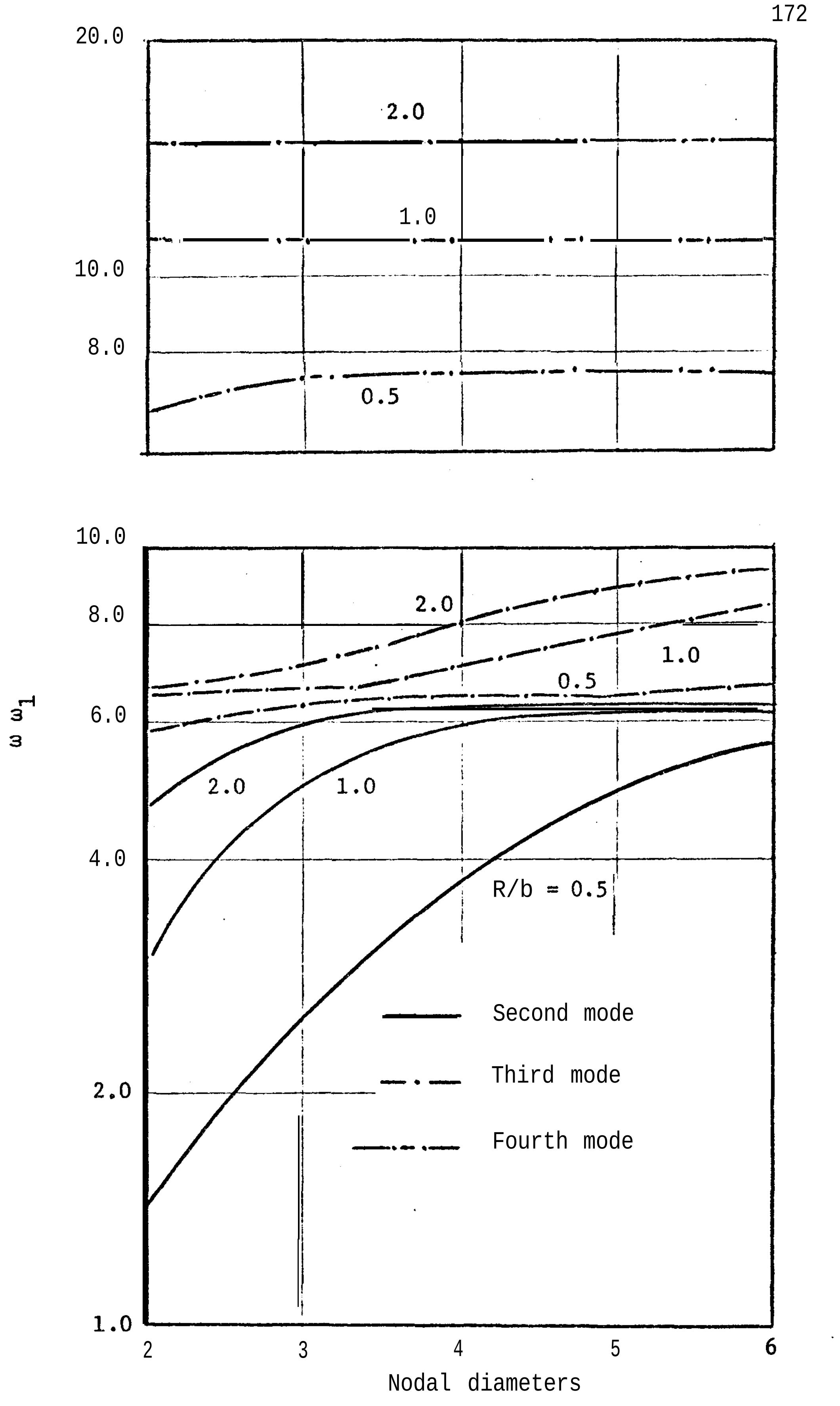

Figure 4.11 Influence of R/b ratio on the higher coupled frequencies.

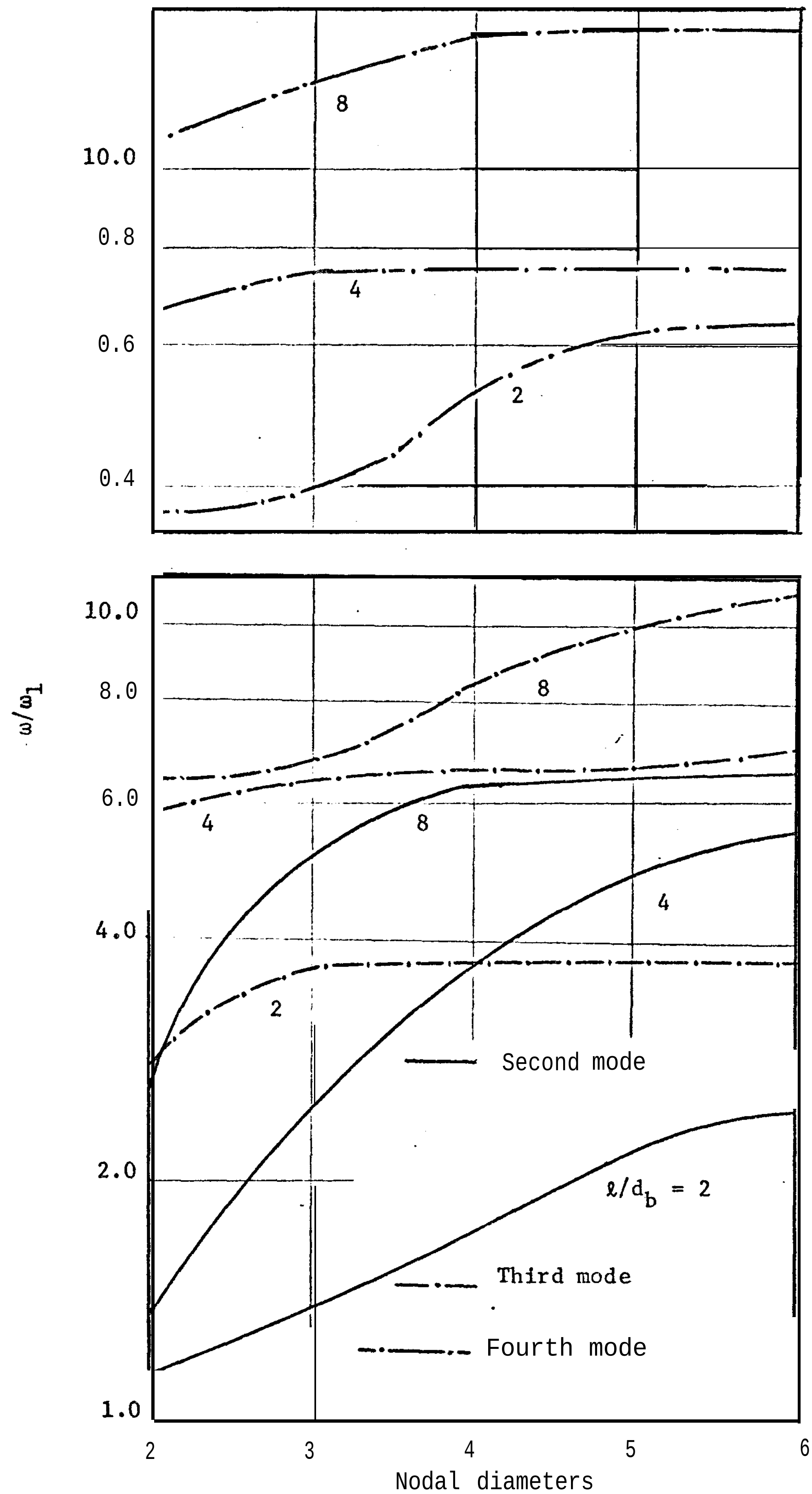

Figure 4.12 Influence of blade aspect ratio on higher coupled frequencies.

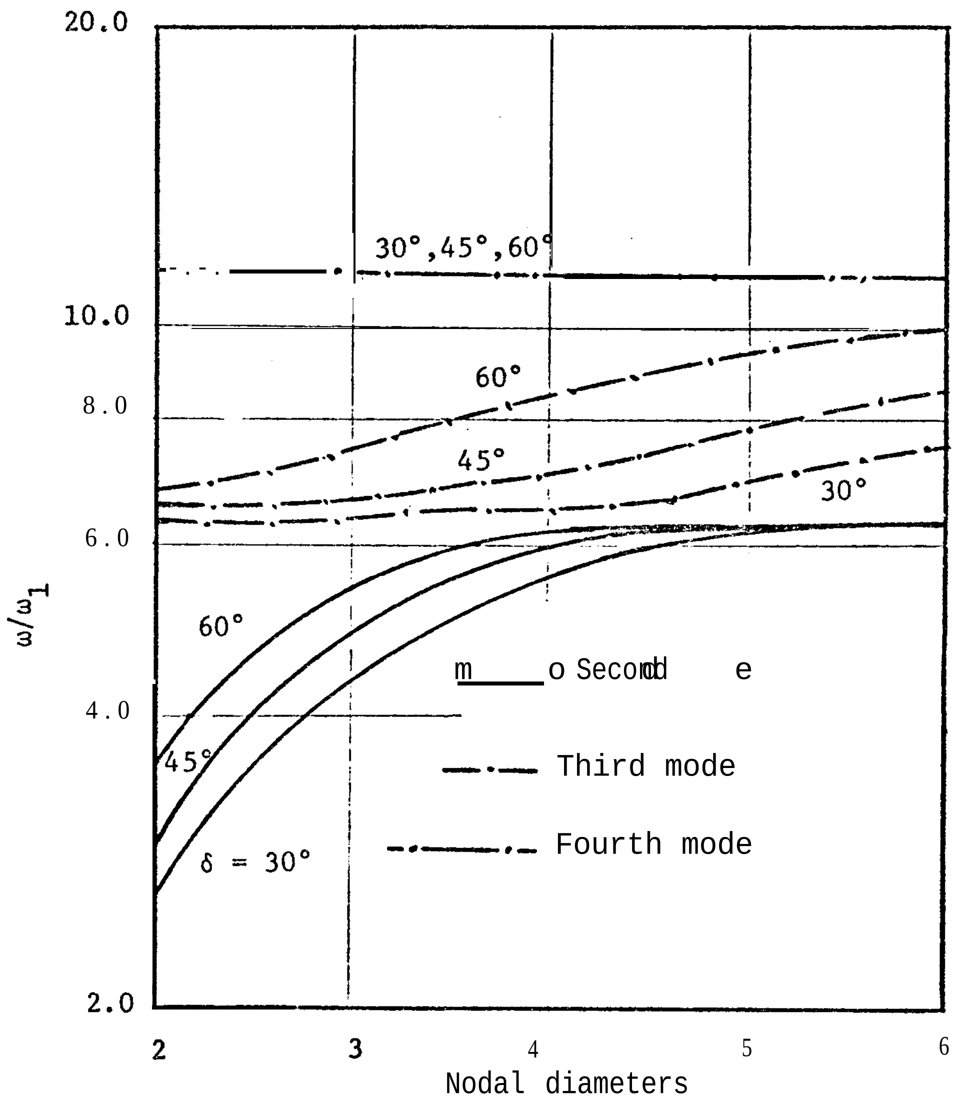

Figure 4.13 Influence of stagger angle on the higher coupled frequencies.

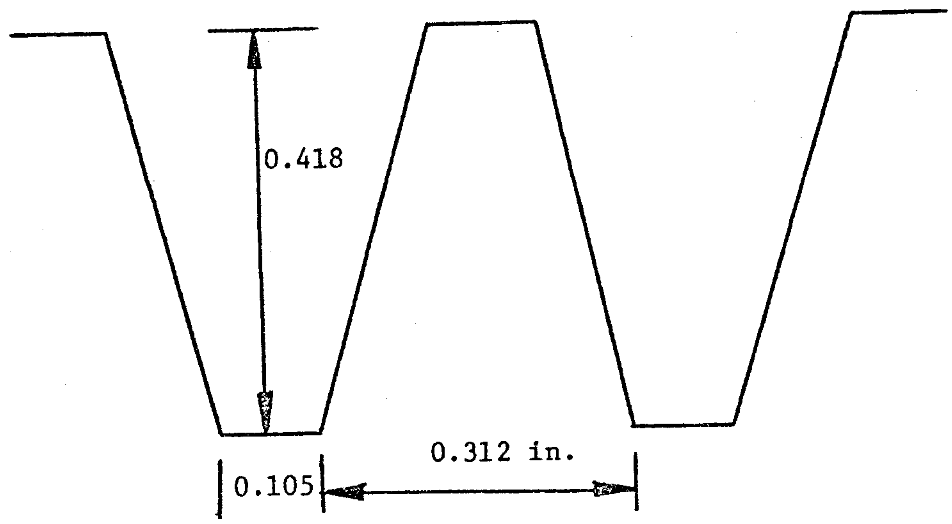

Number of castellations = 113

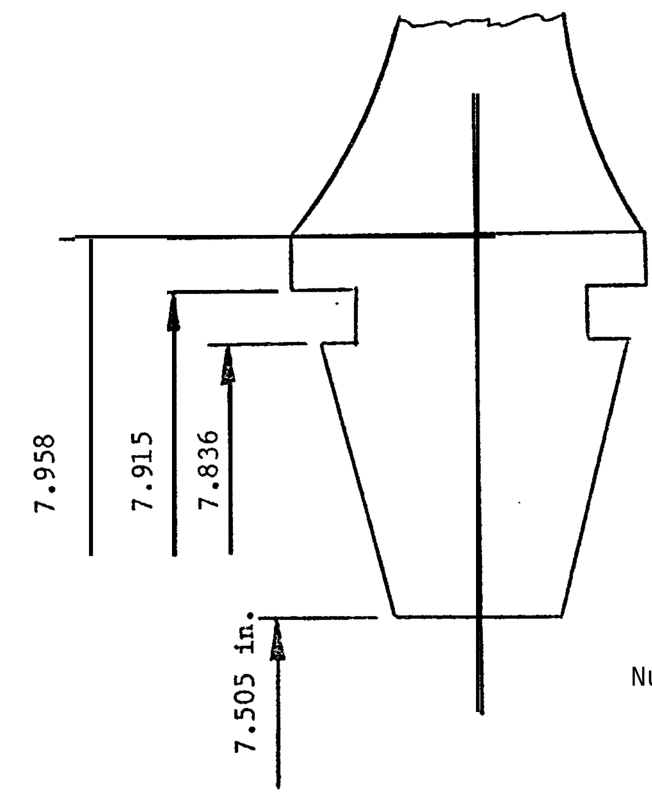

Number of blades = 113

Figure 4.14 Details at the blade disc attachment of the turbine rotor.

TABLE 2.1

Matrix $[B_d]$

$\frac{r_2^2 (r_2 - 3r_1)}{(r_2 - r_1)^3}$	$\frac{r_1 r_2^2}{(r_2 - r_1)^2}$	$\frac{r_1^2 (3r_2 - r_1)}{(r_2 - r_1)^3}$	$\frac{r_1^2 r_2}{r_2 - r_1)^2}$
$\frac{6r_1 r_2}{r_2 - r_1)^3}$	$-\frac{r_2 (2r_1 + r_2)}{(r_2 - r_1)^2}$	$-\frac{6r_1 r_2}{(r_2 - r_1)^3}$	$\frac{r_1 (r_1 + 2r_2)}{(r_2 - r_1)^2}$
$\frac{3 (r_1 + r_2)}{r_2 - r_1)^3}$	$\frac{(r_1 + 2r_2)}{(r_2 - r_1)^2}$	$\frac{3 (r_1 + r_2)}{(r_2 - r_1)^3}$	$\frac{(2r_1 + r_2)}{(r_2 - r_1)^2}$
$\frac{2}{(r_2 - r_1)^3}$	$-\frac{1}{(r_2 - r_1)^2}$	$-\frac{2}{(r_2 - r_1)^3}$	$-\frac{1}{(r_2 - r_1)^2}$

TABLE 2.2

Matrix [kd] of the thin plate bending annular element.

$P_{-3}(m^4+2m^2-2\nu m^2)$	$P_{-2}(m^4-m^2)$	$P_{-1}(m^4-4m^2)$	$P_o(m^4-7m^2-2\nu m^2)$
	$P_{-1}(m^4-2m^2+1)$	$P_o(m^4-3m^2-2\nu m^2+2\nu+2)$	$P_1(m^4-4m^2-6\nu m^2+6\nu+3)$
symmetrical $P_i = \frac{\text{CITE}}{12(1-\nu^2)} \int_{r_1}^{r_2} h^3(r) r^i dr$		$P_1(m^4-2m^2-6\nu m^2+8\nu+8)$	$P_2(m^4-m^2-12\nu m^2+18\nu+18)$
			$P_3(m^4+2m^2-20\nu m^2+36\nu+45)$

TABLE 2.3

Matrix [md] of the thin plate bending annular element.

Q_1	Q_2	Q_3	Q_4
	Q_3	Q_4	Q_5
Symmetrical $Qi = C\pi\rho \int_{r_1}^{r_2} h(r) r^i dr$		Q_5	Q_6
			Q_7

TABLE 2.4

The deflection vector $\{q_d^o\}$ and the matrices $[B_d^o]$, $[k_d^o]$ and $[m_d^o]$ of the thin plate bending circular element with m = 0.

$$\{q_d^o\}^T = [\ \bar{w}_1 \quad \bar{w}_2 \quad \bar{\theta}_2\ ]$$

$$[B_d] = \begin{bmatrix} 1 & 0 & 0 \\ -\dfrac{3}{r_2^2} & \dfrac{1}{r_2} & \dfrac{3}{r_2^2} \\ \dfrac{2}{r_2^3} & -\dfrac{1}{r_2^2} & -\dfrac{2}{r_2^3} \end{bmatrix}$$

$$[k_d^o] = \begin{bmatrix} 0 & 0 & 0 \\ 0 & P_1(8\nu+8) & P_2(18\nu+18) \\ 0 & P_2(18\nu+18) & P_3(36\nu+45) \end{bmatrix}$$

$$[m_d^o] = \begin{bmatrix} Q_1 & Q_2 & Q_4 \\ Q_2 & Q_5 & Q_6 \\ Q_4 & Q_6 & Q_7 \end{bmatrix}$$

$$P_i = 2\pi \frac{E}{12(1-\nu^2)} \int_0^{r_2} h^3(r) r^i dr \ ; \quad Q_i = 2\pi \int_0^{r_2} \rho h(r) r^i dr$$

TABLE 2.5

The deflection vector $\{q_d^o\}$ and the matrices $[B_d^o]$, $[k_d^o]$ and $[m_d^o]$ of the thin plate bending circular element with m = 1.

$$\{q_d^o\}^T = [\bar{\theta}_1 \quad \bar{w}_2 \quad \bar{\theta}_2]$$

$$[B_d^0] = \begin{bmatrix} -1 & 0 & 0 \\ \frac{2}{r_2} & \frac{3}{r_2^2} & \frac{1}{r_2} \\ -\frac{1}{r_2^2} & -\frac{2}{r_2^3} & -\frac{1}{r_2^2} \end{bmatrix}$$

$$[k_d^o] = \begin{bmatrix} 0 & 0 & 0 \\ 0 & P_1(7+2\nu) & P_2(18+6\nu) \\ 0 & P_2(18+6\nu) & P_3(48+16\nu) \end{bmatrix}$$

$$[m_d^o] = \begin{bmatrix} Q_3 & Q_4 & Q_5 \\ Q_4 & Q_5 & Q_6 \\ Q_5 & Q_6 & Q_7 \end{bmatrix}$$

$$P_i = \frac{\pi E}{12(1-\nu^2)} \int_0^{r_2} h^3(r) r^i dr \quad ; \quad Q_i = \pi \int_0^{r_2} \rho h(r) r^i dr$$

TABLE 2.6

The deflection vector $\{q_d^o\}$ ant the matrices $[B_d^o]$, $[k_d^o]$ and $[m_d^o]$ of the thin plate bending circular element with m = 2,4,6,...

$$\{q_d^o\}^T = [\ \bar{w}_1 \quad \bar{\theta}_2\ ]$$

$$[B_d^o] = \begin{bmatrix} -\dfrac{2}{r_2^2} & \dfrac{1}{r_2} \\ \\ \dfrac{2}{r_2^3} & -\dfrac{1}{r_2^2} \end{bmatrix}$$

$$[k_d^o] = \begin{bmatrix} \bar{P}_1(m^4-2m^2-6m^2\nu & P_2(m^4-m^2-12m^2\nu \\ +8\nu+8) & +18\nu+18) \\ \\ P_2(m^4-m^2-12m^2\nu & P_3\ (m^4+2m^2-20m^2\nu \\ +18\nu+18) & +36\nu+45) \end{bmatrix}$$

$$[m_d^o] = \begin{bmatrix} Q_5 & Q_6 \\ Q_6 & Q_7 \end{bmatrix}$$

$$P_i = \frac{\pi E}{12(1-\nu^2)} \int_0^{r_2} h^3(r) r^i dr \quad ; \quad Q_i = \pi \int_0^{r_2} \rho h(r) r^i dr$$

TABLE 2.7

Non-dimensional frequency λ of a uniform thickness circular plate; simply supported at the outer boundary, calculated using thin plate bending circular and annular elements. $\nu = 0.33$

m	n	Number of elements 1	2	4	8	Exact (42)
0	0	4.99	4.98	4.98	4.98	4.97
	1	39.66	30.20	29.78	29.76	29.70
	2		85.78	74.79	74.23	74.13
	3		188.33	143.28	138.65	138.30
1	0	14.68	13.96	13.94	13.94	13.91
	1	60.27	52.19	48.65	48.52	48.58
	2		121.75	104.15	102.91	102.82
	3		219.32	193.34	177.44	176.89
2	0	30.62	25.85	25.66	25.65	25.70
	1		77.67	70.50	70.17	70.06
	2		180.00	137.58	134.54	134.33
	3			237.44	219.23	211.99
4	0	68.07	58.42	56.93	56.88	56.85
	1		145.01	122.79	121.80	121.66
	2		252.82	217.93	206.34	205.92
	3			334.98	311.50	
6	0	140.55	101.30	98.21	98.04	
	1		201.62	187.65	184.12	
	2		475.62	303.76	289.12	
	3			452.45	415.34	

TABLE 2.8

Non-dimensional frequency λ of a uniform thickness circular plate; clamped at the outer boundary, calculated using thin plate bending circular and annular elements. $\nu = 0.33$

m	n	Number of elements 1	2	4	8.	Exact (42)
0	0	10.25	10.22	10.22	10.22	10.24
	1		40.25	39.84	39.78	39.82
	2		115.15	90.12	89.18	89.11
	3			161.71	158.64	158.26
1	0	23.66	21.33	21.27	21.26	21.25
	1		66.58	61.10	60.85	60.84
	2		166.07	121.69	120.25	120.12
	3			218.37	199.91	199.09
2	0		35.21	34.91	34.88	34.81
	1		101.94	85.21	84.63	84.64
	2			156.19	154.13	153.76
	3			273.86	244.10	243.36
4	0		74.46	69.83	69.68	69.72
	1		211.83	141.22	140.23	140.19
	2			245.65	230.20	229.52
	3			388.00	340.90	
6	0		128.22	114.77	114.25	
	1		437.52	210.92	206.33	
	2			345.70	317.24	
	3			518.53	448.94	

TABLE 2.9

Non-dimensional frequency λ of a uniform thickness circular plate, free at the outer boundary, calculated using thin plate bending circular and annular elements. ν = 0.33

m	n	Number of elements				Exact
		1	2	4	8	(42)
0	1		9.06	9.07	9.07	9.06
	2		35.81	38.39	38.50	38.44
	3		76.63	88.14	87.86	87.80
	4		183.79	156.49	157.11	156.75
1	1		20.41	20.52	20.51	20.52
	2		63.72	60.11	59.88	59.75
	3		138.10	120.01	119.18	118.81
	4		278.11	214.48	198.74	197.96
2	0	5.27	5.26	5.26	5.26	5.24
	1	48.83	35.34	35.28	35.25	35.50
	2		94.95	84.91	84.42	84.64
	3		250.66	154.72	153.64	153.51
4	0	21.86	21.54	21.53	21.53	21.50
	1	88.75	75.43	73.52	73.39	73.45
	2		183.58	142.66	142.46	142.33
	3		297.69	242.91	231.60	
6	0	47.19	46.92	46.83	46.81	
	1	171.67	126.29	122.42	122.28	
	2		263.69	213.50	211.81	
	3		494.18	339.32	321.17	

TABLE 2.9

Non-dimensional frequency λ of a uniform thickness circular plate, free at the outer boundary, calculated using thin plate bending circular and annular elements. $\nu = 0.33$

m	n	Number of elements				Exact
		1	2	4	8	(42)
0	1		9.06	9.07	9.07	9.06
	2		35.81	38.39	38.50	38.44
	3		76.63	88.14	87.86	87.80
	4		183.79	156.49	157.11	156.75
1	1		20.41	20.52	20.51	20.52
	2		63.72	60.11	59.88	59.75
	3		138.10	120.01	119.18	118.81
	4		278.11	214.48	198.74	197.96
2	0	5.27	5.26	5.26	5.26	5.24
	1	48.83	35.34	35.28	35.25	35.50
	2		94.95	84.91	84.42	84.64
	3		250.66	154.72	153.64	153.51
4	0	21.86	21.54	21.53	21.53	21.50
	1	88.75	75.43	73.52	73.39	73.45
	2		183.58	142.66	142.46	142.33
	3		297.69	242.91	231.60	
6	0	47.19	46.92	46.83	46.81	
	1	171.67	126.29	122.42	122.28	
	2		263.69	213.50	211.81	
	3		494.18	339.32	321.17	

TABLE 2.10

Non-dimensional frequency λ of a uniform thickness annular plate, simply supported at the outer boundary, calculated using thin plate bending annular elements. $\nu = 0.33$ $a/b = 0.001$

m	n	Number of elements				Exact
		1	2	4	8	(42)
0	0	4.99	4.98	4.98	4.98	4.97
	1	38.80	30.19	29.78	29.76	29.70
	2	176.23	85.68	74.78	74.23	74.13
	3		185.98	143.22	138.65	138.30
1	0	14.68	13.96	13.94	13.94	13.91
	1	60.27	52.18	48.65	48.52	48.58
	2	145.10	121.70	104.15	102.91	102.82
	3		219.33	193.29	177.44	176.89
2	0	30.29	25.84	25.66	25.65	25.70
	1	165.30	77.63	70.49	70.17	70.06
	2	435.67	177.93	139.53	134.53	134.33
	3		516.70	234.47	219.21	211.99
3	0	44.05	41.08	40.02	39.99	39.94
	1	381.80	106.88	95.23	94.62	94.48
	2	907.25	200.24	177.45	169.03	168.74
	3		1176.41	284.08	263.93	
4	0	65.46	58.41	56.93	56.88	56.85
	1	686.25	142.49	122.78	121.80	121.66
	2	1564.89	244.90	217.89	206.34	205.92
	3		2102.24	334.48	311.15	
5	0	94.73	78.36	76.34	76.24	76.21
	1	1077.49	172.75	153.70	151.65	151.29
	2	2409.66	325.78	259.73	246.44	
	3		3290.88	389.94	361.98	
6	0	131.44	101.16	98.21	98.04	
	1	1555.46	201.56	187.62	184.12	
	2	3441.95	438.60	303.66	289.28	
	3		4742.59	451.86	415.32	

TABLE 2.11

Non-dimensional frequency λ of a uniform thickness annular plate, clamped at the outer boundary, calculated using thin plate bending annular elements. $\nu = 0.33$ a/b = 0.001

m	n	Number of elements				Exact
		1	2	4	8	(42)
	0	10.24	10.22	10.22	10.22	10.24
	1		40.24	39.88	39.78	39.82
0	2		114.49	90.11	89.18	89.11
	3		528.76	161.66	158.63	158.26
	0	23.66	21.33	21.27	21.26	21.25
	1		66.56	61.10	60.85	60.84
1	2		165.85	121.70	120.25	120.12
	3			218.23	199.91	199.09
	0	103.70	35.20	34.91	34.88	34.81
	1		101.58	85.20	84.63	84.64
2	2		493.31	156.14	154.13	153.76
	3			273.81	244.08	243.36
	0	248.69	53.47	51.12	51.04	50.98
	1		138.14	112.00	111.10	111.09
3	2		1135.96	199.49	190.79	190.44
	3			329.13	291.10	
	0	450.40	74.35	69.83	69.68	69.72
	1		200.97	141.21	140.23	140.19
4	2		2033.55	245.51	230.20	229.52
	3			386.85	340.89	
	0	709.10	98.65	91.05	90.76	90.82
	1		289.64	174.19	171.98	171.87
5	2		3185.06	294.20	272.36	
	3			447.69	393.53	
	0	1024.98	127.91	114.76	114.25	
	1		401.81	210.87	206.33	
6	2		4591.14	345144	317.23	
	3			517.78	448.93	

TABLE 2.12

Non-dimensional frequency λ of a uniform thickness annular plate, free at the outer boundary, calculated using thin plate bending annular elements. ν = 0.33 a/b = 0.001

m	n	Number of elements 1	2	4	8	Exact (42)
0	1		9.07	9.07	9.07	9.06
	2		35.72	38.38	38.50	38.44
	3		76.84	88.15	87.86	87.80
	4		167.47	156.41	157.10	156.75
1	1		20.56	20.52	20.51	20.52
	2		62.75	60.10	59.88	59.75
	3		129.74	120.13	119.18	118.81
	4		278.12	214.27	198.74	197.96
2	0	5.27	5.26	5.26	5.26	5.24
	1	47.21	35.33	35.28	35.25	35.52
	2	191.88	94.75	84.89	84.42	84.64
	3		245.65	154.68	153.64	153.51
3	0	12.51	12.26	12.25	12.24	12.25
	1	63.01	54.28	53.0'2	52.93	53.00
	2	430.99	127.67	112.58	111.99	111.94
	3		265.01	197.67	191.14	190.72
4	0	21.84	21.54	21.53	21.53	21.53
	1	86.26	75.32	73.52	73.39	73.45
	2	770.95	177.29	142.66	142.46	142.33
	3		294.05	242.81	231.60	
5	0	33.26	33.11	33.07	33.06	33.06
	1	119.00	98.89	96.69	96.53	96.43
	2	1208.66	225.92	176.32	175.75	175.56
	3		355.21	289.99	274.96	
6	0	47.09	46.90	46.83	46.81	
	1	160.85	126.13	122.41	122.28	
	2	1743.73	262.33	213.46	211.81	
	3'		458.67	339.13	321.17	

TABLE 2.13

Non-dimensional frequency λ of a uniform thickness annular plate, simply supported at the outer boundary, calculated using thin plate bending annular elements. $\nu = 0.3$ $a/b = 0.1$

m	n	Number of elements 1	2	4	8	Exact (43)
0	0	4.91	4.87	4.86	4.85	4.86
	1	33.43	29.82	29.52	29.45	29.41
	2	95.77	83.37	75.36	74.88	74.85
	3		176.72	145.31	143.12	
1	0	14.39	13.90	13.88	13.87	13.88
	1	58.65	50.45	48.19	48.03	48.08
	2	162.37	113.95	102.03	100.67	
	3		214.36	178.39	171.86	
2	0	27.95	25.49	25.40	25.40	25.45
	1	83.68	74.73	69.46	69.27	69.23
	2	332.49	155.88	133.84	132.37	
	3		258.08	231.03	214.84	
3	0	43.41	40.40	39.96	39.94	39.99
	1	128.17	101.94	94.81	94.41	
	2	589.09	203.28	171.41	168.27.	
	3		325.32	280.64	261.71	
4	0	60.38	57.88	56.88	56.84	
	1	192.81	131.94	122.32	121.73	
	2	932.38	239.49	213.07	206.07	
	3		447.93	329.02	310.53	
5	0	80.96	77.79	76.27	76.21	
	1	275.54	165.71	152.58	151.58	
	2	1371.87	275.96	256.92	246.19	
	3		614.90	380.85	361.12	
6	0	105.94	100.17	98.10	98.00	
	1	375.82	201.11	185.86	184.04	
	2	1907.00	323.40	302.14	288.97	
	3		818.49	437.80	414.30	

TABLE 2.14

Non-dimensional frequency A of a uniform thickness annular plate, clamped at the outer boundary, calculated using thin plate bending annular elements. $\nu = 0.3$ $a/b = 0.1$

m	n	Number of elements 1	2	4	8	Exact (43)
0	0	10.27	10.21	10.17	10.16	10.16
	1	51.68	39.87	39.65	39.54	39.49
	2		105.67	91.27	90.53	90.38
	3		253.03	166.21	164.71	
1	0	22.64	21.31	21.21	21.20	21.15
	1	126.95	63.14	60.39	60.10	59.98
	2		144.28	119.30	117.31	
	3		332.77	197.84	193.43	
2	0	45.15	34.70	34.56	34.54	34.53
	1	283.22	93.09	83.84	83.50	
	2		201.48	153.20	151.54	83.44
	3		559.97	256.34	238.98	
3	0	83.44	51.89	51.05	50.99	51.06
	1	514.65	127.73	111.49	110.83	
	2		292.84	191.92	189.80	
	3		899.12	316.16	288.33	
4	0	134.84	72.30	69.77	69.67	
	1	829.15	165.91	141.00	140.16	
	2		425.51	236.25	229.85	
	3		1350.27	373.64	339.67	
5	0	199.05	95.89	90.95	90.75	
	1	1229.88	212.79	173.04	171.92	
	2		594.00	284.83	272.04	
	3		1919.23	432.54	392.52	
6	0	276.34	122.80	114.58	114.24	
	1	1718.04	270.79	208.30	206.24	
	2		796.02	336.24	316.84	
	3		2609.34	495.64	447.84	

TABLE 2.15

Non-dimensional_ frequency λ of a uniform thickness annular plate, free at the outer boundary, calculated using thin plate bending annular elements. v = 0.3 a/b= 0.1

m	n	Number of elements 1	2	4	8	Exact (43)
0	1		8.83	8.79	8.78	8.77
	2		35.44	38.18	38.24	38.17
	3		89.89	89.62	89.11	
	4		112.25	159.96	163.01	
1	1		20.50	20.42	20.41	20.49
	2		61.02	59.39	59.11	58.99
	3		133.17	117.80	116.22	
	4		175.70	195.53	192.25	
2	0	5.31	5.31	5.30	5.30	5.30
	1	39.38	34.99	34.96	34.93	34.86
	2	110.10	89.63	83.60	83.30	
	3	351.47	183.34	152.11	151.04	
3	0	12.49	12.44	12.44	12.44	12.44
	1	61.62	53.24	53.03	52.97	53.04
	2	152.80	121.36	112.28	111.76	
	3	611.61	253.48	191.11	190.19	
4	0	21.98	21.85	21.84	21.84	
	1	83.26	74.45	73.65	73.55	
	2	218.44	155.88	142.95	142.49	
	3	965.55	310.02	235.42	321.35	
5	0	33.69	33.52	33.50	33.50	
	1	106.91	98.36	96.92	96.77	
	2	305.23	196.83	176.10	175.86	
	3	1416.29	345.78	283.59	274.83	
6	0	47.57	47.43	47.40	47.38	
	1	134.62	124.92	122.78	122.60	
	2	411.76	243.63	212.30	211.98	
	3	1965.22	382.73	334.17	321.06	

TABLE 2.16

Non-dimensional frequency λ of a uniform thickness annular plate, simply supported at the outer boundary, calculated using thin plate bending annular elements. ν = 0.3 a/b = 0.5

m	n	Number of elements				Exact
		1	2	4	8	(43)
0	0	5.09	5.08	5.08	5.08	5.07
	1	74.42	66.02	65.88	65.84	65.76
	2	274.06	228.44	204.83	203.92	203.23
	3		459.05	427.62	421.60	
1	0	11 .71	11.62	11.61	11.61	11.62
	1	78.35	70.12	69.93	69.89	69.89
	2	277.19	231.35	207.98	207.05	
	3		460.64	430.40	424.37	
2	0	22.78	22.40	22.36	22.36	22.31
	1	89.44	81.57	81.17	81.11	81.13
	2	286.58	239.98	217.30	216.30	
	3		465.36	438.75	432.63	
3	0	36.54	35.70	35.64	35.64	35.69
	1	106.21	98.69	97.77	97.66	
	2	302.30	254.09	232.36	231.23	
	3		473.10	452.60	446.25	
4	0	53.47	52.10	52.04	52.03	
	1	127.54	120.24	118.50	118.34	
	2	324.39	273.35	252.62	251.27	
	3		483.74	471.84	465.02	
5	0	73.64	71.70	71.64	71.64	
	1	153.02	145.84	143.08	142.87	
	2	352.82	297.38	277.52	275.89	
	3		497.26	496.29	488.67	
6	0	96.74	94.27	94.19	94.18	
	1	182.80.	i75.51	171.69	171.44	
	2	387.69	325.87	306.67	304.74	
	3		513.25	525.77	516.93	

TABLE 2.17

Non-dimensional frequency λ of a uniform thickness annular plate, clamped at the outer boundary, calculated using thin plate bending annular elements. $\nu = 0.3$ $a/b = 0.5$

m	n	Number of elements: 1	2	4	8	Exact (43)
0	0	17.76	17.24	17.72	17.72	17.68
	1	131.10	93.68	93.94	93.85	93.85
	2		289.62	253.96	252.34	252.80
	3		736.51	495.48	490.03	
1	0	22.21	22.05	22.02	22.02	21.98
	1	135.43	97.19	97.48	97.38	97.32
	2		292.39	256.85	255.21	
	3		739.88	498.04	492.64	
2	0	33.04	32.22	32.12	32.12	32.05
	-1	148.12	107.35	107.63	107.50	107.56
	2		300.69	265.44	263.72	
	3		750.00	505.72	500.45	
3	0	48.17	45.99	45.83	45.81	45.77
	1	168.39	123.29	123.27	123.07	
	2		314.38	279.52	277.63	
	3		766.86	518.54	513.37	
4	0	67.49	63.24	63.04	63.02	
	1	195.41	144.11	143.36	143.07	
	2		333.30	298.73	296.58	
	3		790.50	536.49	531.27	
5	0	91.22	84.04	83.84	83.82	
	1	228.61	169.35	167.45	167.06	
	2		357.37	322.67	320.15	
	3		820.76	559.54	553.95	
6	0	119.40	108.21	107.99	107.96	
	1	267.79	198.88	195.61	195.14	
	2		386.26	350.98	348.03	
	3		858.16	587.64	581.22	

TABLE 2.18

Non--dimensional frequency λ of a uniform thickness annular plate, free at the outer boundary, calculated using thin plate bending annular elements, ν = 0.3 a/b = 0.5

m	n	Number of elements				Exact
		1	2	4	8	(43)
0	1		9.32	9.31	9.31	9.32
	2		85.79	91.97	92.29	92.36
	3		280.03	250.86	249.53	
	4		330.95	477.12	486.46	
1	1		17.17	17.20	17.20	17.18
	2		95.92	96.34	96.27	96.33
	3		273.85	253.73	252.74	
	4		597.97	492.03	490.07	
2	0	4.27	4.27	4.27	4.27	4.28
	1	31.50	31.21	31.12	31.12	31.06
	2	123.79	107.80	107.66	107.52	
	3	380.23	294.55	263.73	262.30	
3	0	11.43	11.43	11.43	11.43	11.43
	1	48.40	47.66	47.48	47.46	47.42
	2	141.73	125.26	124.87	124.66	
	3	394.27	309.17	279.35	277.75	
4	0	21.08	21.07	21.07	21.07	
	1	68.40	66.99	66.75	66.72	
	2	164.96	147.74	146.75	146.44	
	3	414.03	329.17	300.40	298.57	
5	0	33.00	32.99	32.98	32.98	
	1	91.96	89.66	89.41	89.38	
	2	192.72	174.59	172.68	172.27	
	3	439.56	354.26	326.35	324.20	
6	0	47.10	47.09	47.07	47.06	
	1	119.19	115.74	115.52	115.48	
	2	224.70	205.69	202.61	202.10	
	3	471.07	384.23	356.73	354.23	

TABLE 2.19

Non-dimensional frequency λ of a free circular plate with parabolic thickness variation, modelled with parabolic thickness variation annular thin plate bending elements. ν = 0.3 a/b = 0.001

m	n	Number of elements 1	2	4	8	Exact (46)
0	1		9.55	9.67	9.67	9.67
	2		20.16	29.26	29.80	29.83
	3		42.07	54.79	57.79	57.86
1	1		17.80	17.80	17.80	17.80
	2		42.27	41.93	41.86	41.86
	3		71.12	74.99	73.99	73.88
2	0	5.80	5.80	5.80	5.80	5.80
	1	26.65	25.98	25.88	25.88	25.88
	2	225.72	55.78	54.19	53.91	53.89
	3		125.83	91.90	90.17	89.89
3	0	10.04	10.04	10.04	10.94	10.04
	1	44.97	34.50	33.98	33.94	33.94
	2	537.80	75.03	66.60	65.99	65.92
	3		157.18	109.24	106.45	105.91
4	0	14.64	14.26	14.20	14.20	14.20
	1	75.11	42.72	42.10	42.00	42.00
	2	970.90	95.23	79.08	78.09	77.95
	3		220.04	128.16	122.85	121.93
5	0	20.60	18.50	18.34	18.33	18.33
	1	115.48	52.04	50.28	50.08	50.06
	2	1525.91	115.19	91.72	90.25	89.99
	3		314.87	150.22	139.36	137.96
6	0	28.17	22.70	22.47	22.45	22.45
	1	165.45	62.57	58.50	58.15	58.11
	2	2203.40	138.97	104.83	102.47	102.02
	3		436.97	174.69	155.99	153.98

TABLE 2.20

Non-dimensional frequency λ of a free circular plate with parabolic thickness variation, modelled with linear thickness variation annular thin plate bending elements. ν = 0.3 a/b = 0.001

m	n	Number of elements 1	2	4	8	Exact (46)
0	1		9.33	9.66	9.67	9.67
	2		18.11	28.94	29.78	29.83
	3		41.22	53.07	57.64	57.86
1	1		16.98	17.75	17.80	17.80
	2		38.56	41.26	41.81	41.86
	3		67.72	72.77	73.69	73.88
2	0	4.73	5.75	5.79	5.80	5.80
	1	19.32	23.78	25.71	25.87	25.88
	2	24.55	52.15	52.88	53.80	53.89
	3		123.58	89.30	89.61	89.89
3	0	7.14	9.84	10.03	10.04	10.04
	1	36.79	30.99	33.56	33.92	33.94
	2	593.60	71.19	64.61	65.76	65.92
	3		153.19	106.77	105.53	105.91
4	0	10.12	13.60	14.17	14.20	14.20
	1	64.37	38.49	41.30	41.95	42.00
	2	1074.67	91.30	76.54	77.71	77.95
	3		212.26	125.85	121.49	121.93
5	0	14.25	17.13	18.25	18.33	18.33
	1	100.74	47.23	48.97	49.97	50.06
	2	1690.57	111.09	88.89	89.68	89.99
	3		301.91	147.86	137.64	137.96
6	0	19.57	20.53	22.29	22.44	22.45
	1	145.52	57.10	56.64	57.98	58.11
	2	2442.14	134.48	101.92	101.76	102.02
	3		417.75	172.16	154.25	153.98

TABLE 2.21

Comparision of non-dimensional frequency λ for a uniform free plate, calculated using sector elements (54), and thin plate bending annular elements. $\nu = 0.33$

m	n	3 x 12 grid sector elements D.O.F. = 55	Annular elements a/b = 0.001 N=2 D.O.F.= 6	Annular elements a/b = 0.001 N=4 D.O.F.= 10	Exact (42)
0	1	8.98	9.07	9.07	9.06
	2	38.12	35.72	38.38	38.40
1	1	20.24	20.56	20.52	20.52
	2		62.75	60.10	59.75
2	0	5.91; 5.94	5.26	5.24	5.24
	1	36.01	35.33	35.30	35.50
3	0	12.98	12.26	12.25	12.25
	1		54.28	53.02	53.00
4	0	23.02	21.54	21.53	21.50
	1		75.32	73.52	73.45
5	0	34.18; 34.44	33.11	33.07	33.10
	1		98.89	96.69	96.43

TABLE 2.22

Matrix $[k_d^a]$ of the thin plate bending annular element

$m^2 S_{-1}$	$m^2 S_0$	$m^2 S_1$	$m^2 S_2$
	$R_1 + m^2 S_1$	$2R_2 + m^2 S_2$	$3R_3 + m^2 S_3$
Symmetrical		$4R_3 + m^2 S_3$	$6R_4 + m^2 S_4$
			$9R_5 + m^2 S_5$

$$R_i = C\pi \int_{r_1}^{r_2} r^i h(r) \sigma_r(r)\, dr \; ; \qquad S_i = C\pi \int_{r_1}^{r_2} r^i h(r) \sigma_\xi(r)\, dr$$

TABLE 2.23

Matrix $[k_d^p]$ of the plane stress annular element

Q_{-1}	$(1 + \nu)\, Q_0$	$(1 + 2\nu)\, Q_1$	$(1 + 3\nu)\, Q_2$
	$2(1 + \nu)\, Q_1$	$3(1 + \nu)\, Q_2$	$4(1 + \nu)\, Q_3$
Symmetrical		$(5 + 4\nu)\, Q_3$	$(7 + 5\nu)\, Q_4$
			$(10 + 6\nu)\, Q_5$

$$Q_i = \frac{2\pi E}{1-\nu^2} \int_{r_1}^{r_2} h(r)\, r^i\, dr$$

TABLE 2.24

Matrix $[k_d^p]$ of the plane stress circular element

$2(1+\nu)\ Q_1$	$3(1+\nu)\ Q_2$	$4(1+\nu)\ Q_3$
	$(5+4\nu)Q_3$	$(7+5\nu)\ Q_4$
Symmetrical		$(10+6\nu)\ Q_5$

$$Q_i = \frac{2E}{1-\nu^2} \int_0^{r_2} h(r)\ r^i\ dr$$

TABLE 2.25

Radial stress coefficients p = ($\sigma_r/\rho\ \Omega^2 b^2$) x 10^4 for a uniform annular disc rotating with constant angular velocity Ω
a/b = 0.001   v = 0.3

r/b	Number of elements					Exact
	1	2	4	8	16	
0.001	4428	4475	4536	4604	4652	0
0.063					4096	4107
0.126				4055	4058	4059
0.188					3978	3979
0.251			3864	3865	3866	3866
0.313					3720	3720
0.376				3543	3543	3543
0.438					3333	3333
0.501		3091	3091	3092	3092	3092
0.563					2818	2818
0.625				2512	2512	2512
0.688					2174	2174
0.750			1803	1803	1803	1803
0.813					1401	1401
0,875				966	966	966
0.938					499	499
1.000	-1	0	0	0	0	0

TABLE 2.26

Tangential stress coefficients $q = (\sigma_\xi / \rho\, \Omega^2 b^2) \times 10^4$ for a uniform annular disc rotating with constant angular velocity Ω
$a/b = 0.001 \quad \nu = 0.3$

r/b	Number of elements					Exact
	1	2	4	8	16	
0.001	5153	5332	5594	5960	6473	8250
0.063					4114	4116
0.126				4087	4087	4088
0.188					4041	4041
0.251			3975	3976	3976	3976
0.313					3892	3892
0.376				3790	3790	3790
0.438					3669	3669
0.501		3530	3530	3530	3530	3530
0.563					3372	3372
0.625				3196	3196	3196
0.688					3001	3001
0.750			2788	2788	2788	2788
0.813					2556	2556
0.875				2306	2306	2306
0.938					2037	2037
1.000	1750	1750	1750	1750	1750	1750

TABLE 2.27

Radial stress coefficients $p = (\sigma_r / \rho\, \Omega^2 b^2) \times 10^4$ for a uniform, annular disc rotating with constant angular velocity Ω
$a/b = 0.2 \quad \nu = 0.3$

r/b	Number of elements					Exact
	1	2	4	8	16	
0.20	2023	965	316	77	15	0
0.25					1391	1392
0.30				2074	2084	2085
0.35					2437	2438
0.40			2555	2593	2598	2599
0.45					2640	2640
0.50				2594	2599	2599
0.55					2497	2497
0.60		2247	2335	2346	2347	2347
0.65					2157	2157
0.70				1932	1932	1932
0.75					1676	1676
0.80			1392	1392	1392	1392
0.85					1081	1081
0.90				745	745	745
0.95					384	384
1.00	-314	-41	-2	0	0	0

TABLE 2.28

Tangential stress coefficients $q = (\sigma_\xi / \rho\, \Omega^2 b^2) \times 10^4$ for a uniform annular disc rotating with constant angular velocity Ω
$a/b = 0.2$ $\nu = 0.3$

r/b	Number of elements					Exact
	1	2	4	8	16	
0.20	8736	8579	8413	8343	8324	8320
0.25					6781	6782
0.30				5907	5909	5910
0.35					5346	5346
0.40			4931	4940	4941	4941
0.45					4624	4624
0.50				4356	4356	4356
0.55					4117	4117
0.60		3869	3890	3893	3893	3893
0.65					3677	3677
0.70				3463	3463	3463
0.75					3247	3247
0.80			3027	3028	3028	3028
0.85					2802	2802
0.90				2570	2570	2570
0.95					2329	2329
1.00	1978	2066	2079	2680	2080	2080

TABLE 2.29

Radial stress coefficients $p = (\sigma_r / \rho \Omega^2 b^2) \times 10^4$ for an annular disc with hyperbolic radial thickness variation rotating with constant angular velocity Ω. $a/b = 0.2$ $\nu = 0.3$

r/b	Number of elements					Exact
	1	2	4	8	16	
0.20	1105	507	167	41	8	0
0.25					883	880
0.30				1427	1423	1420
0.35					1771	1767
0.40			2003	1999	1992	1988
0.45					2121	2117
0.50				2184	2176	2173
0.55					2169	2166
0.60		2107	2127	2113	2107	2105
0.65					1995	1993
0.70				1840	1836	1834
0.75					1632	1631
0.80			1398	1389	1386	1385
0.85					1099	1098
0.90				773	772	771
0.95					405	405
1.00	-220	-26	1	0	0	0

TABLE 2.30

Tangential stress coefficients q = (σ_{ξ} /$\rho\Omega^2 b^2$) x 10^4 for an annular disc with hyperbolic radial thickness variation rotating with constant angular velocity Ω.   a/b = 0.2 v = 0.3

r/b	Number of elements					Exact
	1	2	4	8	16	
0.20	5783	4979	4912	4951	4974	4985
0.25					4070	4079
0.30				3582	3602	3609
0.35					3334	3340
0.40			3103	3150	3164	3169
0.45					3043	3047
0.50				2934	2944	2948
0.55					2853	2856
0.60		2638	2724	2751.	2759	2761
0.65					2657	2659
0.70				2537	2543	2546
0.75					2416	2418
0.80			2248	2266	2272	2274
0.85					2111	2113
0.90				1927	1932	1934
0.95					1735	1737
1.00	1403	1449	1499	1514	1519	1520

TABLE 2.31

Radial stress coefficients $p = \{\sigma_r/E\alpha^* T(b)\} \times 10^4$ for a uniform annular disc with linear temperature gradient.
a/b = 0.001 $\nu = 0.3$

r/b	Number of elements 1	2	4	8	16	Exact
0.001	3575	3612	3662	3717	3755	0
0.063					3112	3121
0.126				2910	2912	2914
0,188					2705	2706
0.251			2496	2497	2497	2498
0.313					2289	2289
0.376				2081	2081	2081
0.438					1873	1873
0.501		1664	3.665	1665	1665	1665
0.563					1457	1457
0.625				1249	1249	1249
0.688					1041	1041
0.750			833	833	833	833
0.813					624	624
0.875				416	416	416
0.938					208	208
1.000	-1	0	0	0	0	0

TABLE 2.32

Tangential stress coefficients q = { $\sigma_\xi / E\alpha^* T(b)$} x 10^4 for a uniform annular disc with linear temperature gradient.
a/b = 0.001 ν = 0.3

r/b	Number of elements					Exact
	1	2	4	8	16	
0.001	4157	4301	4512	4808	5222	6657
0.063					2909	2911
0.126				2494	2494	2494
0.188					2078	2078
0.251			1661	1662	1662	1662
0.313					1245	1245
0.376				829	829	829
0.438					413	412
0.501		-4	-3	-3	-3	-3
0.563					-420	-420
0.625				-836	-836	-836
0.688					-1252	-1252
0.750			-1668	-1668	-1668	-1668
0.813					-2085	-2085
0.875				-2501	-2501	-2501
0.938					-2917	-2917
1.000	-3334	-3333	-3333	-3333	-3333	-3333

TABLE 2.33

Radial stress coefficients p = { σ_r /Eα^* T(b)) x 10^4 for a uniform annular disc with linar temperature gradient.
a/b = 0.2 ν = 0.3

r/b	Number of elements					Exact
	1	2	4	8	16	
0.02	1362	650	213	52	10	0
0.25					832	833
0.30				1202	1209	1210
0.35					1370	1371
0.40			1387	1413	1416	1417
0.45					1396	1396
0.50				1332	1333	1333
0.55					1244	1244
0.60		1069	1128	1135	1136	1136
0.65					1015	1015
0.70				884	884	884
0.75					747	747
0.80			602	604	604	604
0.85					457	457
0.90				307	307	307
0.95					155	155
1.00	-212	-28	-1	0	0	0

TABLE 2.34

Tangential stress coefficients $q = \{\sigma_\xi / E\alpha^* T(b)\} \times 10^4$ for a uniform annular disc with linear temperature gradient.
a/b = 0.2 ν = 0.3

a/b	Number of elements					Exact
	1	2	4	8	16	
0.20	5169	5063	4951	4904	4892	4889
0.25					3555	3556
0.30				2677	2679	2679
0.35					2018	2818
0.40			1466	1471	1472	1472
0.45					993	993
0.50				555	556	556
0.55					145	145
0.60		-263	-249	-247	-247	-247
0.65					-626	-626
0.70				-996	-996	-996
0.75					-1358	-1358
0.80			-1716	-171.5	-1715	-1715
0.85					-2068	-2068
0.90				-2418	-2418	-2418
0.95					-2766	-2766
1.00	-3180	-3120	-3112	-3111	-3111	-3111

TABLE 2.35

Frequency coefficients λ for a centrally clamped circular membrane disc when stresses calculated using finite elements are used at the nodes of the finite element model and linear variations of stresses are taken within the elements. $\nu = 0.3$ $a/b = 0.001$

m	n	Number of elements				Exact
		1	2	4	8	(48)
1	0	0.8624	0.9799	0.9977	0.9999	1.00
	1	4.188	5.343	5.799	5.917	5.95
	2		13.340	13.779	14.076	14.20
	3		29.685	25.370	25.514	25.75
2	0	1.941	2.197	2.310	2.340	2.35
	1	7.098	7.885	8.574	8.848	8.95
	2		17.498	18.061	18.561	18.85
	3		37.994	31.284	31.554	32.05
3	0	3.391	3.752	3.969	4.030	4.05
	1	12.294	10.880	11.750	12.144	12.30
	2		23.219	22.290	23.466	23.85
	3		54.763	38.116	38.123	38.70

TABLE 2.36

Frequency coefficients λ for a centrally clamped circular membrane disc when exact stresses are used at the nodes of the finite element model and linear variations of stresses are taken within the elements. $\nu = 0.3$ $a/b = 0.001$

m	n	Number of elements 1	2	4	8	Exact (48)
1	0	0.791	0.963	0.992	0.998	1.00
	1	3.843	5.261	5.763	5.905	5.95
	2		13.185	13.680	14.038	14.20
	3		29.281	25.175	25.429	25.75
2	0	1.803	2.188	2.309	2.340	2.35
	1	6.317	7.796	8.564	8.848	8.95
	2		17.148	18.012	18.556	18.85
	3		36.493	31.125	31.538	32.05
3	0	3,187	3.750	3.969	4.030	4.05
	1	10,742	10.837	11.750	12.144	12.30
	2		22.883	22.891	23.466	23.85
	3		51,045	38.068	38.122	38.70

TABLE 2.37

Frequencies in Hz. of a rotating annular disc, calculated using 8 thin plate bending annular elements, and the variation with speed of rotation.
$a/b = 0.5$, $b = 8.0$ in., $h = 0.04$ in., $E = 30 \times 10^6$ psi,
$\rho g = 0.283$ lb/in^3, $\nu = 0.3$

m	n	Speed of rotation in rpm.				
		0	1000	2000	3000	4000
0	0	79	81	86	93	103
	1	515	517	522	530	541
	2	1477	1479	1483	1491	1502
	3	2917	2919	2923	2931	2942
1	0	81	83	91	102	116
	1	525	527	533	542	555
	2	1488	1489	1494	1502	1514
	3	2928	2930	2934	2942	2953
2	0	89	94	108	127	150
	1	556	558	566	578	594
	2	1519	1521	1527	1537	1550
	3	2961	2963	2968	2977	2989
3	0	112	119	140	168	200
	1	607	610	620	636	659
	2	1573	1575	1582	1594	1610
	3	3016	3018	3024	3034	3048
4	0	155	164	188	222	263
	1	679	683	696	717	746
	2	1648	1651	1660	1674	1694
	3	3094	3096	3103	3115	3131
5	0	216	226	252	291	338
	1	772	777	793	819	854
	2	1746	1750	1760	1778	1802
	3	3194	3197	3205	3218	3237

TABLE 2.38

Frequencies in Hz. of a uniform annular disc rotating with 3000 rpm, calculated using thin plate bending annular elements.

a/b = 0.5, b = 8.0 in., h = 0.04 in., $E = 30 \times 10^6$ psi, $\rho g = 0.283$ lb/in^3, $\nu = 0.3$.

m	n	Number of elements		
		2	4	8
0	0	91	93	93
	1	535	530	530
	2	1844	1502	1491
	3	5500	2976	2931
1	0	100	102	102
	1	548	542	542
	2	1854	1514	1502
	3	5508	2987	2942
2	0	126	127	127
	1	584	578	578
	2	1883	1548	1537
	3	5533	3021	2977
3	0	167	167	168
	1	643	637	636
	2	1933	1605	1594
	3	5573	3078	3034
4	0	222	222	222
	1	723	718	717
	2	2003	1686	1674
	3	5630	3158	3115
5	0	291	291	291
	1	825	820	819
	2	2093	1790	1778
	3	5703	3261	3218

TABLE 2.39

Matrices $[k_d^1]$ and $[k_d^2]$ of the Thick Disc Element-1

$P_{-2}m^2(2-\nu)$	$P_{-1}2m^2$	$P_{-2}m(m^2-\nu+1)$	$P_{-1}m^3$
$P_{-1}(m^2-1)$	$P_0(m^2+m^2\nu-\nu-1)$	$P_{-1}m(m^2-1)$	$P_0m(m^2-1)$
$P_0(m^2\nu-2\nu-2)$	$P_1 2(m^2\nu-2\nu-2)$	$P_0m(m^2-\nu-3)$	$P_1m(m^2-2\nu-2)$
$P_1(2m^2\nu-m^2-6\nu-3)$	$P_2(3m^2\nu-m^2-9\nu-9)$	$P_1m(m^2-5-4\nu)$	$P_2m(m^2-6\nu-3)$

$P_{-1}\frac{1}{2}(m^2-m^2\nu+2)+Q_1$	$P_0\frac{1}{2}(m^2-m^2\nu+\nu+1)+Q_2$	$P_{-1}\frac{1}{2}m(3-\nu)$	P_0m
	$P_1\frac{1}{2}(m^2-m^2\nu+4\nu+4)+Q_3$	$P_0\frac{1}{2}m(3+\nu)$	$P_1m(1+\nu)$
Symmetrical		$P_{-1}\frac{1}{2}(2m^2+1-\nu)+Q_1$	$P_0m^2+Q_2$
			$P_1m^2+Q_3$

$$P_i = C\pi\frac{E}{12(1-\nu^2)}\int_{r_1}^{r_2} h^3(r)r^i dr \quad ; \quad Q_i = C\pi\kappa^2 G\int_{r_1}^{r_2} h(r)r^i dr$$

TABLE 2.40

Matrix $[m_d^1]$ of the Thick Disc Element-1

$P_{-1}m^2$	P_0m^2	P_1m^2	P_2m^2	0	0	P_0	P_1m
	$P_1(1+m^2)$	$P_2(2+m^2)$	$P_3(3+m^2)$	$-P_1$	$-P_2$	P_1m	P_2m
		$P_3(4+m^2)$	$P_4(6+m^2)$	$-2P_2$	$-2P_3$	P_2m	P_3m
			$P_5(9+m^2)$	$-3P_3$	$-3P_4$	P_3m	P_4m
				P_1	P_2	0	0
	Symmetrical				P_3	0	0
						P_1	P_2
							P_3

$$P_i = C\,\pi\,\frac{\rho}{12}\int_{r_1}^{r_2} h^3(r)\,r^i\,dr$$

TABLE 2.41

Matrix $[k_d^s]$ of the Thick Disc Element-2

$Q_{-1}\, m^2$	$Q_0\, m^2$	$Q_1\, m^2$	$Q_2\, m^2$
	$Q_1\,(1+m^2)$	$Q_2\,(2+m^2)$	$Q_3\,(3+m^2)$
		$Q_3\,(4+m^2)$	$Q_4\,(6+m^2)$
$Q_i = C\pi\kappa^2 \int_{r_1}^{r_2} h(r)\, r^i\, dr$			$Q_5\,(9+m^2)$

TABLE 2.42

Matrix $[m_d^s]$ of the Thick Disc Element-2

$P_{-1}\, m^2$	$P_0\, m^2$	$P_1\, m^2$	$P_2\, m^2$
	$P_1\,(1+m^2)$	$P_2\,(2+m^2)$	$P_3\,(3+m^2)$
		$P_3\,(4+m^2)$	$P_4\,(6+m^2)$
$P_i = C\pi \frac{\rho}{12} \int_{r_1}^{r_2} h^3(r)\, r^i\, dr$			$P_5\,(9+m^2)$

TABLE 2.43

Frequencies in Hz. of a uniform circular plate calculated using Thick Disc Element-l. a/b = 0.001; b = 37.5 mm; h = 5 mm; E = 22,000 kg/mm2 ; ρ = 7.85 and ν = 0.3.

m	n	Number of Elements 1	2	4	8	Exact*	Thin plate soln.	Experi-mental.
0	1	6766	7837	7943	7950	7949	8213	7767
	2	23421	30540	31222	31297	31278	34848	30698
	3	153450	63350	65651	64310	64141	79593	
1	1	15050	16875	17419	17440	17408	18603	17012
	2	55174	45134	46786	46417	46246	54169	
	3	332367	97409	89537	82941	82183	107708	
2	0	4781	4774	4765	4754	4742	4754	4620
	1	37746	29627	28883	28797	28714	32202	28117
	2	119687	73842	63216	62101	61901	76731	
3	0	11100	10855	10823	10784	10738	11105	10505
	1	50683	43797	41635	41438	41265	48046	
	2	202583	96747	80979	78333	77973	101476	

* Calculated using Mindlin's plate theory.

TABLS 2.44

Frequencies in Hz. of a uniform circular plate calculated using Thick Disc Element-2. $a/b = 0.001$; $b = 37.5$ mm; $h = 5$ mm; $E = 22{,}000$ kg/mm2 ; $\rho = 7.85$ and $\nu = 0.3$.

m	n	Number of Elements				Exact*	Thin plate soln.	Experi- mental
		1	2	4	8			
0	1	6594	7423	7948	7955	7949	8213	7767
	2'	10341	13289	29948	31297	31278	34848	30698
	3			52618	60020	64141	79593	
1	1	15414	16905	17457	17481	17408	18603	17012
	2	53869	42678	46300	46387	46246	54169	
	3	321156	93328	82498	82519	82183	107708	
2	0	4787	4785	4784	4784	4742	4754	4620
	1	39835	29050	29011	28986	28714	32202	28117
	2	142438	68329	62535	62276	61901	76731	
3	0	11139	10898	10890	10889	10738	11105	10505
	1	52104	42738	41883	41830	41265	48046	
	2	274801	87648	78990	78687	77973	101476	

* Calculated using Mindlin's plate theory.

TABLE 2.45

The fundamental frequency ($m = 2$, $n = 0$) in Hz. of thick uniform plates and rings calculated using Thick Disc Element-1.
$E = 30 \times 10^6$ psi $\rho g = 0.283$ $\nu = 0.3$

	Dimensions(in)			Number of Elements				Experi-mental
	a	b	h	1	2	4	8	
Disc	0.0*	6.4375	3.5	3606	3542	3524	3516	3450
Disc	0.0*	9.375	3.5	1862	1845	1836	1831	1880
Disc	0.0*	5.1875	3.5	5162	5032	5009	4999	5100
Ring	5.375	6.4375	3.5	1315	1303	1292	1289	1350
Ring	5.375	6.4375	1.5	924	923	915	913	920
Ring	8.3125	9.375	3.5	635	632	629	628	640
Ring	8.3125	9.375	2.5	570	568	564	563	575

* Small value assumed so that a/b = 0.001

TABLE 2.46

The fundamental frequency (m = 2, n = 0) in Hz. of thick uniform plates and rings calculated using Thick Disc Element-Z.
E = 30 x 106 psi ρg = 0.283 ν = 0.3

	Dimensions (in)			Number of Elements				Experi-mental
	a	b	h	1	2	4	8	
Disc	0.0*	6.4375	3.5	3630	3627	3627	3627	3450
Disc	0.0*	9.375	3.5	1872	1871	1871	1871	1880
Disc	0.0*	5.1875	3.5	5191	5188	5188	5188	5100
Ring	5.375	6.4375	3.5	2237	2237	2237	2237	1350
Ring	5.375	6.4375	1.5	1071	1071	1071	1071	920
Ring	8.3125	9.375	3.5	1075	1075	1075	1075	640
Ring	8.3125	9.375	2.5	793	793	793	793	575

* Small value assumed so that a/b = 0.001

TABLE 2.47

Frequencies in Hz. of rings calculated using Thick Disc Element-2.
E = 30 x 106 psi   ρg = 0.283   ν = 0.3

m	n	Dimension(in) a	b	h	Number of Elements 1	2	4	8	Exact*	Experi-mental
2	0	4.125	5.1875	0.6215	709	709	703	701	799	720
3	0				1964	1963	1953	1950	2089	2000
2	0			1.5	1453	1450	1436	1432	1429	1470
3	0				4001	3996	3970	3962	3954	4050
2	0			2.5	1867	1855	1837	1832	1828	1900
3	0				5020	4997	4949	4934	4923	
2	0			3.5	1978	1951	1929	1922	1918	1980
3	0				5088	5030	4964	4943	4930	
2	0	5.375	6.4375	3.6215	444	444	441	440	498	435
3	0				1238	1238	1233	1231	1307	1250
2	0			1.5	924	923	915	913	912	920
3	0				2610	2607	2593	2588	2586	2850
2	0			2.5	1215	1210	1201	1198	1195	
3	0				3420	3410	3385	3377	3371	
2	0			3.5	1315	1303	1292	1285	1286	1350
3					3566	3538	3504	3494	3487	

* Calculated using Mindlin's plate theory.

TABLE 2.48

Frequencies in Hz. of stepped discs.
E = 30 x 10^6 psi ρg = 0.283 ν = 0.3

m	n	h	Finite Element*	Experimental
2	0	2.5	3093	3030
2	0	1.5	2416	2310
2	0	0.75	1668	1600

* Five Thick Disc Element-l used.

TABLE 2.49

Thickness of the turbine disc at various radii.

Radius (in)	h (in)	Radius (in)	h (in)	Radius (in)	h (in)	Radius (in)	h (in)
7.50	1.025	6.08	0.625	4.53	0.910	2.80	1.200
7.39	1.025	5.89	0.650	4.33	0.945	2.38	1.395
7.25	0.790	5.70	0.680	4.12	0.980	2.11	1.700
7.10	0.590	5.50	0.725	3.89	1.020	1.80	2.180
6.95	0.480	5.30	0.770	3.66	1.050	1.38	2.220
6.72	0.474	5.08	0.805	3.43	1.095	0.90	2.650
6.45	0.550	4.92	0.840	3.20	1.140		
6.26	0.590	4.72	0.875	3.00	1.170		

TABLE 2.50

Frequencies in Hz. of an actual turbine disc, calculated using thin plate bending annular elements and Thick Disc Element-l.
E = 31.2 x 106 psi ρg = 0.281 v = 0.3

m	n	Eight thin plate elements	Number of Thick Disc Element-l			Experi-mental	Percent-age error *
			4	6	8		
0	1 2 3		1737 5590 11521	1696 5585 11340	1707 5618 11401	1590 5240	7.35 7.20
1	1 2 3		2962 7714 14708	2899 7710 14022	2894 7632 13810	2685	7.80
2	0 1 2 3	1177 5323 12485 22565	1135 4835 10471 18510	1109 4749 10292 16960	1114 4761 10294 16927	1048 4392	6.30 8.30
3	0 1 2 3	1805 7315 16174 27903	1746 6529 13205 23220	1702 6389 12889 20229	1711 6431 12976 20307	1625 5926	5.30 8.50
4	0 1 2 3	2668 9436 19480 32542	2534 8260 15923 26677	2478 8089 15214 23136	2482 8112 15279 23264	2357	5.30
5	0 1 2 3	377s 11880 23001 37197	3503 10121 18830 30170	3436 9947 17585 26055	3440 9960 17618 26135	3256	5.65
6	0 1 2 3	5118 14608 26805 42203	4627 12100 21797 34094	4552 11919 20026 29067	4556 11931 20047 29100	4298	6.00
7	0 1 2 3	6683 17561 30847 47610	5886 14196 24737 38428	5805 13971 22534 32141	5810 13984 22553 32151	5460	6.40

* Error in eight element solution.

TABLE 3.1

Bending stiffness and inertia matrices of a beam element when linear variations in I and A are assumed within the element.

$$\frac{EI_1}{\ell^3}\left|\begin{array}{c|c|c|c}
6(1+\alpha) & -2\ell(1+2\alpha) & -6(1+\alpha) & -2\ell(2+\alpha) \\
\hline
 & \ell^2(1+3\alpha) & 2\ell(1+2\alpha) & \ell^2(1+\alpha) \\
\cline{2-4}
 & & 6(1+\alpha) & 2\ell(2+\alpha) \\
\cline{3-4}
\alpha = \dfrac{I_2}{I_1} & & & \ell^2(3+\alpha)
\end{array}\right|$$

$$\frac{\rho A_1 \ell}{420}\left|\begin{array}{c|c|c|c}
36+120\beta & -\ell(7+15\beta) & 27(1+\beta) & \ell(6+7\beta) \\
\hline
 & \dfrac{\ell^2}{2}(3+5\beta) & -\ell(7+6\beta) & -\dfrac{3}{2}\ell^2(1+\beta) \\
\cline{2-4}
 & & 120+36\beta & \ell(15+7\beta) \\
\cline{3-4}
\beta = \dfrac{A_2}{A_1} & & & \dfrac{\ell^2}{2}(5+3\beta)
\end{array}\right|$$

Subscripts 1 and 2 refer to values at node 1 and node 2 of the element respectively.

TABLE 3.2

Torsional stiffness and inertia matrices of a beam element when linear variations in KG and J are assumed within the element.

$$\frac{G}{2\ell}\begin{bmatrix} K_{G1} + K_{G2} & -(K_{G1} + K_{G2}) \\ -(K_{G1} + K_{G2}) & K_{G1} + K_{G2} \end{bmatrix}$$

$$\frac{\rho\ell}{12}\begin{bmatrix} 3J_1 + J_2 & J_1 + J_2 \\ J_1 + J_2 & J_1 + 3J_2 \end{bmatrix}$$

Subscripts 1 and 2 refer to values at node 1 and node 2 of the element respectively.

TABLE 3.3

Additional bending stiffness matrix, resulting from uniform rotation Ω, for a uniform beam element for bending in the plane of rotation.

$\dfrac{A}{420\ell}$

$\{504\sigma_1+252(\sigma_2-\sigma_1)$ $+156\alpha\}$	$\{-42\sigma_1-42(\sigma_2-\sigma_1)$ $-22\alpha\}\ell$	$\{-504\sigma_1-252(\sigma_2-\sigma_1)$ $+54\alpha\}$	$(-42\sigma_1+13\alpha)\ell$
	$\{56\sigma_1+14(\sigma_2-\sigma_1)$ $+4\alpha\}\ell^2$	$\{42\sigma_1+42(\sigma_2-\sigma_1)$ $-13\alpha\}\ell$	$\{-14\sigma_1-7(\sigma_2-\sigma_1)$ $-3\alpha\}\ell^2$
		$\{504\sigma_1+252(\sigma_2-\sigma_1)$ $+156\alpha\}$	$(42\sigma_1+22\alpha)\ell$
Symmetrical			$\{56\sigma_1+42(\sigma_2-\sigma_1)$ $+4\alpha\}\ell^2$

$\alpha = \ell^2\rho\Omega^2$

σ_1 = stress at node 1 of element

σ_2 = stress at node 2 of element

TABLE 3.4

Additional bending stiffness matrix, resulting from uniform rotation Ω , for a uniform beam element for bending out of the plane of rotation.

$\frac{A}{420\ell}$ ×

$504\sigma_1+252(\sigma_2-\sigma_1)$	$\{-42\sigma_1-42(\sigma_2-\sigma_1)\}\ell$	$-504\sigma_1-252(\sigma_2-\sigma_1)$	$-42\sigma_1\ell$
	$\{56\sigma_1+14(\sigma_2-\sigma_1)\}\ell^2$	$\{42\sigma_1+42(\sigma_2-\sigma_1)\}\ell$	$\{-14\sigma_1-7(\sigma_2-\sigma_1)\}\ell^2$
		$504\sigma_1+252(\sigma_2-\sigma_1)$	$42\sigma_1\ell$
Symmetrical			$\{56\sigma_1+42(\sigma_2-\sigma_1)\}\ell^2$

σ_1 = stress at node 1

σ_2 = stress at node 2

TABLE 3.5

Additional stiffness matrix resulting from uniform rotation Ω for a uniform beam element in torsion.

a + 2β	$-\alpha + \beta$
$-\alpha + \beta$	a + 28

$\alpha \quad = \frac{\rho J}{2\ell} (\sigma_1 + \sigma_2)$

$\beta \quad = - \frac{\rho \Omega^2 \ell}{6} (I_{max} - 1_{min})$ cos 26

σ_1 = stress at node 1 of the element

σ_2 = stress at node 2 of the element

TABLE 3.6

Stiffness and inertia matrices of an uniform Timoshenko beam element of length ℓ in Sending.

$\frac{EI}{\ell^3}$

12	6ℓ	6ℓ	-12	6ℓ	6ℓ
	$4\ell^2$	$3\ell^2$	-6ℓ	$2\ell^2$	$3\ell^2$
		$(3+\frac{\alpha}{3})\ell^2$	-6ℓ	$3\ell^2$	$(3+\frac{\alpha}{6})\ell^2$
$\alpha = \frac{GA\ell^2}{EI}$			12	-6ℓ	-6ℓ
Symmetrical				$4\ell^2$	$3\ell^2$
					$(3+\frac{\alpha}{3})\ell^2$

$\frac{\rho A\ell}{420}$

$156 +504\beta$	$(22+ 42\beta)\ell$	$(22+ 252\beta)\ell$	$54 -504\beta$	$(-13-F 42\beta)\ell$	$(-13+ 252\beta)\ell$
	$(4+ 56\beta)\ell^2$	$(4+ 21\beta)\ell^2$	$(13- 42\beta)\ell^2$	$(-3- 14\beta)\ell^2$	$(-3-F 21\beta)\ell^2$
		$(4+ 126\beta)\ell^2$	$(13- 252\beta)\ell$	$(-3 +21\beta)\ell^2$	$(-3 +126\beta)\ell^2$
$\beta=(\frac{\mu}{\ell})^2$			$156 +504\beta$	$(-22 -42\beta)\ell$	$(-22 -252\beta)\ell$
μ - radius of gyration				$(4+ 56\beta)\ell^2$	$(4+ 21\beta)\ell^2$
Symmetrical					$(4+ 126\beta)\ell^2$

TABLE 3.7

Frequency coefficients λ , for the first mode of vibration of a rotating beam for vibration out of plane of rotation, calculated using four beam finite elements.

R/L	Ω*										
	0	0.1	0.2	0.5	1	2	5	10	20	50	100
0.00	3.516	3.518	3.523	3.557	3.678	4.126	6.407	11.12	21.00	51.09	101.6
0.02	3.516	3.518	3.523	3.559	3.683	4.141	6.467	11.26	21.28	51.83	103.1
0.05	3.516	3.518	3.523	3.560	3.689	4.164	6.556	11.36	21.70	52.91	105.3
0.10	3.516	3.518	3.524	3.563	3.700	4.201	6.701	11.78	22.39	54.67	108.8
0.20	3.516	3.518	3.525	3.569	3.721	4.275	6.982	12.41	23.69	58.03	115.6
0.50	3.516	3.519	3.527	3.585	3.784	4.489	7.764	14.12	27.23	67.04	133.7
1.00	3.516	3.520	3.532	3.612	3.886	4.824	8.913	16.57	32.26	79.78	159.3
2.00	3.516	3.522	3.541	3.666	4.083	5.432	10.84	20.61	40.46	100.5	200.7
5.00	3.516	3.529	3.567	3.823	4.622	6.936	15.20	29.55	58.51	145.8	291.4

TABLE 3.8

Frequency coefficients λ, for the second mode of vibration of a rotatfng beam for vibration out of plane of rotation, calculated using four beam finite elements.

R/L	Ω*										
	0	0.1	0.2	0.5	1	2	5	10	20	50	100
0.00	22.06	22.06	22.07	22.10	22.20	22.62	25.39	23.41	54.57	125.4	246.6
0.02	22.06	22.06	22.07	22.10	22.21	22.64	25.47	23.66	55.17	127.0	249.8
0.05	22.06	22.06	22.07	22.10	22.21	22.66	25.60	34.04	56.07	129.3	254.6
0.10	22.06	22.06	22.07	22.10	22.22	22.70	25.81	34.66	57.52	133.2	262.3
0.20	22.06	22.06	22.07	22.11	22.24	22.78	26.22	35.86	60.32	140.5	277.1
0.50	22.06	22.06	22.07	22.12	22.30	23.00	27.42	39.23	67.97	160.4	317.1
1.00	22.06	22.06	22.07	22.15	22.40	23.38	29.31	44.24	78.99	188.8	374.1
2.00	22.06	22.07	22.08	22.19	22.59	24.10	32.73	52.75	97.19	235.3	467.5
5.00	22.06	22.07	22.11	22.34	23.16	26.16	41.24	72.23	137.7	338.0	673.6

TABLE 3.9

Frequency coefficients λ , for the third mode of vibration of a rotating beam for vibration out of plane of rotation, calculated using four beam finite elements.

R/L	Ω^* = 0	0.1	0.2	0.5	1	2	5	10	20	50	100
0.00	62.18	62.18	62.18	62.21	62.31	62.73	65.58	74.78	103.1	209.8	398.1
0.02	62.18	62.18	62.18	62.21	62.32	62.75	65.67	75.11	104.0	212.3	403.2
0.05	62.18	62.18	62.18	62.21	62.33	62.77	65.81	75.59	105.3	216.0	410.7
0.10	62.18	62.18	62.18	62.22	62.34	62.81	66.05	76.39	107.5	222.1	423.0
0.20	62.18	62.18	62.18	62.22	62.36	62.89	66.52	77.96	111.7	233.6	446.1
0.50	62.18	62.18	62.19	62.24	62.42	63.13	67.89	82.46	123.3	264.9	509,0
1.00	62.18	62.18	62.19	62.26	62.52	63.52	70.12	89.36	140.1	309.5	598.2
2.00	62.18	62.18	62.20	62.31	62.71	64.30	74.34	101.5	168.2	382.4	744.0
5.00	62.18	62.19	62.22	62.40	63.31	66.57	85.55	130.6	231.2	542.8	1066

TABLE 3.10

Frequency coefficients λ, for the first mode of vibration of a rotating beam for vibration in the plane of rotation, calculated using four beam finite elements.

R/L	Ω*										
	0	0.1	0.2	0.5	1	2	5	10	20	50	100
0.00	3.516	3.516	3.517	3.522	3.540	3.609	4.006	4.863	6.396	10.48	17.87
0.02	3.516	3.516	3.517	3.523	3.544	3.626	4.101	5.165	7.279	13.64	24.99
0.05	3.516	3.517	3.518	3.525	3.551	3.652	4.240	5.588	8.432	17.32	32.89
0.10	3.516	3.517	3.518	3.528	3.563	3.694	4.461	6.229	10.06	22.12	42.92
0.20	3.516	3.517	3.519	3.533	3.584	3.778	4.874	7.344	12.71	29.45	57.94
0.50	3.516	3.518	3.522	3.550	3.649	4.019	5.940	9.963	18.48	44.66	88.74
1.00	3.516	3.519	3.526	3.577	3.755	4.390	7.378	13.21	25.31	62.16	123.9
2.00	3.516	3.521	3.535	3.632	3.958	5.050	9.621	18.02	35.17	87.13	174.0
5.00	3.516	3.528	3.562	3.590	4.512	6.641	14.36	27.80	54.99	136.9	273.7

TABLE 3.11

Frequency coefficients λ, for the second mode of vibration of a rotating beam for vibration in the plane of rotation, calculated using four beam finite elements.

R/L	Ω*										
	0	0.1	0.2	0.5	1	2	5	10	20	50	100
0.00	22.06	22.06	22.07	22.09	22.18	22.54	24.89	31.88	50.77	115.0	225.4
0.02	22.06	22.06	22.07	22.09	22.18	22.55	24.97	32.15	51.42	116.7	229.0
0.05	22.06	22.06	22.07	22.09	22.19	22.58	25.10	32.54	52.38	119.3	234.1
0.10	22.06	22.06	22.07	22.10	22.20	22.61	25.32	33.19	53.93	123.4	242.5
0.20	22.06	22.06	22.07	22.10	22.22	22.69	25.74	34.44	56.91	131.3	258.4
0.50	22.06	22.06	22.07	22.11	22.28	22.92	26.96	37.94	64.96	152.4	300.9
1.00	22.06	22.06	22.07	22.14	22.37	23.29.	28.88	43.10	76.42	182.0	360.5
2.00	22.06	22.06	22.08	22.19	22.57	24.02	32.35	51.80	95.11	229.9	456.7
5.00	22.06	22.07	22.10	22.33	23.13	26.08	40.94	71.54	136.3	334.3	666.1

TABLE 3.12

Frequency coefficients λ , for the third mode of vibration of a rotating beam for vibration in the plane of rotation, calculated using four beam finite elements.

R/L	Ω^*									
	0	0.1	0.2	0.5	1	2	5	10	20	50	100
0.00	62.18	62.18	62.18	62.21	62.31	62.70	65.39	74.11	101.2	203.7	385.4
0.02	62.18	62.18	62.18	62.21	62.31	62.72	65.48	74.44	102.1	206.3	390.6
0.05	62.18	62.18	62.18	62.21	62.32	62.74	65.62	74.93	103.4	210.1	398.4
0.10	62.18	62.18	62.18	62.21	62.33	62.78	65.86	75.74	105.6	216.4	410.9
0.20	62.18	62.18	62.18	62.22	62.35	62.86	66.33	77.32	109.9	228.2	434.8
0.50	62.18	62.18	62.18	62.23	62.41	63.10	67.71	81.85	121.6	260.2	499.0
1.00	62.18	62.18	62.19	62.26	62.51	63.49	69.94	88.80	138.7	305.5	589.8
2.00	62.18	62.18	62.20	62.31	62.71	64.27	74.17	101.0	167.0	379.1	737.3
5.00	62.18	62.19	62.22	62.46	63.30	66.54	85.41	130.2	230.3	540.5	1061

TABLE 3.13

Frequency coefficients λ for a vibrating simply supported Timoshenko beam, calculated using the present method.

N	1	2	3	4	5	6	
Mode No.	Number of degrees of freedom						Exact
	4	7	10	13	16	19	(128)
1	9.405	8.684	8.652	8.647	8.646	8.645	8.645
2			27.508	27.106	27.017	26.988	26.960
3			49.701	49.573	48.336	47.967	47.680
4			78.145	87.410	72.476	70.359	68.726

TABLE 3.14

Frequency coefficients λ for a vibrating cantilevered Timoshenko beam calculated using the present method.

N	1	2	3	4	5	6	
Mode No.	Number of degrees of freedom						Exact
	3	6	9	12	15	18	(128)
1	3.304	3.286	3.284	3.284	3.284	3.284	3.284
2	21.590	16.009	15.567	15.512	15.498	15.494	15.488
3	65.361	40.490	36.650	34.821	34.482	34.382	34.301
4		82.112	59.845	57.934	55.036	54.219	53.652

TABLE 3.15

Frequency coefficients λ for a simply supported Timoshenko beam.

	N	1	2	4	Exact (128)
		Number of degrees of freedom			
	Mode No.	4	8	16	
Kapur (128)	1	9.45	8.672	8.646	8.645
	2	30.843	28.577	27.021	26.960
	3		52.198	48.041	47.680
	4		74.236	70.871	68.726
	N	1	2	4	Exact (128)
		Number of degrees of freedom			
	Mode No.	2	4	8	
Archer (79A)	1	10.620	8.831	8.688	8.645
	2	48.583	39.098	28.218	26.960
	3		77.010	54.073	47.680
	4		93.897	85.271	68.726

TABLE 3.16

Frequency coefficients λ for a cantilevered Timoshenko beam.

N		1	2	4	Exact (128)
		Number of degrees of freedom			
	Mode No.	4	8	16	
Kapur (128)	1	3.297	3.285	3.284	3.284
	2	19.432	15.577	15.498	15.488
	3		37.005	34.403	34.301
	4		61.644	54.003	53.652
N		1	2	4	Exact (128)
		Number of degrees of freedom			
	Mode No.	2	4	8	
Archer (79)	1	3.322	3.294	3.286	3.284
	2	26.569	16.147	15.712	15.488
	3		54.494	36.515	34.301
	4		86.711	59.842	53.652

TABLE'3.17

Frequency coefficients A for retwisted cantilever blades.

$\frac{d_b}{b_b}$	δ*	n	Number of Elements 2	3	4	5	Ref. † (85)	Ref. (82)	Ref. (84)
2	30°	1	1.8767	1.8770	1.8771	1.8772	1.8774	1.87	
		2	2.6459	2.6413	2.6398	2.6391	2.6379	2.63	
		3	4.7325	4.7231	4.7223	4.7230	4.7281	4.73	
		4	6.5668	6.5806	6.5667	6.5501	6.5535	6.55	
2	60"	1	1.8798	1.8822	1.8830	1.8834	1.8843	1.88	
		2	2.6282	2.6118	2.6065	2.6041	2.6004	2.57	
		3	4.7868	4.7836	4.7947	4.8017	4.8210	4.82	
		4	6.3333	6.4186	6.3885	6.3739	6.3587	6.35	
2	90°	1	1.8841	1.8903	1.8923	1.8932	1.8957	1.89	
		2	2.6046	2.5698	2.5592	2.5546	2.5485	2.54	
		3	4.8736	4.8753	4.9040	4.9199	4.9591	4.95	
		4	6.0617	6.2273	6.1754	6.1543	6.1397	6.12	
4	30"	1	1.8769	1.8774	1.8776	1.8777	1.8781		1.87
		2	3.6961	3.6566	3.6424	3.6358	3.6245		3.62
		3	4.7691	4.8069	4.8282	4.8401	4.8672		4.90
		4	8.1375	7.7646	7.7162	7.6912	7.6802		7.70
8	30"	1	1.8770	1.8775	1.8777	1.8779	1.8777		1.87
		2	4.5688	4.4123	4.3616	4.3390	4.3066		4.26
		3	5.3353	5.5446	5.6404	5.6893	5.7855		5.76
		4	8.5350	7.8317	7.7798	7.7583	7.7827		7.75
16	30"	1	1.8770	1.8776	1.8778	1.8779	1.8772	1.88	
		2	4.6465	4.5229	4.4779	4.4573	4.4432	4.42	
		3	6.7043	7.1723	7.4609	7.5523	7.5752	7.53	
		4	9.3475	7.9112	7.7894	7.8206	8.2287	8.22	

† Results obtained using fivepretwisted beam elements.

* δ is the total pretwist angle in this case.

TABLE 4.1

Functions A_1 to A_{12}

$$A_1(x) = \frac{m}{r} J_m(x) - k J_{m+1}(x)$$

$$A_2(x) = \frac{m}{r} Y_m(x) - k Y_{m+1}(x)$$

$$A_3(x) = \frac{m}{r} I_m(x) + k I_{m+1}(x)$$

$$A_4(x) = \frac{m}{r} Km(x) - k K_{m+1}(x)$$

$$A_5(x) = c_1 J_m(x) + c_2 J_{m+1}(x)$$

$$A_6(x) = c_1 Y_m(x) + c_3 Y_{m+1}(x)$$

$$A_7(x) = c_2 I_m(x) - c_3 I_{m+1}(x)$$

$$A_8(x) = c_2 Km(x) + c_3 K_{m+1}(x)$$

$$A_9(x) = c_4 J_m(x) + c_5 J_{m+1}(x)$$

$$A_{10}(x) = c_4 Y_m(x) + c_5 Y_{m+1}(x)$$

$$A_{11}(x) = c_6 I_m(x) + c_7 I_{m+1}(x)$$

$$A_{12}(x) = c_6 K_m(x) - c_7 K_{m+1}(x)$$

$$c_1 = \frac{m(m-1)\ (l-v)}{r^2} - k^2$$

$$c_2 = \frac{m(m-1)\ (I-v)}{r^2} + k^2$$

$$c_3 = \frac{k(1-\nu)}{r}$$

$$c_4 = \frac{-mk^2r^2 + (l-v)\ (1-m)\ m^2}{r^3}$$

$$c_5 = \frac{k^3r^3 + kr(1-\nu)\ m^2}{r^3}$$

$$c_6 = \frac{mk^2r^2 + (l-v)\ (l-m)\ m^2}{r^3}$$

$$c_7 = \frac{k^3r^3 - kr(1-\nu)\ m^2}{r^3}$$

TABLE 4.2

Matrix [D]

$$
-\frac{D}{\Delta_m}\left|\begin{array}{c|c}
\begin{array}{c} P_1A_9(kb) - Q_1A_{10}(kb) \\ + R_1A_{11}(kb) - S_1A_{12}(kb) \end{array} & \begin{array}{c} P_1A_5(kb) - Q_1A_6(kb) \\ + R_1A_7(kb) - S_1A_8(kb) \end{array} \\ \hline
\text{Symmetrical} & \begin{array}{c} P_2A_5(kb) - Q_2A_6(kb) \\ + R_2A_7(kb) - S_2A_8(kb) \end{array}
\end{array}\right|
$$

$$
P_1 = \begin{vmatrix} Y_m(ka) & I_m(ka) & K_m(ka) \\ A_2(ka) & A_3(ka) & A_4(ka) \\ A_2(kb) & A_3(kb) & A_4(kb) \end{vmatrix} \quad
Q_1 = \begin{vmatrix} J_m(ka) & I_m(ka) & K_m(ka) \\ A_1(ka) & A_3(ka) & A_4(ka) \\ A_1(kb) & A_3(kb) & A_4(kb) \end{vmatrix}
$$

$$
R_1 = \begin{vmatrix} J_m(ka) & Y_m(ka) & K_m(ka) \\ A_1(ka) & A_2(ka) & A_4(ka) \\ A_1(kb) & A_2(kb) & A_4(kb) \end{vmatrix} \quad
S_1 = \begin{vmatrix} J_m(ka) & Y_m(ka) & I_m(ka) \\ A_1(ka) & A_2(ka) & A_3(ka) \\ A_1(kb) & A_2(kb) & A_3(kb) \end{vmatrix}
$$

$$
P_2 = \begin{vmatrix} Y_m(ka) & I_m(ka) & K_m(ka) \\ A_2(ka) & A_3(ka) & A_4(ka) \\ Y_m(kb) & I_m(kb) & K_m(kb) \end{vmatrix} \quad
Q_2 = \begin{vmatrix} J_m(ka) & I_m(ka) & K_m(ka) \\ A_1(ka) & A_3(ka) & A_4(ka) \\ J_m(kb) & I_m(kb) & K_m(kb) \end{vmatrix}
$$

$$
R_2 = \begin{vmatrix} J_m(ka) & Y_m(ka) & K_m(ka) \\ A_1(ka) & A_2(ka) & A_4(ka) \\ J_m(kb) & Y_m(kb) & K_m(kb) \end{vmatrix} \quad
S_2 = \begin{vmatrix} J_m(ka) & Y_m(ka) & I_m(ka) \\ A_1(ka) & A_2(ka) & A_3(ka) \\ J_m(kb) & Y_m(kb) & I_m(kb) \end{vmatrix}
$$

TABLE 4.2 (Continued)

$$\Delta_m = \begin{vmatrix} J_m(ka) & Y_m(ka) & I_m(ka) & K_m(ka) \\ A_1(ka) & A_2(ka) & A_3(ka) & A_4(ka) \\ J_m(kb) & Y_m(kb) & I_m(kb) & K_m(kb) \\ A_1(kb) & A_2(kb) & A_3(kb) & A_4(kb) \end{vmatrix}$$

TABLE 4.3

Dynamic stiffness matrix [DR] of a thin circular ring.

$$
C\pi R_o \rho \begin{bmatrix} \left(EI_z + \dfrac{GK_G}{m^2}\right)\dfrac{m^4}{R_0^4} - \omega^2 \left(A + J_z \dfrac{m^2}{R_o^2}\right) & (EI_z + GK_G)\dfrac{m^2}{R_0^3} \\ \text{Symmetrical} & (EI_z + m^2\, GK_G)/\,R_o^2 - \omega^2 J_x \end{bmatrix}
$$

E, G	– elastic moduli,
I_z	– moment of inertia about z axis,
K_G	– St. Venant torsion21 stiffness of the ring section,
R_o	– centroidal radius of the ring,
A	– Area of cross-section of ring,
J_z, J_x	– moment of inertia about z and x axes of ring section,

TABLE 4.4

Matrix $[D_b]$

$A_{11}\cos^2\delta$	$A_{12}\cos^2\delta$ $+B_{12}\sin^2\delta$	$(A_{11}-B_{11})\sin 5\cos\delta$	$(A_{12}-B_{12})\sin\delta\cos\delta$	0
	$A_{22}\cos^2\delta$ $+B_{22}\sin^2\delta$	$(A_{12}-B_{12})\sin 6\cos\delta$	$(A_{22}-B_{22})\sin 6\cos\delta$	0
		$A_{11}\sin^2\delta$ $+B_{11}\cos^2\delta$	$A_{12}\sin^2\delta$ $+B_{12}\cos^2\delta$	0
Symmetrical			$A_{22}\sin^2\delta$ $+B_{22}\cos^2\delta$	0
				C_{11}

$$A_{11} = -EI_1\lambda_1^3\left[\frac{\cos\lambda_1\ell\sinh\lambda_1\ell + \sin\lambda_1\ell\cosh\lambda_1\ell}{\cos\lambda_1\ell\cosh\lambda_1\ell + I}\right]$$

$$A_{12} = EI_1\lambda_1^2\left[\frac{\sin\lambda_1\ell\sinh\lambda_1\ell}{\cos\lambda_1\ell\cosh\lambda_1\ell + 1}\right]$$

$$A_{22} = EI_1\lambda_1\left[\frac{\cos\lambda_1\ell\sinh\lambda_1\ell - \sin\lambda_1\ell\cosh\lambda_1\ell}{\cos\lambda_1\ell\cosh\lambda_1\ell\ i- 1}\right]$$

Replace I_1 by I_2 and λ_1 by λ_2 in the above expressions to obtain B_{11}, B_{12} and B_{22} .

$$C_{11} = GK_G\lambda_3\cot\lambda_3\ell$$

TABLE 4.5

Dimensions and other details of bladed disc models I to III .

Model	Disc Dimensions (in)			Rim Dimensions (in)			Blade Dimensions (in)				
	a	b	h	R_o	b_r	d_r	ℓ	b_b	d_b	Z	δ
I	1.0	5.2	0.3	5.6	0.8	0.8	5.875	0.125	1.0	36	45°
II	1.0	5.2	0.3	5.6	0.8	0.8	3.025	0.125	1.0	36	45°
III*	3.5	17.5	0.8		No rim		12.000	0.600	2.0	36	50°

* All dimensions are in cm.

TABLE 4.6

First six cantilevered blade alone frequencies of models I to III.

Mode No.	Model I		Model II		Model III	
	ω^b (Hz)	Type	ω^b (Hz)	Type	ω^b (Hz)	Type
1	116	B_1	439	B_1	342	B_1
2	729	B_1	2427	T	1173	B_2
3	931	B_2	2750	B_1	2206	B_1
4	1250	T	3511	B_2	3498	T
5	2042	B_1	7281	T	6178	B_1
6	3749	T	7702	B_1	7354	B_2

B_1 - Bending in the I_{min} direction

B_2 - Bending in the I_ direction

T - Torsion

TABLE 4.7

Calculated and experimental frequencies in Hz. of bladed disc model I.

$E = 29 \times 10^6$ psi $\rho g = 0.283$ lb/in^3 $\nu = 0.3$

m	Mode NO	Number of disc and blade elements 1	2	3	4	Exact	Experi-mental
2	1	112	112	112	112	112	113
	2	323	321	320	320	320	326
	3	1071	746	743	741	740	
	4	1251	1156	1153	1151	1150	1123
	5	1388	1293	1276	1270	1263	
	6	3851	2482	2080	2072	2056	2094
3	1	116	115	115	115	115	115
	2	602	598	589	589	589	581
	3	1130	750	747	746	745	754
	4	1370	1275	1258	1252	1244	
	5	1782	1749	1720	1715	1712	1687
	6	4619	2531	2148	2144	2130	2159
4	1	117	116	116	116	116	116
	2	760	711	708	707	706	695
	3	1140	778	777	776	776	766
	4	1374	1279	1261	1255	1247	
	5	2727	2378	2024	2013	1998	2010
	6	5724	2888	2820	2814	2807	2792
5	1	117	116	116	116	116	116
	2	836	729	726	724	723	
	3	1145	829	828	828	828	
	4	1375	1280	1262	1256	1248	
	5	3945	2458	2051	2040	2025	2041
	6	7142	3923	3843	3737	3662	3610
6	1	117	116	116	116	116	116
	2	876	733	729	727	726	
	3	1147	862	861	861	861	
	4	1376	1280	1262	1256	1248	
	5	5279	2473	2058	2048	2033	2067
	6	8761	4457	4116	3949	3738	

TABLE 4.8

Calculated and experimental frequencies in Hz. of bladed disc model II.

$E = 29 \times 10^6$ psi $\rho g = 0.283$ lb/in^3 $\nu = 0.3$

m	fode No.	Number of disc and blade elements 1	2	3	4	Exact	Experimental
2	1	347	345	345	345	345	350
	2	580	577	576	576	576	587
	3	2292	2214	2207	2205	2203	2112
	4	2679	2493	2458	2446	2430	
	5	4308	2816	2803	2797	2794	2781
	6	7193	4761:	4705	4689	4676	3958
3	1	427	426	425	425	425	423
	2	1161	1157	1156	1156	1156	1157
	3	2678	2493	2459	2447	2431	
	4	2981	2818	2805	2800	2797	2893
	5	4332	2971	2968	2966	2965	
	6	7693	5671	5629	5619	5610	
4	1	436	434	434	434	434	436
	2	1912	1880	1878	1877	1876	1802
	3	2685	2500	2466	2454	2438	
	4	3838	2828	2816	2811	2808	
	5	4441	3936	3933	3932	3931	3789
	6	8558	7121	6964	6945	6924	
5	1	439	437	436	436	436	436
	2	2494	2375	2360	2355	2347	2228
	3	2713	2535	2509	2501	2492	
	4	4238	2859	2849	2844	2842	
	5	5410	5294	5278	5273	5269	5018
	6	9880	8664	7645	7715	7290	
6	1	440	438	437	437	437	436
	2	2654	2472	2439	2427	2412	2458
	3	2936	2680	2666	2661	2659	
	4	4287	2952	2946	2944	2942	
	5	7167	7061	6902	6872	6827	6551
	6	11691	8716	7947	7713	7336	

TABLE 4.9

Calculated and experimental frequencies in Hz. of bladed disc model III

$E = 29 \times 10^6$ psi $\rho g = 0.283$ lb/in^3 $\nu = 0.3$

m	Mode No.	Number of disc and blade elements 1	2	3	4	Exact	Jager Calculated	(120) Experimental
2	1	157	155	154	154	154	154	164
	2	466	463	463	463	462	450	430
	3	1032	1008	1005	1004	1003	1005	985
	4	2979	2120	2107	2103	2099	2040	1930
	5	3860	3187	3151	3138	3128		
	6	4929	3610	3559	3542	3519		
3	1	226	225	225	225	225	230	237
	2	522	521	521	521	521	515	490
	3	1277	1267	1266	1265	1264	1270	1215
	4	3082	2224	2214	2210	2208	2145	2050
	5	3866	3534	3494	3479	3461		
	6	5036	3760	3729	3717	3706		
4	1	275	273	273	273	273	276	280
	2	598	596	596	596	596	599	585
	3	1661	1579	1575	1574	1573	1600	1500
	4	3283	2376	2370	2366	2364	2275	2200
	5	3885	3613	3563	3545	3523		
	6	5261	4422	4372	4364	4358		
5	1	304	298	298	298	298		
	2	678	667	666	666	666		
	3	2043	1823	1814	1812	1811		
	4	3561	2621	2618	2614	2611		
	5	3956	3668	3617	3600	3578		
	6	5734	5193	5099	5088	5081		
6	1	321	313	312	312	312		
	2	760	728	726	726	726		
	3	2331	1957	1946	1943	1941		
	4	3717	2935	2924	2918	2912		
	5	4174	3768	3719	3702	3682		
	6	6623	5928	5811	5798	5786		

TABLE 4.10

Dimensions and other details of cases 1 through 7

Case	Disc Dimensions (in)			Blade Dimensions (in)			Z	δ	ℓ/b	ℓ/d_b
	a	b	h	ℓ	d_b	b_b				
1	0.1	6.0	0.3	6.0	1.0	0.08	36	45°	1.0	6.0
2	0.1	8.0	0.3	4.0	1.0	0.08	36	45°	0.5	4.0
3	0.1	4.0	0.3	8.0	1.0	0.08	36	45°	2.0	8.0
4	0.1	8.0	0.3	4.0	0.5	0.04	72	45°	0.5	8.0
5	0.1	8.0	0.3	4.0	2.0	0.16	18	45°	0.5	2.0
6	0.1	6.0	0.3	6.0	1.0	0.08	36	30°	1.0	6.0
7	0.1	6.0	0.3	6.0	1.0	0.08	36	60°	1.0	6.0

TABLE 4.11

First four cantilevered blade alone frequencies of cases 1 through 7.

$E = 29 \times 10^6$ psi $\rho g = 0.283$ $v = 0.3$

Mode No.	Case Number									
	1,2 and 7		3		4		5		6	
1	71	B_1	161	B_1	40	B_1	80	B_1	321	B_1
2	447	B_2	1007	B_1	252	B_1	503	%	1198	T
3	**799**	T	1198	T	502	B_2	1004	B_2	2013	B_1
4	**892**	B_2	2008	B_2	599	T	1198	T	3594	T

B_1 - Bending in the I_{min} direction B_2 - Bending in the I_ direction

T - Torsion

TABLE 4.12

Coupled frequencies in Hz. of cases 1 through 7, calculated by the exact method.

$E = 29 \times 10^6$ psi $\rho g = 0.283$ lb/in^3 $\nu = 0.3$

	Mode	Case Number						
m	No.	1	2	3	4	5	6	7
2	I	69	137	40	79	130	70	68
	2	212	220	186	210	375	186	250
	3	462	947	262	510	901	452	483
	4	796	1054	597	880	1202	795	797
3	1	71	155	40	80	225	71	70
	2	348	402	24.1	430	442	308	387
	3	469	1030	287	529	1193	454	526
	4	798	1200	597	1022	1281	797	798
4	I	71	158	40	80	272	71	71
	2	419	607	248	. 496	553	395	427
	3	501	1040	327	685	1205	459	602
	4	798	1201	598	1192	1700	798	799
5	1	71	159	40	80	291	71	71
	2	437	784	250	500	680	436	437
	3	554	1056	357	808	1212	487	661
	4	798	1203	598	1197	2034	798	799
6	1	71	159	40	80	300	71	71
	2	442	905	251	502	799	443	441
	3	600	1092	378	a67	1221	531	703
	4	798	1208	598	1197	2054	798	799

TABLE 4.13

Frequency ratios ω/ω_1^b of the first four modes of cases 1 through 7.

m	Mode No.	Case Number 1	2	3	4	5	6	7
2	1	0.9718	0.8509	1.0000	0.9875	0.4050	0.9859	0.9577
	2	2.986	1.367	4.650	2.625	1.168	2.620	3.521
	3	6.507	5.882	6.550	6.375	2.807	6.366	6.803
	4	11.211	6.547	14.925	11.000	3.745	11.197	11.225
3	1	1.0000	0.9627	1.0000	1.0000	0.7009	1.0000	0.9859
	2	4.901	2.497	6.025	5.375	1.377	4.338	5.451
	3	6.606	6.398	7.175	6.613	3.717	6.394	7.409
	4	11.239	7.453	14.950	12.775	3.991	11.225	11.239
4	1	1.0000	0.9814	1.0000	1.0000	0.8474	1.000	1.0000
	2	5.901	3.770	6.200	6.200	1.723	5.563	6.014
	3	7.056	6.460	8.175	8.563	3.754	6.465	8.479
	4	11.239	7.460	14.950	14.900	5.296	11.239	11.254
5	1	1.0000	0.9876	1.0000	1.0000	0.9065	1.0000	1.0000
	2	6.155	4.870	6.250	6.250	2.118	6.141	6.155
	3	7.803	6.559	8.925	10.100	3.776	6.859	9.310
	4	11.239	7.472	14.950	14.963	6.337	11.239	11.254
6	1	1.0000	0.9876	1.0000	1.0000	0.9346	1.0000	1.0000
	2	6.225	5.621	6.275	6.275	2.489	6.239	6.211
	3	8.451	6.783	9.450	10.838	3.804	7.479	9.901
	4	11.239	7.503	14.950	14.963	6.399	11.239	11.254

TABLE 4.14

Variation of frequencies (in Hz.) of bladed disc model I with speed of rotation.

$E = 29 \times 10^6$ psi $\quad \rho g = 0.283$ lb/in^3 $\quad \nu = 0.3$

m	Mode No.	Speed of rotation in rpm. 0	3500	7000
2	1	112	140	200
	2	320	327	347
	3	741	773	858
	4	1151	1158	1178
	5	1270	1271	1273
	6	2072	2106	2205
3	1	115	145	208
	2	589	596	612
	3	746	775	860
	4	1252	1252	1252
	5	1715	1724	1750
	6	2144	2174	2266
4	1	116	145	209
	2	707	729	761
	3	776	791	861
	4	1255	1255	1255
	5	2013	2045	2136
	6	2814	2822	2844
5	1	116	146	209
	2	724	756	827
	3	828	834	866
	4	1256	1256	1256
	5	2040	2075	2173
	6	3737	3754	3761
6	1	116	146	210
	2	727	760	848
	3	861	865	881
	4	1256	1256	1256
	5	2048	2083	2182
	6	3949	3955	3962

TABLE 4.15

Frequencies in Hz. of bladed disc model I calculated including transverse shear and rotary inertia.

$E = 29 \times 10^6$ psi $\rho g = 0.283$ lb/in^3 $\nu = 0.3$

m	Mode No.	Number of disc and blade elements			Experiment
		2	3	4	
2	1	112	112	112	113
	2	332	328	327	326
	3	744	740	739	
	4	1165	1157	1154	1123
	5	1293	1275	1269	
	6	2481	2076	2063	2094
3	1	115	115	115	115
	2	596	592	589	581
	3	750	744	743	754
	4	1274	1256	1250	
	5	1734	1705	1700	1687
	6	2520	2140	2132	2159
4	1	116	116	116	116
	2	710	705	703	695
	3	772	768	766	766
	4	1277	1259	1253	
	5	2357	2014	2000	2010
	6	2823	2744	2738	2792
5	1	116	116	116	116
	2	728	723	722	
	3	815	811	809	
	4	1278	1260	1254	
	5	2445	2043	2029	2041
	6	3719	3646	3585	3610
6	1	116	116	116	116
	2	731	727	725	
	3	843	839	838	
	4	1278	1260	1254	
	5	2460	2050	2037	2067
	6	4342	4075	3939	

TABLE 4.16

Frequencies in Hz. of bladed disc model II calculated including transverse shear and rotary inertia.

$E = 29 \times 10^6$ psi $\rho g = 0.283$ lb/in^3 $\nu = 0.3$

m	Mode No.	Number of disc and blade elements			Experimeni
		2	3	4	
2	1	353	351	350	350
	2	582	579	578	587
	3	2360	2276	2255	2112
	4	2490	2455	2443	
	5	2788	2769	2763	2781
	6	6428	4463	4408	3958
3	1	426	425	425	423
	2	11.58	1152	1149	1157
	3	2493	2458	2446	
	4	2783	2767	2761	2893
	5	3034	3006	2989	
	6	7113	5395	5347	
4	1	434	434	433	436
	2	1839	1827	1820	1802
	3	2501	2466	2454	
	4	2790	2773	2768	
	5	3894	3878	3868	3789
	6	8132	684.9	6744	
5	1	436	436	436	436
	2	2295	2273	2264	2228
	3	2528	2495	2484	
	4	2801	2786	2780	
	5	5118	5080	5072	5018
	6	8655	7680	7653	
6	1	437	437	437	436
	2	2443	2410	2399	2458
	3	2631	2603	2593	
	4	2832	2817	2811	
	5	6655	6521	6493	6551
	6	8709	7843	7676	

TABLE 4.17

Section properties of the turbine blade

Radius (in)	Area (in^2)	I_{min} (in^4)	I_{max} (in^4)	δ (°)
8.182	0.1196	0.0005994	0.007063	10.32
8.780	0.0960	0.0004300	0.005400	16.00
9.390	0.0771	0.0002736	0.003857	22.71
10.050	0.0630	0.0001700	0.002800	29.50
10.720	0.0461	0.0000822	0.002048	32.27

TABLE 4.18

Calculated and measured frequencies in Hz. of the turbine blade
5 Timoshenko beam elements used in the calculations.

$E = 29.3 \times 10^6$ psi $\rho g = 0.283$ lb/in^3 $\nu = 0.3$

Mode No.	Calculated	Experiment
1	1151	1150
2	3553	2560
3	5482	
4	12108	

TABLE 4.19

Dimensions and section properties at nodal points of the finite element model of the turbine.

DISC

Node	Radius (in)	Thickness (in)
1	0.900	2.650
2	2.380	1.395
3	3.430	1.095
4	5.700	0.680
5	6.950	0.480
6	7.390	1.025
7	7.836	1.025

BLADE

Node	Radius (in)	Area (in^2)	I_{min} (in^4)	I_{max} (in^4)	δ (°)
1	7.836	0.1350	0.0007400	0.007400	8.00
2	8.182	0.1196	0.0005994	0.007063	10.32
3	8.780	0.0960	0.0004300	0.005400	16.00
4	9.380	0.0771	0.0002736	0.003857	22.71
5	10.050	0.0630	0.0001700	0.002800	29.50
6	10.855	0.0435	0.0000720	0.001900	32.30

TABLE 4.20

Calculated and experimental frequencies, in Hz., of the turbine rotor. 6 disc elements and 5 blade elements used in the calculations.

pg = 0.281 (disc) , pg = 0.283 (blade) $\nu = 0.3$ $E_{blade} = 29.3 \times 10^6$ psi

m	Mode No.	Calculated $E_d = 31.2$ psi $\times 10^6$	Calculated $E_d = 28.4$ psi $\times 10^6$	Experiment
2	1	700	669	618
	2	1168	1166	
3	1	1010	974	860
	2	1208	1197	975
4	1	1131	1126	1044
	2	1523	1466	1290
5	I	1143	1142	1173
	2	1947	1877	1563
6	1	1146	1146	
	2	2308	2237	1871

APPENDIX A

APPLICATION OF THE THIN PLATE BENDING ELEMENTS TO STATIC BENDING ANALYSIS OF CIRCULAR AND ANNULAR PLATES

A.1 INTRODUCTION

The annular and circular thin plate bending elements developed in Chapter 2, although primarily developed for the vibration analysis of turbine discs with radial thickness variations, can be readily applied in the static bending analysis of axisymmetric circular and annular plates.

Here a few examples have been chosen to show the accuracy and use of these elements in such static analysis. When plates with axisymmetric loading are considered, annular and circular elements with $m = 0$ are to be used, Loads which are not axisymmetric can also be considered if they can be expanded into Fourier series, In such cases each Fourier component is considered seperately and for the i^{th} component elements with nodal diameters $m = i$ are used. Required number of' Fourier terms are taken and the individual contributions of deflection etc. are superposed together to get the complete solution of the problem.

A.2 NUMERICAL APPLICATIONS

The first example is the axisymmetric circular plate with radial thickness variation subjected to uniform load q, shown in Figure A.1. Annular and circular elements with m = 0 are used and the load q is replaced by consistent load. The central deflection and bending moments obtained are given in Table A.1, along with exact solutions. Plates with $h_o/h_1 = 1.0$ and 1.5 are considered. The same problem is solved by considering annular plates with a/b = 0.001, and using only annular elements, The results are given in Table A.2. Comparing results of Table A.1 and A.2, it is seen that when the plates are approximated by annular plates with very small inner radius the bending moments obtained at the centre are not accurate, whereas they are not much affected at points away from the centre,

The second example chosen is an axisymmetric annular plate with variable thickness shown in Figure A.2. The maximum deflection for this plate with b/a = 1.25, 2, and 5, obtained with models with annular elements are given in Table A.3 with exact solutions.

Axisymmetric plates with nonsymmetric loads can also be considered, As already mentioned these loads are expanded in Fourier series and each Fourier component is considered separately. A uniform annular plate fixed at the inner radius a and free at the outer radius b, and subjected to a single concentrated load P at a point on the outer boundary as shown in Figure A.3 is considered. Deflection under the load obtained for this problem using annular elements are given for plates with a/b = 0.5 in Table A.4 along with exact solutions. Humber of Fourier components taken for the calculations were 11, 21, 51, and 101. The results show that the number of Fourier components taken has more influence on the results than the number of elements used. Olson and Lindberg (54) have used sector elements to solve this problem and their results are given in Table A.5.

The next example is a clamped circular plate with a single concentrated load P applied anywhere in the plate, as shown in Figure A.4. The plate is approximated with an annular plate with a/b = 0.001. The deflection under the load when the first 21 Fourier components of the load are taken are given in Table A.6 with exact solutions and solutions obtained by Olson and Lindberg (54) using sector elements. The load is applied at a point with radius ratio c/b = 0.5.

A.3 DISCUSSION

The numerical examples considered show that for axisymmetric plates, although sector elements (54,55,56) and triangular elements (57) can be used in the static bending analysis, the use of annular and circular elements offer substantial computational advantages since the number of degrees of freedom involved are much less than the other cases. At the same time there is no loss in accuracy. The relative ease with which radial thickness variation can be taken into account when annular and circular elements are used is an added advantage. Eventhough a set of problems equal to the number of Fourier components taken, are to be solved in the case of loads which are not axisymmetric, still use of these elements offer computational advantages in terms of storage and time.

But the application of these elements are limited only to complete axisymmetric circular and annular plates.

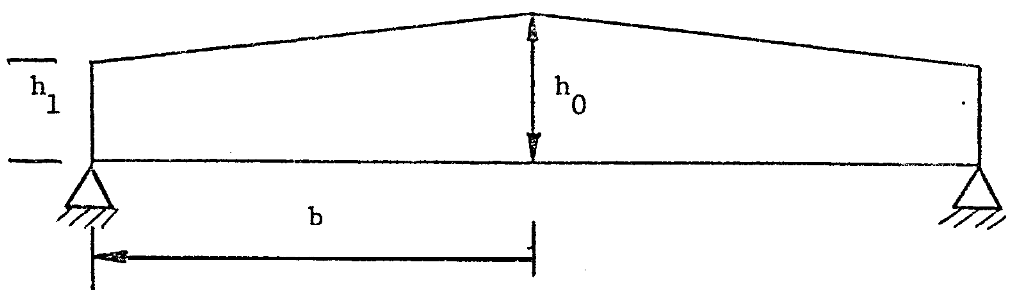

Figure A.1 Circular plate with radial linear thickness variation.

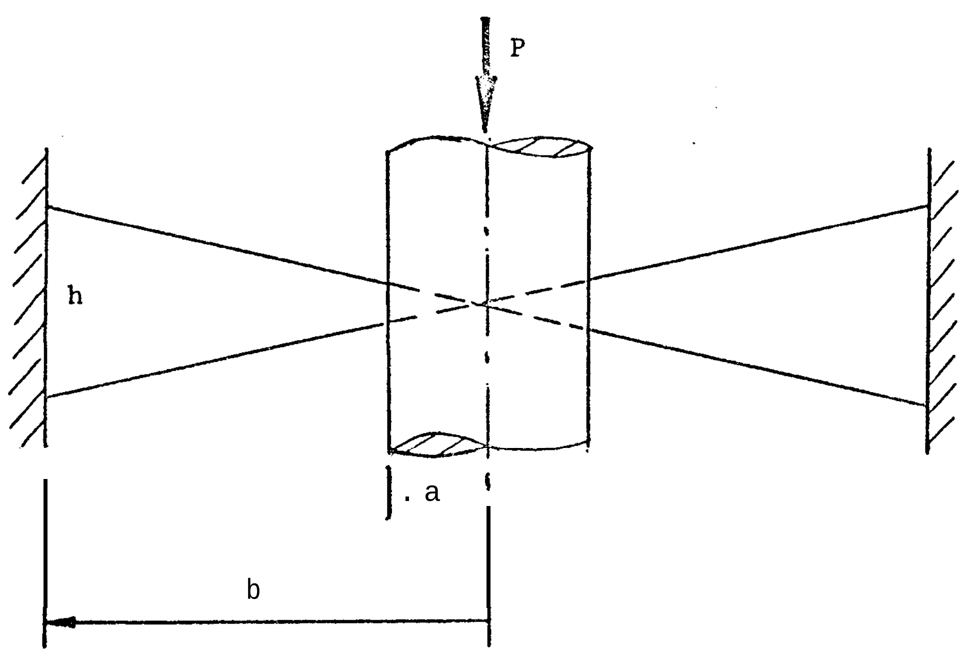

Figure A.2 Annular plate with radial linear thickness variation.

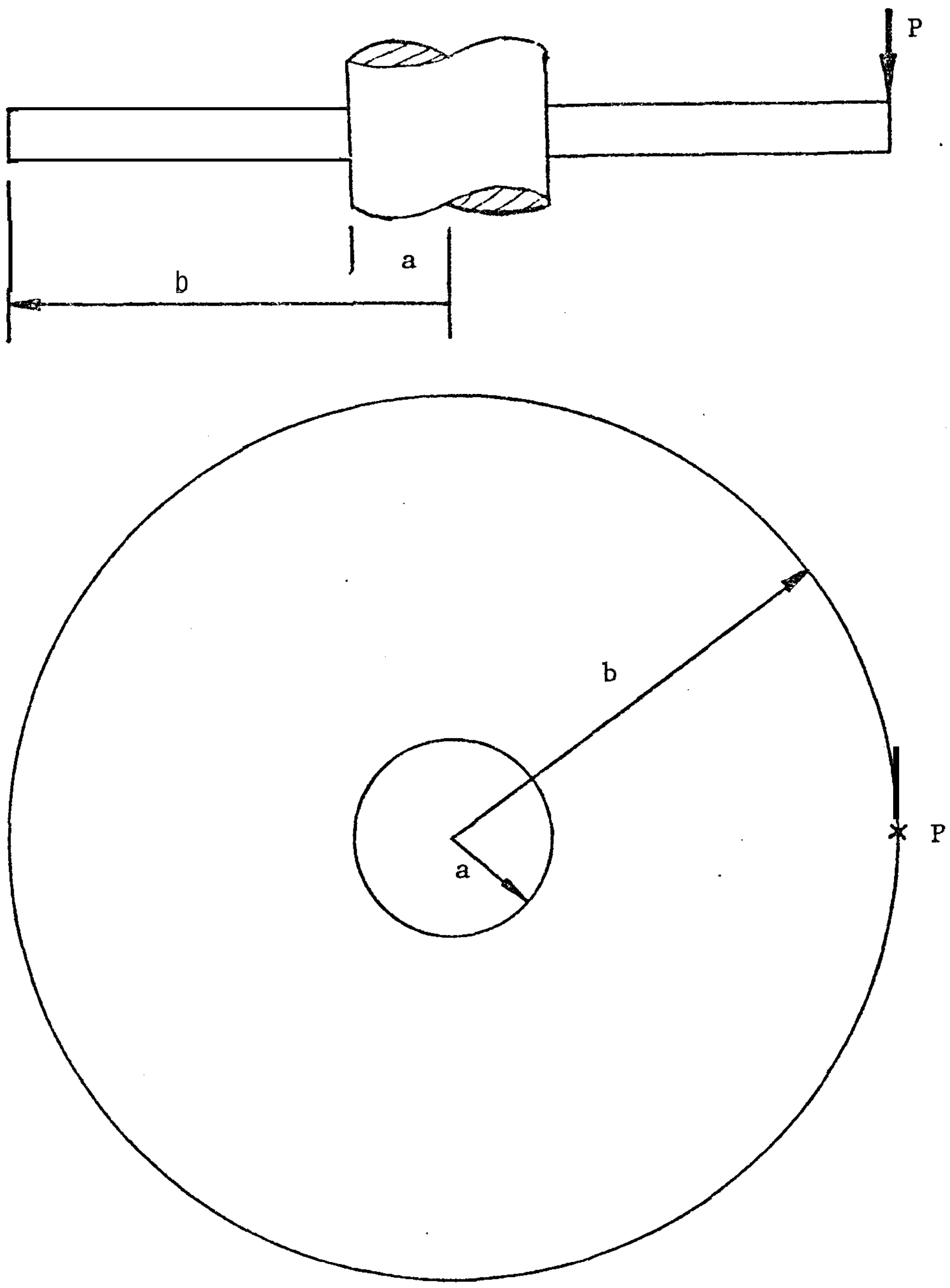

Figure A.3 Uniform annular plate loaded with a concentrated load at the outer boundary.

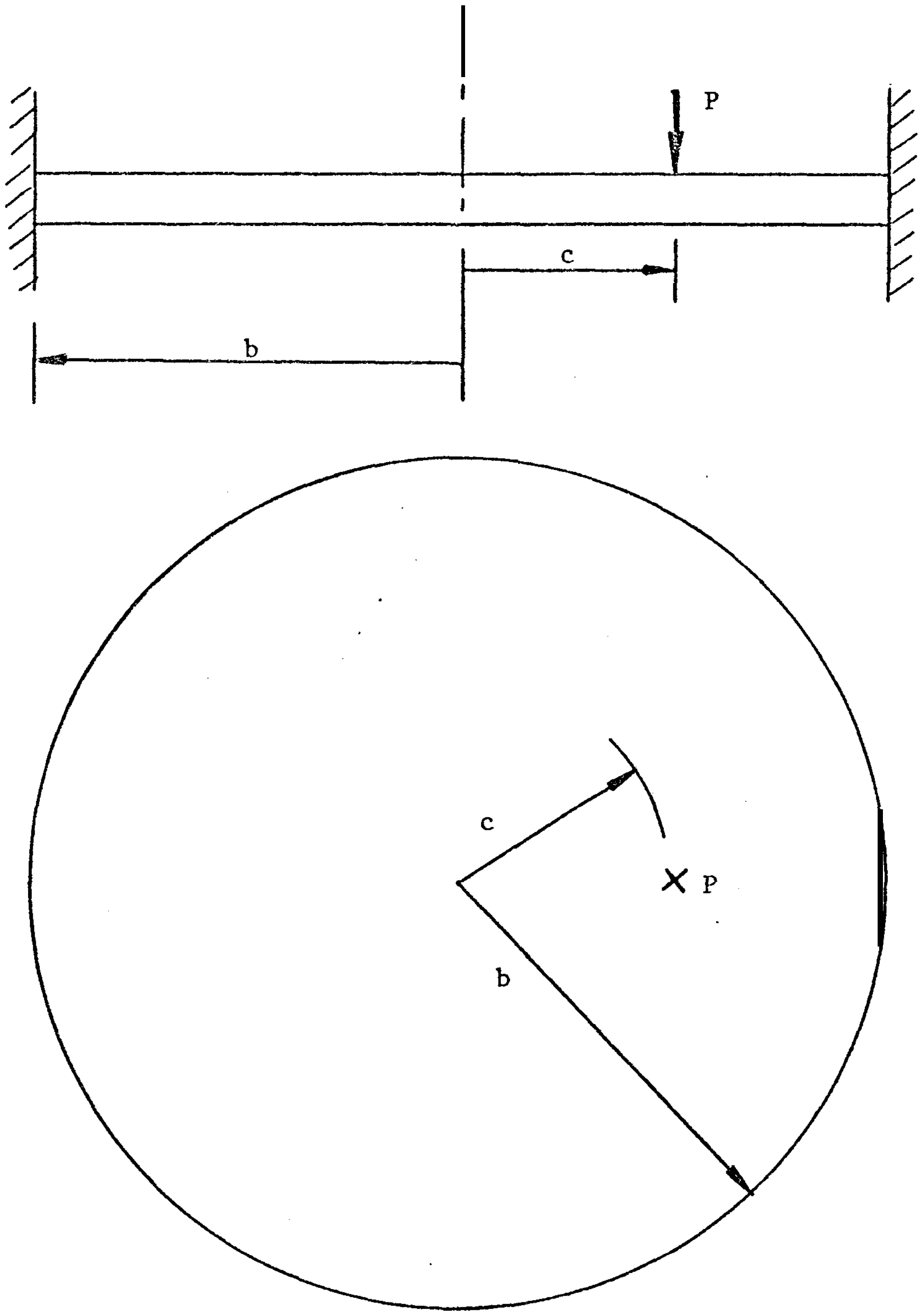

Figure A.4 Uniform circular plate loaded with a concentrated load anywhere on the plate.

TABLE A.1

Deflections and bending moments of simply supported plates under uniform pressure q, modelled with one circular and several annular thin plate bending elements.

h_o i i		r	Number of elements 2	4	8	16	Exact (124)
1	$w_{max}\frac{Eh_0^3}{qb^4}$	0	0.7391	0.7383	0.7383	0.7383	0.738
	M_r/qb^2	0	0.2147	0.2060	0.2038	0.2033	0.203
		b/2	0.1599	0.1543	0.1528	0.1525	0.152
	M_t/qb^2	0	0.2147	0.2060	0.2038	0.2033	0.203
		b/2	0.1775	0.1763	0.1759	0.1758	0.176
		b	0.0955	0.0942	0.0939	0.0938	0.094
1.5	$w_{max}\frac{Eh_0^3}{qb^4}$	0	1.2660	1.2660	1.2660	1.2660	1.260
	M_r/qb^2	0	0.2689	0.2593	0.2577	0.2574	0.257
		b/2	0.1927	0.1799	0.1772	0.1766	0.176
	M_t/qb^2	0	0.2689	0.2593	0.2577	0.2574	0.257
		b/2	0.1760	0.1730	0.1724	0.1722	0.173
		b	0.0588	0.0556	0.0545	0.0541	0.054

TABLE A.2

Deflections and bending moments of simply supported plates under uniform pressure q, modelled with annular thin plate bending elements only with a/b = 0.001.

$\frac{h_0}{h}$		r	Number of elements: 2	4	8	16	Exact (124)
1	$w_{max}\frac{Eh_0^3}{qb^4}$	0	0.7389	0.7384	0.7383	**0.7383**	0.738
	M_r/qb^2	0	0.1639	0.2111	0.2191	0.2220	0.203
		b/2	0.1595	0.1542	0.1527	0.1524	0.152
	M_t/qb^2	0	0.0073	0.2275	0.2709	0.2935	0.203
		b/2	0.1774	0.1762	0.1759	0.1758	0.176
		b	0.0955	0.0942	0.0939	0.0938	0.094
1.5	$w_{max}\frac{Eh_0^3}{qb^4}$	0	1.2650	1.2650	1.2650	1.2650	1.260
	M_r/qb^2	0	0.2202	0.2713	**0.2783**	0.2814	0.257
		b/2	0.1925	0.1797	0.1771	0.1765	0.176
	M_t/qb^2	0	0.0693	0.3099	0.3478	0.3731	0.257
		b/2	0.1758	0.1729	0.1723	0.1721	0.173
		b	0.0588	0.0556	0.0544	0.0541	0.054

TABLE A.3

Deflection coefficients $w_{max}\frac{Eh^3}{Pb^2}$ of an annular disc of varying thickness (Figure A.2).

b/a	Number of elements					Exact (124)
	1	2	4	8	16	
1.25	0.001652	0.001733	0.001739	0.001739	0.001739	0.00174
2.00	0.039770	0.057250	0.060320	0.060610	0.060630	0.0606
5.00	0.208200	0.542600	0.780800	0.861900	0.874900	0.876

TABLE A.4

Deflection coefficient w_{max} D/P for a uniform annular plate with a single concentrated load, calculated using thin plate bending annular elements.

n*	Number of Elements				Exact (124)
	2	4	8	16	
11	0.047737	0.047785	0.047789	0.047789	0.050718
21	0.049910	0.049960	0.049964	0.049965	
51	0.050537	0.050591	0.050595	0.050596	
101	0.050616	0.050682	0.050687	0.050688	

n* - number of Fourier terms

TABLE A.5

Deflection coefficient w_{max} D/P for a uniform annular plate with a single concentrated load, calculated using sector elements (54).

Sector Element Grids	N.D.F.	w_{max} D/P	Exact (124)
1x6	19	0.050896	0.050718
2x12	74	0.051372	
3x18	165	0.051027	
4x24	292	0.050885	

TABLE A.6

Deflection coefficient w D/P of a uniform circular plate with a single concentrated load P applied any where in the plate. c/b = 0.5

Number of Elements	N.D.F.	n*	wD/P	
			Finite element	Exact (124)
2	6	21	0.0104559	
4	10	21	0.0109955	
8	18	21	0.0111291	
12	26	21	0.0111483	0.0111906
2x4*	18	-	0.0113155	
4x6*	63	-	0.0112715	
6x8*	133	-	0.0109738	

* Sector element grid (54)

n* - number of Fourier terms

APPENDIX B

VIBRATION OF CIRCULAR AND ANNULAR PLATES WITH TRANSVERSE SHEAR AND ROTARY INERTIA

B.1 INTRODUCTION

Based on Mindlin's Plate theory (62), which takes into account transverse shear and rotary inertia, Callahan (66), and Bakshi and Callahan (67) have derived frequency determinants for circular and annular plates with various boundary conditions. These determinants can be used in the calculation of natural frequencies of moderately thick circular and annular plates. A brief summary of the theory as applied to annular plates is given here with the frequency determinant of a free-free annular plate.

B.2 MINDLIN'S PLATE THEORY

When transverse shear and rotary inertia are considered, the governing differential equations, in polar coordinates, of a vibrating plate is

$$\frac{\partial^2 w_i}{\partial r^2} - \frac{1}{r}\frac{\partial w_i}{\partial r} + \frac{1}{r^2}\frac{\partial^2 w_i}{\partial \xi^2} + \delta_i w_i = 0 \qquad \text{(B.1)}$$

$$(i = 1,2,3.)$$

where w_1 and w_2 are component parts' of the total deflection w;

and w_3 is a potential function giving rise to twist about normal to plate; and

$$\delta_{1,2}^2 = \frac{1}{2}\delta_o^4 \{ (R + S) \pm [(R - S)^2 + 4\delta_o^{-4}]^{\frac{1}{2}} \}$$

$$\delta_3^2 = 2(R\delta_o^4 - S^{-1}) / (1 - \nu) \qquad \text{(B.2)}$$

$$\delta_o^4 = \rho\, \omega^2 h / D$$

$$R = h^2/12 ; \quad S = D/\kappa^2 Gh ; D = E h^3 / 12(1 - \nu^2)$$

E, G, ν are the Young's modulus, the shear modulus and Poisson's ratio, respectively, and $\kappa^2 = \pi^2/12$

Now,

$$w = w_1 + w_2$$

$$\psi_r = (\sigma_1 - 1)\frac{\partial w_1}{\partial r} + (\sigma_2 - 1)\frac{\partial w_2}{\partial r} + \frac{1}{r}\frac{\partial w_3}{\partial \xi}$$

(B.3)

$$\psi_\xi = (\sigma_1 - 1)\frac{1}{r}\frac{\partial w_1}{\partial \xi} + (\sigma_2 - 1)\frac{1}{r}\frac{\partial w_2}{\partial \xi} - \frac{\partial w_3}{\partial r}$$

where

$$\sigma_1, \sigma_2 = (\delta_2^2, \delta_1^2)(R\,\delta_o^4 - S^{-1})^{-1}$$

The above equations give the deflection and rotations of the plate, and the plate stresses are given by the following relations.

$$M_r = D\left[\frac{\partial\psi_r}{\partial r} + \frac{\nu}{r}\left(\psi_r + \frac{\partial\psi_\xi}{\partial\xi}\right)\right]$$

$$M_\xi = D\left[\frac{1}{r}\left(\psi_r + \frac{\partial\psi_\xi}{\partial\xi}\right) + \nu\frac{\partial\psi_r}{\partial r}\right.$$

$$M_{r\xi} = \frac{D}{2}(1-\nu)\left[\frac{1}{r}\left(\frac{\partial\psi_r}{\partial\xi} - \psi_\xi\right) + \frac{\partial\psi_\xi}{\partial r}\right] \qquad \text{(B.4)}$$

$$Q_r = \kappa^2 Gh\left(\psi_r + \frac{\partial w}{\partial r}\right)$$

$$Q = \kappa^2 Gh\left(\psi_\xi + \frac{1}{r}\frac{\partial w}{\partial\xi}\right)$$

Now, δ_1^2 is always positive for positive values of ω ; but δ_2^2 and δ_3^2 are positive only when $\omega < \omega$, where $\bar{\omega}$ is the frequency of the first thickness shear mode of an infinite plate, and is given by, $\bar{\omega} = \pi(G\ /\rho)^{1/2} / h$

Hence, the most general solutions of Equations (B.1), for an annular plate when $\omega < \bar{\omega}$ are

$$w_1 = \sum_{m=0}^{\infty}\{a_m^1 J_m(r\delta_1) \; 4 \; b_m^1 Y_m(r\delta_1)\}(\cos m\xi + \sin m\xi)$$

$$w_2 = \sum_{m=0}^{\infty}\{a_m^2 I_m(r\delta_2') + b_m^2 K_m(r\delta_2')\}(\cos m\xi + \sin m\xi)$$

$$w_3 = \sum_{m=0}^{\infty}\{a_m^3 \, Im(r\delta_3') + b_m^3 K_m(r\delta_3')\}(\cos m\xi + \sin m\xi) \qquad \text{(B.5)}$$

where a_m^i, b_m^i ($i = 1,2,3.$) are arbitrary constants,

J_m, Y_m, I_m, and K_m are Bessel functions of order m,

$$(\delta'_2)^2 = \left| (\delta_2)^2 \right| \;; \qquad (\delta'_3)^2 = \left| (\delta_3)^2 \right|$$

Substituting (B.5) into (B.4) we arrive at expressions for the plate stress components involving the six arbitrary constants a^i_m, b^i_m ($i = 1,2,3.$).

B.3 ANNULAR PLATE WITH FREE BOUNDARIES

Let us consider an annular plate with both boundaries free, as an example. Then on both boundaries where $r = a$ and $r = b$.

$$Q_r = M_{r\xi} = M_r = 0 \tag{B.6}$$

Now,

$$
\begin{aligned}
Q_r \; = \;& a^1_m A^1_m (\delta_1 r) + b^1_m B^1_m (\delta_1 r) + a^2_m A^2_m (\delta'_2 r) + b^2_m B^2_m (\delta'_2 r) \\
& a^3_m A^3_m (\delta'_3 r) + b^3_m B^3_m (\delta'_3 r) \\
M_{r\xi} \; = \;& a^1_m C^1_m (\delta_1 r) + b^1_m D^1_m (\delta_1 r) + a^2_m C^2_m (\delta'_2 r) + b^2_m D^2_m (\delta'_2 r) \\
& a^1_m C^1_m (\delta'_3 r) + b^1_m D^1_m (\delta'_3 r) \\
M_r \; = \;& a^1_m E^1_m (\delta_1 r) + b^1_m F^1_m (\delta_1 r) + a^2_m E^2_m (\delta'_2 r) + b^2_m F^2_m (\delta'_2 r) \\
& a^3_m E^3_m (\delta'_3 r) + b^3_m F^3_m (\delta'_3 r)
\end{aligned}
\tag{B.7}
$$

Where the expressions A_m^i, B_m^i, etc., (i = 1,2,3) are combnations of Bessel functions and are given in Table B.l.

When the above expressions are equated to zero when r =a and r = b , satisfying boundary conditions (B.6), we get a set of homogeneous simultaneous equations. Nontrivial solution of these is obtained by equating to zero the following determinant.

$$\Delta = \begin{vmatrix} A_m^1(\delta_1 a) & B_m^1(\delta_1 a) & A_m^2(\delta_2' a) & B_m^2(\delta_2' a) & A_m^3(\delta_3' a) & B_m^3(\delta_3' a) \\ A_m^1(\delta_1 b) & B_m^1(\delta_1 b) & A_m^2(\delta_2' b) & B_m^2(\delta_2' b) & A_m^3(\delta_3' b) & B_m^3(\delta_3' b) \\ C_m^1(\delta_1 a) & D_m^1(\delta_1 a) & C_m^2(\delta_2' a) & D_m^2(\delta_2' a) & C_m^3(\delta_3' a) & D_m^3(\delta_3' a) \\ C_m^1(\delta_1 b) & D_m^1(\delta_1 b) & C_m^2(\delta_2' b) & D_m^2(\delta_2' b) & C_m^3(\delta_3' b) & D_m^3(\delta_3' b) \\ E_m^1(\delta_1 a) & F_m^1(\delta_1 a) & E_m^2(\delta_2' a) & F_m^2(\delta_2' a) & E_m^3(\delta_3' a) & F_m^3(\delta_3' a) \\ E_m^1(\delta_1 b) & F_m^1(\delta_1 b) & E_m^2(\delta_2' b) & F_m^2(\delta_2' b) & E_m^3(\delta_3' b) & F_m^3(\delta_3' b) \end{vmatrix} = 0 \qquad \text{(B.8}$$

Por other boundary conditions similar determinants are readily derived. Similar procedure is followed when a circular plate is considered. This problem has been treated by Callahan (66).

The natural frequencies of the plate are obtained by systematic searching of values of ω which make the value of the appropriate frequency determinant corresponding to the required boundary conditions, zero.

TABLE B.1

$$A^1_m(x) = \sigma_1 J'_m(x)\, \kappa^2 Gh \qquad B^1_m(x) = \sigma_1 Y'_m(x)\, \kappa^2 Gh$$

$$A^2_m(x) = \sigma_1 I'_m(x)\, \kappa^2 Gh \qquad B^2_m(x) = \sigma_1 K'_m(x)\, \kappa^2 Gh$$

$$A^3_m(x) = -\frac{m}{r} I_m(x)\, \kappa^2 Gh \qquad B^3(x) = -\frac{m}{r} K_m(x)\, \kappa^2 Gh$$

$$C^1_m(x) = [(\sigma_1-1)\{\frac{m}{r} J'_m(x) - \frac{m}{r^2} J_m(x)\}](1-\nu) D$$

$$C^2_m(x) = [(\sigma_2-1)\{\frac{m}{r} I'_m(x) - \frac{m}{r^2} I_m(x)\}](1-\nu) D$$

$$C^3_m(x) = -\frac{1}{2}[I''_m(x) - \frac{1}{r} I'_m(x) + \frac{m^2}{r^2} I_m(x)](1-\nu) D$$

$$D^1_m(x) = [(\sigma_1-1)\{\frac{m}{r} Y'_m(x) - \frac{m}{r^2} Y_m(x)\}](1-\nu) D$$

$$D^2_m(x) = [(\sigma_2-1)\{\frac{m}{r} K'_m(x) - \frac{m}{r^2} K_m(x)\}](1-\nu) D$$

$$D^3_m(x) = -\frac{1}{2}[K''_m(x) - \frac{1}{r} K'_m(x) + \frac{m^2}{r^2} K_m(x)](1-\nu) D$$

$$E^1_m(x) = [(\sigma_1-1)\{J''_m(x) + \frac{\nu}{r} J'_m(x) - \frac{\nu m^2}{r^2} J_m(x)\}] D$$

$$E^2_m(x) = [(\sigma_2-1)\{I''_m(x) + \frac{\nu}{r} I'_m(x) - \frac{\nu m^2}{r^2} I_m(x)\}] D$$

$$E^3_m(x) = [-\frac{m}{r} I'_m(x) + \frac{m}{r^2} I_m(x)](1-\nu) D$$

$$F^1_m(x) = [(\sigma_1-1)\{Y''_m(x) + \frac{\nu}{r} Y'_m(x) - \frac{\nu m^2}{r^2} Y_m(x)\}] D$$

$$F^2_m(x) = [(\sigma_2-1)\{K''_m(x) + \frac{\nu}{r} K'_m(x) - \frac{\nu m^2}{r^2} K_m(x)\}] D$$

$$F^3_m(x) = [-\frac{m}{r} K'_m(x) + \frac{m}{r^2} K_m(x)](1-\nu) D$$

APPENDIX C

FINITE ELEMENT ANALYSIS OF THICK RECTANGULAR PLATES IN BENDING

C.1. INTRODUCTION

Pryor and Barber (125) have developed a twenty degree of freedom rectangular element for the bending analysis of rectangular plates including the effects of transverse shear. In'the formulation of this element, in addition to the total deflection w and rotations ϕ_x and ϕ_y normally considered in plate bending, the average transverse shear strains $\bar{\gamma}_x$ and $\bar{\gamma}_y$ are taken as the additional degrees of freedom. Numerical results presented demonstrate good agreement with Reissner theory, and a substantial improvement over previous formulations (133,134).

In the exact analysis of problems based on Reissner theory, Salarno and Goldberg (135) have separated the contributions due to bending and transverse shear. Such an alternative approach, when used in the finite element formulation, offers significant computational advantages. Following this approach, a (12 x 12) shear stiffness matrix is derived which is used seperately to yield the transverse shear effects.

Since the notations used here are different from those used elsewhere in this work, a separate list is given at the end of this Appendix.

C.2. FINITE ELEMENT FORMULATION

The governing equations of the Reissner theory give the following relations for the stress resultants, (124),

$$
\begin{aligned}
M_x &= D\left[\frac{\partial\phi_x}{\partial x} + \nu\frac{\partial\phi_y}{\partial y} + \frac{\nu k}{2Gh}q\right] \\
M_y &= D\left[\frac{\partial\phi_y}{\partial y} + \nu\frac{\partial\phi_x}{\partial x} + \frac{\nu k}{2Gh}q\right] \qquad (C.1) \\
M_{xy} &= -\frac{D(1-\nu)}{2}\left[\frac{\partial\phi_x}{\partial y} + \frac{\partial\phi_y}{\partial x}\right]
\end{aligned}
$$

where

$$
\begin{aligned}
\phi_x &= -\frac{\partial w}{\partial x} + k\frac{Q_x}{Gh} \\
& \qquad\qquad\qquad\qquad (C.2) \\
\phi_y &= -\frac{\partial w}{\partial y} + k\frac{Q_y}{Gh}
\end{aligned}
$$

Implicit in the theory is the value $k = 6/5$ accounting for the variation in transverse shear strain across the section. Equations C.1 and C.2 together with the equilibrium relations, result in the governing differential Equation

$$D\nabla^4 w = q - \frac{h^2}{12}\left(\frac{2-\nu}{1-\nu}\right)\nabla^2 q \qquad (C.3)$$

This equation has been solved by Salerno and Goldberg (135), and these exact solutions were used for comparison purposes with the finite element method in reference (125)

In Equations C.1 the tenn $\frac{\nu k}{2Gh} q$ arises from consideration of the transverse normal stress σ_z. The effect of the stress is not accounted for in the finite element formulation of Barber et al or in the following, Accordingly, dropping this term, but retaining $k = 6/5$, results in the governing Equation

$$D\nabla^4 w = q - \frac{h^2}{10}\left(\frac{2}{1-\nu}\right)\nabla^2 q \qquad (C.4)$$

It may be noted that solutions to Equation C.4 can be obtained by minor modification of the Salerno and Goldberg solutions, and that these modified solutions should be used to assess the finite element method which discounts the effects of transverse normal stress.

In the finite element formulation to be described it is assumed that the contributions of bending and transverse shear to the plate deflection w, may be separated ; thus

$$w = w^b + w^s \tag{C.5}$$

Further we assume that that the rotations ϕ_x and ϕ_y can be obtained from the deflection resulting from bending only; thus,

$$\phi_x = -\frac{\partial w^b}{\partial x} \qquad \phi_y = -\frac{\partial w^b}{\partial y} \tag{C.6}$$

The resulting relations for the stress resultants become;

$$M_x = -D\left[\frac{\partial^2 w^b}{\partial x^2} + \nu\frac{\partial^2 w^b}{\partial y^2}\right]$$

$$M_Y = -D\left[\frac{\partial^2 w^b}{\partial y^2} + \nu\frac{\partial^2 w^b}{\partial x^2}\right]$$

$$M_{xy} = D\ (1-\nu)\ \frac{\partial^2 w^b}{\partial x \partial y}$$

$$Q_x = -\frac{Gh}{k}\ \frac{\partial w^s}{\partial x} \qquad (C.7)$$

$$Q_y = -\frac{Gh}{k}\ \frac{\partial w}{\partial y}$$

Thus the bending and twisting moments are these given by classical thin plate theory. The strain energy relations for the deformed plate are then,

$$U = \frac{1}{2} \iint\ [u_b]^T\ [D]\ [u_b]\ dx\,dy + \frac{1}{2} \iint [u_s]^T\ [G]\ [u_s]\ dx\ \ dy$$

(C.8)

where,

$$[u_b]^T = [\ w^b_{xx}\ \ w^b_{xx}\ \ w^b_{xy}\ ]$$

$$[D] = \begin{bmatrix} D & D\nu & 0 \\ D\nu & D & 0 \\ 0 & 0 & 2D(1-\nu) \end{bmatrix}$$

$$[u_s]^T = [\ w_x^s \ w_y^s \ ]$$

and

$$[G] = \begin{bmatrix} Gh/k & 0 \\ 0 & Gh/k \end{bmatrix} \qquad (C.9)$$

The effects of bending and transverse shear on the deflection are thus uncoupled and the contributions of each may be calculated separately.

Considering bending contributions first, for the rectangular element shown in Figure C.1 if we take as deflection function,

$$w^b = [\ 1 \ x \ y \ x^2 \ xy \ y^2 \ x^3 \ x^2y \ xy^2 \ y^3 \ x^3y \ xy^3\ ] \ [a] \qquad (C.10)$$

and as generalised co-ordinates the nodal deflection vector,

$$[\bar{w}_b]^T = [\ w_i^b \ w_{xi}^b \ w_{yi}^b\ ] \qquad i = 1,\ 2,\ 3,\ 4 \qquad (C.11)$$

there results the well known stiffness matrix for thin plate bending obtained and studied by many workers (123). Such elements may be assembled and solved in the usual way to yield the contribution of bending to the total plate displacement, and to give stress resultants according to thin plate theory,

In the same way we take for the transverse shear deflection,

$$w^s = [\, 1 \;\; x \;\; y \;\; x^2 \;\; xy \;\; y^2 \;\; x^3 \;\; x^2y \;\; xy^2 \;\; y^3 \;\; x^3y \;\; xy^3 \,]\,[b] \qquad (C.12)$$

together with the nodal deflection vector,

$$[\overline{w}_s]^T = [\; w_i^s \;\; w_{xi}^s \;\; w_{yi}^s \;] \qquad i = 1, 2, 3, 4 \qquad (C.13)$$

and by substitution in the energy relation for transverse shear, Equation C.8 , a (12 x 12) shear stiffness matrix Is obtained for the element, This matrix is given In Table C.l. These shear stiffness matrices may now be assembled and solved in the usual way to yield the contribution of transverse shear to the plate total deflection, and to give the stress resultants Q_x and Q_Y, Equation C.7 .

The boundary condition constraints to be enforced with the bending element contribution are those normally considered.

In the shear stiffness contribution the following will apply for the edge condition

For an edge x = constant,

Clamped and Simply supported

$$w^s = 0 \quad ; \quad w^s_x \neq 0 \quad \text{and} \quad w^s_y = 0 \tag{C.14}$$

and

Free

$$w^s \neq 0 \; ; \quad w^s_x = 0 \quad \text{and} \quad w^s_y = 0 \; .$$

Before examining the numerical application of this proposed method, two significant computational advantages will be noted, which result from separating the effects of bending and shear, First for a given finite element mesh two sets of simultaneous equations must be solved, corresponding to the assembled matrices obtained from the (12 x 12) bending and (12 x 12) shear element matrices. However these resulting sets of equations are of much lower order than that which must be stored and solved using the (20 x 20) finite element formulation of reference (125). For example, a 6 x 6 mesh used to solve a simplv supported quarter plate system will involve two (147 x 147) matrices by the method described here, compared with a single (245 x245) matrix using the method of reference (125) substantial advantages in computing time and storage are evident with the present method. Secondly, the deflection of the plate can be written, (135), as

$$w_{max} = [\, a + \beta\ (h/a)^2\ ]\ qa^4/Eh^3 \tag{C.15}$$

in which the coefficient a derives from classical thin plate theory, while β gives the additional deflection resulting from transverse shear. Thus for a given aspect ratio (b/a) of the plate, it is necessary to calculate α and β for one thickness only; the effect of transverse shear in a plate of identical aspect ratio, but differing (h/a) ratio is then readily obtained from Equation C.15.

C.3. NUMERICAL APPLICATIONS

To examine the accuracy and convergence of the method, the central deflection of a uniform thickness, uniformly loaded, simply- supported square plate has been calculated for various finite element meshes. Using symmetry the model comprised a quarter plate system having N elements per side, where N was varied from 1 to 6. The value k = 6/5 was used, and thus the Solution to Equation C.4 obtained by modifying those obtained in reference (135) have been used to compare with the finite element results. The calculatedvalues of the coefficients α and β, Equation C.15, are given in Tables C.2 and C.3 in Table C.2 a consistent load formulation has been used, while in Table C.3 lumping of the distributed load at the nodes has been used. Good agreement with the exact values is obtained. Convergence of the shear contribution with a consistent load formulation is extremely rapid, and indicates that the use of precision bending elements would be most profitable to increase the accuracy of the bending conribution. With lumped loading of the nodes, convergence of the shear contribution is much slower, but it is interesting to note that the bending contribution is indeed improved for this particular bending element.

In Table C.4 the deflection coefficient for a uniform simply supported square plate of various thicknesses is given, and compared with the results given in reference (125) exact values, obtained from Equation 3 in reference (135) this case a 6 x 6 finite element mesh has been used for the quarter plate system, and the value k = 1 suggested in reference employed. Again agreement between the various solutions is good, but it is worth noting once more the advantages in computing time and storage, and in the use of' Equation C.15 for different thickness when assessing the proposed method.

C.4 NOTATION

[a], [b]	- vectors of constants;
b, s	- subscripts and superscripts denoting bending and shear;
D	- flexural rigidity of the plate;
E	- modulus of elasticity of material;
G	- shear modulus of material;
h	- thickness of plate;
k	- constant denoting resistance of section to warping;
M_x, M_y, M_{xy}	- moment stress resultants;
Q_x, Q_y	- transverse shear stress resultants;
4	- transverse uniform distributed pressure;
U	- strain energy;
w	- total deflection of plate;
w^b	- deflection of plate due to bending;
w^s	- deflection of plate due to transverse shear;
$[w_b]$	- nodal displacements due to bending;
$[\bar{w}_s]$	- nodal displacements due to transverse shear;
x, y, z	- coordinates'of plate element; subscripts denoting partial differentials;
α, β	- deflection coefficients due to bending and transverse shear;.

$\bar{\gamma}_x$, $\bar{\gamma}_y$	- average transverse shear strains;
∇^2	$= \dfrac{\partial^2}{\partial x^2} + \dfrac{\partial^2}{\partial y^2}$;
ν	- Poisson's ratio;
σ_z	- normal stress in the z direction;
ϕ_y, ϕ_y	- total rotations of sections x = constant and y = constant.

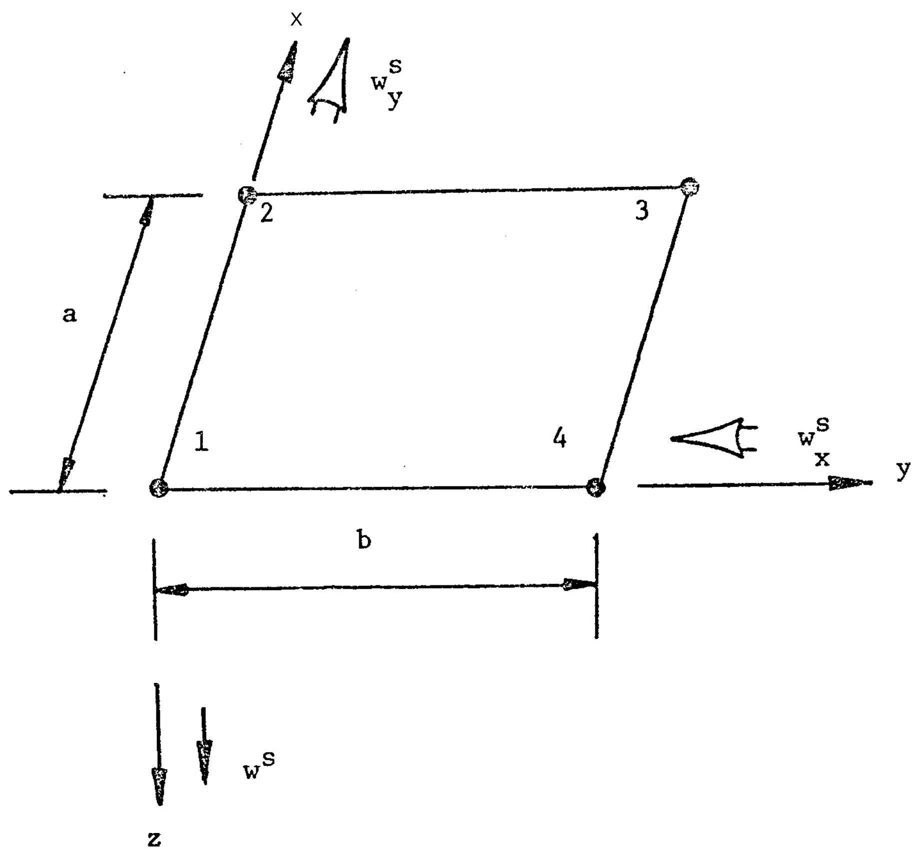

Figure C.1 Rectangular plate shear deformation element.

TABLE C.1

Shear stiffness matrix for a rectangular element.

$\frac{Gh}{1260k}\left(\frac{b}{a}\right)$

$P = (a/b)^2$

Symmetric

552(1+P)											
6(7+11P)	4(14+3P)										
6(11+7P)	0	4(3+14P)									
12(-46+17P)	3(-14+13P)	3(-22+7P)	552(1+P)								
3(14-13P)	-(14+9P)	0	-6(7+11P)	4(14+3P)							
3(-22+7P)	0	4(-3+7P)	6(11+7P)	0	4(3+14P)						
-204(1+P)	-3(7+13P)	-3(13+7P)	12(17-46P)	3(-7+22P)	3(13-14P)	552(1+P)					
3(7+13P)	-7+9P	0	3(-7+22P)	4(7-3P)	0	-6(7+11P)	4(14+3P)				
3(13+7P)	0	9-7P	3(-13+14P)	0	-(9+14P)	-6(11+7P)	0	4(3+14P)			
12(17-46P)	3(7-22P)	3(13-14P)	-204(1+P)	3(7+13P)	-3(13+7P)	12(-46+17P)	3(14-13P)	3(22-7P)	552(1+P)		
3(7-22P)	4(7-3P)	0	-3(7+13P)	-7+9P	0	3(-14+13P)	-(14+9P)	0	6(7+11P)	4(14+3P)	
3(-13+14P)	0	-(9+14P)	3(13+7P)	0	9-7P	3(22-7P)	0	4(-3+7P)	-6(11+7P)	0	4(3+14P)

TABLE C.2

Coefficients $w_{max}Eh^3/qa^4$ for central deflection of a uniformly loaded simply supported square plate. $\nu = 0.3$ $k = G/5$

N	Classical Theory	Reissner Theory Eqn. C.4	Finite Element (consistent load)			
	a	β	a	% error	β	% error
1	0.04437	0.2299	0.05529	24.6	0.2259	-1.7
2			0.04726	6.5	0.2300	0.0
3			0.04566	2.9	0.2299	0.0
4			0.04509	1.6	0.2299	0.0
5			0.04483	1.0	0.2299	0.0
6			0.04469	0.7	0.2299	0.0

TABLE C.2

Coefficients $w_{max}Eh^3/qa^4$ for central deflection of a uniformly loaded simply supported square plate. $\nu = 0.3$ $k = G/5$

N	Classical Theory	Reissner Theory Eqn. C.4	Finite Element (consistent load)			
	a	β	a	% error	β	% error
1	0.04437	0.2299	0.05529	24.6	0.2259	-1.7
2			0.04726	6.5	0.2300	0.0
3			0.04566	2.9	0.2299	0.0
4			0.04509	1.6	0.2299	0.0
5			0.04483	1.0	0.2299	0.0
6			0.04469	0.7	0.2299	0.0

TABLE C.3

Coefficients $w_{max}\ Eh^3/qa^4$ for central deflection of a uniformly loaded simply supported square plate. $\nu = 0.3$ $k = 6/5$

N	Classical Theory	Reissner Theory Eqn. C.4	Finite Element (Lumped load)			
	α	β	a	% error	β	% error
1	0.04437	0.2299	0.03763	-15.2	0.2226	-3.2
2			0.04302	- 3.0	0.2161.	-6.0
3			0.04378	- 1.3	0.2230	-3.0
4			0.04404	- 0.7	0.2259	-1.7
5			0.04416	- 0.5	0.2273	-1.1
6			0.04422	- 0.3	0.2281	-0.8

TABLE C.4

Coefficients $w_{max}\ Eh^3/qa^4$ for central deflection of a uniformly loaded simply supported square plate. $\nu = 0.3$ $k = 1.0$

h/a	Reissner Theory (135)	Finite Element		
		Pryor et al (125)	Present Method	
			Const. Load	Lumped Load
0.01	0.04439	0.04423	0.04471	0.04424
0.05	0.04486	0.04469	0.04517	0.04470
0.10	0.04632	0.04612	0.04660	0.04612
0.15	0.04876	0.04852	0.04900	0.04850
0.20	0.05217	0.05186	0.05235	0.05182
0.25	0.05656	0.05617	0.05666	0.05610

APPENDIX D

DETAILS OF COMPUTER PROGRAMS

D.1 INTRODUCTION

For numerical calculations several FORTRAN programs were written and most of the calculations in this investigation can be done with one of the programs described here. Several options, which facilitate the use of these programs either for the analysis of the entire rotor system or the component parts, are given. Furthermore these programs can be easily modified to meet particular requirements. Complete listings of the programs are given in section D.4. Brief description of the programs along with the definition of input and output variables are given below. Use of the various options are explained.

D.2 FORTRAN PROGRAM FOR THE ANALYSIS OF ROTORS OF SIMPLE GEOMETRY - PROGRAM-1

D.2.1 General Description

This program was written for the numerical calculations involved in the exact method of analysis of rotors, described in chapter 4, section 4.3. Hence the use of this program is restricted to rotors of simple geometry. In this program a systematiciterative search is made for the values of the natural frequency ω of the system which makes the value of the frequency determinant of the system to be zero. Ofcourse' specified amount of tolerance is allowed on this condition.

In principle the value of ω can be initiated with zero, as the starting value, and the iteration continued with some specified step size until a change of sign in the value of the determinant is noticed. Then the step size may be reduced and this procedure repeated until a very small step size is reached. But this procedure requires considerable amount of computer time if the initial step size is small. For that reason if the initial step size is increased, it is very likely that some of the natural frequency values are missed. This happens because of the complex behaviour of the value of the frequency determinant with the change of ω. As seen in Figure D.l, the value of the determinant some times jumps from $-\infty$ to $+\infty$ and again changes sign within a very small increment of ω. Since the elements of the determinant contain combinations of trigonametric, hyperbolic and Bessel functions it is impossible to foresee such jumps.

Because of the above reasons this program is made to utilize approximate frequency values of the rotor obtained from finite element analysis. Thus this program is mainly used for refining and assessing the accuracy and convergence of the finite element results.

The following procedure is followed. First, a range is specified within which the exact frequency is expected to lie. Then the approximate frequency corresponding to a particular mode of vibration is read in. The iterations are performed with a small step size, within the range. When a change of sign of the value of the frequency determinant is noticed, it is checked whether there was a jump from either side of infinities. If this did not happen, then the step size is cut down and the iterations continued until the allowable step size is reached. If a jump had taken place then the iterations are simply continued until change of sign is again noticed. This procedure is repeated for other modes.

A flow diagram of the program is given in Figure D.2, which shows how the input data is provided and how the iterations are performed. The notation used in this flow diagram are explained below in section D.2.2 along with the variables used in the program.

D.2.2 Input and Output Variables

Brief descriptions of the input and output variables used in PROGRAM-1 are given below in their order of appearance in the program. Corresponding symbols used in the flow diagrams are given immediately following these variables where applicable.

Input and related variables.

ALL		- allowable error in the value of Bessel functions given as a factor.
FAC(N)		- N! (factorial N).
FI(N)		- function $Q(N) = 1 + \frac{1}{2} + \frac{1}{3} + \ldots + \frac{1}{N}$
SM	S	- initial step size.
ALØW	α	- factor used to get the final allowable step size where the iteration is stopped.
XXX	x	- factor used to multiply the approximate frequency to get starting value.
YYY	y	- factor used to multiply the approximate frequency to get the final value beyond which iterations are not carried out.
NDS	m_s	- starting value of nodal diameters.
ND	m_e	- final value of nodal diameters.
NC	n_r	- required number of frequencies in each nodal diameter case.
IRNG	i_R	- rim option.
ED	E_d	- Youngs modulus of disc material.
EB	E_b	- Youngs modulus of blade material.

RØD	ρ_d	– mass density of disc material.
RØB	ρ_b	– mass density of blade material.
PRD	ν_d	– Poisson's ratio of disc material.
PRB	ν_b	– Poisson's ratio of blade material.
RDI	a	– inner radius of disc.
RDØ	b	– outer radius of disc.
TD	h	– thickness of disc.
BB	b_b	– width of blade.
BD	d_b	– depth of blade
BL	ℓ	– length of blade.
BANG	δ	– blade stagger angle.
Z	Z	– number of blades in the rotor,
ER	E_r	– Youngs modulus of rim material.
RØR	ρ_r	– mass density of the rim material.
PRR	ν_r	– Poisson's ratio of the rim material.
RR	R_0	– the rim centroidal radius.
RJ	K_G	– St. Venant torsional stiffness of the rim section.
RIZ	I_{zz}	– moment of inertia of the rim section about Oz axis.
RLX	I_{xx}	– moment of inertia of the rim section about Ox axis.
E1	e_1	– distance between the inner boundary and the centroid of the rim,
E2	e_2	– distance between the centroid and the outer boundary of the rim.
RA	A_r	– area of cross-section of the rim.
AFR(,)	ω_a	– approximate frequencies of the rotor.

Output variables

M	m	- number of nodal diameters.
N	n	- mode number.
FF	ω_t	- trial value of the frequency.
NIT	i	- number of iterations.
AFR(,)	ω_r	- refined frequencies.

D.2.3 Subroutines Used In PROGRAM-1

The subroutines and functions used in PROGRAM-1 are given below.

(1) Main program.

MAIN-1

(2) Subroutines used to obtain disc dynamic stiffness matrix.

EXTDSK

DETERM

(3) Functions used for the computation of the values of Bessel functions.

XJN

XIN

XYN

XKN

FACT

PHI

D.3 FORTRAN PROGRAMS FOR THE ANALYSIS OF ROTORS OF GENERAL GEOMETRY - PROGRAM-2 and PROGRAM-3

D.3.1 General Description

For the stress and vibration analysis of rotors of general geometry two programs, PROGRAM-2 and PROGRAM-3, were written. Roth of these are based on the finite element method of analysis of the rotor described in chapter 4. The effects of transverse shear and rotary inertia are not considered in PROGRAM-Z, whereas these effects are considered in PROGRAM-3. Also in the latter the rim of the rotor, if present, is considered to be a part of the disc.

In both these programs all the necessary input statements are included so that input data closely describing rotors of general geometry can be fed in. The materials of the disc, rim and blades may be of different materials. The programs are featured with several options which allow the user to either consider the entire rotor or the parts. Also the effect of rotation and temperature gradient can be included when they are thought necessary.

The meaning and use of the various options available in these programs are given below. The symbols used here are the same used in the programs. A flow diagram is given in

Figure D.3, showing how the input data are provided and the symbols used in this diagram are explained along with those used in the programs in section D.3.3.

D.3.2 Options Available In PROGRAM-2 AND PROGRAM-3

(1) IØPT - General option.

value	description
1	Vibration of the disc alone is considered.
2	Vibration of the blade alone is considered.
3	Vibration of the bladed disc is considered.
4	Stress analysis of the disc alone is considered.

(2) IRNG - Rim option

value	description
0	No rim present.
1	A rim is present.

(3) ITED - Disc thermal gradient option

value	description
0	No temperature gradient present.
1	Temperature gradient present.

(4) ISTB - Blade initial stress option.

value	description
0	Blade has no initial stresses.
1	Blade has initial stresses.

(5) IEDE - Blade general option.

value	description
1	Vibration of a single blade in the principal directions and in torsion are considered seperately.
2	The coupled bending-bending vibration of a pretwisted blade is considered.
3	The vibration of a single or group of blades with or without initial stresses is considered.

D.3.3 Input and Output Variables

Brief descriptions of the input and output variables used in PROGRAM-2 and PROGRAM-3 are given below, in the order of their appearance in the programs. Corresponding symbols used in the flow diagrams are given immediately following these variables where applicable.

Variables used in PROGRAM-2 and PROGRAM-3

IØPT	i	- general option.
IRNG	i_R	- rim option.
NF	n	- number of frequencies to be calculated for each diametral node configuration.
ØMGA	Ω	- speed of rotation in rad./sec.

ND	m_e	- final value of nodal diameters.
MDS	m_s	- starting value of nodal diameters.
NDE	N_d	- number of disc elements.
ITED	i_T^d	- temperature option of the disc
ED	E_d	- Young's modulus of the disc material.
RØD	ρ_d	- mass density of the disc material.
PRD	ν_d	- Poisson's ratio of the disc material.
ALD	α_d	- coefficient of thermal expansion of the disc material.
SRI	σ_a	- radial stress at the inner boundary of the disc.
SRØ	σ_b	- radial stress at the outer boundary of the disc.
NTD		- number of degrees of freedom in the disc.
R(I)	r(i)	- the radii at the inner and outer boundaries of all the disc elements' taken in increasing order.
T(I)	h(i)	- the thicknesses at the inner and outer boundaries of all the disc elements taken in increasing order.
TE(I)	T(i)	- values of temperature at the inner and outer boundaries of all the disc elements taken in increasing order.
NBE	N_b	- number of blade elements.
NB	Z	- number of blades present.
ISTB	i_s^b	- blade initial stress option.
IBDE	i_b	- blade general option.
NSB		- number of stations in the blade.

NTB		number of degrees of freedom in the blade.
EB	E_b	- Young's modulus of blade material.
RØB	ρ_b	- mass density of blade material.
PRB	ν_b	- Poisson's ratio of blade material.
BX(I)	x(i)	- distancees of stations in the blade from the root.
BB(I)	$I_1(i)$	- I_{min} of the blade at the stations considered.
BD(I)	$I_2(i)$	- I_{max} of the blade at the stations considered.
ARA(I)	A(i)	- area of cross-section of blade at the stations.
BKG(I)	$K_G(i)$	- St. Venant's torsional stiffness of the blade section at the stations.
ANG(I)	$\delta(i)$	- pretwist angles at the stations.
SIG(I)	$\sigma(i)$	- initial stresses in the blade at the stations.
ER	E_r	- Young's modulus of rim material.
RØR	ρ_r	- mass density of rim material.
PRR	ν_r	- Poisson's ratio of rim material..
ALR	α_r	- coefficient of thermal expansion of rim material.
RRI	R_i	- inner radius of rim.
RRØ	R_o	- outer radius of rim.
RTI	t_i	- thickness of rim at inner radius.
RTØ	t_o	- thickness of rim at outer radius.
RTEI	T_i	- temperature at inner radius of rim.
RTEØ	T_o	- temperature at outer radius of rim.

Additional variables used in PROGRAM-2 alone.

E1	e_1	- distance from inner boundary to centroid of rim.
E2	e_2	- distance from centroid to outer boundary of rim.

RIZ	I_z	- moment of inertia about Oz axis of rim section.
RIX	I_x	- moment of inertia about Ox axis of rim section.
RJ	K_G	- St. Venant's torsional stiffness of rim section.

Additional variables used in PROGRAM-3 alone.

SCD	k_d	$= 1/\kappa^2$, where κ^2 is shear constant of disc.
SCR	k_r	$= 1/\kappa^2$, where κ^2 is shear constant of rim.
SCB	k_b	$= 1/k$, where k is shear constant of blade.

D.3.4 Subroutines used in PROGRAM-Z and PROGRAM-3.

The subroutines used in PROGRAM-2 and PROGRAM-3 are divided in to the following sections.

(1) Main programs.

(2) Subroutine calculating the blade subsystem matrices.

(3) Subroutine calculating the disc subsystem matrices.

(4) Subroutine assembling the subsystem matrices in to the system matrices.

(5) Subroutine calculating the stresses in the disc.

(6) Subroutines used to solve the eigenvalue problem.

(7) General purpose subroutines.

Sections (1) to (4) are different for the two programs, whereas sections (5) to (7) are the same for both the programs. The subroutines used in these sections are given below.

<table>
<tr><th>Section</th><th>PROGRAM-1</th><th>PROGRAM-2</th></tr>
<tr><td>1</td><td>MAIN2</td><td>MAIN3</td></tr>
<tr><td>2</td><td>BLADE</td><td>THKBDE</td></tr>
<tr><td>3</td><td>DISC</td><td>THKDSC</td></tr>
<tr><td>4</td><td>SYSTEM</td><td>THKSYS</td></tr>
<tr><td>5</td><td colspan="2">INLSTR</td></tr>
<tr><td>6</td><td colspan="2">EIGVAL
MAX
QUICK
INVT
ASMBLE
SYSLOD
REDUCE
TRIMUL
MATMUL</td></tr>
</table>

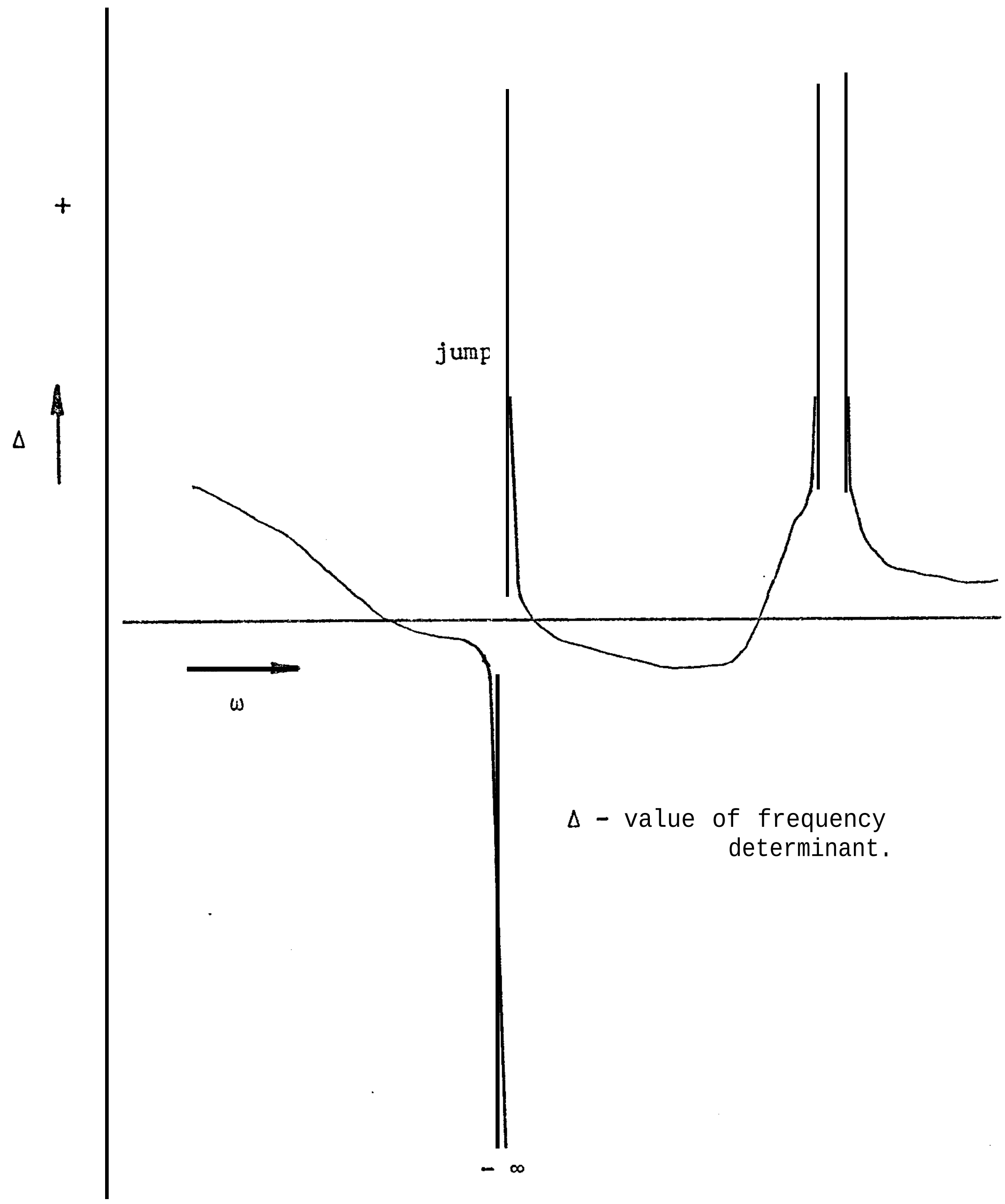

Figure D.l Variation of the value of the frequency determinant with increasing values of trial values of ω

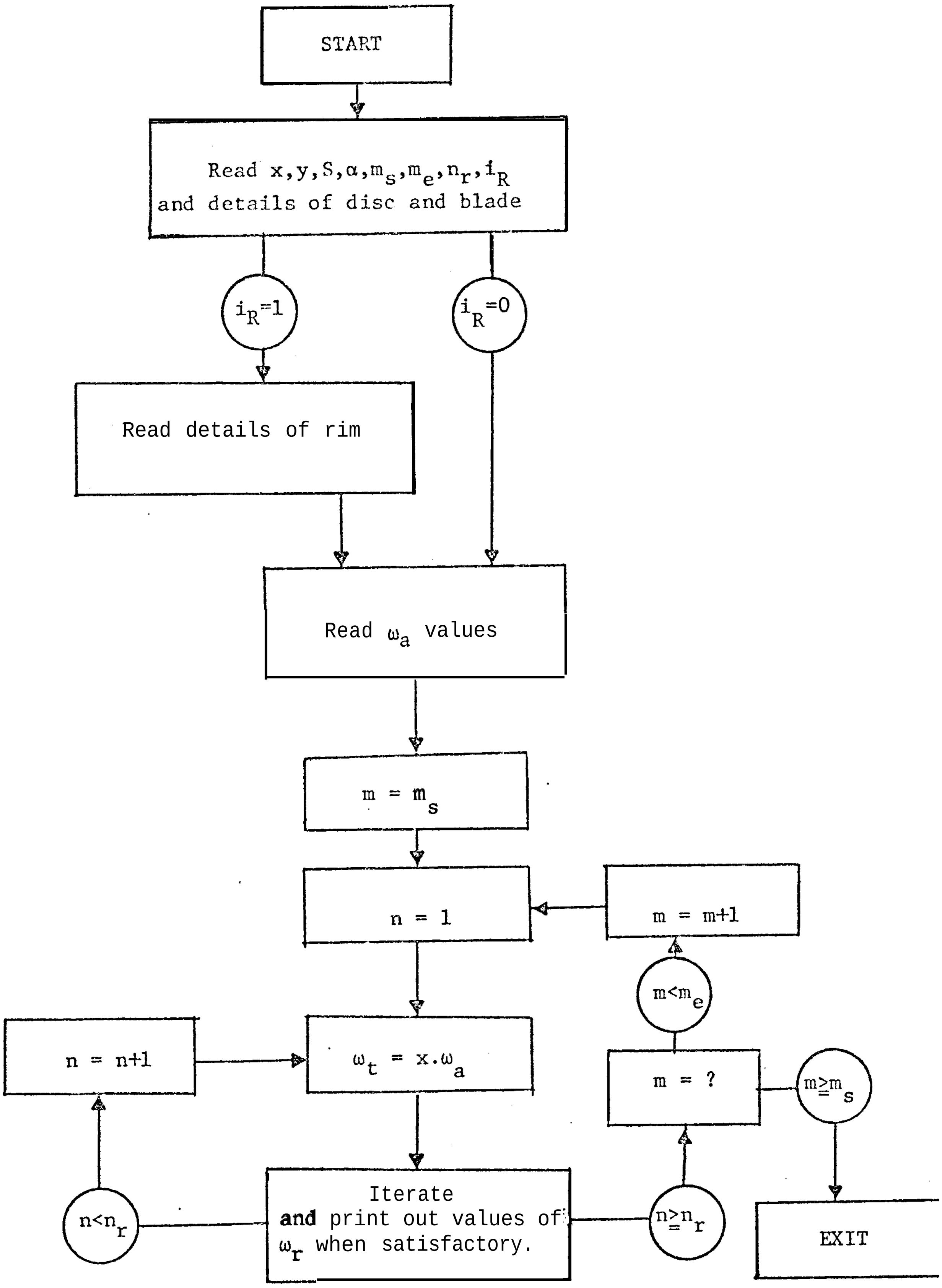

Figure D.2 Flow diagram for PROGRAM-1.

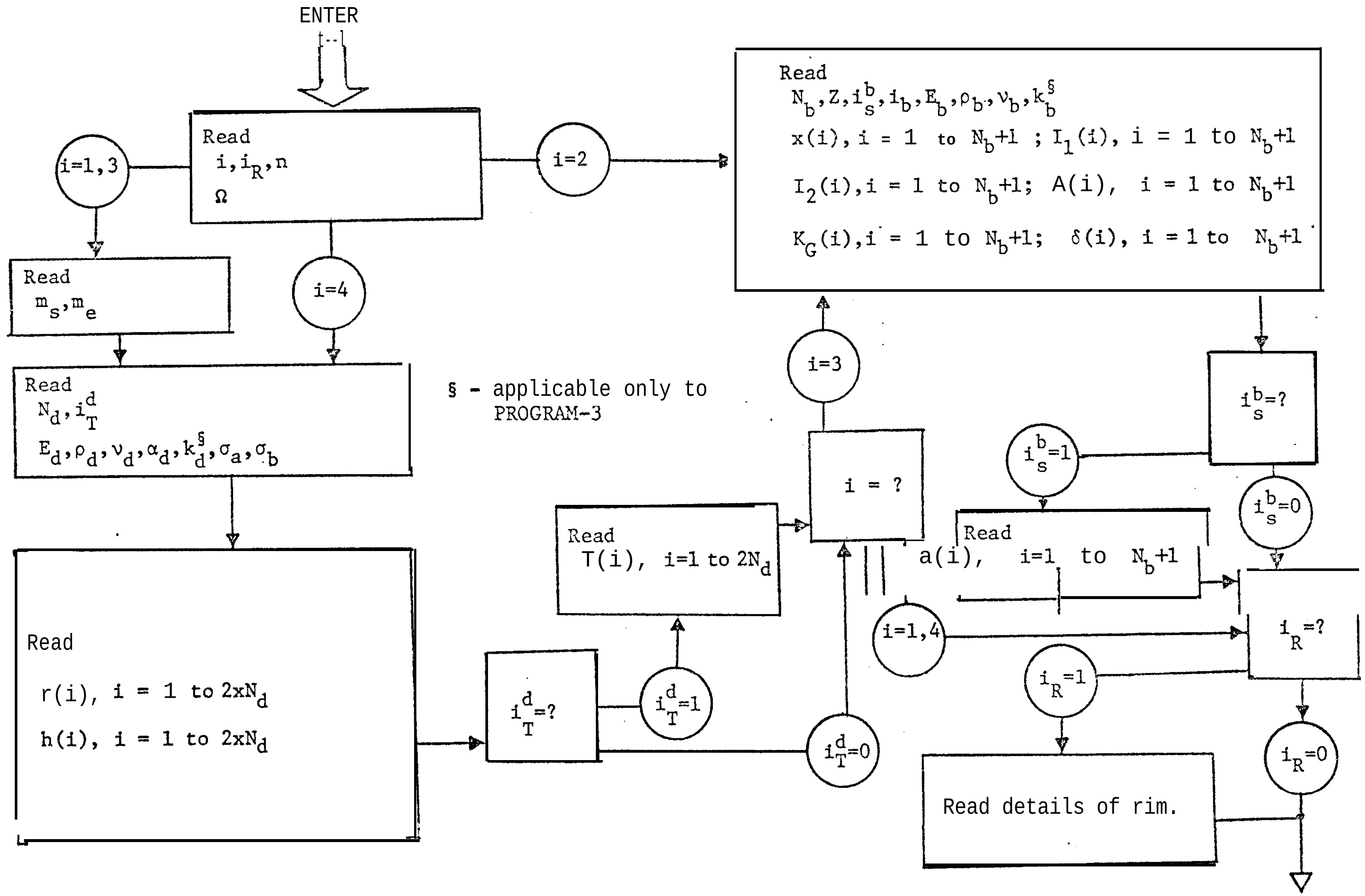

Figure D.3 Flow diagram for PROGRAM-2 and PROGRAM-3, showing how the input data is provided.

D.4 PROGRAM LISTING

D.4.1 Subroutines used in PROGRAM-1

```
C     ************************************************
C     *                                              *
C     *  MAIN-1 -- MAIN PRØGRAM ØF PRØGRAM-1         *
C     *                                              *
C     ************************************************
C     *  THIS PRØGRAM REFINES THE APPRØXIMATE FREQUENCIES *
C     *  ØF A BLADED RØTØR USING THE 'EXACT METHØD'  *
C     *  THE DIMENSIØNS ØF ALL THE ARRAYS ARE FIXED AND NØ *
C     *  CHANGES ARE NECESSARY AT ANY TIME           *
C     ************************************************
      DIMENSIØN S(2,2),C(2,2)
      DIMENSIØN AFR(0/10,10)
      CØMMØN PI,PRD,ED,TD,AK,BK,RDI,RDØ,CDL,FCC
      CØMMØN/ØNE/FAC(0/60),FI (0/60),ALL
      ALL=0.1E-10
C     ************************************************
C     *  CALCULATE AND STØRE THE VALUES ØF FACTØRIALS AND *
C     *  THE PHI FUNCTIØN FØR VALUES ØF N FRØM 0 TØ 55 *
C     ************************************************
      DØ 18 I=0,55
      FAC(I)=FACT(I)
   18 FI(I)=PHI(I)
   16 CØNTINUE
      PRINT 7
      NØP=0
C     ************************************************
C     *  READ IN VALUES ØF INITIAL STEP SIZE AND FACTØRS *
C     *  FØR FINAL STEP SIZE AND RANGE               *
C     ************************************************
      READ 10,SM,ALØW,XXX,YYY
      PRINT10,SM,ALØW,XXX,YYY
C     ************************************************
C     *  READ INITIAL AND FINAL NUMBERS ØF NØDAL DIAMETERS *
C     *  TO BE CØNSIDERED, THE NUMBER ØF FREQUENCIES TØ BE *
C     *  CALCULATED AND RING ØPTIØN                  *
C     ************************************************
      READ 11,NDS,ND,NC,IRNG
      PRINT11,NDS,ND,NC,IRNG
```

```
C     ****************************************************
C     *  READ IN VALUES ØF THE DISC AND BLADE ELASTIC     *
C     *  CØNSTANTS AND DIMENSIØNS                         *
C     ****************************************************
      READ 12,ED,EB
      PRINT12,ED,EB
      READ 12,RØD,RØB
      PRINT12,RØD,RØB
      READ 10,PRD,PRB
      PRINT10,PRD,PRB
      READ 10,RDI,RDØ,TD
      PRINT10,RDI,RDØ,TD
      READ 10,BB,BD,BL,BANG,Z
      PRINT10,BB,BD,BL,BANG,Z
      RRR=RDØ
      E1=0.0
      E2=0.0
      IF(IRNG.EQ.0)GØ TØ 19
C     ****************************************************
C     *  IF RIM IS PRESENT, READ IN THE VALUES OF THE RIM *
C     *  ELASTIC CØNSTANTS AND DIMENSIØNS                 *
C     ****************************************************
      READ 12,ER,RØR,PRR
      PRINT12,ER,RØR,PRR
      READ 10,RR,RJ,RIZ,RIX,E1,E2,RA
      PRINT10,RR,RJ,RIZ,RIX,E1,E2,RA
      RRR=RR+E2
      A1 =1.0/RR
      A2=A1 *ill
      A3=A1 *A2
      A4=A1*A3
      A5=A1 *A4
      GR=0.5*ER/(1.0+PRR)
   19 CØNTINUE
C     ****************************************************
C     *  READ IN THE VALUES ØF THE APPPRØXIMATE FREQUENCY *
C     *  VALUES FØR THE SPECIFIED VALUES ØF NØDAL DIAMETER*
C     ****************************************************
      READ 6,((AFR(I,J),J=1,NC),I=NDS,ND)
      PRINT6,((AFR(I,J),J=1,NC),I=NDS,ND)
      x2 = 1.0/RRR/RRR
      PI=3.141592653589793
      CCC=2.0*PI
      BIX=BD*BB*BB*BB/12.0
      BIY=BB*BD*BD*BD/12.0
      BJ=BB*BB*BB*BD*(1./3.-.21*BB/BD*(1.-BB/BD*BB/BD*BB/BD*BB/BD/12.0)
      CD=SQRT(SQRT(12.0*RØD*(1.0-PRD*PRD)/ED/TD/TD))
      CX=SQRT(SQRT( 12.0*RØB/EB/BB/BB))
      CY=SQRT(SQRT(12.0*RØB/EB/BD/BD))
      CT=SQRT(2.0*RØB*(1.0+PRB)/EB)
      BA=BANG*PI/180.0
      SNA= SIN(BA)
```

```
      CSA= CØS(BA)
      RSNA=E2*SNA
      RCSA=E2*CSA
      SAS =SNA*SNA
      CAS=CSA*CSA
      SRS =RSNA*RSNA
      CRS=RCSA*RCSA
      PQ=0.5/(1.0+PRB)
      PRINT 3
      M=NDS-1
   20 CØNTINUE
C     ***************************************************
C     *  SELECT THE NUMBER ØF NØDAL DIAMETERS           *
C     ***************************************************
      M=M+1
      IF(M.GT.ND) GØ TØ 90
      PRINT 1
      AN=M
      AN2 =AN*AN
      AN4=AN2*AN2
      PRINT 5
      FF=0.0
      FCC=0.5
      IF(M.EQ.0) FCC=1.0
      IF(IRNG.NE.0) CR=2.0*PI*FCC*RR
      N=0
   30 CØNTINUE
      NIT=0
      AM=SM
C     ***************************************************
C     *  SELECT THE NUMBER ØF NØDAL CIRCLES             *
C     ***************************************************
      N=N+1
      XN=N
      IF(N.GT.NC) GØ TØ 20
C     ***************************************************
C     *  SET LØWER AND UPPER LIMITS FØR ITERATIØN       *
C     ***************************************************
      FF=XXX*AFR(M,N)
      ZZZ=YYY*AFR(M,N)
   25 CØNTINUE
C     ***************************************************
C     *  SPCIFY STE? SIZE                               *
C     ***************************************************
      STEP=AM
      GO TØ 37
   33 CØNTINUE
      FF=XXX*AFR(M,N)
      AM=AM*0.5
      STEP=AM
      IF(STEP.LT.0.05) GC TØ 30
   37 CØNTINUE
```

```
C       *********************************************************
C       *  SPECIFY THE ALLØWABLE  STEP  SIZE  TØ END ITERATIØN *
C       *********************************************************
        ALLØW=ALØW*XN
        KK= 1
        KKK= 1
   40   CØNTINUE
        FF=FF+STEP
   52   CØNTINUE
C       *********************************************************
C       *  START  ITERATING                                     *
C       *********************************************************
        NIT=NIT+1
        IF(NIT.GT.500)GØTØ  30
        NØP=NØP+1
        XY=FF
        IF(FF.GT.ZZZ) GØ TØ  33
        FR=FF*CCC
        SFR=      SQRT(FR)
        CDL=CD*SFR
        AK=CDL*RDI
        BK=CDL*RDØ
C       *********************************************************
C       *  CØMPUTE THE DYNAMIC  STIFFNESS  CØEFFICIENTS FØR     *
C       *  THE DISC                                             *
C       *********************************************************
        CALL  EXTDSK(C,M)
C       *********************************************************
C       *  CØMPUTE THE DYNAMIC  STIFFNESS  CØEFFICIENTS FØR    *
C       *  ARRAY ØF BLADES                                     *
C       *********************************************************
        CXL=CX*SFR
        CYL=CY*SFR
        CTL=CT*FR
        CXR=CXL*BL
        CYR=CYL*BL
        CTR=CTL*BL
        SNX= SIN(CXR)
        SNY= SIN(CYR)
        CSX=  CØS(CXR)
        CSY= CØS(CYR)
        SNT= SIN(CTR)
        CST= CØS(CTR)
        SHX=S INH(CXR )
        SHY=S INH(CYR)
        CHX=CØSH(CXR )
        CHY=CØSH(CYR)
        DX=EB*Z*FCC*BIX/(CSX*CHX+1.0)
        DY=EB*Z*FCC*BIY/(CSY*CHY+1.0)
        PX=-DX*CXL*CXL*CXL*(CSX*SHX+SNX*CHX)
        PY=-DY*CYL*CYL*CYL*(CSY*SHY+SNY*CHY)
        RX=DX*CXL*CXL*SNX*SHX
        RY=DY*CYL*CYL*SNY*SHY
        TX=DX*CXL*(CSX*SHX-SNX*CHX)
```

```
      TY=DY*CYL*(CSY*SHY-SNY*CHY)
      AT=-PQ*BJ*CTL*SNT/CST*Z*FCC*EB
      RMA=0.0
      RMB=0.0
      RMC=0.0
      IF(IRNG.EQ.0) GO TØ 45
C     ****************************************************
C     *  IF A RIM IS PRESENT CØMPUTE THE DYNAMIC STIFFNESS *
C     *  CØEFFICIENTS FØR THE RIM                          *
C     ****************************************************
      RMA=CR*(ER*RIZ+GR*RJ/AN2)*AN4*A4-CR*FR*FR*RØR*(RA
     .+RIZ*AN2*A2)
      RMB=CR*(ER*RIZ+GR*RJ)*AN2*A3
      RMC=CR*(ER*RIZ+AN2*GR*RJ)*A2-CR*FR*FR*RØR*(RIX+RIZ)
   45 CØNTINUE
      DO 50 I=1,2
      DØ 50 J=1,2
   50 S(I,J)=0.0
C     ****************************************************
C     *  CØMBINE THE SUBSYSTEM MATRICES TO GET THE SYSTEM *
C     *  DYNAMIC STIFFNESS MATRIX                          *
C     ****************************************************
      AZ=SAS*PX+CAS*PY+AN2*X2*AT+RMA
      BZ=-E2*SAS*PX-E2*CAS*PY+SAS*RX+CAS*RY+RMB-AN2*X2*AT*E2
      CZ=SRS*PX+CRS*PY+SAS*TX+CAS*TY-2.0*E2*SAS*RX
     .-2.0*E2*CAS*RY+RMC+AN2*X2*AT*E2*E2
      S(1,1)=C(1,1)+AZ
      S(1,2)=C(1,2)-E1*AZ+BZ
      S(2,2)=C(2,2)+E1*E1*AZ-2.0*E1*BZ+CZ
C     ****************************************************
C     *  CALCULATE THE VALUE ØF THE FREQUENCY DETERMINANT *
C     ****************************************************
      DET=S(1,1)*S(2,2)-S(1,2)*S(1,2)
      IF(KK.EQ.1) GØ TO 75
C     ****************************************************
C     *  CHECK IF VALUE ØF DETERMINANT CHANGES SIGN        *
C     ****************************************************
      AAA=ABS(PV)+ABS(DET)
      BBB=ABS(PV+DET)
      IF(AAA.NE.BBB) KKK=2
      DIF=ABS(PV)+ABS(DET)
   75 PV=DET
      KK=2
      IF(KKK.EQ.1) GØ TØ 40
      IF(STEP.LT.AM) GØ TØ 80
      FF=FF-STEP
      DIFA=DIF
      STEP=ALLØW
      KK=1
      KKK=1
      GØ TØ 52
   80 DIFB=DIF
```

```
C      ***************************************************
C      *  CHECK IF VALUE ØF DETEMINANT JUMPS FRØM ØNE  E N D  TØ*
C      *  THE ØTHER ENDØF  INFINITY                           *
C      ***************************************************
       IF(DIFA.LT.DIFB) GØ  T O   2 5
       AFR(M,N) =FF
C      ***************************************************
C      *  PRINT ØUT THE RESULTS  WHEN SAT ISFACTARY           *
C      ***************************************************
       PRINT 15,M,N,FF,NIT
       GØ TØ  3 0
   9  0   CØNT INUE
C      ***************************************************
C      *  PRINT  EUT SUMMARYØF  ALL  THE  RESULTS             *
C      ***************************************************
       DØ  9 5  IJK=1,5
       PRINT  3
       PRINT10,RDI,RDØ,TD
       IF(IRNG.NE.0) PRINT10,RR,RA,E1,E2
       PRINT10,BB,BD,BL,BANG,BN
   95  PRINT  2,((AFR(I,J),J=1,NC),I=NDS,ND)
       GØ TØ   16
  103  CALL  EXIT
    1  FØRMAT (///// )
    2  FØRMAT(/6F12.4)
    3 FØRMAT(1H1,5X,' EXACT  SØLUTIØN--FREQUNCIES  IN CPS.'//)
    5  FØRMAT(3X,46HNØDAL  D I A    MØDE NO    FREQUENC IES    ITERATIØNS)
    6  FØRMAT(6F10.4)
    7 FØRMAT(1H1,5X,'VIBRATIØNØF  BLADED  DISC  --  EXACT SØLUTIØN'
      .//5X,'INPUT DATA' //)
   10  FØRMAT(8F10.3)
   11  FØRMAT(16I5)
   12  FØRMAT(4F20.9)
   15  FØRMAT(/2(6X,I3),3X,F13.4,I10)
       END
```

```
      SUBRØUTINE DETERM(AA,N,D)
C     ****************************************************
C     *  THIS SUBRØUTINE EVALUATES THE VALUE D ØF THE     *
C     *  DETERMINANTØF ARRAY AA (N,N).                     *
C     *  BEFORE ENTERING THE SUBRØUTINE DEFINE ALL THE    *
C     *  ELEMENTS ØF ARRAY AA                             *
C     ****************************************************
      DIMENSIØN AA(4,4),A(4,4)
      DØ 200 I=1,N
      DØ 200 J=1,N
  200 A(I,J)=AA(I,J)
      D=1.
      K=1
    1 CØNTINUE
      KK=K+ 1
      IS=K
      IT=K
      B= ABS(A(K,K))
      DØ 2 I=K,N
      DØ 2 J=K,N
      IF( ABS(A(I,J))-B)2,2,21
   21 IS=I
      IT=J
      B= ABS(A(I,J))
    2 CØNT INUE
      IF(IS-K)3,3,31
   31 DO 32 J=K,N
      C=A(IS,J)
      A(IS,J)=A(K,J)
   32 A(K,J)=-C
    3 CØNTINUE
      IF( IT-K)4,4,41
   41 DØ 42 I=K,N
      C=A(I,IT)
      A(I,IT)=A(I,K)
   42 A(I,K)=-C
    4 CØNT I NUE
      D=A(K,K)*D
      IF(A(K,K))5,71,5
    5 CØNT INUE
      DO 6 J=KK,N
      A(K,J)=A(K, J)/A(K,K)
      DØ 6 I=KK,N
      W =A(I,K)*A(K,J)
      A(I,J)=A(I,J)-W
    6 CØNTINUE
      K=KK
      IF(K-N)1,70,1
   70 D=A(N,N)*D
   71 RETURN
      END
```

```
      SUBRØUTINE EXTDSK(C,M)
C     ****************************************************
C     *  THIS SUBRØUTINE CALCULATES THE EXACT STIFFNESS   *
C     *  MATRIX C(2,2) ØF AN UNIFØRM DISC, CLAMPED AT THE *
C     *  INNER BØUNDARY AND FREE AT THE ØUTER BOUNDARY    *
C     ****************************************************
      DIMENSION A(4,4),C(2,2)
      CØMMØN PI,PR,ED,TD,AK,BK,RDI,RDØ,CDL,FCC
      L=M+1
      D=TD*TD*TD/12.0/(1.0-PR*PR)*ED
      A2=CDL*CDL
      A3 =A2*CDL
C     ****************************************************
C     *  CALCULATE AND STØRE ALL THE BESSEL FUNCTIØNS TØ  *
C     *  BE USED LATER                                    *
C     ****************************************************
      AJM=XJN(M,AK)
      BJM=XJN(M,BK)
      AJL=XJN(L,AK)
      BJL=XJN(L,BK)
      AYM=XYN(M,AK,AJM)
      BYM=XYN(M,BK,BJM)
      AYL=XYN(L,AK,AJL)
      BYL=XYN(L,BK,BJL)
     AIM=XIN(M,AK)
      BIM=XIN(M,BK)
      AIL=XIN(L,AK)
      BIL=XIN(L,BK)
      AKM=XKN(M,AK,AIM)
      BKM=XKN(M,BK,BIM)
      AKL=XKN(L,AK,AIL)
      BKL=XKN(L,BK,BIL)
      AM=M
      AM2 =AM*AM
      RI2=RDI*RDI
      RI3=RI2*RDI
      RØ2=RDØ*RDØ
      RØ3=RØ2*RDØ
      AX=AM/RDI
      BX=AM/RDØ
      BY=AM*(AM-1.)*(1.-PR)/RØ2-A2
      BZ=AM*(AM-1.)*(1.-PR)/RØ2+A2
      AA=CDL*(1.-PR)/RDI
      BB=CDL*(1.-PR)/RDØ
      AN1 =AX*AJM-CDL*AJL
      AN2=AX*AYM-CDL*AYL
      AN3=AX*AIM+CDL*AIL
      AN4=AX*AKM-CDL*AKL
      BN1=BX*BJM-CDL*BJL
      BN2=BX*BYM-CDL*BYL
      BN3=BX*BIM+CDL*BIL
      BN4=BX*BKM-CDL*BKL
      BN5=BY*BJM+BB*BJL
      BN6=BY*BYM+BB*BYL
      BN7=BZ*BIM-BB*BIL
```

```
      BN8=BZ*BKM+BB*BKL
      BP=(-AM*A2*RO2+(1.-PR)*(1.-AM)*AM2)/RØ3
      BQ=( AM*A2*RO2+(1.-PR)*(1.-AM)*AM2)/RØ3
      BR= (A3 *ii03 +CDL*RDØ*(1.-PR)*AM2)/RØ3
      BS=(A3*RØ3-CDL*RDØ*(1.-PR)*AM2)/RØ3
      BN23=BP*BJM+BR*BJL
      BN24=BP*BYM+BR*BYL
      BN25=BQ*BIM+BS*BIL
      BN26=BQ*BKM-BS *BKL
c     ******************************************************
C     *  CALCULATE ANDSTØRE THE VALUES ØF THE DETERMINANTS*
C     *  APPEARING IN THE DYNAMIC STXFFIJESS MATRIX OF DISC *
C     ******************************************************
      A(1,1)=AJM
      A(1,2)=AYM
      A(1,3)=AIM
      A(1,4)=AKM
      A(2,1)=AN1
      A(2,2)=AN2
      A(2,3)=AN3
      A(2,4)=AN4
      A(3,1)=BJM
      A(3,2)=BYM
      A(3,3)=BIM
      A(3,4)=BKM
      A(4,1)=BN1
      A(4,2)=BN2
      A(4,3)=BN3
      A(4,4)=BN4
      CALL DETERM(A,4,DM)
      A(1,1)=AYM
      A(1,2)=AIM
      A(1,3)=AKM
      A(2,1)=AN2
      A(2,2)=AN3
      A(2,3)=AN4
      A(3,1)=BYM
      A(3,2)=BIM
      A(3,3)=BKM
      CALL DETERM(A,3,DMPA)
      A(1,1)=AJM
      A(2,1)=AN1
      A(3,1  )=BJM
      CALL DETERM(A, 3, DMPB)
      A(1,2)=AYM
      A(2,2)=AN2
      A(3,2)=BYM
      CALL DETERM(A,3,DMPC)
      A(1,3)=AIM
      A(2,3)=AN3
      A(3,3   )=BIM
      CALL DETERM(A,3,DMPD)
```

```
      A(1,1)=AYM
      A(1,2)=AIM
      A(1,3)=AKM
      A(2,1)=AN2
      A(2,2)=AN3
      A(2,3)=AN4
      A(3,1)=BN2
      A(3,2)=BN3
      A(3,3)=BN4
      CALL DETERM(A,3,DMSA)
      A(1,1)=AJM
      A(2,1)=AN1
      A(3,1)=BN1
      CALL DETERM(A,3,DMSB)
      A(1,2)=AYM
      A(2,2)=AN2
      A(3,2)=BN2
      CALL DETERM(A,3,DMSC)
      A(1,3)=AIM
      A(2,3)=AN3
      A(3,3)=BN3
      CALL DETERM(A,3,DMSD)
C     ********************************************************
C     *  CALCULATE THE VALUES ØF THE ELEMENTS ØFTHE DISC *
C     *  DYNAMIC STIFFNESS MATRIX                            *
C     ********************************************************
      CØNST=-D/DM*PI*RDØ*2.0*FCC
      C(1,1)=CØNST*(DMSA*BN23-DMSB*BN24+DMSC*BN25-DMSD*BN26)
      C(1,2)=CØNST*(DMPA*BN23-DMPB*BN24+DMPC*BN25-DMPD*BN26)
      C(2,2)=CØNST*(DMPA*BN5-DMPB*BN6+DMPC*BN7-DMPD*BN8)
      RETURN
      END
```

```
      FUNCTIØN PHI(N)
C     ******************************************************
C     *  PHI(N)=1+1/2+1/3+...  1/N                         *
C     ******************************************************
      PHI=0.0
      IF(N.EQ.0) RETURN
      DO 10 I=1,N
      XI=I
   10 PHI=PHI+1.0/XI
      RETURN
      END
```

```
      FUNCTIØN FACT(N)
C     ******************************************************
C     *  THIS FUNCTIØN  CALCULATES  FACTØRIAL N            *
C     ******************************************************
      FACT=1.0
      IF(N.EQ.0) RETURN
      DO 10 I=1,N
      AI=I
   lb FACT=FACT*AI
      RETURN
      'END
```

```
      FUNCTIØN XIN(N,X)
C     ******************************************************
C     *  TIIIS FUNCTION CALCULATES MØDIFIED BESSEL FUNCTION *
C     *. OF THE FIRST KIND OF INTEGER ØRDER N AND REAL      *
C     *  PARAMETER X                                        *
C     ******************************************************
      CØMMØN/ØNE/FAC(0/60),FI(0/60),ALL
      XIN=0.0
      K=-1
   10 K=K+1
      XX=(X/2.0)**(N+2*K)/FAC(K)/FAC(N+K)
      XIN=XIN+XX
      ALLØW=ABS(XIN)*ALL
      IF(ABS(XX).GT.ALLØW) GØ TØ 10
      RETURN
      END
```

```
      FUNCTIØN XJN(N,X)
C     ******************************************************
C     *  THIS FUNCTIØN CALCULATES 3ESSEL FUNCTIØN OF THE    *
C     *  FIRST KIND ØF INTEGER ORDER N AND REAL PARAMETER X*
C     ******************************************************
      CØMMØØN/ØNE/FAC(0/60),FI(0/60),ALL
      XJN=0.0
      K=-1
   10 K=K+1
      XX=(X/2.0)**(N+2*K)/FAC(K)/FAC(N+K)
      XJN=XJN+XX*(-1.0)**K
      ALLØW=ABS(XJN)*ALL
      IF(ABS(XX).GT.ALLØW) GØ TO 10
      RETURN
      END
```

```
      FUNCTIØN XYN(N,X,XJNX)
C     ****************************************************
C     *  THISFUNCTIØN CALCULATES BESSELFUNCTIØNØFSECØND*
C     *  KIND OF INTEGER ORDER N AND REAL PARAMETER X     *
C     *  XJNX IS THE EESSEL FUNCTIØNØF THE SAME TYPE AND *
C     *  SHØULD BE DEFINED BEFØRE ENTERING                *
C     ****************************************************
      CØMMØN/ØNE/FAC(0/60),FI(0/60),ALL
     PI=3.141592653589793
      EC=0.5772 1566490 1533
      XYN=2.0/PI*( LØG(X/2.0)+EC)*XJNX
      XX=0.0
      IF(N.EQ.0)GØ TO 15
      NN=N-1
      DO   10   I=0,NN
   10 XX=XX+FAC(N-I-1 )*(X*0.5)**(2*I-N)/FAC(I)
      XYN=XYN-(1.0/PI)*XX
   15 CONTINUE
      K=-1
      IF(N.EQ.0)  K=0
   20 K=K+1
      YY=1.0/PI*(-1.0)**K*(FI(K)+FI(N+K))*(0.5*X)**(2*K+N)/FAC(K)
     ./FAC(N+K)
      XYN=XYN-YY
      ALLØW=ABS(XYN) *ALL
      IF(ABS(YY).GT.ALLØW) GO TØ 20
      RETURN
      END

      FUNCTIØN XKN(N,X,XINX)
C     ****************************************************
C     *  THIS FUNCTIØN CALCULATES MØDIFIED BESSEL FUNCTIØN*
C     *  ØF THE SECØND KIND ØF INTEGER ØRDER N AND REAL   *
C     *  PARAMETER X                                      *
C     *  XINX IS THE BESSEL FUNCT IØNØF THE SAME TYPE AND *
C     *  SHØULD 2E DEFINED BEFØRE ENTERING                *
C     ****************************************************
      CØMMØN/ØNE/FAC(0/60),FI(0/60),ALL
      EC=0.577215664901533
      XKN=(-1.0)**(N+1)*( LØG(X*0.5)+EC)*XINX
      XX=0.0
      IF(N.EQ.0) GO TØ 15
      NN=N-1
      DØ 10 I=0,NN
   10 XX=XX+(-1.0)**I*FAC(N-I-1 )*(X*0.5)**(2*I-N)/FAC(I)
      XKN=XKN+0.5*XX
   15 CØNTINUE
      K=-1
      IF(N.EQ.0) K=0
   20 K=K+1
      YY=0.5*(-1.0)**N*(0.5*X)**(N+2*K)*(FI(K)+FI(K+N))/FAC(K)/FAC(N+K)
      XKN=XKN+YY
      ALLØW=ABS(XKN) *ALL
      IF(ABS(YY).GT.ALLØW)GØ TO 20
      RETURN
      END
```

D.4.2 Subroutines used in PROGRAM-2

```
C       ***************************************************
C       *                                                 *
C       *  MAIN2 -- MAIN PRØGRAM ØF PRØGRAM2              *
C       *                                                 *
C       ***************************************************
C       *  THIS IS A GENERAL PRØGRAM TØ BE USED IN THE    *
C       *  ANALYSIS ØF BLADED RØTØRS. TRANSVERSE SHEAR AND *
C       *  RØTARY INERTIA ARE IGNØRED BØTH IN THE DISC AND *
C       *  THE BLADES. ØPTIØNS FACILITATING THE USE OF THIS *
C       *  PRØGRAM FØR THE VIBRATIØN ANALYSIS ØF EITHER THE *
C       *  ENTIRE RØTØR SYSTEM ØR ITS CØMPØNENT PARTS MAY BE *
C       *  SPECIFIED. VARIABLE DIMENSIØNS ARE USED REQURING *
C       *  THE CHANGING ØF THE DIMENSIØNS ØNLY IN THE MAIN *
C       *  PRØGRAM AT ANY TIME AND SPECIFYING THE APPRØPRIATE*
C       *  VALUES ØF MS1 AND MS2.                         *
C       ***************************************************
        DIMENSIØN SK(24,24),SM(24,24),SKB(30,30),SMB(30,30)
        DIMENSIØN R(24),T(24),TE(24),W(24),P(24)
        DIMENSIØN BB(24),BD(24),BX(24),SIG(24),ANG(24),ARA(24),BKG(24)
        DIMENSIØN SGR(24),SGT (24 )
        DIMENSIØN D(24,24),F(24,24),B(24),C(24),X(24)
        DIMENSIØN ERR(24),B7(24),B8(24),B9(24),FR(20,10)
        CØMMØN/ØPTIØN/IØPT,IRNG,ITHD,ITED,ITHB, IST3
        CØMMØN/ØNE/AM,AM2,AM4,AMPR
        CØMMØN/TWØ/S1,S2,S3,S4,CKD,CKR,CMD,CMR,CC,CCC,CK,CP,CT
        CØMMØN/THRE/RDI,RDØ,RRI,RRØ,RTI,RTØ,E1,E2,RIZ,RIX,RJ,RA,STR
        CØMMØN/FØUR/PI,ED,ER,EB,RØD,RØR,RØB,ALD,ALR,PRD,PRR,PRB
        CØMMØN/FIVE/SRI,SRØ,ØMGA
        CØMMØN/SIX/CØNST,M,NF
        EQUIVALENCE (SK,F)
        MS1=24
        MS2=30
     15 CØNTINUE
C       ***************************************************
C       *  READ GENERAL ØPTIØN,RIM ØPTIØN,AND NUMBER ØF   *
C       *  FREQUENCIES REQUIRED FØR EACH DIAMETRAL NØDE.  *
C       ***************************************************
        READ 12,IØPT,IRNG,NF
        PRINT12, IØPT,IRNG,NF
C       ***************************************************
C       *  READ SPEED OF RØTATIØN ØF THE RØTØR IN RAD./SEC.*
C       ***************************************************
        READ 6, ØMGA
        PRINT6,ØMGA
```

```
      GØ TØ(20,50,20,21),IØPT
C     ***************************************************
C     * READ FINAL AND STARTING VALUES ØF NØDAL DIAMETERS *
C     ***************************************************
   20 READ 12,ND,MDS
      PRINT12,ND,MDS
C     ***************************************************
C     * READ NUMBER ØF DISC ELEMENTS, DISC ØPTIØNS, DISC *
C     * MATERIAL PRØPERTIES, AND    BØUNDARY LØADINGS. *
C     ***************************************************
   21 READ 12 ,NDE,ITED
      PRINT 12, NDE,ITED
      READ 6,ED,RØD,PRD,ALD
      PRINT6,ED,RØD,PRD,ALD
      READ 10,SRI,SRØ
      PRINT10,SRI,SRØ
      NSD=NDE+1
      NPD=2*NDE
      NTD=2*NSD
C     ***************************************************
C     * READ DISC DIMENSIØNS                            *
C     ***************************************************
      READ 10,(R(I),I=1,NPD)
      PRINT10,  (R(I),I=1,NPD)
      READ 10,(T(I),I=1,NPD)
      PRINT10,(T(I),I=1,NPD)
      RDI=R(1)
      RDØ=R(NPD)
      IF(ITED.EQ.0)GØ TØ 49
      READ 10,(TE(I),I=1,NPD)
      PRINT10,(TE(I),I=1,NPD)
   49    GØ      TØ(70,50,50,70),IØPT
   50 CØNTINUE
C     ***************************************************
C     * READ NUMBER ØF BLADE ELEMENTS, NUMBER ØF BLADES,  *
C     * AND BLADE ØPTIØNS.                               *
C     ***************************************************
      READ 12,NBE,NB,ISTB,IBDE
      PRINT12,NBE,NB,ISTB,IBDE
      NSB=NBE+1
      NTB=5*NSB
C     ***************************************************
C     * READ BLADE MATERIAL PRØPERTIES                  *
C     ***************************************************
      READ 6,EB,RØB,PRB
      PRINT6,EB,RØB,PRB
C     ***************************************************
C     * READ BLADE DIMENSIØNS                           *
C     ***************************************************
      READ 10,(BX(I),I=1,NSB)
      PRINT10,(BX(I),I=1,NSB)
      READ 10,(BB(I),I=1,NSB)
      PRINT10,(BB(I),I=1,NSB)
```

```
      READ 10, (BD(I),I=1,NSB)
      PRINT10,(BD(I),I=1,NSB)
      READ 10,(BKG(I),I=1,NSB)
      PRINT10,(BKG(I),I=1,NSB)
      READ 10,(ARA(I),I=1,NSB)
      PRINT10,(ARA(I),I=1,NSB)
      READ 10,(ANG(I),I=1,NSB)
      PRINT10,(ANG(I),I=1,NSB)
      IF(ISTB.EQ.1) READ 6,(SIG(I),I=1,NSB)
      IF(ISTB.EQ.1) PRINT6, (SIG(I),I=1,NSB)
   70 IF (IRNG.EQ.0)GØ TO 80
C     ***************************************************
C     *  IF RIM IS PRESENT, READ THE RIM MATERIAL PRØPER-*
C     *  TIES, DIMENSIØNS, AND ELASTIC PRØPERTIES        *
C     ***************************************************
      READ 6,ER,RØR,PRR
      PRINT6,ER,RØR,PRR
      READ 10,RRI,RRØ,RTI,RTØ,RTEI,RTEØ
      PRINT10,RRI,RRØ,RTI,RTØ,RTEI,RTEØ
      READ 10,E1,E2,RIZ,RIX,RJ,RA
      PRINT10,E1,E2,RIZ,RIX,RJ,RA
      T(NPD+1)=RTI
      T(NPD+2)=RTØ
      TE(NPD+1)=RTEI
      TE(NPD+2)=RTEØ
      R(NPD+1)=RRI
      R(NPD+2)=RRØ
   80 CØNTINUE
      PI=3.14159265358979
      CØNST=0.5/PI
      S1=1./3.
      S2=1./6.
      S3=1./7.
      S4=1./9.
      GO TØ(95,85,85,95),IØPT
   85 CØNTINUE
C     ***************************************************
C     *  CALCULATE BLADE SUBSYSTEM STIFFNESS AND MASS    *
C     *  MATRICES AND STØRE THEM                         *
C     ***************************************************
      CALL BLADE(SKB,SMB,BX,BB,BD,ANG,SIG,ARA,BKG,NBE,IBDE,MS2)
      GØ TØ(95,90,95),IØPT
   90 CØNTINUE
C     ***************************************************
C     *  CØMPUTE BLADE FREQUENCIES ACCØRDING TØ THE BLADE *
C     *  GENERAL ØPTIØNS                                  *
C     ***************************************************
      IF(IRNG.NE.0)GØ TØ 102
      IJK=1
      M=0
      IF(IBDE.NE.1) GØ TØ 94
      DØ 91 I=3,2*NSB
      II=I-2
```

```
      DØ 91 J=3,2*NSB
      JJ= J-2
      SK(II,JJ)=SKB(I,J)
   91 SM(II,JJ)=SMB(I,J)
      N1=2*NSB-2
      PRINT 1
      CALL EIGVAL(SK,SM,D,F,FR,B,C,X,ERR,B7,B8,B9,IJK,N1,MS1)
      DØ 92 I=2*NSB+3,4*NSB
      II=I-2-2*NSB
      DØ 92 J=2*NSB+3, 4 *NSB
      JJ=J-2-2*NSB
      SK(II,JJ)=SKB(I,J)
   92 SM(II,JJ)=SMB(I,J)
      PRINT 2
      CALL EIGVAL(SK,SM,D,F,FR,B,C,X,ERR,B7,B8,B9,IJK,N1,MS1)
      DØ 93 I=4*NSB+2,NTB
      II=I-1-4*NSB
      DO 93 J=4*NSB+2, NTB
      JJ=J-1-4*NSB
      SK(II,JJ)=SKB(I,J)
   93 SM(II,JJ)=SMB(I,J)
      N1=NSB-1
      PRINT 4
      CALL EIGVAL(SK,SM,D,F,FR,B,C,X,ERR,B7,B8,B9,IJK,N1,MS1)
      GØ TØ 15
   94 IF(IBDE.NE.2)GØ TØ 97
      NM=NTB
      DØ 195 I=NBE,1,-1
      II=5*I
      CALL REDUCE(SKB,NM,II,1,MS2)
      CALL REDUCE (SMB,NM,II,1,MS2)
      NM=NM- 1
  195 CØNTINUE
      DO 96 I=5,4*NSB
      II=I-4
      DØ 96 J=5,4*NSB
      JJ=J-4
      SK(II,JJ)=SKB(I,J)
   96 SM(II,JJ)=SMB(I,J)
      N1=4*NSB-4
      PRINT 5
      GØ TØ 99
   97 CØNTINUE
      DØ 98 I=6,NTB
      II=I-5
      DØ 98 J=6,NTB
      JJ=J-5
      SK(II,JJ)=SKB(I,J)
   98 SM(II,JJ)=SMB(I,J)
      N1=NTB-5
      PRINT 7
   99 CALL EIGVAL(SK,SM,D,F,FR,B,C,X,ERR,B7,B8,B9,IJK,N1,MS1)
      GØ TØ 15
```

```
   95 CØNTINUE
      CK=2.0*PI*ED/(1.0-PRD*PRD)
      CP=2.0*PI*RØD*ØMGA*ØMGA
      CT=2.0*PI*ED*ALD/(1.0-PRD)
C     ****************************************************
C     *  CALCULATETHE INITIAL STRESSES INTHE DISC DUE TØ*
C     *  RØTATIØN, TEMPERATURE GRADIENT, AND ØTHER BØUNDARY*
C     *  LØADINGS                                        *
C     ****************************************************
      CALL INLSTR(SK,R,T,TE,W,P,SGR,SGT,NSD,MS1)
      IF(IØPT.EQ.4) GØ TØ 15
      NT=NTD
      IF(IØPT.EQ.3) NT=NTD+NTB-5
      STR=0.5*(SGT(NPD-1)+SGT(NPD))*RA
      GØ TØ 105
  102 CØNTINUE
      READ 10,SRØ
      PRINT10,SRØ
      STR=RØR*RA*ØMGA*ØMGA*(RRI+E1)*(RRI+E1)+SRØ*(RRI+E1)
      NTD=2
      NT=NTD+NTB-5
  105 CØNTINUE
      IJK=1
      M=MDS-1
      IF(IØPT.EQ.3)  Z=NB
  100 CØNTINUE
C     ****************************************************
C     *  SELECT NUMBERØF NØDAL DIAMETERS                 *
C     ****************************************************
      M=M+1
      PRINT 3,M
      FAC=1.0
      IF(M.EQ.0) FAC=2.0
      IF(IØPT.NE.2) CKD=FAC*PI*ED/(1.0-PRD*PRD)/12.0
      IF(IØPT.NE.2) CMD=FAC*PI*RØD
      IF(IRNG.EQ.1 )CKR=FAC*PI*(RRI+E1)
      IF(IRNG.EQ.1 )CMR=FAC*PI*(RRI+E1)
      IF(IØPT.NE.1) CC=Z*FAC/2.0
      IF(IØPT.NE.2) CCC=FAC*PI
      AM=M
      AM2=AM*AM
      AM4=AM2*AM2
      AM6=AM4*AM2
      IF(IØPT.NE.2) AMPR=AM2*PRD
      DØ 110 I=1,NT
      DO 110 J=1,NT
      SK(I,J)=0.0
  110 SM(I,J)=0.0
C     ****************************************************
C     *  CALCULATE DISC SUBSYSTEM STIFFNESS AND MASS     *
C     *  MATRICES ANDSTØRETHEM                           *
C     ****************************************************
      CALL DISC(SK,SM,R,T,SGR,SGT,NSD,MS1)
```

```
C      ****************************************************
C      *  GET THE SYSTEM STIFFNESS AND MASS MATRICES FRØM  *
C      * THE SUBSYSTEM MATRICES                            *
C      ****************************************************
       CALL SYSTEM (SK,SM,SKB,SMB,NTD,NTB,MS1,MS2)
C      ****************************************************
C      *  APPLY BØUNDARY CØNDITIONS                        *
C      ****************************************************
       CALL REDUCE(SK,NT,1,2,MS1)
       CALL REDUCE(SM,NT,1,2,MS1)
       N1=NT-2
C      ****************************************************
C      *  SØLVE THE EIGEN VALUE PRØBLEM AND GET THE SYSTEM*
C      *  FREQUENCIES                                     *
C      ****************************************************
       CALL EIGVAL(SK,SM,D,F,FR,B,C,X,ERR,B7,B8,B9,IJK,N1,MS1)
       IF(M.LT.ND)GØ TØ 100
       GØ TO 15
  200  CALL EXIT
     1 FØRMAT(1H1,5X,'BLADE SENDING FREQUENCIESINI-MINDIRECTIØN'//)
     2 FØRMAT(1H1, S?:, 'BLADE BENDING FREQUENCIES INI-MAXDIRECTIØN'//)
     3 FØRMAT(///26HNUMBER OF NØDAL DIAMETERS=,I2///)
     4 FØRMAT(1H1,5X,'BLADE TØRTIØNAL FREQUENCIES'//)
     5 FØRMAT(1H1,5X,'TWISTED BLADE BENDING FREQUENCIES'//)
     6 FØRMAT(4F20.10)
     7 FØRMAT(1H1,5X,'BLADE FREQUENCIES WITH INITIAL STRESSES'//)
    10 FØRMAT(8F10.7)
    11 FØRMAT(/8E13.6)
    12 FØRMAT(1 615 )
       END
```

```
      SUBRØUTINE BLADE(SKB,SMB,BX,BB,BD,ANG,SIG,ARA,BKG,NBE,IBDE,L)
C     ****************************************************
C     *  THIS SUBRØUTINE CALCULATES THE BLADE SUBSYSTEM      *
C.    *  STIFFNESS MATRIX SKB(L,L) AND MASS MATRIX SMB(L,L)*
C     *  TRANSVERSE SHEAR AND RØTARY INERTIA ARE IGNØRED   *
C     *  ADDITIØNAL STIFFNESS DUE TØ INITIAL STRESSES CAN *
C     *  ALSO BE INCLUDED                                  *
C     ****************************************************
      DIMENSIØN       SKB(L,L),SMB(L,L),EK(10,10),EM(10,10)
      DIMENSIØN R(10,10),B(10,10),C(10,10),D(10,10)
      DIMENSIØN    BX(L),BB(L),BD(L),ANG(L),SIG(L),ARA(L),BKG(L)
      CØMMØN/ØPTIØN/IØPT,IRNG, PTHD, ITED,ITHB, ISTB
      CØMMØN/FØUR/PI,ED,ER,EB,RØD,RØR,RØB,ALD,ALR,PRD,PRR,PRB
      CØMMØN/FIVE/SRI,SRØ,ØMGA
      RX(I,AI)=ALFS*ALFA*XX(I+1,AI+1.0)+(ALFS*BETA+BETS*ALFA)*
     .XX(I+2,AI+2.0)+BETS*BETA*XX(I+3,AI+3.0)
      SX(I,AI)=RØB*ØMGA*ØMGA*(ALFA*XX(I+1,AI+1.0)+BETA*XX(I+2,AI+2.0))
      XX(I,AI)=(BX2**I-BX1**I)/AI
      NTB=5*(NBE+1)
      DØ 10 I=1,NTB
      DO 10 J=1 ,NTB
      SKB(I,J)=0.0
   10   SMB(I,J)=0.0
      PRINT 1
      K=0
   20CØNT INUE
      DØ 15 I=1,10
      DØ 15 J=1,10
      B(I,J)=0.0
      EK(I,J)=0.0
      EM(I,J)=0.0
   15 R(I,J)=0.0
C     ****************************************************
C     *  SELECT THE NUMBER K ØF THE ELEMENT AND GET THE      *
c     *  VALUES ØFSECTIØN PRGPERTIES ØF THE BLADE AT         *
C     *  ENDS ØF THE ELEMENT.                                *
C     ****************************************************
      K=K+1
      KP1=K+1
      BX1=BX(K)
      BX2=BX(KP1)
      PRINT 2,K,BX1,BX2
      ARA1=ARA(K)
      ARA2 =ARA(KP1)
      ANG 1 =ANG(K)
      ANG2=ANG(KP1)
      BA=0.5*(ANG1+ANG2)
      SN=SIN(BA/180.0*PI)
      CS=CØS(BA/180.0*PI)
```

```
      GB=0.5*EB/(1.0+PRB)
      BMI1=BB(K)
      BMI2=BB(KP1)
      BMX1=BD(K)
      BMX2=BD(KP1       )
      BJ1=BKG(K)
      BJ2=BKG(KP1)
      EL=BX2-BX1
      XK1=EB*BMI 1 /EL/EL/EL
      XK2=EB*BMI2/EL/EL/EL
      YK1=EB*BMX1/EL/EL/EL
      YK2=EB*BMX2/EL/EL/EL
      ZK1=GB*BJ1/2.0/EL
      ZK2=GB*BJ2/2.0/EL
      XM1=RØB*ARA1*EL/420.0
      XM2=RØB*ARA2*EL/420.0
      ZM1=RØB*(BMI1+BMX1)*EL/12.0
      ZM2=RØB*(BMI2+BMX2)*EL/12.0
C     ***************************************************
C     *   CALCULATE THE RØTATIØN MATRIX  R              *
C     ***************************************************
      R(1,1)=CS
      R(2,2)=CS
      R(3,6)=CS
      R(4,7)=CS
      R(5,3)=CS
      R(6,4)=CS
      R(7,8)=CS
      R(8,9)=CS
      R(1,3)=SN
      R(2,4)=SN
      R(3,8)=SN
      R(4,9)=SN
      R(5,1)=-SN
      R(6,2)=-SN
      R(7,6)=-SN
      R(8,7)=-SN
      R(9,5)=1.0
      R(10,10)=1.0
C     ***************************************************
C     *  CALCULATE THE ELEMENT STIFFNESS MATRIX EK      *
C     ***************************************************
      EK(1,1)=6.0*XK1+6.0*XK2
      EK(1,2)=-2.0*EL*XK1-4.0*EL*XK2
      EK(1,3)=-6.0*XK1-6.0*XK2
      EK(1,4)=-4.0*EL*XK1-2.0*EL*XK2
      EK(2,2)=EL*EL*XK1+3.0*EL*EL*XK2
      EK(2,3)=2.0*EL*XK1+4.0*EL*XK2
      EK(2,4)=EL*EL*XK1+EL*EL*XK2
      EK(3,3)=6.0*XK1+6.0*XK2
      EK(3,4)=4.0*EL*XK1+2.0*EL*XK2
      EK(4,4)=3.0*EL*EL*XK1+EL*EL*XK2
      EK(5,5)=6.0*YK1     +6.0*YK2
```

```
      EK(5,6)=-2.0 *EL*YK 1 -4.0 *EL*YK2
      EK(5,7)=-6.0*YK1-6.0*YK2
      EK(5,8)=-4.0*EL*YK1-2.0*EL*YK2
      EK(6,6)=EL*EL*YK1+3.0*EL*EL*YK2
      EK(6,7)= 2.0*EL*YK1+4.0*EL*YK2
      EK(6,8)=EL*EL*YK1+EL*EL*YK2
      EK(7,7)=6.0*YK1+6.0*YK2
     EK(7,8)=    4.0*EL*YK1+2.0*EL*YK2
      EK(8,8)=3.0*EL*EL*YK1+EL*EL*YK2
      EK( 9, 9)=ZK1+ZK2
      EK(9,10)=-ZK1-ZK2
      EK(10, 13)=ZK1+ZK2
C     **************************************************
C     * 'CALCULATE THE ELEMENT MASS MATRIX EM          *
C     **************************************************
      EM(1, 1)=36.0*XM1+120.0*XM2
      EM(1,2)=-7.0*EL*XM1-15.0*EL*XM2
      EM(1,3)=27.0*XM1+27.0*XM2
      EM(1,4)= 6.0*EL*XM1+7.0*EL*XM2
      EM(2,2)=1.5*EL*EL*XM1+2.5*EL*EL*XM2
      EM(2,3)=-7.0*EL*XM1-6.0*EL*XM2
      EM(2,4 >=-1 .5*EL*EL*XM1-1 .5*EL*EL*XM2
      EM(3,3)=120.0*XM1+36.0*XM2
      EM(3,4)= 15 .0*EL*XM1+7.0*EL*XM2
      EM(4,4)=2.5*EL*EL*XM1+1.5*EL*EL*XM2
      EM(5,5)=36.0*XM1+120.0*XM2
      EM(5,6)=-7.0*EL*XM1-15.0*EL*XM2
      EM(5,7)=27.0*XM1+27.0*XM2
      EM(5,8)=    6.0*EL*XM1+7.0*EL*XM2
      EM(6,6)=1.5*EL*EL*XM1+2.5*EL*EL*XM2
      EM(6,7)=-7.0*EL*XM1-6.0*EL*XM2
      EM(6,8)=-1.5*EL*EL*XM1-1.5*EL*EL*XM2
      EM(7,7)=120.0*XM1+36.0*XM2
      EM(7,8)= 15.0*EL*XM1+7.0*EL*XM2
      EM(8,8)=2.5*EL*EL*XM1+1.5*EL*EL*XM2
      EM(9,9)=3.0*ZM1 i-Z?12
      EM(9, 1 0)=ZM1+ZM2
      Et.1(10,10)=ZM1+3.0*ZM2
      DØ 30 I=1,9
      II=I+1
      DO 30 J=II,10
      EK(J,I)=EK(I, J)
   30 EM(J, 1)=EM(I, J)
C     **************************************************
C     *  STØRE THE ELEMENT MATRICES INTØ THE BLADE SYSTEM  *
C     *  MATRICES IN THE APPRØPRIATE PØSITIØNS ACCØRDING TØ*
C     *  THE BLADE GENERAL ØPTIØN                          *
C     **************************************************
      IF(IBDE.NE.1) GØ TØ 32
      KK=2*(K-1)
      CALL ASMBLE(SKB,EK,KK,KK,1,4,10,L)
      CALL ASMBLE(SMB,EM,KK,KK,1,4,10,L)
      KK=2*(NBE+1)+2*(K-1)
      CALL ASMBLE(SKB,EK,KK,KK,5,8,10,L)
      CALL ASMBLE(SMB,EM,KK,KK,5,8,10,L)
```

```
      KK=4*(NBE+1)+I?-1
      CALL ASMBLE(SKB,EK,KK,KK,9,10,10,L)
      CALL ASMBLE(SMB,EM,KK,KK,9,10,10,L)
      IF(K.LT.NBE) GØ TØ 20
      RETURN
3     2    CØNTINUE
      CALL TRIMUL(R,EK,C,D,10,10,10,10,10)
      CALL TRIMUL(R,EM,C,D,10,10,10,10,10)
      IF(ISTB.EQ.0) GO TO 50
C     ****************************************************
C     *  CALCULATE THE'3' MATR IX                         *
C     ****************************************************
      B(1,1)=1.0
      B(1,2)=BX1
      B(1,3)=BX1*BX1
      B(1,4)=BX1*BX1*BX1
      B(2,2)=-1.O
      B(2,3)=-2.0*BX1
      B(2,4)=-3.0*BX1*BX1
      B(6,1)=1.o
      B(6,2)=BX2
      B(6,3)=BX2*BX2
      B(6,4)=BX2*BX2*BX2
      B(7,2)=-1.O
      B(7,3)=-2.0*BX2
      B(7,4)=-3.0*BX2*BX2
      B(5,9)=1 .0
      B(5,10)=BX1
      B(10,9)=1.0
      B(10,10)=BX2
      DØ 25 I=1,2
      DØ 25 J=1,4
      B(I+2,J+4)=B(I,J)
25    B(I+7,J+4)=B(I+5,J)
      CALL INVT(B,10,10)
C     ****************************************************
C     *  CALCULATE ADDITIØNAL STIFFNESS VALUES IF INITIAL *
C     *  STRESSES ARE PRESENT                             *
C     ****************************************************
      SIG1=SIG(K)
      SIG2=SIG(KP1)
      ALFS=(BX2*SIG1-BX1*SIG2)/EL
      BETS=(SIG2-SIG1 >/EL
      ALFA=(BX2*ARA1-BX1*ARA2 >/EL
      BETA=(ARA2-ARA1) /EL
      ALIU=(BX2*BMI1-BX1*BMI2)/EL
      BETU=(BMI2-BMI1)/EL
      ALIW=(BX2*BMX1-BX1*BMX2 >/EL
      BETW=(BMX2-BMX1) /EL
      DØ 35 I=1,10
      DØ 35 J=1,10
35.   R(I,J)=0.0
      R(1,1)=-SX(0,0.0)
      R(1,2)=-SX(1,1.0)
```

```
      R(1,3)=-SX(2,2.0)
      R(1,4)=-SX(3,3.0)
      R(2,2)=RX(0,0.0)-SX(2,2.0)
      R(2,3)=2.0*RX(1,1.0)-SX(3,3.0)
      R(2,4)=3.0*RX(2,2.0)-SX(4,4.0)
      R(3,3)=4.0*RX(2,2.0)-SX(4,4.0)
      R(3,4)=6.0*RX(3,3.0)-SX(5,5.0)
      R(4,4)=9.0*RX(4,4.0)-SX(6,6.0)
      R(6,6)=RX(0,0.0)
      R(6,7)=2.0*RX(1,1.0)
      R(6,8)=3.0*RX(2,2.0)
      R(7,7)=4.0*RX(2,2.0)
      R(7,8)=6.0*RX(3,3.0)
      R(8,8)=9.0*RX(4,4.0)
      R( 9,9)=-RØB*ØMGA*ØMGA*CØS(2.0*BA)*((ALFW+ALFU)*XX(1,1.0)+BETW+
     .BETU)*XX(2,2.0))
      R(9,10)=-RØB*ØMGA*ØMGA*CØS(2.0*BA)*((ALFW+ALFU)*XX(2,2.0)+BETW+
     .BETU)*XX(3,3.0))
      R(10,10)=-RØB*ØMGA*ØMGA*CØS(2.*BA)*((ALFW+ALFU)*XX(3,3.0)+BETW+
     .BETU)*XX(4,4.0))
     .ALFS*ALFJ*XX(1,1.0)+(ALFS*BETJ+BETS*ALFJ)*XX(2,2.0)
     .+(BETS*BETJ)*XX(3,3.0)
      DO 40 I=1,9
      II=I+1
      DØ 40 J=II,10
   40 R(J,I)=R(I,J)
      CALL TRIMUL(B,R,C,D,10,10,10,10,10)
      DØ 45 I=1,10
      DO 45 J=1,10
   45 EK(I,J)=EK(I,J)+R(I,J)
   50 KK=5*(K-1)
      CALL ASMBLE(SKB,EK,KK,KK,I,10,10,L)
      CALL ASMBLE(SMB,EM,KK,KK,1,10,10,L)
      IF(K.LT.NBE) GØ TØ 20
      RETURN
    1 FØRMAT(1H1,//5X,'BLADE    DIMENSIØNS'//)
    2 FØRMAT(5X,I5,8F8.3/)
    3 FØRMAT(5E13.5)
      END
```

```
      SUBRØUTINE DISC(SK,SM,R,T,SRR,STT,NS,L)
C     ****************************************************
C     *  THIS SUBRØUTINE CALCULATES THE ELEMENT STIFFNESS *
C     *  AND MASS MATRICES AND STØRES THE VALUES INTØ THE *
C     *  DISC  SUBSYSTEM MATRICES SK(L,L)AND SM(L,L)      *
C     *  THE ADDITIØNAL  STIFFNESS CØEFFICIANTS DUE TØ    *
C     *  INITIAL  STRESSES  SRR(L) AND STT(L)  ARE  ALSO  *
C     *  CALCULATED AND ADDED TO THE RENDING STIFFNESS.   *
C     *  SHEAR DEFØRMATIØNS AND RØTARY  INERTIA  ARE IGNØRED.*
C     *  WHILE  ENTERING THE SUBRØUTINE ZERØ ALL THE TERNS *
C     *  ØF THE MATRICES SK AND SM.  INITIALISE ALL THE   *
C     *  TERMS ØF THE RADIUS AND THICKNESS VECTØRS R AND T.*
C     ****************************************************
      DIMENSIØN SK(L,L),SM(L,L),R(L),T(L)
      DIMENSIØN   SRR(L),STT(L),ES(4,4)
      DIMENSIØN           EK(4,4),EM(4,4),B(4,4),C(4,4),D(4,4)
      CØMMØN/ØPTIØN/IØPT,IRNG,ITHD,ITED,ITHB,ISTB
      CØMMØN/ØNE/AM,P2, P I ,P3
      CØMMØN/TWØ/S1,S2,S3,S4,CKD,CKR,CMD,CMR,CC,CCC,CK,CP,CT
      CØMMØN/FØUR/PI,ED,ER,EB,RØD,RØR,RØB,ALD,ALR,PRD,PRR,PRB
      K=0
      N=NS-1
      PR=PRD
   30 CØNTINUE
C     ****************************************************
C     *  SELECT THE NUMBER K OF THE ELEMENT               *
C     ****************************************************
      K=K+1
      K1=2*K-1
      K2=2 *K
C     ****************************************************
C     *  GET THE VALUES ØF RADIUS AND THICKNESS AT NØDES  *
C     ****************************************************
      R1=R(K1)
      R2=R(K2)
      T1=T(K1)
      T2=T(K2)
      DO 40 I=1,4
      DØ 40 J=1,4
       B(I,J)=0.0
      EK(I,J)=0.0
   40 EM(I,J)=0.0
      DD=R2-R1
      D1=DD*DD
      D2=D1*DD
      ALFA=(R2*T1-R1*T2)/DD
      BETA=(T2-T1)/DD
      X1 =ALFA*ALFA*ALFA*CKD
      X2=ALFA*ALFA*BETA*CKD
      X3=ALFA*BETA*BETA*CKD
      X4=BETA*BETA*BETA*CKD
```

```
C     ****************************************************
C     *  CALCULATE THE 'B' MATRIX                         *
C     ****************************************************
      B(1,1)=R2*R2*(R2-3.*R1)/D2
      B(1,3)=R1*R1*(3.*R2-R1)/D2
      B(1,2)= R1*R2*R2/D1
      B(1,4)= Ri *R1*R2/D1
      B(2,1)=6.*R1*R2/D2
      B(2,3)=-B(2,1)
      B(2,2)=-R2*(2.0*R1+R2)/D1
      B(2,4)=-R1*(R1+2.0*R2)/D1
      B(3,1)=-3.*(R1+R2)/D2
      B(3,3)=-B(3,1)
      B(3,2)= (R1+2.*R2)/D1
      B(3,4)= (2.*R1+R2)/D1
      B(4,1 )= 2./D2
      B(4,3)=-B(4,1)
      B(4,2)=-1.0/D1
      B(4,4)=B(4,2)
      A1=R1*R2
      A2=A1    *A1
      A3=R2-R1
      A4=R2 *a2 -R1**2
      A5=R2**3-R1**3
      A6=R2**4-R1**4
      A7=R2**5-R1**5
      A8=R2**6-R1**6
      A9=R2**7-R1**7
      A10=R2**8-R1**8
      A11=R2**9-R1**9
      A12=R2**10-R1**10
      C5=ALØG   (R2/R1)
      E1=X1*.5*A4/A2+X2*3.*A3/A1 +X3*3 .*C5+X4*A3
      E2=X1*A3/A1+X2*3.*C5+X3*3.*A3+X4*.5*A4
      E3=X1*C5+X2*3.*A3+X3*1.5*A4+X4*S1*A5
      E4=X1*A3+X2*1.5*A4+X3*A5+X4*.25*A6
      E5=X1*.5*A4+X2*A5+X3*.75*A6+X4*.2*A7
      E6=X1   *S1*A5+X2*.75*A6+X3*.6*A7+X4*S2*A8
      E7=X1*.25*A6+X2*.6*A7+X3*.5*A8+X4*S3*A9
C     ****************************************************
C     *  CALCULATE THE 'SMALLK' MATRIX                    *
C     ****************************************************
      EK(1,1)=E1*(P1+2.*P2-2.*P3)
      EK(1,2)=E2*(P1-P2)
      EK(2,1)=EK(1,2)
      EK(1,3)=E3*(P1-4.*P2)
      EK(3,1)=EK(1,3)
      EK(1,4)=E4*(P1-7.*P2-2.*P3)
      EK(4,1)=EK( 1,4)
      EK(2,2)=E3*(P1-2.*P2+1.)
      EK(2,3)=E4*(P1-3.*P2-2.*P3+2.*PR+2.)
      EK(3,2)=EK(2,3)
      EK(2,4)=E5*(P1-4.*P2+3.-6.*P3+6.*PR)
      EK(4,2)=EK(2,4)
      EK(3,3)=E5*(P1-2.*P2+8.-6.*P3+8.*PR)
```

```
      EK(3,4)=E6*(P1-P2+18.-12.*P3+18.*PR)
      EK(4,3)=EK(3,4)
      EK(4,4)=E7*(P1+2.*P2+45.-20.*P3+36.*PR)
      CA=(R2*SRR(K1    )-R1*SRR(K2))/DD
      DA=(SRR(K2)-SRR(K1))/DD
      EE=(R2*STT(K1)-R1*STT(K2))/DD
      FF=(STT(K2)-STT(K1))/DD
      X1=CCC*ALFA*EE*P2
      X2=CCC*P2*(ALFA*FF+BETA*EE)
      X3=CCC*BETA*FF*P2
      E1 =X1*C5+X2*A3+0.5*X3*A4
      E2=X1*A3+0.5*X2*A4+S1*X3*A5
      E3=0.5*X1*A4+S1*X2*A5+0.25*X3*A6
      E4=S1*X1*A5+0.25*X2*A6+0.2*X3*A7
      E5=0.25*X1*A6+0.2*X2*A7+S2*X3*A8
      E6=0.2*X1*A7+S2*X2*A8+S3*X3*A9
      E7=S2*X1*A8+S3*X2*A9+0.125*X3*A10
      X1=CCC*ALFA*CA
      X2=CCC*(ALFA*DA+BETA*CA)
      X3=CCC*BETA*DA
      F1=0.5*X1*A4+S1*X2*A5+0.25*X3*A6
      F2=S1*X1*A5+0.25*X2*A6+0.2*X3*A7
      F3=0.25*X1*A6+0.2*X2*A7+S2*X3*A8
      F4=0.2*X1*A7+S2*X2*A8+S3*X3*A9
      F5=S2*X1*A8+S3*X2*A9+0.125*X3*A10
C     ***************************************************
C     *  CALCULATE ADDITIØNAL STIFFNESS FØR INITIAL STRESS *
C     ***************************************************
      ES(1,1)=E1
      ES(1,2)=E2
      ES(1,3)=E3
      ES(1,4)=E4
      ES(2,2)=E3+F1
      ES(2,3)=E4+2.0*F2
      ES(2,4)=E5+3.0*F3
      ES(3,3)=E5+4.0*F3
      ES(3,4)=E6+6.0*F4
      ES(4,4)=E7+9.0*F5
      ES(2,1)=ES(1,2)
      ES(3,1)=ES(1,3)
      ES(3,2)=ES(2,3)
      ES(4,1)=ES(1,4)
      ES(4,2)=ES(2,4)
      ES(4,3)=ES(3,4)
      DØ 45 I=1,4
      DØ 45 J=1,4
   45 EK(I,J)=EK(I,J)+ES(I,J)
      ALFA=ALFA*CMD
      BETA=BETA*CMD
C     ***************************************************
C     *  CALCULATE THE'SMALL M'MATRIX                    *
C     ***************************************************
      EM(1,1)=ALFA*.5*A4+BETA*S1*A5
      EM(1,2)=ALFA*S1*A5+BETA*.25*A6
```

```
      EM(1,3)=ALFA*.25*A6+BETA*.2*A7
      EM(1,4)=ALFA*.2*A7+BETA*S2*A8
      EM(2,1)=EM(1,2)
      EM(2,2)=EM(1,3)
      EM(2,3)=EM(1,4)
      EM(2,4)=ALFA*S2*A8+BETA*S3*A9
      EM(3,1)=EM(1,3)
      EM(3,2)=EM(2,3)
      EM(3,3)=EM(2,4)
      EM(3,4)=ALFA*S3*A9+BETA*.125*A10
      EM(4,1)=EM(1,4)
      EM(4,2)=EM(2,4)
      EM(4,3)=EM(3,4)
      EM(4,4)=ALFA*.125*A10+BETA*S4*A11
C     ****************************************************
C     *  CALCULATE  THE  STIFFNESS  AND MASS MATRICES     *
C     ****************************************************
      CALL  TRIMUL(B,EK,C,D,4,4,4,4,4)
      CALL TRIMUL(B,EM,C,D,4,4,4,4,4)
      KK=2*(K-1)
C     ****************************************************
C     *  PUT THE ELEMENT MATRICES INTØ SUBSYSTEM MATRICES  *
C     ****************************************************
      CALL ASMBLE(SK,EK,KK,KK,1,4,4,L)
      CALL ASMBLE(SM,EM,KK,KK,1,4,4,L)
C     ****************************************************
C     *  GØ BACK AND REPEAT CALCULATIØNS FØR ØTHER ELEMENTS*
C     ****************************************************
      IF(K-N)30,50,50
   50 CØNTINUE
      RETURN
      END
```

```
      SUBROUTINE SYSTEM(SK,SM,SKB,SMB,NTD,NTB,L,LL)
C     ****************************************************
C     *  T H I S  SUBROUTINE ASSEMBLES THE STIFFNESS AND MASS *
C     *  MATRICES OF THE THREE SUB SYSTEMS INTO THE SYSTEM *
C     *  MATRICES . THE MATRICES RK(2,2) AND RM(2,2) OF  T H E *
C     *  RIM SUBSYSTEM ARE CALCULATED BEFORE ASSEMBLING.     *
C     *  THE DISC SUBSYSTEM MATRICES SK(L,L)  A N D  SM(L,L) *
C     *  ARE THEMSELF USED AS SYSTEM MATRICES.              *
C     *  BEFORE ENTERING THE SUBROUTINE INITIALISE ALL THE *
C     *  TERMS OF  T H E  SUBSYSTEM MATRICES SK,SM,SKB,AND SMB.*
C     ****************************************************
      DIMENSION SK(L,L),SM(L,L),SKB(LL,LL),SMB(LL,LL)
      DIMENSION DK(10,10),DM(10,10),T(10,10),C(10,10),D(10,10)
      DIMENSION RK(2,2),RM(2,2),CR(2,2),DR(2,2),TT(2,2)
      COMMON/OPTION/IOPT,IRNG,ITHD,ITED,ITHB,ISTB
      COMMON/ONE/AM,AM2,AM4,AMPR
      COMMON/TWO/S1,S2,S3,S4,CKD,CKR,CMD,CMR,CC,CCC,CK,CP,CT
      COMMON/THRE/RDI,RDO,RRI,RRO,RTI,RTO,E1,E2,RIZ,RIX,RJ,RA,STR
      COMMON/FOUR/PI,ED,ER,EB,ROD,ROR,ROB,ALD,ALR,PRD,PRR,PRB
      IF(IOPT.EQ.1) GO TO 35
      RR=RRO
      IF(IRNG.EQ.0)  RR=RDO
      DO 10 I=1,10
      DO 10 J=1,10
      DK(I,J)=SKB(I,J)
      DM(I,J)=SMB(I,J)
   10 T(I,J)=0.0
C     ****************************************************
C     *  APPLY THE CONSTRAINT CONDITIONS TO THE BLADE       *
C     *  SUBSYSTEM MATRICES.                                 *
C     ****************************************************
      T(3,1)=1.0
      T(3,2)=-E1-E2
      T(4,2)=1.0
      T(5,1)=-AM/RR
      T(5,2)=AM/RR*(E1+E2)
      T(6,3)=1.0
      T(7,4)=1.0
      T(8,5)=1.0
      T(9,6)=1.0
      T(10,7)=1.0
      CALL TRIMUL(T,DK,C,D,10,7,10,10,10)
      CALL TRIMUL(T,DM,C,D,10,7,10,10,10)
      DO 15 I=1,10
      DO 15 J=1,10
      C(I,J)=SKB(I,J)
   15 DC I,J)=SMB(I,J)
      DO 20 I=1,7
      II=I+3
      DO 20 J=1,7
      JJ=J+3
      SKB(II,JJ)=DK(I,J)
   20 SMB(II,JJ)=DM(I,J)
```

```
C     ******************************************************
C     *  ASSEMBLE THE DISC AND BLADE MATRICES INTØ THE     *
C     *  SYSTEM MATR ICES .                                *
C     ******************************************************
      DØ 30 I=4,NTB
      II=I+NTD-5
      D5 30 J=4,NTB
      JJ= J+NTD-5
      SK(II,JJ)=SK(II,JJ)+CC*SKB(I,J)
   30 SM(II,JJ)=SM(II,JJ)+CC*SMB(I,J)
      DØ 35I=1, 10
      DO 35 J=1,10
      SKB(I,J)=C(I,J)
      SMB(I,J)=D(I,J)
   35 CØNT INUE
      IF(IRNG.EQ.0)GØ TO 50
C     ******************************************************
C     *  CALCULATE THE RIM MATRICES                        *
C     ******************************************************
    A1=1 .0/(RRI+E1)
      A2=A1*A1
      A3 =A2 *A 1
    A4=A3*A1
      AR=0.5*(RRØ-RRI)*(RTØ+RTI)
      GR=0.5*ER/(1.0+PRR)
    RK(1,1)=CKR*(ER*RIZ+GR*RJ/AM2)*AM4*A4+AM2*A2*STR*CKR
      RK(1,2)=CKR*(ER*RIZ+GR*RJ)*AM2*A3
      RK(2,1)=RK(1,2)
      RK(2,2)=CKR*(ER*RIZ+AM2*GR*RJ)*A2
      RM(1,1)=CMR*RØR*(RA+RIZ*AM2*A2)
      RM(1,2)=0.0
      RM(2,1)=0.0
      RM(2,2)=CMR*RØR    *(RIX+RIZ)
      TT(1,1)=1.0
      TT(1,2)=-E1
      TT(2,1)=0.0
      TT(2,2)=1.0
      CALL TRIMUL(TT,RK,CR,DR,2,2,2,2,2)
      CALL TRIMUL(TT,RM,CR,DR,2,2,2,2,2)
C     ******************************************************
C     *  ASSEMBLE THE R I M  MATRICES INTØ  T H E  SYSTEM MATRICES*
C     ******************************************************
      DO 40 I=1,2
      II=NTD-2+I
      DØ 40 J=1,2
      JJ=NTD-2+J
      SK(II,JJ)=SK(II,JJ)+RK(I,J)
   40 SM(II,JJ)=SM(II,JJ)+RM(I,J)
   SO RETURN
    2 FØRMAT(5X,I5,5E13.6/)
      E N D
```

D.4.3 Subroutines used in PROGRAM-3

```
C     ****************************************************
C     *                                                  *
C     *  MAIN-3 --MAIN PRØGRAM OF PRØGRAM3               *
C     *                                                  *
C     ****************************************************
C     *  THIS IS A GENERAL PRØGRAMTØ BE USED INTHE       *
C     *  ANALYSIS ØF BLADED RØTØRS.  TRANSVERSE SHEAR AND *
C     *  RØTARYINERT IA ARE INCLUDEDBØTH IN THE DISC AND *
C     *  BLADES. ØPTIØNS FACILITATING THE USE OF THIS    *
C     *  PRØGRAMFØR THE VIBRATIØN ANALYS IS ØF EITHER THE *
C     *  ENT IRE RØTØR SYSTEM ØR ITS CØMPØNENT PARTS MAY BE *
C     *  SPECIFIES. VARIABLE DIMENSIØNS ARE USED REQUIRING *
C     *  THE CHANGINGØF THE DIMENSIØNS ØNLY IN THE MAIN *
C     *  PRØGRAM AT ANY TIMEANDSPECIFYING THE APPRØPRIATE*
C     *  VALUES SF MS1ANDMS2.                            *
C     ****************************************************
      DIMENSIØN SK(49,49),SM(49,49),SKB(35,35),SMB(35,35)
      DIMENSIØN     R(49),T(49),TE(49),W(49),P(49)
      DIMENSIØN BB(49),BD(49),BX(49),SIG(49),ANG(49),ARA(49),BKG(49)
      DIMENSIØN SGR(49),SGT(49)
      DIMENSIØN      D(49,49),F(49,49),B(49),C(49),X(49)
      DIMENSIØN ERR(49),B7(49),B8(49),B9(49),FR(20,10)
      CØMMØN/ØPTIØN/IØPT,IRNG,ITHD,ITED,ITHB, I STB
      CØMMØN/ØNE/AM,AM2,AM4,AMPR
      CØMMØN/TWØ/S1,S2,S3,S4,CKD,CKR,CMD,CMR, CC, CCC, CK, C?, CT, CSD,CSR
      CØMMØN/THRE/RDI,RDØ,RRI,RRØ,RTI,RTØ,E1,E2,RIZ,RIX,RJ
      CØMMØN/FØUR/PI,ED,ER,EB,RØD,RØR,RØB,ALD,ALR,PRD,PRR,PRB,SCB
      CØMMØN/FIVE/SRI,SRØ,ØMGA
      CØMMØN/SIX/CØNST,M,NF
      EQUIVALENCE (SK,F)
      MS1=49
      MS2=35
   15 CØNTINUE
C     ****************************************************
C     *  READ GENERAL ØPTIØN,RIMØPTIØN, AND NUMBER ØF    *
C     *  FREQUENCIES REQUIRED FØREACH DIAMETRAL NØDE.    *
C     ****************************************************
      READ 12, IØPT,IRNG,NF
      PRINT 12, IØPT,IRNG,NF
```

```
C     ****************************************************
C     *  READ SPEED ØF RØTATIØN ØF THE RØTØR IN RAD./SEC.  *
C     ****************************************************
      READ 6,ØMGA
      PRINT6,ØMGA
      GØ TØ(20,50,20,21),IØPT
C     ****************************************************
C     *  READ FINAL AND STARTING VALUES ØF NØDAL DIAMETERS *
C     ****************************************************
   20 READ 12,ND,MDS
      PRINT12,ND,MDS
C     ****************************************************
C     *  READ NUMBER ØF DISC ELEMENTS, DISC ØPTIØNS, DISC  *
C     *  MATERIAL PRØPERTIES AND BØUNDARY LØADING.         *
C     ****************************************************
   21 READ 12,NDE,ITED
      PRINT12,NDE,ITED
      READ 6,ED,RØD,PRD,ALD,SCD
      PRINT6,ED,RØD,PRD,ALD,SCD
      READ 10,SRI,SRØ
      PRINT10,SRI,SRØ
      NSD=NDE+1
      NPD=2*NDE
      NTD=4*NSD
      IF(IRNG.NE.0) NTD=4*(NSD+1)
C     ****************************************************
C     *  READ DISC DIMENSIØNS                              *
C     ****************************************************
      READ 10,(R(I),I=1,NPD)
      PRINT10,(R(I),I=1,NPD)
      READ 10,(T(I),I=1,NPD)
      PRINT10,(T(I),I=1,NPD)
      RDI=R(1)
      RDØ=R(NPD)
      IF(ITED.EQ.0) GØ TØ 49
C     ****************************************************
C     *  READ TEMPERATURE GRADIENT ØF THE DISC             *
C     ****************************************************
      READ 10,(TE(I),I=1,NPD)
      PRINT10,(TE(I),I=1,NPD)
   49 GØ TØ(70,50,50,70),IØPT
   50 CØNTINUE
C     ****************************************************
C     *  READ NUMBER ØF BLADE ELEMENTS, NUMBER ØF BLADES,  *
C     *  AND BLADE ØPTIØNS                                 *
C     ****************************************************
      READ 12,NBE,NB,ISTB,IBDE
      PRINT12,NBE,NB,ISTB,IBDE
      NSB=NBE+1
      NTB=7*NSB
C     ****************************************************
C     *  READ BLADE MATERIAL PRØPERTIES                    *
C     ****************************************************
      READ 6,EB,RØB,PRB,SCB
      PRINT6,EB,RØB,PRB,SCB
```

```
C      ****************************************************
G      *  READ BLADE DIMENSIONS                           *
G      ****************************************************
       READ 10,(BX(I),I=1,NSB)
       PRINT10, (BX(I ), I=1,NSB)
       READ 10,(BB(I),I=1,NSB)
       PRINT10,(BB(I),I=1,NSB)
       READ 10,(BD(I),I=1,NSB).
       PRINT10,(BD(I),I=1,NSB)
       READ 10,(ARA(I),I=1,NSB)
       PRINT10,(ARA(I),I=1,NSB)
       READ 10,(BKG(I),I=1,NSB)
       PRINT10,(BKG(I),I=1,NSB)
       READ 10,(ANG(I),I=1,NSB)
       PRINT10,(ANG(I),I=1,NSB)
       IF(ISTB.EQ.1) READ 6,(SIG(I),I=1,NSB)
       IF(ISTB.EQ.1) PRINT6,(SIG(I),I=1,NSB)
   70  IF(IRNG.EQ.0) GØ TØ 80
G      ****************************************************
C      *   IF RIM IS PRESENT,READ THE RIM MATERIAL PRØPER- *
G      *  TIES, DIMENSIØNS AND ELASTIC PRØPERTIES          *
G      ****************************************************
       READ 6,ER,RØR,PRR,ALR,SCR
       PRINT6,ER,RØR,PRR,ALR,SCR
       READ 10,RRI,RRØ,RTI,RTØ,RTEI,RTE3
       PRINT10,RRI,RRØ,RTI,RTØ,RTEI,RTEØ
       T(NPD+1)=RTI
       T(NPD+2)=RTØ
       TE(NPD+1)=RTEI
       TE(NPD+2)=RTEØ
       R(NPD+1)=RRI
       R(NPD+2)=RRØ
   80  CØNTINUE
       PI=3.14159265358979
       CØNST=0.5/PI
       S1=1./3.
       S2=1./6.
       S3=1./7.
       S4=1./9.
       GØ TØ(95,85,85,95),IØPT
   85  CØNTINUE
G      ****************************************************
G      *  CALCULATE BLADE SUBSYSTEM STIFFNESS AND MASS     *
G      *  MATRICES AND STØRE THEM                          *
G      ****************************************************
       GALL THKBDE(SKB,SMB,BX,BB,BD,ANG,SIG,ARA,BKG,NBE,IBDE,MS2)
       GØ TØ(95,90,95),IØPT
   90  CØNTINUE
       IF(IRNG.NE.0) GØ TØ   95
G      ****************************************************
C      *  CØMPUTE BLADE FREQUENCIES ACCØRDING TØ THE BLADE *
C      *  GENERAL OPTIØNS                                  *
C      ****************************************************
       IJK=1
       M=0
```

```
      IF(IBDE.NE.1)GØ TO 94
      DØ 91 I=3,3*NSB-1
      II=I-2
      DO 91 J=3,3*NSB-1
      JJ=J-2
      SK(II,JJ)=SKB(I,J)
   91 SM(II,JJ)=SMB(I,J)
      N1=3*NSB-3
      PRINT 1
      CALL EIGVAL(SK,SM,D,F,FR,B,C,X,ERR,B7,B8,B9,IJK,N1,MS1)
      DØ 92 I=3*NSB+3,6*NSB-1
      II=I-2-3*NSB
      DØ 92 J=3*NSB+3,6*NSB-1
      JJ=J-2-3*NSB
      SK(II,JJ)=SKB(I,J)
   92 SM(II,JJ)=SMB(I,J)
      PRINT 2
      CALL EIGVAL(SK,SM,D,F,FR,B,C,X,ERR,B7,B8,B9,IJK,N1,MS1)
      DØ 93 I=6*NSB+2,NTB
      II=I-1-6*NSB
      DØ 93 J=6*NSB+2,NTB
      JJ=J-1-6*NSB
      SK(II,JJ)=SKB(I,J)
   93 SM(II,JJ)=SMB(I,J)
      N1=NSB-1
      CALL EIGVAL(SK,SM,D,F,FR,B,C,X,ERR,B7,B8,B9,IJK,N1,MS1)
      GØ TO 15
   94 IF(IBDE.NE.2) GO TØ97
      NM=NTB
      DO 195 I=NBE,1,-1
      II=7*I
      CALL REDUCE(SKB,NM,II,1,MS2)
      CALL REDUCE(SMB,NM,II,1,MS2)
      NM=NM-1
  195 CØNTINUE
      CALL REDUCE (SKB,NM,6*NSB-3,1,MS2)
      CALL REDUCE(SMB,NM,6*NSB-3,1,MS2)
      CALL REDUCE(SKB,NM-1,4,2,MS2)
      CALL REDUCE(SMB,NM-1,4,2,MS2)
      CALL REDUCE(SKB,NM-3,1,2,MS2)
      CALL REDUCE(SMB,NM-3,1,2,MS)
      N1=NM-6
      PRINT 5
      GØTØ 99
   97 CØNTINUE
      NM=NTB
      CALL REDUCE(SKB,NM,7*NSB-1,      1,MS2)
      CALL REDUCE(SMB,NM,7*NSB-1,1,MS2)
      CALL REDUCE(SKB,NM-1,7*NSB-4,1,MS2)
      CALL REDUCE(SMB,NM-1,7*NSB-4,1,MS2)
      CALL REDUCE(SKB,NM-2,4,2,MS2)
      CALL REDUCE(SMB,NM-2,4,2,MS2)
      CALL REDUCE(SKB,NM-4,1,2,MS2)
      CALL REDUCE (SMB, NH-4,1,2,MS2)
```

```
      N1=NM-6
      PRINT 7
   99 CALL EIGVAL(SKB,SMB,D,F,FR,B,C,X,ERR,B7,B8,B9,IJK,N1,MS2)
      GØ TØ 15
   95 CØNTINUE
      CK=2.0*PI*ED/(1.0-PRD*PRD)
      CP=2.0*PI*RØD*ØMGA*ØMGA
      CT=2.0*PI*ED*ALD/(1.0-PRD)
C     *****************************************************
C     *  CALCULATE THE INITIAL STRESSES IN THE DISC DUE TØ *
C     *  RØTATIØN, TEMPERATURE GRADIENT AND ØTHER BØUNDARY *
C     *  LØADINGS                                          *
C     *****************************************************
      CALL INLSTR(SK,R,T,TE,W,P,SGR,SGT,NSD,MS1)
      IF(IØPT.EQ.4) CALL EXIT
      NT =NTD
      IF(IØPT.EQ.3) NT=NTD+NTB-6
      IJK=1
      M=MDS-1
      IF(IØPT.EQ.3)      Z=NB
  100 CØNTINUE
C     *****************************************************
C     *  SELECT NUMBER OF NØDAL DIAMETERS                  *
C     *****************************************************
      M=M+1
      PRINT 3,M
      FRC-1.0
      IF(M.EQ.0) FAC=2.0
      CKD=FAC*PI*ED/(1.0-PRD*PRD)/12.0
      CMD=FAC*PI*RØD
      IF(IRNG.EQ.1) CKR=FAC*PI*ER/(1.0-PRR*PRR)/12.0
      IF(IRNG.EQ.1) CMR=FAC*PI*RØR
      IF(IØPT.EQ.3) CC=Z*FAC/2.0
      CCC=FAC*PI
      CSD=0.5*PI*FAC*ED/SCD/(1.0+PRD)
      IF(IRNG.NE.0) CSR=0.5*PI*FAC*ER/SCR/(1.0+PRR)
      AM=M
      AM2 =AM*AM
      AM4=AM2*AM2
      AM6 =AM4 *AM2
      AMPR =AM2 *PRD
      DØ 105 I=1,NT
      DØ 10.5 J=1,NT
      SK(I,J)=0.0
  105 SM(I,J)=0.0
C     *****************************************************
C     *  CALCULATE DISC SUBSYSTEM STIFFNESS AND MASS       *
C     *  MATRICES AND STØRE THEM                           *
C     *****************************************************
      CALL  THKDSC(SK,SM,R,T,SGR,SGT,NSD,MS1)
```

```
C       ***************************************************
C       *  GET THE SYSTEM STIFFNESS  AND  MASS MATRICES FROM   *
C       *  THE SUBSYSTEM MATRICES                              *
C       ***************************************************
        IF(IØPT.EQ.3) CALL THKSYS(SK,SM,SKB,SMB,
       .CC,RDØ,RRØ,NTD,NTB,MS1,MS2)
C       ***************************************************
C       *  APPLY BØUNDARY CØNDITIØNS                           *
C       ***************************************************
        CALL REDUCE(SK,NT,NT-1,1,MS1)
        CALL REDUCE(SM,NT,NT-1,1,MS1)
        IF(IØPT.EQ.1) GØ TØ 110
        CALL REDUCE(SK,NT-1,NT-4,1,MS1)
        CALL REDUCE(SM,NT-1,NT-4,1,MS1)
        CALL REDUCE(SK,NT-2,1,2,MS1)
        CALL REDUCE(SM,NT-2,1,2,MS1)
        N1=NT-4
        GØ TØ 120
  110   CONTINUE
        CALL REDUCE(SK,NT-1,3,1,MS1)
        CALL REDUCE(SM,NT-1,3,1,MS1)
        N1=NT-2
  120   CØNTINUE
C       ***************************************************
C       *  SØLVE THE EIGENVALUE PRØBLEM AND GET THE SYSTEM     *
C       *  FREQUENCIES                                         *
C       ***************************************************
        CALL EIGVAL(SK,SM,D,F,FR,B,C,X,ERR,B7,B8,B9,IJK,N1,MS1)
        IF(M.LT.ND) GØ TØ 100
        GØ TØ 15
  200   CALL EXIT
    1   FØRMAT(1H1,5X,'BLADE BENDING FREQUENCIES IN I-MIN DIRECTIØN'//)
    2   FØRMAT(1H1,5X,'BLADE BENDING FREQUENCIES IN I-MAX DIRECTIØN'//)
    3   FØRMAT (///, 27HNUMBER ØF NØDAL DIAMETERS =, I3// )
    4   FØRMAT(1H1,5X,' BLADE TØRTIØNAL FREQUENCIES '//)
    5   FØRMAT(1H1,5X,'TWISTED BLADE BENDING FREQUENCIES'//)
    6   FØRMAT(4F20.10)
    7   FØRMAT(1H1,5X,' BLADE FREQUENCIES WITH INITIAL STRESSES '//)
   10   FØRMAT(8F10.6)
   11   FØRMAT(/8E13.6)
   12   FØRMAT(16I5)
        END
```

```
      SUBRØUTINE THKBDE(SKB,SMB,BX,BB,BD,ANG,SIG,ARA,BKG,NBE,IBDE,L)
C     ****************************************************
C     * THIS SUBRØUTINE CALCULATES THE BLADE SUBSYSTEM    *
C     * STIFFNESS MATRIX SKB(L,L) AND MASS MATRIX SMB(L,L)*
C     * TRANSVERSE SHEAR AND RØTARY INERTIA ARE INCLUDED  *
C     * ADDITIØNAL STIFFNESS DUE TØ INITIAL STRESSES CAN  *
C     * ALSO BE INCLUDED                                  *
C     ****************************************************
      DIMENSIØN SKB(L,L),SMB(L,L),EK(14,14),EM(14,14)
      DIMENSIØN R(14,14),B(14,14),C(14,14),D(14,14)
      DIMENSIØN BX(L),BB(L),BD(L),ANG(L),SIG(L)
      CØMMØN/FØUR/PI,ED,ER,EB,RØD,RØR,RØB,ALD,ALR,PRD,PRR,PRB,SCB
      CØMMØN/FIVE/SRI,SRØ,ØMGA
      RX(I,AI)=ALFS*ALFA*XX(I+1,AI+1.0)+(ALFS*BETA+BETS*ALFA)*
     .XX(I+2,AI+2.0)+BETS*BETA*XX(I+3,AI+3.0)
      SX(I,AI)=RØB*ØMGA*ØMGA*(ALFA*XX(I+1,AI+1.0)+BETA*XX(I+2,AI+2.0))
      XS(I,AI)=YYY*(ALFA*XX(I+1,AI+1.0)+BETA*XX(I+2,AI+2.0))
      XR(I,AI)=XXX*(AL*XX(I+1,AI+1.0)+BE*XX(I+2,AI+2.0))
      XX(I,AI)=(BX2**I-BX1**I)/AI
      NTB=7*(NBE+1)
      DØ 10 I=1,NTB
      DØ 10 J=1,NTB
      SKB(I,J)=0.0
   10 SMB(I,J)=0.0
      PRINT 1
      K=0
   20 CØNTINUE
      DØ 15 I=1,14
      DØ 15 J=1,14
      B(I,J)=0.0
      EK(I,J)=0.0
      EM(I,J)=0.0
   15 R(I,J)=0.0
C     ****************************************************
C     * SELECT THE NUMBER K ØF THE ELEMENT AND GET THE    *
C     * VALUES OF SECTIØN PRØPERTIES OF THE BLADE AT THE  *
C     * ENDS ØF THE ELEMENT                               *
C     ****************************************************
      K=K+1
      KP1=K+1
      BX1=BX(K)
      BX2=BX(KP1)
      ARA1=ARA(K)
      ARA2=ARA(KP1)
      ANG1=ANG(K)
      ANG2=ANG(KP1)
      PRINT 2,K,BX1,BX2
      SIG1=SIG(K)
      SIG2=SIG(KP1)
      BA=0.5*(ANG1+ANG2)
```

```
      SN=SIN(BA/180.0*PI)
      CS=COS(BA/180.0*PI)
    GB=0.5*EB/(1  .0+PRB)
      BMI1=BB(K)
      BMI2=BB(KP1)
      BMX1=BD (IO
      BMX2=BD(KP1)
      BJ 1=BKG(K)
      B J2=BKG(KP1)
      EL=BX2 -3X1
    ALFS=(BX2*SIG1-BX1*SIG2)/EL
      BETS=(SIG2-SIG1 )/EL
      ALFA=(BX2*ARA1-BX1*ARA2)/EL
      BETA= (ARA2-ARA1) /EL-
      ALFJ=(BX2*BJ1-BX1*BJ2)/EL
      BETJ=(BJ2-BJ1 )/EL
      ALIU=(BX2*BMI1-BX1*BMI2 >/EL
      BEIU=(BMI2-BMI1 >/EL
      ALIW=(BX2*BMX1-BX1*BMX2 )/EL
      BEIW=(BMX2-BMX1)/EL
C     ***************************************************************
C     *  CALCULATE THE '3' MATRIX                                   *
C     ***************************************************************
      B(1,1)=1.0
      B(1,2)=BX1
      B(1,3)=BX1*BX1
      B(1,4)=BX1*BX1*BX1
      B(2,2)=-1.0
      B(2,3)=-2.0*BX1
      B(2,4)=-3.0*BX1*BX1
      B(2,5)=1.0
      B(2,6)=BX1
      B(3,5)=1.0
      B(3,6)=BX1
      B(4,1)=1.0
      B(4,2)=BX2
      B(4,3)=BX2*BX2
      B (4,4)=BX2*BX2*BX2
      B(5,2)=-1.0
      B(5,3)=-2.0*BX2
      B(5,4)=-3.0*BX2*BX2
     B(5,5)=1.0
      B(5,6)=BX2
      B(6,5)=1.0
      B(6,6)=BX2
      DO 25 I=1,6
      II=I+6
      DO 25 J=1,6
      JJ= J+6
   25 B(II,JJ)=B(I,J)
      B(13,13)=1.0
      B(13,14)=BX1
      B(14,13)=1.0
      B(14,14)=BX2
      CALL INVT(B,14,14)
```

```
C     ******************************************************
C     *  CALCULATE THE RØTATIØN MATRIX R                   *
C     ******************************************************
      R(1,1)=CS
      R(2,2)=CS
      R(3,3)=CS
      R(4,8)=CS
      R(5,9)=CS
      R(6,10)=CS
      R(7,4)=CS
      R(8,5)=CS
      R(9,6)=CS
      R(10,11)=CS
      R(10,11)=CS
      R(11,12)=CS
      R(12,13)=CS
      R(1,4)=SN
      R(2,5)=SN
      R(3,6)=SN
      R(4,11)=SN
      R(5,12)=SN
      R(6,13)=SN
      R(7,1)=-SN
      R(8,2)=-SN
      R(9,3)=-SN
      R(10,8)=-SN
      R(1 1,9)=-SN
      R(12, IO)=-SN
      R(13,7)=1 .O
     R(14,14)=1  .0
C     ******************************************************
C     *  CALCULATE THE ELEMENT STIFFNESS MATRIX EK         *
C     ******************************************************
      KKK=0
      AL=ALIU
      BE=BEIU
      I=0
      J=O
      XXX=EB
      YYY=GB/SCB
   30 CØNT INUE
      KKK=KKK+1
      EK(I+3,   J+3)=4.0*XR(0,0.0)
      EK(I+3,J+4)=12.0*XR(1,1.0)
      EK(I+3,J+6)=-2.0*XR(0,0.0)
      EK(I+4,J+4)=36.0*XR(2,2.0)
      EK(I+4,J+6)=-6.0*XR(1,1.0)
      EK(I+5,J+5)=XS(0,0.0)
      EK(I+5,J+6)=XS(1,1.0)
      EK(I+6,J+6)=XR(0,0.0)+XS(2,2.0)
      IF(KKK.EQ.2)GØ TØ  3 5
      I=6
      J=6
```

```
      AL=ALIW
      BE=BEIW
      GØ TØ 30
   35 CØNTINUE
      EK(14,14)=GB*(ALFJ*XX(1,1.0)+BETJ*XX(2,2.0))
C     ***************************************************
C     *  CALCULATE THE ELEMENT MASS MATRIX EM            *
C     ***************************************************
      KKK=0
      I=0
      J=O
      AL=ALIU
      BE=BEIU
      XXX=RØB
      YYY=RØB
   40 CØNTINUE
      KKK=KKK+1
      EM(I+1,J+1)=XS(0,0.0)
      EM(I+1,J+2)=XS(1,1.0)
      EM(I+1,J+3)=XS(2,2.0)
      EM(I+1,J+4)=XS(3,3.0)
      EM(I+2,J+2)=XS(2,2.0)+XR(0,0.0)
      EM(I+2,J+3)=XS(3,3.0)+2.0*XR(1,1.0)
      EM(I+2,J+4)=XS(4,4.0)+3.0*XR(2,2.0)
      EM(I+2,J+5)=-XR(0,0.0)
      EM(I+2,J+6)=-XR(1,1.0)
      EM(I+3,J+3)=XS(4,4.0)+4.0*XR(2,2.0)
      EM(I+3,J+4)=XS(5,5.0)+6.0*XR(3,3.0)
      EM(I+3,J+5)=-2.0*XR(1,1.0)
      EM(I+3,J+6)=-2.0*XR(2,2.0)
      EM(I+4,J+4)=XS(6,6.0)+9.0*XR(4,4.0)
      EM(I+4,J+5)=-3.0*XR(2,2.0)
      EM(I+4,J+6)=-3.0*XR(3,3.0)
      EM(I+5,J+5)=XR(0,0.0)
      EM(I+5,J+6)=XR(1,1.0)
      EM(I+6,J+6)=XR(2,2.0)
      IF(KKK.EQ.2) GO TØ 45
      AL=AL IW
      BE=BEIW
      I=6
      J=6
      GØTØ 40
   45 CØNTINUE
      AL=(ALIU+ALIW)*RØB
      BE=(BEIU+BEIW)*RØB
      EM(13,13)=AL*XX(1,1.0)+BE*XX(2,2.0)
      EM(13,14)=AL*XX(2,2.0)+BE*XX(3,3.0)
      EM(14,14)=AL*XX(3,3.0)+BE*XX(4,4.0)
      DØ 50 I=1,13
      II=I+1
      DØ 50 J=II,14
      EK( JP I)=EK(I, J)
   50 EM(J,I)=EM(I,J)
```

```
      CALL TRIMUL(B,EK,C,D, 14, 14,14,14,14)
      CALL TRIMUL(B,EM,C,D, 14, 14, 14, 14, 14)
C     *****************************************************
C     *  STØRE THE ELEMENT MATRICES INTØ THE BLADE SYSTEM*
C     *  MATRICES IN THE APPRØPRIATE PØSITIØNS ACCØRDING TØ*
C     *  THE BLADE GENERAL ØPTIØN                          *
C     *****************************************************
      IF(IBDE.NE.1) GØ TØ 60
      KK=3*(K-1)
      CALL ASMBLE(SKB,EK,KK,KK,1,6,14,L)
      CALL ASMBLE(SMB,EM,KK,KK,1,6,14,L)
      KK=3*(NBE+1)+3*(K-1)
      CALL ASMBLE(SKB,EK,KK,KK,7,12,14,L)
      CALL ASMBLE(SMB,EM,KK,KK,7,12,14,L)
      KK=6*(NBE+1)+K-1
      CALL ASMBLE(SKB,EK,KK,KK,13,14,14,L)
      CALL ASMBLE(SMB,EM,KK,KK,13,14,14,L)
      IF(K.LT.NBE) GØ TØ 20
      RETURN
   60 CØNTINUE
      CALL TRIMUL(R,EK,C,D, 14, 14, 14, 14, 14)
      CALL TRIMUL(R,EM,C,D,14,14,14,14, 14)
      IF(ØMGA.EQ.0.0) GO TO 80
      DØ 70 I=1,14
      DØ 70 J=1,14
      B(I,J)=0.0
   70 R(I,J)=0.0
C     *****************************************************
C     *  CALCULATE ADDITIØNAL STIFFNESS VALUES IF INITIAL*
C     *  STRESSES ARE PRESENT                              *
C     *****************************************************
      B(1,1)=1.0
      B(1,2)=BX1
      B(1,3)=BX1*BX1
      B(1,4)=BX1*BX1*BX1
      B(2,2)=-1.0
      B(2,3)=-2.0*BX1
      B(2,4)=-3.0*BX1*BX1
      B(2,5)=1.0
      B(2,6)=BX1
      B(3,5)=1.0
      B(3,6)=BX1
      B(4,7)=1.0
      B(4,8)=BX1
      B(4,9)=BX1*BX1
      B(4,10)=BX1*BX1*BX1
      B(5,8)=1.0
      B(5,9)=-2.0*BX1
      B(5,10)=-3.0*BX1*BX1
      B(5,11)=1.0
      B(5,12)=BX1
      B(6,11)=1.0
      B(6,12)=BX1
      B(7,13)=1.0
```

```
      B(7,14)=BX1
      B(8,1)=1.0
      B(8,2)=BX2
      B(8,3)=BX2*BX2
      B(8,4)=BX2*BX2*BX2
      B(9,2)=-1.0
      B(9,3)=-2.0*BX2
      B(9,4)=-3.0*BX2*BX2
      B(9,5)=1.0
      B(9,6)=BX2
      B(10,5)=1.0
      B(10,6)=BX2
      B(11,7)=1.0
      B(11,8)=BX2
      B(11,9)=BX2*BX2
      B(11,10)=BX2*BX2*BX2
      B(12,8)=-1.0
      B(12,9)=-2.0*BX2
      B(12,10)=-3.0*BX2*BX2
      B(12,11)=1.0
      B(12,12)=BX2
      B(13,11)=1.0
      B(13,12)=BX2
      B(14,13)=1.0
      B(14,14)=BX2
      R(1,1)=-SX(0,0.0)
      R(1,2)=-SX(1,1.0)
      R(1,3)=-SX(2,2.0)
      R(1,4)=-SX(3,3.0)
      R(2,2)=RX(0,0.0)-SX(2,2.0)
      R(2,3)=2.0*RX(1,1.0)-SX(3,3.0)
      R(2,4)=3.0*RX(2,2.0)-SX(4,4.0)
      R(3,3)=4.0*RX(2,2.0)-SX(4,4.0)
      R(3,4)=6.0*RX(3,3.0)-SX(5,5.0)
      R(4,4)=9.0*RX(4,4.0)-SX(6,6.0)
      R(8,8)=RX(0,0.0)
      R(8,9)=2.0*RX(1,1.0)
      R(8,10)=3.0*RX(2,2.0)
      R(9,9)=4.0*RX(2,2.0)
      R(9,10)=6.0*RX(3,3.0)
      R(10,10)=9.0*RX(4,4.0)
      R(13,13)=-RØB*ØMGA*ØMGA*CØS(2.0*BA)*((ALFW+ALFU)*XX(1,1.0)
     .+(BETW+BETU)*XX(2,2.0))
      R(13,14)=-RØB*ØMGA*ØMGA*CØS(2.*BA)*((ALFW+ALFU)*XX(2,2.0)+(BETW+
     .BETU)*XX(3,3.0))
      R(14,14)=-RØB*ØMGA*ØMGA*CØS(2.*BA)*((ALFW+ALFU)*XX(3,3.0)+(BETW+
     .BETU)*XX(4,4.0))
     .+ALFS*ALFJ*XX(1,1.0)+(ALFS*BETJ+BETS*ALFJ)*XX(2,2.0)
     .+BETS*BETJ*XX(3,3.0)
      CALL TRIMUL(B,R,C,D,14,14,14,14,14)
      DØ 80 I=1,14
      DØ 80 J=1,14
      EK(I,J)=EK(I,J)+R(I,J)
   80 CØNT INUE
```

```
      KK=7*(K-1)
      CALL ASMBLE(SKB,EK,KK,KK,1,14,14,L)
      CALL ASMBLE(SMB,EM,KK,KK,1,14,14,L)
      IF(K.LT.NBE)GØ TO 20
      RETURN
    1 FØRMAT(1H1,//5X,'BLADE DIMENSIØNS'//)
    2 FØRMAT(5X,I5,8F8.3/)
    3 FØRMAT(7E13.5)
      END
```

```
      SUBRØUTINE THKDSC(SK,SM,R,T,SRR,STT,NSD,L)
C     ***************************************************
C     *  THISSUBRØUTINE CALCULATES THEELEMENT STIFFNESS *
C     *  AND MASSMATRICESANDSTØRESTHE VALUES INTO TEE *
C     *  DISC SUBSYSTEMMATRICES SK(L,L) AND SM(L,L)      *
C     *  THE ADDITIØNAL STIFFNESS CØEFFICIENTS DUE TØ    *
C     *  INITIAL STRESSESSRR(L) AND STT(L) ARE ALSO      *
C     *  CALCULATED AND ADDED TØTHEBENDING STIFFNESS .   *
C     *  TRANSVERSE SHEARANDRØTARYINERT IA ARE INCLUDED.*
C     *  BEFØRE ENTERING THESUBRØUTINE ZERO ALL THE TERMS*
C     *  OF THE MATRICESSK AND SM. INITIALISE ALL THE    *
C     *  TERNS ØFTHE RADIUS ANDTHICKNESS VECTOR R AND T. *
C     ***************************************************
      DIMENSIØN SK(L,L),SM(L,L),R(L),T(L)
      DIMENSIØN SRR(L),STT(L),ES(8,8)
      DIMENSIØN EK(8,8),EM(8,8),B(8,8),C(8,8),D(8,8)
      CØMMØN/ØPTIØN/IØPT,IRNG, ITHD, ITED, ITH3, ISTB
      CØMMØN/ØNE/AM,P2,P1,P3
      CØMMØN/TWØ/S1,S2,S3,S4,CKD,CKR,CMD,CMR,CC,CCC,CKK,CP,CT,CSD,CSR
      CØMMØN/FØUR/PI,ED,ER,EB,RØD,RØR,RØB,ALD,ALR,PRD,PRR,PRB,SCB
      K=0
      NS-NSD'
      IF(IRNG.EQ.1)NS=NSD+1
      N=NS-1
      PR=PRD
      CK=CKD
      CM=CMD
      CS=CSD
   30 CØNT INUE
C     ***************************************************
C     *  SELECT THENUMBERKØF THE ELEMENT                 *
C     ***************************************************
      K=K+1
      K1=2*K-1
      K2=2*K
C     ***************************************************
C     *  GET THE VALUES ØF 'RADIUS ANDTHICKNESS AT NØDES *
C     ***************************************************
      R1=R(K1)
      R2=R(K2)
      T1=T(K1)
      T2=T(K2).
      DØ 40 I=1,8
      DO 40 J=1,8
      B(I,J)=0.0
      EK(I,J)=0.0
   40 EM(I,J)=0.0
      IF(K.NE.NSD) GØTØ 42
      PR=PRR
```

```
      P3=PRR*P2
      CK=CKR
      CM=CMR
      CS=CSR
   42 CØNTINUE
      DD=R2-R1
      D1=DD*DD
      D2=D1*DD
      ALFA=(R2*T1-R1*T2)/DD
      BETA= (T2-T1)/DD
      X1=ALFA*ALFA*ALFA*CK
      X2=ALFA*ALFA*BETA*CK
      X3=ALFA*BETA*BETA*CK
      X4=BETA*BETA*BETA*CK
C     ******************************************************
C     *  CALCULATE THE 'B' MATRIX                          *
C     ******************************************************
      B(1,1)=1.0
      B(1,2)=R1
      B(1,3)=R1*R1
      B(1,4)=R1*R1*R1
      B(2,2)=-1.0
      B(2,3)=-2.0*R1
      B(2,4)=-3.0*R1*R1
      B(2,5)=1.0
      B(2,6)=R1
      B(3,5)=1.0
      B(3,6)=R1
      B(4,7)=1.0
      B(4,8)=R1
      B(5,1)=1.0
      B(5,2)=R2
      B(5,3)=R2*R2
      B(5,4)=R2*R2*R2
      B(6,2)=-1.0
      B(6,3)=-2.0*R2
      B(6,4)=-3.0*R2*R2
      B(6,5)=1.0
      B(6,6)=R2
      B(7,5)=1.0
      B(7,6)=R2
      B(8,7)=1.0
      B(8,8)=R2
      CALL INVT(B,8,8)
C     ******************************************************
C     *  CALCULATE THE 'SMALLK'MATRIX                      *
C     ******************************************************
      A1=R1*R2
      A2=A1*A1
      A3=R2-R1
      A4=R2**2-R1**2
      A5=R2**3-R1**3
      A6=R2**4-R1**4
      A7=R2**5-R1**5
```

```
A8=R2**6-R1**6
A9=R2**7-R1**7
A10=R2**8-R1**8
A11=R2**9-R1**9
A12=R2**10-R1**10
C5=ALØG(R2/R1)
E1=X1*.5*A4/A2+X2*3.*A3/A1+X3*3.*C5+X4*A3
E2=X1*A3/A1+X2*3.*C5+X3*3.*A3+X4*.5*A4
E3=X1*C5+X2*3.*A3+X3*1.5*A4+X4*S1*A5
E4=X1*A3+X2*1.5*A4+X3*A5+X4*.25*A6
E5=X1*.5*A4+X2*A5+X3*.75*A6+X4*.2*A7
E6=X1 *S1 *A5+X2*.75*A6+X3*.6*A7+X4*S2*A8
E7=X1*.25*A6+X2*.6*A7+X3*.5*A8+X4*S3*A9
EK(1,1)=E1*(P1+2.*P2-2.*P3)
EK(1,2)=E2*(P1-P2)
EK(1,3)=E3*(P1-4.*P2)
EK(1,4)=E4*(P1-7.*P2-2.*P3)
EK(2,2)=E3*(P1-2.*P2+1.)
EK(2,3)=E4*(P1-3.*P2-2.*P3+2.*PR+2.)
EK(2,4)=E5*(P1-4.*P2+3.-6.*P3+6.*PR)
EK(3,3)=E5*(P1-2.*P2+8.-6.*P3+8.*PR)
EK(3,4)=E6*(P1-P2+18.-12.*P3+18.*PR)
EK(4,4)=E7*(P1+2.*P2+45.-20.*P3+36.*PR)
EK(1,5)=E2*(2.0*P2-P3)
EK(1,6)=E3*2.0*P2
EK(1,7)=E2*(P2*AM-AM*PR+AM)
EK(1,8)=E3*P2*AM
EK(2,5)=E3*(P2-1.0)
EK(2,6)=E4*(P2+P3-PR-1.0)
EK(2,7)=E3*(P2*AM-AM)
EK(2,8)=E4*(P2*AM-AM)
EK(3,5)=E4*(P3-2.0*PR-2.0)
EK(3,6)=E5*(2.0*P3-4.0*PR-4.0)
EK(3,7)=E4*(P2*AM-AM*PR-3.0*AM)
EK(3,8)=E5*(P2*AM-2.0*AM*PR-2.0*AM)
EK(4,5)=E5*(2.0*P3-P2-6.0*PR-3.0)
EK(4,6)=E6*(3.0*P3-P2-9.0*PR-9.0)
EK(4,7)=E5*(P2*AM-5.0*AM-4.0*AM*PR)
EK(4,8)=E6*(P2*AM-6.0*AM*PR-3.0*AM)
EK(5,5)=E3*(1.0-0.5*P3+0.5*P2)
EK(5,6)=E4*(1.0+PR-0.5*P3+0.5*P2)
EK(5,7)=E3*(1.5*AM-0.5*AM*PR)
EK(5,8)=E4*AM
EK(6,6)=E5*(2.0+2.0*PR-0.5*P3+0.5*P2)
EK(6,7)=E4*(1.5*AM+0.5*AM*PR)
EK(6,8)=E5*(AM+AM*PR)
EK(7,7)=E3*(P2+0.5-0.5*PR)
EK(7,8)=E4*P2
EK( 8, 8)=E5*P2
X1 =ALFA*CS
X2=BETA*CS
E1 =X1*0.5*A4+X2*S1*A5
E2=X1*S1*A5+X2*0.25*A6
```

```
      E3=X1*0.25*A6+X2*0.2*A7
      EK(5,5)=EK(5,5)+E1
      EK(5,6)=EK(5,6)+E2
      EK(6,6)=EK(6,6)+E3
      EK(7,7)=EK(7,7)+E1
      EK(7,8)=EK(7,8)+E2
      EK(8,8)=EK(8,8)+E3
C     *****************************************************
C     *  CALCULATE  ADDITIØNAL STIFFNESS FØR INITIAL  STRESS *
C     *****************************************************
      CA=(R2*SRR(K1)-R1*SRR(K2))/DD
      DA=(SRR(K2)-SRR(K1))/DD
      EE=(R2*STT(K1)-R1*STT(K2))/DD
      FF=(STT(K2)-STT(K1))/DD
      X1=CCC*ALFA*EE*P2
      X2=CCC*P2*(ALFA*FF+BETA*EE)
      X3=CCC*BETA*FF*P2
      E1=X1*C5+X2*A3+0.5*X3*A4
      E2=X1*A3+0.5*X2*A4+S1*X3*A5
      E3=0.5*X1*A4+S1*X2*A5+0.25*X3*A6
      E4=S1*X1*A5+0.25*X2*A6+0.2*X3*A7
      E5=0.25*X1*A6+0.2*X2*A7+S2*X3*A8
      E6=0.2*X1*A7+S2*X2*A8+S3*X3*A9
      E7=S2*X1*A8+S3*X2*A9+0.125*X3*A10
      X1=CCC*ALFA*CA
      X2=CCC*(ALFA*DA+BETA*CA)
      X3=CCC*BETA*DA
      F1=0.5*X1*A4+S1*X2*A5+0.25*X3*A6
      F2=S1*X1*A5+0.25*X2*A6+0.2*X3*A7
      F3=0.25*X1*A6+0.2*X2*A7+S2*X3*A8
      F4=0.2*X1*A7+S2*X2*A8+S3*X3*A9
      F5=S2*X1*A8+S3*X2*A9+0.125*X3*A10
      ES(1,1)=E1
      ES(1,2)=E2
      ES(1,3)=E3
      ES(1,4)=E4
      ES(2,2)=E3+F1
      ES(2,3)=E4+2.0*F2
      ES(2,4)=E5+3.0*F3
      ES(3,3)=E5+4.0*F3
      ES(3,4)=E6+6.0*F4
      ES(4,4)=E7+9.0*F5
C     *****************************************************
C     *  CALCULATE THE 'SMALL II' MATRIX                  *
C     *****************************************************
      X1=CM/12.0*ALFA*ALFA*ALFA
      X2=CM/12.0*ALFA*ALFA*BETA*3.0
      X3=CM/12.0*ALFA*BETA*BETA*3.0
      X4=CM/12.0*BETA*BETA*BETA
      ALFA=ALFA*CM
      BETA=BETA*CM
      EM(1,1)=ALFA*.5*A4+BETA*S1*A5
      EM(1,2)=ALFA*S1*A5+BETA*.25*A6
```

```
      EM(1,3)=ALFA*.25*A6+BETA*.2*A7
      EM(1,4)=ALFA*.2*A7+BETA*S2*A8
      EM(2,2)=EM(1,3)
      EM(2,3)=EM(1,4)
      EM(2,4)=ALFA*S2*A8+BETA*S3*A9
      EM(3,3)=EM(2,4)
      EM(3,4)=ALFA*S3*A9+BETA*.125*A10
      EM(4,4)=ALFA*.125*A10+BETA*S4*A11
      E3=X1*C5+X2*A3+0.5*X3*A4+S1*X4*A5
      E4=X1*A3+0.5*X2*A4+S1*X3*A5+0.25*X4*A6
      E5=0.5*X1*A4+S1*X2*A5+0.25*X3*A6+0.2*X4*A7
      E6=S1*X1*A5+0.25*X2*A6+0.2*X3*A7+S2*X4*A8
      E7=0.25*X1*A6+0.2*X2*A7+S2*X3*A8+S3*X4*A9
      E8=0.2*X1*A7+S2*X2*A8+S3*X3*A9+0.125*X4*A10
      E9=S2*X1*A8+S3*X2*A9+0.125*X3*A10+S4*X4*A11
      EM(1,1)=EM(1,1)+E3*P2
      EM(1,2)=EM(1,2)+E4*P2
      EM(1,3)=EM(1,3)+E5*P2
      EM(1,4)=EM(1,4)+E6*P2
      EM(2,2)=EM(2,2)+E5*(1.0+P2)
      EM(2,3)=EM(2,3)+E6*(2.0+P2)
      EM(2,4)=EM(2,4)+E7*(3.0+P2)
      EM(3,3)=EM(3,3)+E7*(4.0+P2)
      EM(3,4)=EM(3,4)+E8*(6.0+P2)
      EM(4,4)=EM(4,4)+E9*(9.0+P2)
      EM(1,7)=EM(1,7)+E4*AM
      EM(1,8)=EM(1,8)+E5*AM
      EM(2,5)=EM(2,5)-E5
      EM(2,6)=EM(2,6)-E6
      EM(2,7)=EM(2,7)+E5*AM
      EM(2,8)=EM(2,8)+E6*AM
      EM(3,5)=EM(3,5)-2.0*E6
      EM(3,6)=EM(3,6)-2.0*E7
      EM(3,7)=EM(3,7)+E6*AM
      EM(3,8)=EM(3,8)+E7*AM
      EM(4,5)=EM(4,5)-3.0*E7
      EM(4,6)=EM(4,6)-3.0*E8
      EM(4,7)=EM(4,7)+E7*AM
      EM(4,8)=EM(4,8)+E8*AM
      EM(5,5)=EM(5,5)+E5
      EM(5,6)=EM(5,6)+E6
      EM(6,6)=EM(6,6)+E7
      EM(7,7)=EM(7,7)+E5
      EM(7,8)=EM(7,8)+E6
      EM(8,8)=EM(8,8)+E7
      DØ 45 I=1,7
      II=I+1
      DØ 45 J=II,8
      EK(J,I)=EK(I,J)
      EM(J,I)=EM(I,J)
   45 CØNTINUE
```

```
C      ****************************************************
C      *  CALCULATE  THE  STIFFNESS  AND MASS  MATRICES       *
C      ****************************************************
       CALL  TRIMUL(B,EK,C,D,8,8,8,8,8)
       CALL  TRIMUL(B,EM,C,D,8,8,8,8,8)
C      ****************************************************
C      *  PUT  THE  ELEMENT MATRICES INTØ SUBSYSTEM  MATRICES  *
C      ****************************************************
       KK=4*(K-1)
       CALL  ASMBLE(SK,EK,KK,KK,1,8,8,L)
       CALL  ASMBLE(SM,EM,KK,KK,1,8,8,L)
C      ****************************************************
C      *  GØ BACK AND  REPEAT  CALCULATIONS  FØR  ØTHER ELEMENTS*
C      ****************************************************
       IF(K-N)30,50,50
    50 CØNTINUE
       RETURN
       END
```

```
      SUBRØUTINE    THKSYS(SK,SM,SKB,SMB,CC,RDØ,RRØ,NTD,NTB,L,LL)
C     ****************************************************
C     *  THIS SUBRØUT INE ASSEMBLESTHE STIFFNESS AND MASS*
C-    *  MATRICES ØF THE TWØ SUB SYSTEMSINTØTHESYSTEM    *
C     *  MATRICES. THE DISC SUBSYSTEMSMATRICESSK(L,L) AND*
C     *  SM(L,L) ARE THEMSELF USED AS SYSTEM MATRICES.   *
C     *  BEFØREENTERING THE SUBRØUTINE INITIALISE ALL THE *
C     *  TERNS ØFTHESUBSYSTEM MATRICES SK,SM,SKB,ANDSMB *
C     ****************************************************
      DIMENSIØN     SK(L,L),SM(L,L),SKB(LL,LL),SMB(LL,LL)
      DIMENSIØNDK( 14, 14),DM( 14, 14),T(14,14),C(14,14),D(14,14)
      CØMMØN/ØPTIØN/IØPT,IRNG,ITHD,ITED,ITHB,ISTB
      CØMMØN/ØNE/AM,AM2,AM4,AMPR
     RR=RDØ
      IF(IRNG.NE.0)    RR=RRØ
      DØ 10 I=1,14
      DO 10 J=1,14
      DK(I,J)=SKB(I,J)
      DM(I,J)=SMB(I,J)
   10 T(I,J)=0.0
C     ****************************************************
C     *  APPLY THE CØNSTRAINT CØNDITIØNSTØ THE BLADE     *
C     *  SUBSYSTEMMATRICES                               *
C     ****************************************************
     T(3,5)=1.0
      T(4,1)=1.0
      T(5,2)=1.0
      T(6,3)=1.0
      T(7,1)=-AM/RR
      T(7,4)=1.0
      T(8,6)=1.0
      T(9,7)=1.0
     T(10,8)=1.0
      T(11,9)=1.0
      T(12,10)=1.0
      T(13,11)=1.0
      T(14,12)=1.0
      CALL TRIMUL(T,DK,C,D, 141 12, 14, 14,14)
      CALL TRIMUL(T,DM,C,D,14,12,14, 14, 14)
      DØ 15 I=1,14
      DO 15 J=1,14
      C(I,J)=SKB(I,J)
   15 D(I,J)=SMB(I,J)
      DØ 20 I=1,12
      II=I+2
      DO 20 J=1,12
```

```
      JJ=J+2
      SKB(II,JJ)=DK(I,J)
   20 SMB(II,JJ)=DM(I,J)
C     ****************************************************
C     *  ASSEMBLE THE DISC AND BLADE MATRICES INTO THE     *
C     *  SYSTEM MATRICES                                   *
C     ****************************************************
      DØ 30 I=3,NTB
      II=I+NTD-6
      DO 30 J=3,NTB
      JJ=J+NTD-6
      SK(II,JJ)=SK(II,JJ)+CC*SKB(I,J)
   30 SM(II,JJ)=SM(II,JJ)+CC*SMB(I,J)
      DO 35 I=1,14
      DO 35 J=1,14
      SKB(I,J)=C(I,J)
   35 SMB(I,J)=D(I,J)
      RETURN
      END
```

D.4.4 Subroutines Used Both in PROGRAM-2 and PROGRAM-3

```
      SUBRØUTINE INLSTR(SK,R,T,TE,W,P,SGR,SGT,NSD,MS)
C     ***************************************************
C     * THIS SUBRØUTINE CALCULATES RADIAL AND TANGENTIAL *
C     * STRESSES SGR(L) AND SGT(L) AT THE NØDAL PØINTS ØF *
C     * AN AXISYMMETRIC NØN UNIFØRM DISC WITH ØR WITHØUT *
C     * A RIM DUE TØ UNIFØRM RØTATIØN AND AXISYMMETRIC   *
C     * TEMPERATURE GRADIENT TE(L)                        *
C     * WHILE ENTERING THE SUBRØUTINE INITIALISE ALL THE *
C     * TERMS ØF THE RADIUS VECTØR R(L), THE THICKNESS    *
C     * VECTØR T(L), AND THE TEMPERATURE VECTØR TE(L)     *
C     ***************************************************
      DIMENSIØN SK(MS,MS), W(MS),P(MS),R(MS),T(MS),TE(MS)
      DIMENSIØN SGR(MS),SGT(MS)
      DIMENSIØN EK(4,4),B(4,4),C(4,4),D(4,4),EP(4),EE(4)
      CØMMØN/ØPTIØN/IØPT,IRNG,ITHD,ITED,ITHB, ISTB
      CØMMØN/TWØ/S1,S2,S3,S4,CKD,CKR,CMD,CMR,CC,CCC,CK,CP,CT
      CØMMØN/FØUR/PI,ED,ER,EB,RØD,RØR,RØB,ALD,ALR,PRD,PRR,PRB
      CØMMØN/FIVE/SRI,SRØ
      NS=NSD
      IF(IRNG.EQ.1) NS=NSD+1
      NN=2*NS
      DØ 20 I=1,NN
      P(I)=0.0
      DØ 20 J=1,NN
   20 SK(I,J)=0.0
      PRINT 3
      K=0
      N=NS-1
      PR-PRD
   30 CØNTINUE
C     ***************************************************
C     * SELECT THE NUMBER K OF THE ELEMENT               *
C     ***************************************************
      K=K+1
      IF(K.EQ.NSD) PR=PRR
      K1=2*I<-1
      K2=2*K
C     ***************************************************
C     * GET THE VALUES ØF RADIUS AND THICKNESS AT NØDES  *
C     ***************************************************
      R1=R(K1)
      R2=R(K2)
      T1=T(K1)
      T2=T(K2)
      KK=2*(K-1)
```

```
      DØ   40   I=1,4
      DO 40 J=1,4
      B(I,J)=0.0
   40 EK(I,J)=0.0
      DD=R2-R1
      D1=DD*DD
      D2=D1*DD
      ALFA=(R2*T1-R1*T2)/(R2-R1)
      BETA=(T2-T1)/(R2-R1)
      X1 =ALFA*CK
      X2 =BETA*CK
      IF(K.EQ.NSD) X1=X1*ER/ED*(1.0-PRD*PRD)/(1.0-PRR*PRR)
      IF(K.EQ.NSD) X2=X2*ER/ED*(1.0-PRD*PRD)/(1.0-PRR*PRR)
      B(1,1)=R2*R2*(R2-3.*R1)/D2
      B(1,3)=R1*R1*(3.*R2-R1)/D2
      B(1,2)=-R1*R2*R2/D1
      B(1,4)=-R1*R1*R2/D1
      B(2,1)=6.*R1*R2/D2
      B(2,3)=-B(2,1)
      B(2,2)= R2*(2.0*R1+R2)/D1
      B(2,4)= R1*(R1+2.0*R2)/D1
      B(3,1)=-3.*(R1+R2)/D2
      B(3,3)=-B(3,1)
      B(3,2)=-(R1+2.*R2)/D1
      B(3,4)=-(2.*R1+R2)/D1
      B(4,1)=      2./D2
      B(4,3)=-B(4,1)
      B(4,2)=   1.0/D1
      B(4,4)=B(4,2)
      A1=R1*R2
      A2=A1*A1
      A3=R2-R1
      A4=R2**2-R1**2
      A5=R2**3-R1**3
      A6=R2**4-R1**4
      A7=R2**5-R1**5
      A8=R2**6-R1**6
      A9=R2**7-R1**7
      C5=ALØG(R2/R1)
      E1 =X1*C5+X2*A3
      E2 =X1*A3+X2*0.5*A4
      E3=X1*0.50*A4+X2*S1*A5
      E4=X1*S1*A5+X2*0.25*A6
      E5=X1*0.25*A6+X2*0.2*A7
      E6=X1*0.2*A7+X2*S2*A8
      E7=X1*S2*A8+X2*S3*A9
C     ***************************************************************
C     *  CALCULATE THE SMALL 'SMALL  K' M A T R I X                 *
C     ***************************************************************
      EK(1,1)=E1
      EK(1,2)=E2*(1.0+PR)
      EK(1,3)=E3*(1.0+2.0*PR)
      EK(1,4)=E4*(1.0+3.0*PR)
      EK(2,2)=E3*(2.0+2.0*PR)
      EK(2,3)=E4*(3.0+3.0*PR)
```

```
      EK(2,4)=E5*(4.0+4.0*PR)
      EK(3,3)=E5*(5.0+4.0*PR)
      EK(3,4)=E6*(7.0+5.0*PR)
      EK(4,4)=E7*(10.0+6.0*PR)
      EK(2,1  )=EK(1,2)
      EK(3,1)=EK(1,3)
      EK(4,1)=EK(1,4)
      EK(3,2)=EK(2,3)
      EK(4,2)=EK(2,4)
      EK(4,3)=EK(3,4)
      Y1=ALFA*CP
      Y2=BETA*CP
      IF(K.EQ.NSD) Y1=Y1*RØR/RØD
      IF(K.EQ.NSD) Y2=Y2*RØR/RØD
C     ****************************************************
C     *  CALCULATE CØNSISTANT LØAD VECTØR FØR RØTATIØN    *
C     ****************************************************
      EP(1)=Y1*S1*A5+Y2*0.25*A6
      EP(2)=Y1*0.25*A6+Y2*0.2*A7
      EP(3)=Y1*0.2*A7+Y2*S2*A8
      EP(4)=Y1*S2*A8+Y2*S3*A9
      IF(ITED.EQ.0) GO TØ 42
C     ****************************************************
C     *  GET THE VALUES ØF TEMPERATURE AT NODES           *
C     ****************************************************
      TE1=TE(K1)
      TE2=TE(K2)
      PRINT 2,K,R1,R2,T1,T2,TE1,TE2
      ALFT=(R2*TE1-R1*TE2)/DD
      BETT=(TE2-TE1)/DD
      Z1=ALFA*ALFT*CT
      Z2=ALFA*BETT*CT+BETA*ALFT*CT
      Z3=BETA*BETT*CT
      IF(K.EQ.NSD) Z1=Z1 *ER/ED*ALR/ALD
      IF(K.EQ.NSD) Z2=Z2*ER/ED*ALR/ALD
      IF(K.EQ.NSD) Z3=Z3*ER/ED*ALR/ALD
C     ****************************************************
C     *  CALCULATE CØNS ISTANT LØAD VECTØR FØR TEMPERATURE *
C     ****************************************************
      EP(1)=EP(1)+Z1*A3+Z2*0.5*A4+Z3*S1*A5
      EP(2)=EP(2)+Z1*A4+Z2*2.0*S1*A5+Z3*0.5*A6
      EP(3)=EP(3)+Z1*A5+Z2*0.75*A6+Z3*0.6*A7
      EP(4)=EP(4)+Z1*A6+Z2*0.8*A7+Z3*2.0*S1*A8
      GØ TØ 43
   42 CØNTINUE
      PRINT 2,K,R1,R2,T1,T2
   43 DØ 45 I=1,4
      DO 45 J=1,4
   45 C(I,J)=B(J,I)
C     ****************************************************
C     *  CALCULATE LØAD VECTØR AND STIFFNESS MATRIX       *
C     ****************************************************
      CALL MATMUL(C,EP,EE,4,4,4,1,4)
      CALL TRIMUL(B,EK,C,D,4,4,4,4,4)
```

```
C      *****************************************************
C      *  PUT  THE  ELEMENT MATRICES INTØ SUBSYSTEM MATRICES *
C      *****************************************************
       CALL ASMBLE(SK,EK,KK,KK,1,4,4,MS)
       CALL SYSLØD(P,EE,KK,4,4,MS)
C      *****************************************************
C      *  GØBACK AND REPEAT  CALCULATIØNS FØR ØTHER ELEMENTS*
C      *****************************************************
       IF(K-N)30,50,50
   50 CØNTINUE
       P(1)=P(1)+SRI
       P(NN-1)=P(NN-1)+SRØ
       CALL INVT(SK,NN,MS)
       CALL MATMUL(SK,P,W,NN,NN,NN,1,MS)
C      *****************************************************
C      *  CALCULATE STRESSES AT NØDESØF EACH ELEMENT        *
C      *****************************************************
       PRINT 1
       DØ 60 K=1,N
       E=ED
       PR=?RD
       ALFA=ALD
       IF(K.EQ.NSD) E=ER
       IF(K.EQ.NSD) PR=PRR
       IF(K.EQ.NSD) ALFA=ALR
       CS=E/(1.0-PR*PR)
       K1=2*K-1
       K2=K1+1
       K3=K2+1
     K4=K3+1
       SGR(K1)=CS*(W(K2)+PR*W(K1)/R(K1))
       SGR(K2)=CS*(W(K4)+PR*W(K3)/R(K2))
       SGT(K1)=CS*(W(K1)/R(K1)+PR*W(K2))
       SGT(K2)=CS*(W(K3)/R(K2)+PR*W(K4))
       IF(ITED.EQ.0) GØ TØ 60
       SGR(K1)=SGR(K1)-CS*ALFA*TE(K1)*(1.0+PR)
       SGR(K2)=SGR(K2)-CS*ALFA*TE(K2)*(1.0+PR)
       SGT(K1)=SGT(K1)-CS*ALFA*TE(K1)*(1.0+PR)
       SGT(K2)=SGT(K2)-CS*ALFA*TE(K2)*(1.0+PR)
   60 PRINT 2,K,SGR(K1),SGR(K2),SGT(K1),SGT(K2)
       RETURN
    1 FØRMAT(1H1,//5X,' STRESSES IN THE DISC '//2X,'ELEMENT
     .RADIAL STRESS              TANGENTIAL  STRESS'//)
    2 FØRMAT(/2X,I5,5E13.5)
    3 FØRMAT(1H1,/5X,'DISC DIMENSIØNS'//)
    5 FØRMAT (4E13.6 )
   10 FØRMAT(2X,5E13.6)
       END
```

```
      SUBROUTINE EIGVAL(SK,SM,D,F,FR,B,C,X,ER,B7,B8,B9,IJK,N1,L)
C     ******************************************************
C     *  THIS SUBROUTINE SOLVES THE EIGEN VALUE PROBLEM       *
C     *  RELATE3 TO THE VIBRATION PROBLEM CONSIDERED.         *
C     *  SK(L,L) AND SM(L,L) ARE THE STIFFNESS AND MASS       *
C     *  MATRICES OF THE VIBRATING SYSTEM AND THESE SHOULD *
C     *  BE DEFINED BEFORE ENTERING THE SUBROUTINE. ALL THE*
C     *  OTHER ARRAYS AND VECTORS NEED NOT BE DEFINED.        *
C     *  IJK - THE POSITION OF THE ELEMENT OF THE MODAL       *
C     *  VECTOR WHICH IS KEPT AS UNITY WHILE ITERATING.       *
C     *  N1 - SIZE OF THE ARRAYS SK AND SM                    *
C     *  L -DIMENSION GIVEN TO SK AND SM                      *
C     ******************************************************
      DIMENSION SK(L,L),SM(L,L),D(L,L),F(L,L),B(L),C(L),X(L),ER(L)
      DIMENSION B7(L),B8(L),B9(L),FR(20,10)
      COMMON/SIX/CONST,MrKK
      ALLOW=0.00000001
      MA=M+1
      IF(N1.LT.KK) KK=N1
C     ******************************************************
C     *  FORM THE DYNAMIC STIFFNESS MATRIX D(L,L)             *
C     ******************************************************
      CALL INVT(SK,N1,L)
      CALL MATMUL(SK,SM,D,N1,N1,N1,N1,L)
C     ******************************************************
C     *  SPECIFY MAXIMUM NUMBER OF ITERATIONS BEYOND WHICH *
C     *  ITERATION SHOULD BE STOPPED                          *
C     ******************************************************
      MI=95
      DO 30 I=1,N1
      X(I)=1.0
   30 C(I)=1.0
      MM=0
  150 MM=MM+1
      NI=0
      LN=7
      LL=LN
C     ******************************************************
C     *  S T A R T   ITERATION                                *
C     ******************************************************
   50 NI=NI+1
      ML=LL+1
      NN=ML+1
   41 DO 31 I=1,N1
      B(I)=0.0
      DO 31 K=1,N1
   31 B(I)=B(I)+D(I,K)*C(K)
C     ******************************************************
C     *  EVERY SEVENTH ITERATION GO TO THE QUICK ROUTINE      *
C     *  AND REFINE THE ASSUMED VECTOR'                       *
C     ******************************************************
      IF(NI-LL)51,52,53
   53 IF(NI-ML)51,54,55
   55 IF(NI-NN)51,56,51
```

```
   52 DO 44 I=1,N1
      B7(I)=B(I)
   44 C(I)=B(I)
      GØ TØ 50
   54 DØ 45 I=1,N1
      B8(I)=B(I)
   45 C(I)=B(I)
      GO TO 50
   56 DØ 46 I=1,N1
      B9(I)=B(I)
   46 CØNTINUE
   60 CALL MAX(B,BMAX,M1,N1,L)
      B(M1)=0.0
   61 CALL MAX(B,BMAX,M2,N1,L)
   62 CALL QUICK(B7,B8,B9,C,X,N1,M1,M2,L)
      LL=LL+LN
      GØ TØ 50
   51 BMAX=ABS(B(IJK)9
   90 DØ 32 I=1,N1
      B(I)=B(I)/BMAX
   32 ER(I)=B(I)-C(I)
  320 CALL MAX(ER,ERMAX,M3,N1,L)
C     ****************************************************
c.    *  CHECK CØNVERGENCE                                 *
C     ****************************************************
      ERMAX=2.0*ERMAX/(ABS(B(M3 9)+ABS(C(M3))9
      IF(ERMAX.LT.ALLØW) GØ TØ 42
   43 DØ 49 I=1,N1
   49 C(I)=B(I)
      IF(N1-M1)50,50,42
   42 CØNTINUE
C     ****************************************************
C     *  PRINTØUTFREQUENCY VALUE AND THE MØDALVECTØR       *
C     ****************************************************
      PRINT 80,MM,N1
      FREQ=CØNST/SQRT(BMAX)
      FR(MA,MM9=FREQ
      PRINT 81,FREQ
      PRINT83
      PRINT84,(B(I),I=1,N1 9
      DO 65 I=1,N1
      C(I)=0.0
      DO 65 K=1,N1
   65 C(I 9-C(I)+B(K)*SM(K,I)
      ALFA=0.0
      DØ 66 I=1,N1
   66 ALFA=ALFA+C(I)*B(I)
      BETA=SQRT(ALFA9
      DØ 67 I=1,N1
   67 B7(I)=B(I)/BETA
```

```
      IF(MM-KK)59, 100, 100
   59 DØ 68 I=1,N1
      DØ 68 J=1,N1
      F(I,J)=0.0
   68 F(I,J)=F(I,J)+B(I)*C(J)
      G=BMAX/ALFA
C     ****************************************************
C     *  FØRM THE NEW DYNAMIC STIFFNESS MATRIX           *
C     ****************************************************
      DO 69 I=1,N1
      DØ 69 J=1,N1
   69 D(I,J)=D(I,J)-G*F(I,J)
      DØ 95 I=1,N1
   95 C(I)=X(I)
      GO TO 150
  100 RETURN
   80 FØRMAT(5X,'MØDE NUMBER =' ,I2,4X,'ITERATIØNS =',I3/)
   81 FØRMAT(5X,'FREQUENCY IN HZ.=',E14.8/)
   83 FØRMAT (20X,'MØDAL VECTØR'/)
   84 FØRMAT(/5X,5E13.6)
      END
```

```
      SUBRØUT INE  I NVT(A,N,L)
C     **************************************************
C     *  THIS SUBRCUT I NE  INVERTS  T H E  MATRIX A(N,N) AÑD     *
C     *  STØRES THE INVERSE IN THE SAME  MATRIX                   *
C     **************************************************
      DIMENSIØN A(L,L),INDEX(100,2)
      IS=1
      DØ 108 I=1,N
 108  INDEX(I,1)=0
      II=0
 109  AMAX=-1.
      DO 110I=1,N
      IF(INDEX(I,1))110,111,110
 1i1  DØ 112  J=1,N
      IF(INDEX(J,1))112,113,112
 113  TEMP=ABS(A(I,J))
      IF(TEMP-AMAX)112,112, 114
 114  IRØW=I
      ICØL=J
      AMAX=TEMP
 112  CØNT        INUE
 110  CØNTINUE
      IS=IS+1
 10   FØRMAT(I6,E13.6)
      IF(AMAX)225,115,116
 116  INDEX(ICØL,1)=IRØW
      IF(IRØW-ICØL)119,118,119
 119  DØ 120  J=1,N
      TEMP=A(IRØW,J)
      A(IRØW,J)=A(ICØL,J)
 120  A(ICØL,J)=TEMP
      II=II+1
      INDEX(II,2)=ICØL
 118  PIVØT=A(ICØL,ICØL)
      A(ICØL,ICØL)=1.
      PIVØT=1./PIVØT
      D O   1 2 1  J=1,N
 121  A(ICØL,J)=A(ICØL,J)*PIVØT
      DØ 122 I=1,N
      IF(I-ICØL)123,122,123
 12;  TEMP=A( I; ICØL)
      A(I,ICØL)=0.
      DØ 124 J=1,N
 124  A(I,J)=A(I,J)-A(ICØL,J)*TEMP
 122  CØNTINUE
      GO TØ 109
 125  ICØL=INDEX(II,2)
      IRØW=INDEX(ICØL,I)
      DO 126 I=1,N
      TEMP=A(I,IRØW)
      A(I,IRØW)=A(I,ICØL)
 126  A(I,ICØL)=TEMP
      II=II-1
 225  IF(II)125,127,125
 115  PRINT 150
 150  FØRMAT(1HO,10HZERØ PIVØT,/)
 1'27 CØNTINUE
      RETURN
      END
```

```
      SUBRØUTINE MAX(A,Z,M,N,L)
C     ******************************************************
C     *  THIS SUBRØUTINE FINDS ØUT THE ABSØLUTE MAXIMUM    *
C     *  Z AND PØSITIØN M ØF THE ELEMENTS ØF THE VECTØR    *
C     *  A(N)                                              *
C     ******************************************************
      DIMENSIØN A(L)
    1 Z= ABS(A(1))
      M=1
      DØ   2   I=2,N
      Y= ABS(A(I))
      IF(Y-Z)2,2,3
    3 Z=Y
      M=I
    2 CØNTINUE
    4 RETURN
      END

      SUBRØUTINE QUICK(B7,B8,B9,A,B,N,M1 ,M2,L)
C     ******************************************************
C     *  THIS SUBRØUTINE REFINES THE MØDAL VECTØR FØR QUICK*
C     *  CØNVERGENCE                                       *
C     ******************************************************
      DIMENSIØN    B7(L),B8(L),B9(L),A(L),B(L)
      DR=B8(M1)*B7(M2)-B7(M1)*B8(M2)
    2 A1=(B9(M1)*B8(M2)-B8(M1)*B9(M2))/DR
      A2=(B9(M1)*B7(M2)-B7(M1)*B9(M2))/DR
      A3=0.5*SQRT(A2**2-4.*A1)
    3 C1=0.5*A2+A3
      C2=0.5*A2-A3
      DØ 10 I=1,N
      A(I)=B9(I)-C2*B8(I)
   10 B(I)=B9(I)-C1*B8(I)
   11 RETURN
      EIJD

      SUBRØUTINE MATMUL(A,B,C,MA,NA,MB,NB,L)
C     ******************************************************
C     *  THIS SUBRØUTINE MULTIPLIES THE MATRICES A AND B   *
C     *  AND THE RESULTING MATRIX IS STØRED IN THE ARRAY C *
C     *  MA - NUMBER ØF RØWS IN MATRIX  A                  *
C     *  NA - NUMBER ØF CØLUMNS IN MATRIX  A               *
C     *  MB - NUMBER ØF RØWS IN MATRIX B                   *
C     *  NB - NUMBER ØF CØLUMNS IN MATRIX  B               *
C     ******************************************************
      BIMENSIØN A(L,L),B(L,L),C(L,L)
      DØ 5 I=1,MA
      DØ 5 J=1,NB
      C(I,J)=0.0
      DØ 5 K=1,NA
    5 C(I,J)=C(I,J)+A(I,K)*B(K,J)
    6 RETURN
      END
```

```
      SUBRØUTINE TRIMUL(A,B,C,D,MA,NA,MB,NB,L)
C     ******************************************************
C     *  THIS SUBRØUT INE PREMULTIPLIES THE MATRIX B BY THE *
C     *  TRANSPØSE ØF A AND THEN PØSTMULTIPLIES THE PRØDUCT*
C     *  BY THE MATRIX A AND GIVES THE RESULTING MATRIX     *
C     *  STØRED IN THE ARRAY B ITSELF                       *
C     *  MA - NUMBER ØF RØWS IN MATRIX A                    *
C     *  NA - NUMBER ØF CØLUMNS IN MATRIX A'                *
C     *  MB - NUMBER OF RØWS IN MATRIX B                    *
C     *  NB - NUMBER ØF CØLUMNS IN MATRIX B                 *
C     ******************************************************
      DIMENSIØN A(L,L),B(L,L),C(L,L),D(L,L)
      DØ 10 I=1,MA
      DØ 10 J=1,NA
   10 C(J,I)=A(I,J)
      C A L L   MATMUL(C,B,D,NA,MA,MB,NB,L)
      C A L L   MATMUL(D,A,B,NA,NB,MA,NA,L)
      RETURN
      END
```

```
      SUBRØUTINE REDUCE(A,N,L,K,M)
C     ******************************************************
C     *  THIS SUBRØUTINE REDUCES THE SIZE OF THE ARRAY A    *
C     *  FRØM ( N X N ) TØ ( N-K X N-K ) BY SCØRING OUT     *
C     *  RØWS A N D CØLUMNS FRØM L TØ L+K                   *
C     ******************************************************
      DIMENSIØN A(M,M)
      NM1=N-K
      DØ 1 0 I=L,NM1
      DØ 1 0 J=1,N
      II=I+K
   10 A(I,J)=A(II,J)
      DØ 2 0 I=1,N
      DØ 2 0 J=L,NM1
      JJ=J+K
   20 A(I,J)=A(I,JJ)
      RETURN
      END
```

```
      SUBRØUTINE  ASMBLE(A,B,M,N,KS,K,LL,L)
C     ****************************************************
C     *  THIS SUBRØUTINE ASSEMBLES THE ELEMENT MATRIX .   *
C     *  B(LL,LL) INTØ THE SYSTEM MATRIX A(L,L)           *
C     ****************************************************
      DIMENSIØN A(L,L),B(LL,LL)
      DØ 10 I=KS,K
      MM=M+ I -KS +1
      DO 10 J=KS,K
      NN=N+J-KS+1
   IO A(MM,NN)==A(MM,NN)+B(1,J)
      RETURN
      END
```

```
      SUBRØUTINE SYSLØD(A,B,M,NN,LL,L)
C     ****************************************************
C     *  THIS SUBRØUTINE ASSMBLES THE ELEMENT LØAD VECTØR *
C     *  B(LL) INTØ THE SYSTEM LØAD VECTØR A(L)
C     ****************************************************
      DIMENSIØN A(L),B(LL)
      DØ 10 I=1,NN
      MM=M+I
   10 A(MM)=A(MM)+B(I)
      RETURN
      END
```